ENGINEERING MICROBIAL CELLS FOR BIOMETALLIC CATALYSIS

A thesis submitted to The University of Manchester for the degree of Doctor of Philosophy in the Faculty of Engineering and Physical Sciences

2011

JOANNE MARIE FOULKES

SCHOOL OF EARTH, ATMOSPHERIC AND ENVIRONMENTAL SCIENCES

Contents

51,576 words

Figures

Tables

Abbreviations

Δp	Protonmotive force
A	Absorbance
aa	Amino acid
A. niger	*Aspergillus niger*
ATP	Adenosine triphosphate
bioPd	Biogenic cell-supported palladium
B. sphaericus	*Bacillus sphaericus*
C. antarctica	*Candida antarctica*
CASTing	Combinatorial active-site saturation testing
cfu	Colony-forming units
CIP	Cahn, Ingold and Prelog system
D	Attenuation
D. desulfuricans	*Desulfovibrio desulfuricans*
D. fructosovorans	*Desulfovibrio fructosovorans*
DAB	3,3'-diaminobenzidine
DHAP	Dihydroxyacetone phosphate
DKR	Dynamic kinetic resolution
DMS	Dimethyl sulfide
DMSO	Dimethyl sulfoxide
EC	Enzyme Commission
E. coli	*Escherichia coli*
EDS/EDX	Energy dispersive X-ray spectroscopy
EDTA	Ethylenediaminetetraacetic acid
e.e.	Enantiomeric excess
E_m	Midpoint potential

EM	Electron microscopy/microscope
epPCR	Error-prone polymerase chain reaction
ES	Electrospray
ESEM	Environmental scanning electron microscopy
ESRF	European Synchrotron Radiation Facility
ETC	Electron transport chain
EXAFS	Extended X-ray absorption fine structure
FAD/$FADH_2$	Flavin adenine dinucleotide/reduced FAD
FDH	Formate dehydrogenase
FDH-H	H_2-generating formate dehydrogenase
FDH-O	Aerobic formate dehydrogenase
FDH-N	Anaerobic formate dehydrogenase
FHL	Formate hydrogenlyase
Gly-3-P	Glycerol-3-phosphate
HPLC	High-performance liquid chromatography
HRP	Horseradish peroxidase
Hyd-1(2/3/4)	Hydrogenase-1(2/3/4)
ICP-MS	Inductively coupled plasma mass spectrometry
IPTG	Isopropyl β-D-1-thiogalactopyranoside
k_{cat}	Catalytic constant
K_d	Partition coefficient
LB	Luria-Bertani
LC-MS	Liquid chromatography with mass spectrometry
Linac	Linear accelerator
MAO	Monoamine oxidase
MAO-A/MAO-B	Two mammalian isoforms of monoamine oxidase

MAO-N	Monoamine oxidase from *Aspergillus niger*
MAO-N-D5	Monoamine oxidase from *Aspergillus niger*, variant D5
mao-N-D5	Variant gene expressing the MAO-N-D5 enzyme
MDQ	1-methyl-3,4-dihydroisoquinoline
MIQ	1-methylisoquinoline
MOPS	Morpholinepropanesulfonic acid buffer
M_r	Relative molecular mass
MS	Mass spectrometry
MTBE	Methyl-tert-butyl ether
MTQ	1-methyltetrahydroisoquinoline
NAD^+/NADH	Nicotinamide adenine dinucleotide, oxidised/reduced form
OD_{600}	Optical density (attenuation) at 600 nm
PACE	Phage-assisted continuous evolution
P. aeruginosa	*Pseudomonas aeruginosa*
PAO	Polyamine oxidases
PCR	Polymerase chain reaction
Pd/C	Palladium on a carbon support
PGM	Platinum group metals
PFL	Pyruvate formate lyase
PLP	Pyridoxal 5'-phosphate
PrAO	Primary amine oxidase
QEXAFS	Quick-scanning extended X-ray absorption fine structure
(*R*)-MTQ	(*R*)-enantiomer of 1-methyltetrahydroisoquinoline
rac-MTQ	racemic 1-methyltetrahydroisoquinoline
RSC	Royal Society of Chemistry
RSD	Relative standard deviation

SLS	Swiss Light Source
(*S*)-MTQ	(*S*)-enantiomer of 1-methyltetrahydroisoquinoline
SOC medium	Super optimal broth with catabolite repression
spp.	Species
SRB	Sulfate-reducing bacteria
StEP	Staggered extension process
TEM	Transmission electron microscopy
TCPP	Tris(chloroisopropyl)phosphate
TMA	Trimethylamine
TMAO	Trimethylamine *N*-oxide
UV-Vis	Ultraviolet-visible
V	Volts
WT	Wild-type
XANES	X-ray absorption near-edge spectroscopy
XAS	X-ray absorption spectroscopy
XRD	X-ray diffraction

Abstract

This study investigates the use of palladised *Escherichia coli* as a biometallic catalyst with a view to its use in deracemisation reactions. Some bacteria can reduce metals by their use as the terminal electron acceptor in the respiratory chain, and recent work using *Desulfovibrio* spp. and other obligate and facultative anaerobes has led to the generation of palladium bionanocatalysts with superior activity to commercially available carbon-supported Pd(0) nanoparticles. This current study has investigated the use of formate as an electron donor for the reduction of soluble Pd(II) to insoluble Pd(0) nanoparticles by *E. coli*, and investigates the biological mechanisms responsible for the bioreduction, and for the extracellular location of the nanoparticles.

Previous work has been done at the Manchester Interdisciplinary Biocentre with the directed evolution of the monoamine oxidase enzyme of *Aspergillus niger* (known as MAO-N), which catalyses the oxidative deamination of terminal amines. The result has been to produce an enzyme with enhanced activity in the production of enantiomerically pure chiral amines. The modified enzyme catalyses the oxidation of the (*S*)-enantiomer to the corresponding imine, which is then reduced using a chemical reductant back to either the (*S*)- or the (*R*)-enantiomer, leading to an enantiomeric excess (*e.e.*) of the latter. After several cycles, enantiomerically pure amines are produced. In this study, *E. coli* transformed with a plasmid containing the variant *mao-N-D5* gene insert demonstrated good activity in catalysing the oxidation of the (*S*)-enantiomer of the secondary amine 1-methyltetrahydroisoquinoline (MTQ) to the imine 1-methyl-3,4-dihydroisoquinoline (MDQ), as measured by HPLC. The ability of *E. coli* to reduce Pd(II) to Pd(0) was exploited in order to use the supported nanoparticles in place of the chemical reductant, catalysing the reduction of the imine back to MTQ. Following five cycles of oxidation and reduction, racemic MTQ was converted to (*R*)-MTQ with an enantiomeric excess of up to 93%. The activity of the biometallic catalyst immobilised in alginate beads was also assessed, and found to be the same as planktonic cells. The recyclability and long-term storage of the immobilised biocatalyst was also investigated, and it was found that freeze-drying maintained the stability of the beads for up to six weeks, which was the limit of the experiment.

Declaration

No portion of the work referred to in this thesis has been submitted in support of an application for another degree or qualification of this or any other university or other institute of learning.

Copyright statement

i. The author of this thesis (including any appendices and/or schedules to this thesis) owns any copyright in it (the "Copyright") and she has given The University of Manchester the right to use such Copyright for any administrative, promotional, educational and/or teaching purposes.

ii. Copies of this thesis, either in full or in extracts, may be made only in accordance with the regulations of the John Rylands University Library of Manchester. Details of these regulations may be obtained from the Librarian. This page must form part of any such copies made.

iii. The ownership of any patents, designs, trademarks and any and all other intellectual property rights except for the Copyright (the "Intellectual Property Rights") and any reproductions of copyright works, for example graphs and tables ("Reproductions"), which may be described in this thesis, may not be owned by the author and may be owned by third parties. Such Intellectual Property Rights and Reproductions cannot and must not be made available for use without the prior written permission of the owner(s) of the relevant Intellectual Property Rights and/or Reproductions.

iv. Further information on the conditions under which disclosure, publication and exploitation of this thesis, the Copyright and any Intellectual Property Rights and/or Reproductions described in it may take place is available from the Head of School of Earth, Atmospheric and Environmental Sciences (or the Vice-President).

Acknowledgements

I would like to thank my supervisor, Professor Jon Lloyd, who has provided much help and support over the course of my PhD, and who has made the experience a lot less painful than at times I thought it would be. Thanks also to my co-supervisor Professor Nick Turner, and to Kirk Malone at MIB, who helped me with my HPLC troubles, finding reagents/bench space/pipettes/a cup of tea/the pub as necessary, and with the undiscovered country of chemistry in general. Thanks to Maeve, who came along at just the right time, and to all the postdocs who helped me with my presentations. Thanks to Vicky Coker who knows everything, and without whom my synchrotron experiences would have been much less useful, and thanks to Richard Patrick for waking me up on the night shift (and also for letting me sleep).

Most of all I would like to thank my family. Firstly my sister Alison, who always gave me good advice and made me feel like I was doing the right thing, even though she made me eat lentils. Also my parents, Leone and Alvin, who have provided emotional and financial support, and allowed my to do this without seeming to worry too much about me settling down. Now I promise I'll get a job. And not forgetting Muppet and Daisy, who always provided a friendly ear and an affectionate nibble, and who never judged as long as they were fed on time.

Most of all I would like to thank my wonderful husband Jon, the one person without whom this adventure truly would not have been possible. Thank you for allowing me to go half-way across the country to follow my dream, for coming to see me every weekend, for never blaming me for making us poor, for understanding when you had to go out alone so that I could stay at home and work, for going without a holiday for so long, for buying me dinner and paying the bills, for washing the dishes and cleaning the bathroom even though I hardly ever noticed you doing it, for bringing me cups of coffee, for listening to your music on headphones, and for keeping me sane. Thank you for loving me in spite of all this. Now it's your turn.

The Author

The author has the following qualifications and research experience:

Qualifications

Staffordshire University:	MSc Molecular Biology. Pass with merit. 2007
University of Sheffield:	MSc Pathological Science. Special option in microbiology. 2001
University of Bradford:	BSc (Hons) Biomedical Science. Special option in microbiology. 1995

Research experience

In addition to the publications detailed in this thesis, the author also has the following publication:

Ludlam, H., Howard, J., Kingston, B., Donachie, L., Foulkes, J., Guha, S., Curran, M. D. (2009) “Epidemiology of pharyngeal carriage of Fusobacterium necrophorum” *Journal of Medical Microbiology* 58:1264-5

Chapter 1: Thesis structure and aims

1.1 Structure

The thesis is presented in an alternative format, whereby publications arising from the research have been included in place of traditional chapters. This style of thesis presentation encourages the preparation of manuscripts suitable for publication during the course of the research.

Chapter 2 includes the introduction and literature review.

Chapter 3 outlines the methods and materials.

Chapter 4 is the first publication, *Engineering a biometallic whole cell catalyst for enantioselective deracemization reactions*. This publication is in press with ACS Catalysis.

Contributions of co-authors and collaborators:

Joanne M. Foulkes – first author, designed and performed experimental work.

Kirk L. Malone – technical support for HPLC analyses, proof-reading.

Victoria S. Coker – assistance with EDX and QEXAFS.

Nicholas J. Turner – co-supervisor, assistance with design of experimental work, proof-reading.

Jonathan R. Lloyd – main supervisor, assistance with design of experimental work, assistance with manuscript preparation and drafting of abstract, proof-reading.

John Charnock – analysis of QEXAFS data.

Valentin Koehler – assistance with developing HPLC protocol.

John Waters – provision of XRD data.

Roger Meadows (EM facility) – preparation of sections for TEM, assistance with imaging.

Paul Lythgoe – provision of ICP-MS data.

Chapter 5 is the second publication, *A novel aerobic mechanism for palladium bioreduction and recovery by Escherichia coli*. This publication is in preparation for submission to Microbiology.

Contributions of co-authors and collaborators:

Joanne M. Foulkes – first author, designed and performed experimental work.

Kevin Deplanche – provision of some of TEM data.

Frank Sargent – provision of bacterial strains for experimental work, proof-reading.

Lynne E. Macaskie – proof-reading.

Jonathan R. Lloyd – main supervisor, assistance with design of experimental work, assistance with manuscript preparation, proof-reading.

John Charnock – analysis of EXAFS data.

John Waters – performance of XRD.

Roger Meadows (EM facility) – preparation of sections for TEM, assistance with imaging.

Paul Lythgoe – performance of ICP-MS

Chapter 6 is the third publication, *The immobilisation of a biometallic whole cell catalyst for multi-step transformations*. This publication is in preparation for submission to Applied Microbiology and Biotechnology.

Contributions of co-authors and collaborators:

Joanne M. Foulkes – first author, designed and performed experimental work.

Kirk L. Malone – technical support for HPLC analyses, proof-reading.

Nicholas J. Turner – co-supervisor, discussion of experimental work.

Jonathan R. Lloyd – main supervisor, assistance with design of experimental work, assistance with manuscript preparation, proof-reading.

Valentin Koehler – assistance with developing HPLC protocol.

John Waters – provision of XRD data, assistance with ESEM.

Roger Meadows (EM facility) – preparation of sections for TEM, assistance with imaging.

Paul Lythgoe – provision of ICP-MS data.

Chapter 7 is the fourth publication, *The use of monoamine oxidase and biogenic palladium in the deracemization of the secondary amine 1-methyltetrahydroiso-quinoline*. This publication will be submitted to Practical Methods for Biocatalysis and Biotransformations.

Contributions of co-authors and collaborators:

Joanne M. Foulkes – first author, designed and performed experimental work.

Kirk L. Malone – technical support for HPLC analyses, proof-reading.

Nicholas J. Turner – co-supervisor, assistance with design of experimental work, proof-reading.

Jonathan R. Lloyd – main supervisor, assistance with design of experimental work, assistance with manuscript preparation, proof-reading.

Valentin Koehler – assistance with developing HPLC protocol.

Roger Meadows (EM facility) – preparation of sections for TEM, assistance with imaging.

Chapter 8 provides the conclusions and proposals for future work in this area.

Appendix 1 – this section includes a description of the experimental techniques throughout this project, and provides information on the information that can be provided using these techniques and their limitations.

Appendix 2 – this section includes any experimental work that has not been published.

Appendix 3 – this section includes the conferences I have attended.

1.2 Aims and objectives

At present, multi-step chemical biotransformations require the use of separate, sequential processes. This thesis describes work to generate a novel dual function biometallic catalyst as a model system for deracemisation reactions. The project used *E. coli* as this bacterium grows easily under laboratory conditions without strict environmental controls, and is amenable to genetic engineering. The microorganism

can also reduce Pd(II) to nanoscale bioPd without H_2S production, which is a problem with the sulfate-reducing bacteria that have been used in previous studies (Redwood *et al.*, 2008a).

The aims of this study were to demonstrate the feasibility of the manufacture of a genetically engineered biometallic whole cell catalyst and to optimise its activity as appropriate, attempting to demonstrate expression of the recombinant enzyme and bioreduction of palladium in a single bacterial culture. An assessment of the impact of cell immobilisation on the biometallic catalyst was made, including the selection of an appropriate immobilisation matrix and the impact of freeze-drying on prolonging the activity of cells during storage. The biochemistry of the process of Pd(II) reduction in aerobic cultures was also studied, using physiological and genetic approaches.

A number of techniques were used to achieve these aims in an attempt to build a full picture of the processes involved, including spectroscopy, electron microscopy, molecular biology and the use of deletion mutants, physiological manipulations, analytical chemistry, and immobilised cell technology.

Chapter 2: Introduction

The requirement for enantiomerically pure chiral amines in the pharmaceutical and agrochemicals industries has led to the need to develop dynamic kinetic resolution (DKR) and deracemisation techniques that can efficiently and rapidly produce products, theoretically with 100% yield and 100% enantiomeric excess (*e.e.*) (Alexeeva *et al.*, 2002). Previously published work has investigated the use of lipases and transaminases, using lipases for hydrolysis reactions and transaminases for the conversion of ketones to chiral amines. Lipases are also suitable for use with primary amines and some secondary amines only, with no activity towards tertiary amines (Dunsmore et al., 2006). Using a conceptually different approach, monoamine oxidase-N (MAO-N), attracted attention as a result of its enantioselectivity towards the (*S*)-form of the primary amine α-methylbenzylamine (Alexeeva *et al.*, 2002). MAO-N is a tetrameric flavoprotein that catalyses the oxidative deamination of terminal amine groups. Use of a modified version of the enzyme (MAO-N-D5) for the cyclic deracemisation of chiral amines is based on the creation of imine intermediates by oxidation of the (*S*)-enantiomer (see Figure 2.1).

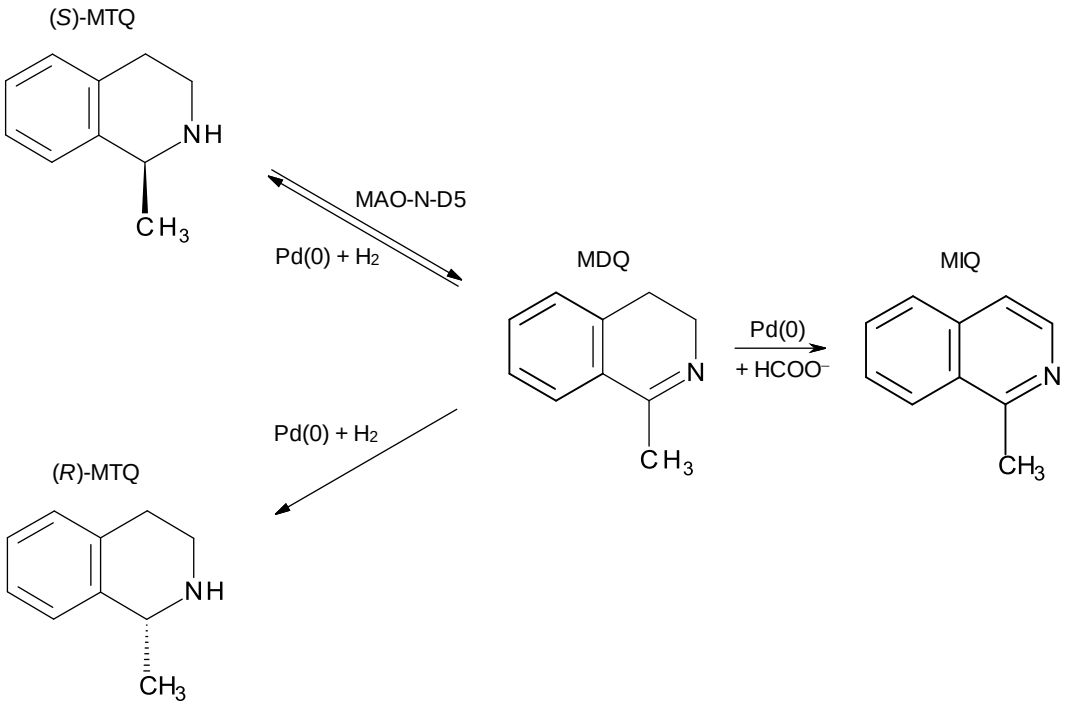

Figure 2.1: The cyclic deracemisation of 1-methyltetrahydroisoquinoline (MTQ) via the imine 1-methyl-3,4-dihydroisoquinoline (MDQ) using palladised biocatalyst with the

mao-N-D5 gene (adapted from Carr et al, 2003). 1-methylisoquinoline (MIQ) is formed when using formate as the electron donor in the reduction step (see section 3.2.5).

The addition of a chemical reductant such as ammonia-borane or palladium results in the non-selective conversion of the imine back to the racemic amine. After several oxidation/reduction cycles, a very high enantiomeric excess and yield of the (*R*)-enantiomer is achieved.

It has been known for more than a century that some bacteria can reduce metals by use as the terminal electron acceptor in the respiratory chain. For example, the sulfate-reducing bacterium (SRB) *Desulfovibrio desulfuricans* has been shown to reduce soluble Pd(II) to insoluble Pd(0), which is located in the periplasm as nanoparticles (Lloyd *et al.*, 1998a). This property has allowed the use of the palladised organism (known as bioPd) directly in industrially important reactions, showing good activity compared with a commercially available carbon-supported palladium catalyst (Baxter-Plant *et al.*, 2003; Creamer *et al.*, 2007b; De Windt *et al.*, 2005; Mabbett *et al.*, 2004; 2006).

This research project investigates the activity of palladised *E. coli* transformed with the MAO-N-D5 enzyme towards the secondary amine 1-methyltetrahydroisoquinoline (MTQ), and assesses its potential in the development of a one-pot method for the deracemisation of chiral amines.

2.1 Bacterial respiration

During respiration in eukaryotic cells, the electrons donated by a low-redox-potential molecule such as nicotinamide adenine dinucleotide (NADH) are transferred to a high-redox-potential electron acceptor such as oxygen, by means of a series of redox reactions involving molecules embedded in the mitochondrial membrane known as the electron transport chain (ETC). The molecules in the ETC include enzymes, quinones (electron and proton carriers), flavoproteins and cytochromes (electron carriers with heme groups). The energy generated during this process is used to drive

the flow of protons across the mitochondrial membrane, which sets up an electrochemical gradient, or protonmotive force (Δp) (Richardson, 2000). The return flow of protons through the membrane generates the high-energy molecule adenosine triphosphate (ATP). The electron-transfer process is similar in bacteria, although the ETC molecules vary depending on the availability of organic molecules for oxidation, and a much wider range of electron acceptors is utilised. This includes sulfate (Hamilton, 1998), nitrate and nitrite (Berks *et al.*, 1995), arsenate (Macy *et al.*, 1996), selenate (Macy *et al.*, 1989), transition metals (Lovley, 1991), and radionuclides (Lloyd *et al.*, 2000; Lloyd & Renshaw, 2005; Lovley *et al.*, 1991). Such substrate flexibility allows microorganisms to exploit a diverse range of environments.

2.1.2 Respiration in *Escherichia coli*

E. coli may obtain energy for growth by aerobic or anaerobic respiration, or by fermentation, depending on environmental conditions. The ETC consists of several different dehydrogenases and terminal reductases or oxidases, linked by quinones (mobile electron shuttles).

Aerobic respiration: during aerobic respiration, one of two terminal oxidases may be used to transfer electrons to oxygen – the cytochrome *o* oxidase complex, or the cytochrome *d* complex, depending on whether oxygen is abundant or limited respectively (Anraku & Gennis, 1987; Poole, 1983).

Anaerobic respiration: during anaerobic respiration, one of ten different terminal reductases may be expressed, depending on the electron acceptor available. There are also 15 different dehydrogenases, leading to a considerable amount of variability in the ETC, although not all combinations of enzymes are possible due to energetic constraints (Unden & Bongaerts, 1997). Each dehydrogenase requires a redox pair, of which one molecule is oxidised and the other reduced, and the midpoint potential (energy in volts released upon oxidation/reduction, E_m) for these redox pairs varies. Table 2.1 lists all dehydrogenases, reductases, and oxidases of *E. coli* and their redox pairs (similar enzymes such as formate dehydrogenases are listed together).

Fermentation: fermentation occurs under anaerobic conditions in the absence of electron donors suitable for respiration. During the process of fermentation, sugars are converted to acetate, ethanol, lactate, formate and succinate, with the production

of substantial amounts of hydrogen and carbon dioxide. The ETC does not operate under fermentative conditions, and so the recycling of NADH (which is normally reoxidised by the ETC) occurs during the conversion of pyruvate to fermentation products.

Table 2.1: Respiratory chain enzymes of *E. coli*, with redox couples and midpoint potentials (adapted from Unden and Bongaerts, 1997)

Enzyme	**Redox couple**	E_m **(V)**
FDH	HCO_3^-/ HCO_2^-	–0.43
Hydrogenase	H^+/H_2	–0.42
NADH dehydrogenase	NAD^+/NADH	–0.32
Glycerol-3-phosphate dehydrogenase	DHAP/Gly-3-P	–0.19
Pyruvate oxidase	acetate+CO_2/pyruvate	?
Lactate dehydrogenase	pyruvate/lactate	–0.19
Amino acid dehydrogenase	2-oxoacid+NH_4^+/aa	?
Glucose dehydrogenase	glucose/gluconate	–0.14
Succinate dehydrogenase	fumarate/succinate	+0.03
Quinol oxidase (cytochrome complex *o*/*d*)	O_2/H_2O	+0.82
Nitrate reductase	NO_3^-/ NO_2^-	+0.42
Nitrite reductase	NO_2^-/ NH_4^+	+0.36
DMSO reductase	DMSO/DMS	+0.16
TMAO reductase	TMAO/TMA	+0.13
Fumarate reductase	fumarate/succinate	+0.03

? = no information available

2.2 Microbial reduction of metals

A wide range of bacteria and Archaea are capable of reducing metals in order to conserve energy for growth (known as dissimilatory metal reduction processes). For example, a diverse group of iron-reducing species are capable of reducing Fe(III) to Fe(II) in subsurface environments. Some bacteria, such as the sulfate-reducers, are

also capable of reducing Fe(III) although there is no evidence that they are able to utilise this process for growth (Lloyd, 2003).

In some cases, microbial reduction leads to the mobilisation of toxic metals, which could have potentially harmful effects on flora and fauna (including humans). In other cases however, reduction of metals can produce ions that are less harmful or less soluble, for example the reduction of Cr(VI) to Cr(III), or the reduction of the soluble radionuclide Tc(VII) to an insoluble black precipitate (Lloyd et al., 1997). Microbial reduction can therefore be used in the bioremediation of contaminated land, but also has potential uses in the reclamation of valuable metals from wastes, such as gold (Kashefi *et al.*, 2001) and palladium (Mabbett et al., 2006).

2.2.1 Dissimilatory metal reduction

Iron reduction

Iron is the most abundant redox-active metal in the Earth's crust, followed by manganese (Lovley, 2000), and most organisms that reduce one also reduce the other (Lovley *et al.*, 2004). The term 'dissimilatory' reduction is used as the organisms do not accumulate the reduced Fe(II) intracellularly. It is probable that Fe(III) reduction to Fe(II) was the first respiratory process to evolve, as Fe(III) is abundant and its reduction is thermodynamically driven, not requiring specialist enzymes (Lovley, 1991; Lovley, 2000; Richardson, 2000). The Fe(III) acts as the terminal electron acceptor in the ETC, whereby electrons flow along a series of membrane-bound proteins towards a more positive redox potential with the associated conversion of energy (Lloyd, 2003). Fe(III) reduction using hydrogen as the electron donor is highly conserved in hyperthermophilic organisms (Lovley *et al.*, 2004), which also points towards an early evolutionary development. However, different mechanisms exist amongst Fe(III) reducers, indicating that the capacity for Fe(III) reduction evolved more than once. For example *Geobacter* species, which have been isolated from a variety of diverse sedimentary environments (Coates *et al.*, 1996), require direct contact with Fe(III) for reduction to take place. *Shewanella* and *Geothrix* species on the other hand produce chelators and electron shuttles to effect Fe(III) reduction at a distance (Lovley *et al.*, 2004).

The dissimilatory reduction of Fe(III) and Mn(IV) has a strong influence on the biogeochemical cycles of many other components of sediments, groundwater, and aquatic environments, due to the use of these components as electron donors or their co-precipitation or dissolution with iron (Lovley, 1991). Competition with sulfate-reducing bacteria (SRB) and methanogens for organic carbon, for example, interferes with the cycling of sulfate and the production of methane (Megonigal *et al.*, 2003). However, it is the ability of Fe(III)-reducing organisms to oxidise organic compounds to carbon dioxide and reduce a variety of other metals which provides potential candidates for bioremediation.

2.2.2 Bioremediation

Organic contaminants

Fe(III) is the predominant electron acceptor in anaerobic zones, which are often extensive in petroleum-contaminated aquifers. If the aromatic hydrocarbons benzene or toluene oxidation were coupled to Fe(III) reduction therefore, this would present a useful bioremediation tool for use in contaminated aquifers (Anderson *et al.*, 1998; Lovley & Anderson, 2000). The dissimilatory Fe(III)-reducing genus *Geobacter* is the only genus known to degrade aromatic hydrocarbons coupled with Fe(III) reduction, and these species may therefore be exploited for their ability to oxidise organic contaminants (Anderson *et al.*, 1998; Lovley *et al.*, 1993; Lovley & Anderson, 2000; Megonigal *et al.*, 2003). Early work on the oxidation of benzene and toluene in aquifer sediments showed that *in vitro* oxidation only occurred when sediments were supplemented with a Fe(III) chelator, such as nitrilotriacetic acid (Lovley *et al.*, 1994), ethylenediaminetetraacetic acid (EDTA), N-methyliminodiacetic acid, ethanol diglycine, and phosphates (Lovley *et al.*, 1996b). In the latter study, humics were also used, but it was later realised that the humics were in fact behaving as electron shuttles between the bacterial cells and the insoluble Fe(III) oxides (Lovley *et al.*, 1996a). It was subsequently demonstrated that microbial communities consisting predominantly of *Geothrix* spp. were not capable of oxidising [^{14}C]benzene to $^{14}CO_2$ without a considerable lag time, but in sediments containing *Geobacteriaceae*, the oxidisation of benzene was rapid, and did not require the addition of chelators or humics (Anderson *et al.*, 1998).

Toxic metals

Many Fe(III) reducing species are capable of substituting other metals as the terminal electron acceptor (Lovley & Anderson, 2000), causing the precipitation and immobilisation of metals in the subsurface. Examples include the reduction of U(VI) to U(IV) by *Geobacter metallireducens* and *Shewanella putrifaciens* (Lovley *et al.*, 1991), the reduction of Tc(VII) to Tc(IV) by the same two species (Lloyd & Macaskie, 1996), and the reduction of Cr(VI) to Cr(III) (Lovley, 1995). The sulfate-reducing bacterium *D. desulfuricans* is capable of reducing Fe(III), U(VI) (Lovley & Phillips, 1992), Cr(VI) (Mabbett *et al.*, 2002; Tucker *et al.*, 1998), Tc(VII) (Lloyd *et al.*, 1998b), Mo(VI) (Tucker *et al.*, 1998), and Pd(II) (Lloyd *et al.*, 1998a) using hydrogen as the electron donor, although without obtaining energy for growth (Lloyd *et al.*, 2001). the formation of insoluble precipitates immobilises toxic and radioactive metals in the subsurface, limiting their bioavailability and their spread. The reduced forms may also be less toxic, as in the case of chromium. Cr(VI) is 1000 times more toxic and mutagenic than Cr(III), and in the trivalent form chromium is also less mobile as it precipitates as Cr(III) minerals (Lovley, 2000). However, the reverse can also be true, and insoluble metals can be reduced to more soluble and toxic forms (Lloyd, 2003).

Different mechanisms are used by *D. desulfuricans* for the reduction of Tc(VII), Cr(VI), Se(IV), and Te(IV), and it is impossible to predict the reduction sequence from the redox potentials due to the preferential reduction of some contaminants over others. This would need to be taken into account if bioremediation of contaminated land was under consideration, and the electron donor would need to be chosen with a particular acceptor in mind (Lloyd *et al.*, 2001).

2.2.3 Recovery of metals

The use of microorganisms in mining for metals has been considered, for example whereby Fe(III) is reduced to soluble Fe(II) and leached from ores. However, biomining has been rejected as the process is too slow, making it impractical against other extraction methods (Lovley, 1991). In the processing of industrial wastes however, bioreduction may present a viable method of recovering precious metals. The recovery of Pd, Pt and Rh from both industrial wastes (Yong *et al.*, 2002a) and the

aqua regia leachates from spent automotive catalysts (Yong *et al.*, 2003) has been demonstrated, using a *D. desulfuricans* biofilm in a flow-through bioreactor. The recovered Pd(0) nanoparticles have also been successfully used as catalysts, in the liberation of hydrogen from hypophosphite (Yong *et al.*, 2002a), and the continuous reduction of Cr(VI) to Cr(III) in a flow-through reactor (Mabbett *et al.*, 2006).

2.3 Palladium

Palladium is a lustrous silvery metal, of the platinum group of metals (PGM), a group that also includes platinum and rhodium. Its symbol is Pd, atomic number 46, and its relative atomic mass is 106.5. It was first discovered by W. H. Wollaston in 1803, and is named after the then recently discovered asteroid Pallas. It resists corrosion, and has the unique property that hydrogen gas is able to filter through it. At room temperature palladium can absorb up to 900 times its own volume of hydrogen (RSC, 2008). Finely divided palladium is used as a catalyst in hydrogenation and dehydrogenation reactions. Supported palladium nanoparticles demonstrate enhanced catalytic properties (Eberhardt, 2002; Grunwaldt *et al.*, 2007; Kim *et al.*, 2004b); however, growth of the palladium nanoparticles by coalescence or ripening would render the catalyst less active, and interventions to prevent this are expensive (Creamer *et al.*, 2007b).

Some palladium is used in jewellery and dental amalgams, although the majority is used in catalysts. Demand for palladium grew to 6.84 million ounces in 2007 (Jollie, 2008), with almost two thirds of this amount (4.45 million ounces) required to replace the platinum in autocatalysts due to the rising cost of platinum. However, only 1.00 million ounces of palladium was recovered from spent autocatalysts (Jollie, 2008), as methods for reclaiming palladium are ineffective and expensive (Yong et al., 2002a).

2.3.1 Production of Pd nanoparticles

For optimal performance, palladium nanoparticles should be well-dispersed and have identical properties. The conventional synthesis of nanoparticles involve the reduction of salts precipitated onto a support or in a super-saturated solution, using high

temperatures or chemical reduction (Burton *et al.*, 2011; Liu *et al.*, 2009). Nucleation sites form throughout the nanoparticle growth stage and metal clusters also form, which leads to a broad distribution of particles size and shape, and capping agents are required to prevent aggregation (Liu *et al.*, 2009).

Flame spray pyrolysis allows the formation of supported metal catalysts in a single step, by the spraying and combusting of a liquid precursor in a flame. Particle size can be controlled by altering the experimental conditions, such as precursor concentration and feed flow rate (Mekasuwandumrong *et al.*, 2011). The flame used is a methanol/oxygen flame in a ~1:2 mixture, and the liquid precursor is dispersed by oxygen (Madler *et al.*, 2003). This leads to the synthesis of PdO crystals, which can be reduced to Pd(0) using a chemical reductant such as sodium borohydride (Ma *et al.*, 2011).

In a partially biological process for the production of palladium nanoparticles, the antioxidants in an extract from the plant *Gardenia jasminoides Ellis* have been used to reduce palladium chloride (Jia *et al.*, 2009). The nanoparticles produced were 3-5 nm in diameter, and were successfully used for the hydrogenation of *p*-nitrotoluene. The same group later used a broth made from the leaves of the tree *Cinnamomum camphora* for the same purpose, although the catalytic activity of the nanoparticles produced was not determined (Yang *et al.*, 2010).

2.4 Bioreduction of palladium

Physical and chemical techniques for the production of palladium nanoparticles require the use of specialised equipment, which carries a considerable expense. The biogenic generation of nanoparticles offers an inexpensive 'green' alternative, with a narrow range of nanoparticles formed and no additional processing required.

The bioreduction of soluble Pd(II) to insoluble Pd(0) was first performed experimentally using the sulfate-reducing bacterium (SRB) *D. desulfuricans*, with a view to the recovery of palladium from waste (Lloyd *et al.*, 1998a). *D. desulfuricans*

was chosen for its high metal reductase activity and broad specificity. Using pyruvate, formate, and hydrogen as electron donors, the bacteria were involved in catalysing the reduction of Pd(II), which formed clusters of approximately 50 nm on the cell surface (detected by electron microscopy). Energy dispersive X-ray microanalysis (EDX) showed these electron-dense areas to be composed of palladium, which was further identified as elemental palladium, or Pd(0), by X-ray diffraction (XRD). It was hypothesised that the enzyme catalysing this reaction was a hydrogenase enzyme, possibly also with cytochrome c_3 (a component of the electron transport chain), due to the use of H_2 as an electron donor under aerobic conditions as well as anaerobic, the periplasmic location of hydrogenases in SRB, and the inhibition of the reaction by Cu^{3+}. H_2 was used under both aerobic and anaerobic conditions with equal success, but in a later study using formate, the reaction proceeded only under anaerobic conditions (Yong *et al.*, 2002c). Use of *D. fructosovorans* mutants has shown that the reduction of Pd(II) by this species is mediated by the periplasmic [NiFe]-hydrogenase (Mikheenko et al., 2008). Other bacteria that have been used to produce bioPd are shown in Table 2.2 (page 35). In the case of a study using *E. coli*, the culture was grown aerobically, then switched to anaerobic conditions before palladisation of the cells (Mabbett *et al.*, 2006). A more recent study has confirmed the role of hydrogenases in formate-dependent palladium reduction by anaerobic cultures of *E. coli*, by using mutant strains (Deplanche *et al.*, 2010).

The role of the bacterial cell in the reduction of Pd(II) to Pd(0) is to provide nucleation sites where the Pd(II) sorbs onto the cell. A one-hour biosorption step is critical in SRB, during which time the metal ions bind to amine groups, on or near a hydrogenase enzyme (de Vargas et al., 2004). The cell also provides initial electrons via the enzymes, with the concurrent oxidation of H_2. The reaction then proceeds autocatalytically, with the cell acting as a scaffold for the growth of Pd(0) crystals (Creamer *et al.*, 2007b; Yong *et al.*, 2002b). In the case of Gram-negative bacteria, with which most studies have been performed, the crystals are located in the periplasm between the cytoplasmic and outer membranes, often bursting through the outer membrane (Macaskie et al., 2005) (see Figure 2.4.1). In Gram-positive bacteria the enzymes involved in the reduction of Pd(II) are unknown, although the nanoparticles formed by

B. sphaericus have been observed by electron microscopy to be located between the peptidoglycan and the S-layer (Creamer *et al.*, 2007b).

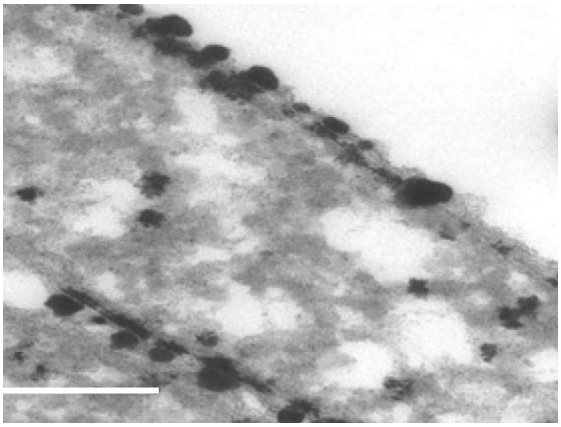

Figure 2.4.1: TEM image of Pd(0) nanoparticles located in the periplasm of *D. desulfuricans* (adapted from Macaskie et al., 2005). Scale bar = 500 nm.

The bioreduction of palladium by bacteria allows Pd(0) to be recovered directly from waste leachates (Creamer *et al.*, 2006; Mabbett *et al.*, 2006; Yong *et al.*, 2002b; Yong *et al.*, 2002c), and the resultant bioPd can be used directly as a palladium catalyst without further refining (Yong *et al.*, 2002b). An added advantage of bioPd is that the palladised cells settle out of suspension easily, whereas palladium on a carbon matrix is difficult to separate from the reaction products (Creamer *et al.*, 2007b).

2.4.1 Uses of bioPd

A number of studies have investigated the catalytic activity of bioPd and demonstrated its use in a variety of reduction reactions as shown in Table 2.2. At 3-10 nm (Redwood *et al.*, 2008a), the bionanoparticles are around half the size of those produced abiotically indicating a likely increase in activity of the palladium catalyst due to the increased surface area (Yong *et al.*, 2002b). In most cases where the bioPd was compared with an abiotically-produced palladium catalyst (finely-divided or supported on a carbon matrix), the bioPd was more active or at least as active as the commercially available alternative. When utilised for the dehalogenation of the flame retardant material and possible pollutant tris(chloroisopropyl)phosphate (TCPP), bioPd was five times more active than the commercially available Pd(0) catalyst

(Deplanche *et al.*, 2009). BioPd has also been used in reactions in methanol, in the conversion of 4-azidoaniline to 1,4-phenylenediamine (Creamer *et al.*, 2008).

Table 2.2: Microbial cell-supported Pd(0) nanocatalysts and their applications (Adapted from Deplanche *et al.*, 2011; and Schröfel & Kratošová, 2011).

Microorganism	**Catalytic application**	**References**
Gram-negative bacteria		
Bacteroides vulgatus	Dehalogenation of diatrizoate	(Hennebel *et al.*, 2011)
Citrobacter braakii	Dehalogenation of diatrizoate	(Hennebel *et al.*, 2011)
Clostridium butyricum	Dehalogenation of diatrizoate	(Hennebel *et al.*, 2011)
Cupriavidus necator	Suzuki–Miyaura and Mizoroki–Heck reactions. Evolution of H_2 from hypophosphite	(Gauthier *et al.*, 2010; Sobjerg *et al.*, 2009; 2011) (Bunge *et al.*, 2010)
Cupriavidus metallidurans	Mizoroki–Heck reaction of *n*-butylacrylate with 4-iodoanisole	(Gauthier *et al.*, 2010)
Desulfovibrio desulfuricans	Evolution of H_2 from hypophosphite. Dehalogenation reactions. Reduction of Cr(VI) to Cr(III). Fuel cell. Hydrogenation of 2-pentyne.	(Yong *et al.*, 2002a; Yong *et al.*, 2002b) (Baxter-Plant *et al.*, 2003; 2004; Harrad *et al.*, 2007; Redwood *et al.*, 2008a) (Humphries *et al.*, 2006; Mabbett *et al.*, 2004; 2006) (Orozco *et al.*, 2010; Yong *et al.*, 2007; 2010) (Bennett *et al.*, 2010)
Desulfovibrio fructosovorans	None	(Mikheenko *et al.*, 2008)
Desulfovibrio vulgaris	Dehalogenation of chlorophenol and polychlorinated biphenyls. Reduction of Cr(VI) to Cr(III).	(Baxter-Plant *et al.*, 2003; 2004) (Humphries *et al.*, 2006)
Escherichia coli	Fuel cell.	(Orozco *et al.*, 2010; Yong

	Dehalogenation of diatrizoate.	*et al.*, 2010) (Hennebel *et al.*, 2011)
Klebsiella pneumoniae	Dehalogenation of diatrizoate	(Hennebel *et al.*, 2011)
Paracoccus denitrificans	Evolution of H_2 from hypophosphite	(Bunge *et al.*, 2010)
Plectonema boryanum	None	(Lengke *et al.*, 2007)
Pseudomonas putida	Suzuki–Miyaura and Mizoroki–Heck reactions. Evolution of H_2 from hypophosphite.	(Sobjerg *et al.*, 2009) (Bunge *et al.*, 2010)
Rhodobacter capsulatus	Partial hydrogenation of 2-butyne-1,4-diol to 2-butene-1,4-diol.	(Wood *et al.*, 2010)
Rhodobacter sphaeroides	Dehalogenation of polychlorinated biphenyls and pentachlorophenol.	(Redwood *et al.*, 2008a)
Serratia sp.	Reduction of Cr(VI) to Cr(III).	(Beauregard *et al.*, 2010)
Shewanella oneidensis	Dehalogenation reactions. Fuel cell.	(De Windt *et al.*, 2005; 2006; Hennebel *et al.*, 2011; Mertens *et al.*, 2007) (Ogi *et al.*, 2011)
Gram-positive bacteria		
Arthrobacter oxydans	Partial hydrogenation of 2-butyne-1,4-diol to 2-butene-1,4-diol.	(Wood *et al.*, 2010)
Bacillus sphaericus	Hydrogenation of itaconic acid.	(Creamer *et al.*, 2007a)
Enterococcus faecium	Dehalogenation of diatrizoate in a membrane bioreactor.	(Hennebel *et al.*, 2011)
Clostridium pasteurianum	Reduction of Cr(VI) to Cr(III).	(Chidambaram *et al.*, 2010)
Staphylococcus sciuri	Suzuki–Miyaura cross coupling reaction and hydrogenation reactions.	(Sobjerg *et al.*, 2011)

2.5 Hydrogenases and formate dehydrogenases in *Escherichia coli*

Formate and molecular hydrogen are both important energy sources for anaerobic bacteria. Formate is a highly reducing, high-energy compound, produced in anaerobically growing *E. coli* by the cleavage of pyruvate, catalysed by pyruvate formate lyase (PFL) (Sawers, 2005). At neutral pH, formate is excreted from the cell into the periplasm, the area between the cytoplasmic and outer membranes in Gram-negative bacteria where the peptidoglycan cell wall is situated. Here, the formate is made available to formate dehydrogenases (Sawers, 1994).

E. coli synthesises three formate dehydrogenase isoenzymes and four hydrogenase isoenzymes, all of which are membrane-bound (see Figure 2.5.1). The three formate dehydrogenases (FDH) consist of α, β, and γ subunits (Abaibou *et al.*, 1995; Sawers, 1994), and catalyse the oxidation of formate. All three FDH are dependent on molybdenum cofactors, derived from molybdopterin complexed with molybdenum and selenium (Sawers, 1994). They have more specific designations based on the growth conditions which lead to their optimal expression, i.e. FDH-O (also known as formate oxidase) is synthesised aerobically or anaerobically in the presence of nitrate (Sawers *et al.*, 1991), FDH-N is synthesised during anaerobic growth in the presence of nitrate, and the synthesis of FDH-H is optimal when *E. coli* grows fermentatively (Sawers, 1994). FDH-O is always present in the cell in small amounts and is very active (Sawers, 1994). A possible role for FDH-O is to allow bacteria to adapt rapidly to a sudden shift from aerobic respiration to anaerobiosis, before FDH-N has been produced in sufficient amounts to continue formate metabolism (Abaibou *et al.*, 1995).

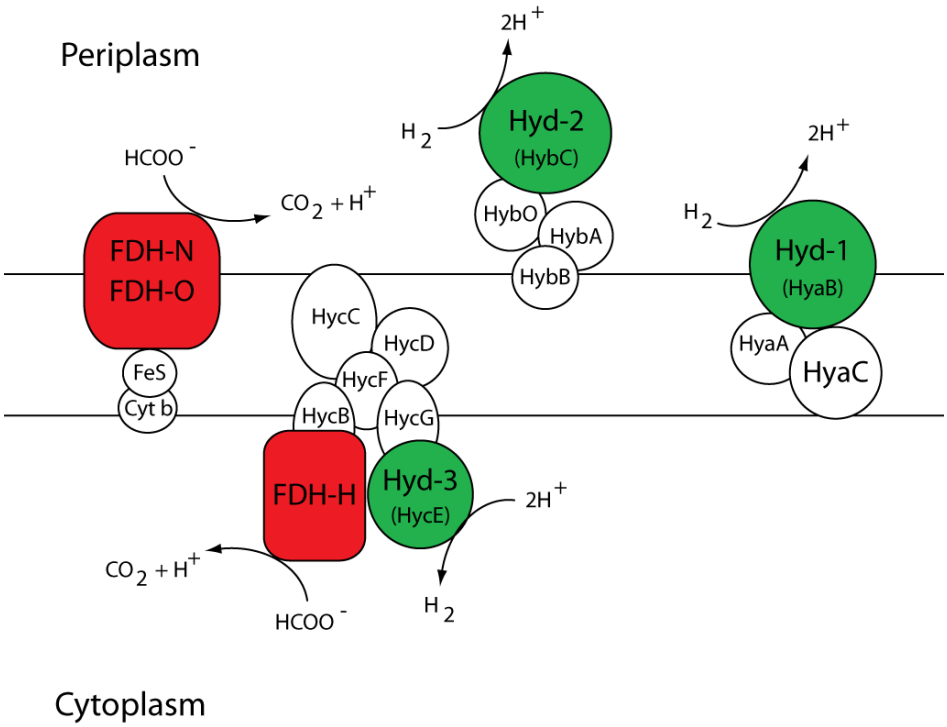

Figure 2.5.1: Locations and orientations of the formate dehydrogenases and hydrogenases 1-3 within the cytoplasmic membrane. Adapted from Sawers (1994), and Forzi & Sawers (2007).

The four hydrogenase enzymes are [NiFe]-hydrogenases, as they have both a nickel and an iron atom at their active site, and they are named in the order of their discovery. Hyd-1 and Hyd-2 are uptake hydrogenases, and catalyse the reversible oxidation of H_2 linked to the reduction of electron acceptors such as nitrate or fumarate (during anaerobic growth), or oxygen (during aerobic growth). Hyd-1 and Hyd-2 consist of αβ heterodimers, with the large α-subunit containing the bimetallic active site (Vignais, 2008). They are linked to the quinone pool of the respiratory chain by cytochrome *b*, which anchors the dimeric proteins to the cytoplasmic membrane (Vignais & Billoud, 2007). Hyd-1 is the most abundant hydrogenase in *E. coli*, and its role may be to recycle H_2 produced under fermentative conditions by the FHL complex (Sawers *et al.*, 1985). Hyd-2 is synthesised at high levels when cells are grown with glycerol and fumarate or H_2 and fumarate (Forzi & Sawers, 2007). Expressed only under strictly anaerobic conditions (Vignais et al., 2001), the multimeric Hyd-3 forms part of the formate hydrogenlyase (FHL) complex, which also includes two electron

carriers and FDH-H, and is involved in the evolution of H_2 and CO_2 from the metabolism of formate (Sawers, 1994). Hyd-3 has already been shown to catalyse the reduction of Tc(VII), using formate or H_2 as electron donors (Lloyd et al., 1997). One group has reported that H_2 uptake decreases with FHL- or Hyd-3-deficient mutants (Maeda et al., 2007), although another group has reported that there is no significant uptake activity with Hyd-2-deficient mutants (Redwood et al., 2008b). There is also a putative hydrogenase-4, although little is known about this enzyme as yet (Vignais & Billoud, 2007). It is possible that Hyd-4 is part of a second FHL complex, which is active at higher pH than FHL complex I (Mnatsakanyan et al., 2002).

All the isoenzymes have abundant iron-sulfur clusters, which are involved in the transfer of electrons between the enzyme and the donors or acceptors (Vignais, 2008). There are also numerous ancillary proteins involved in the maturation and assembly of these enzymes, about the majority of which little is known (Sawers, 1994).

The genes responsible for the encoding of the isoenzymes are shown in Table 2.3 below.

Table 2.3: Operons encoding the formate dehydrogenase and hydrogenase isoenzymes.

Isoenzyme	**Operon**	**Reference**
FDH-O	*fdo*	(Plunkett *et al.*, 1993)
FDH-N	*fdn*	(Berg *et al.*, 1991)
FDH-H	*fdhF* gene	(Zinoni *et al.*, 1986)
Hyd-1	*hya*	(Menon *et al.*, 1990)
Hyd-2	*hyb*	(Menon *et al.*, 1994)
Hyd-3	*hyc*	(Bohm *et al.*, 1990)
Hyd-4	*hyf*	(Andrews *et al.*, 1997)

2.6 Biocatalysis

Biocatalysis is the use of enzymes , or whole cells containing enzymes, for the chemical modification of organic compounds. Enzymes are used in the manufacture of foods, detergents, textiles, diagnostic assays (Demain & Adrio, 2008; Kirk *et al.*, 2002), and in the production of agrochemicals, pharmaceuticals, and fine chemicals (Panke *et al.*, 2004; Straathof *et al.*, 2002). There are a number of advantages to using enzymes in organic synthesis, as the mild conditions under which enzymes are active (typically ambient temperatures, atmospheric pressure, ca. pH 7.0) are easy to achieve; they are naturally produced and so are compatible with requirements for 'green' technology; reactions performed by enzymes may otherwise be difficult or impossible to achieve chemically; and they usually exhibit high selectivity. Attributes of particular interest are chemoselectivity (a preferential reaction with one functional group over others), regioselectivity (one direction or site of bond making or breaking occurs preferentially, forming an excess of one structural isomer), and stereoselectivity (preferential formation of one stereoisomer over another). The production of optically pure compounds by means of enantioselective enzymes is of particular interest, as this is difficult to achieve by chemical means. These compounds are often used as building blocks, and are combined with other molecules to obtain the final product (Turner, 2009).

Microbial cells are usually used in the production of biocatalysts as they are easier to cultivate than animal or plant cells, grow more quickly and are less nutritionally demanding. Biocatalysts may be used as whole cells, or as purified enzymes. With purified enzymes there is no interference from other enzymes that are present in the cell, and the enzymes may also be more tolerant to solvents and the formation of toxic products. However, the purification of enzymes is an expensive process during which the target enzyme may be exposed to cellular proteases, the yield is typically low, enzyme co-factors must be added to the reaction mix or recycled, and the long-term stability of the enzyme is reduced; also, the conformation of the enzyme may change once outside the cell, rendering it inactive (Ishige *et al.*, 2005; Roberts *et al.*, 1995).

Enzymes are classified according to the Enzyme Commission (EC) classification system, which divides enzymes into one of six classes. The choice of enzymes for biotransformations is vast, although some classes of enzyme have proved more useful than others.

EC 1 Oxidoreductases

Oxidoreductases catalyse oxidation and reduction reactions, such as the interconversions of ketones and alcohols, the reduction of double bonds, and the oxidation of amines to imines. Examples include alcohol dehydrogenase, lactate dehydrogenase, and amine oxidases. As oxidoreductases are usually dependent on a co-factor, this must be supplied in excess or recycled during the biotransformation, which can be expensive.

EC 2 Transferases

The transfer of groups between molecules is catalysed by transferases, such as transaminases (transfer of amino groups), kinases (transfer of phosphate groups), and glucosyl transferases (transfer of sugars). The transfer of sugars can be problematic, as the donors for these groups are nucleotides, which are expensive. An enantioselective transaminase has also been used in the manufacture of sitagliptin, an antidiabetic drug, to catalyse the amination of the prositagliptin ketone to form sitagliptin phosphate (Mutti *et al.*, 2011; Savile *et al.*, 2010).

The generation of 2-amino-1,3-diols, which are a component of the broad-spectrum antimicrobial compound chloramphenicol, may be achieved by the transfer of an amino group from an donor molecule to α,α'-dihydroxy ketone, as demonstrated in Figure 2.6.1 (Hailes *et al.*, 2010).

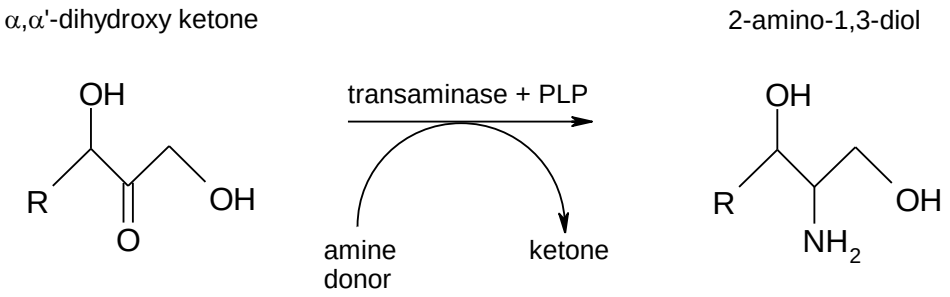

Figure 2.6.1: Transfer of an amino group from a donor molecule to α,α'-dihydroxy ketone via the enzyme co-factor pyridoxal 5'-phosphate (PLP), producing 2-amino-1,3-diol.

EC 3 Hydrolases

A hydrolysis reaction is one in which bonds are cleaved with the addition of water. Examples of hydrolases include lipases, esterases, proteinases, phosphatases, and glycosidases. Lipases and proteinases are the two most commonly used hydrolases in biotransformations (Grogan, 2009). A benefit of using lipase is that it is possible to catalyse the reverse reaction, e.g. transesterfication using *Candida antarctica* lipase B. Figure 1.7.4 shows an example of such a lipase-catalysed biotransformation. Hydrolysis of racemic *N*-acetylbenzylamine to generate (*S*)-1-methylbenzylamine has been performed using whole-cell preparations of the microorganisms *Nocardia erythropofis* and *Cellulomonas fimi* (Ogawa *et al.*, 1994).

EC 4 Lyases

Lyases catalyse the addition of water or ammonia across a double bond. Examples include aldolases, aspartase, and fumarase. Phenylalanine ammonia lyase is used in the synthesis of chiral amines (Gloge *et al.*, 2000).

EC 5 Isomerases

Isomerases and racemases catalyse isomerisation reactions. Alanine racemase, produced by *Salmonella typhimurium*, has been used in a multi-step process for the production of D-amino acids (Fotheringham, 2000). During this process, alanine racemase catalyses the conversion of L-alanine to D-alanine, which is then used as the

amino donor in the transaminase-catalysed conversion of an α-keto acid to a D-amino acid (see Figure 2.6.2).

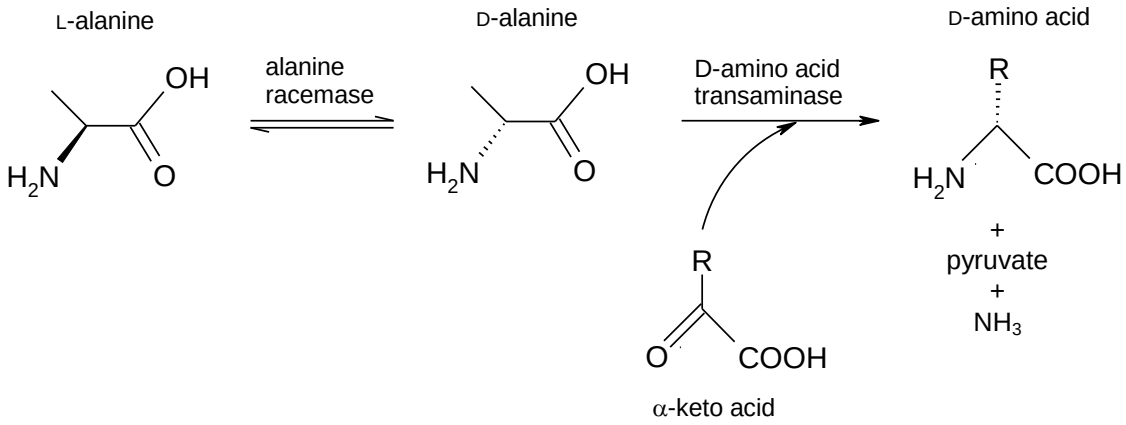

Figure 2.6.2: The multi-step production of D-amino acids.

EC 6 Ligases

Ligases catalyse the formation of bonds between molecules, and whilst they are very useful in molecular biology, they are of limited use in biotransformations.

2.7 Synthesis of optically pure compounds

2.7.1 Chirality

When stereoisomers are chiral molecules, i.e. non-superimposable mirror images of each other, they are also known as enantiomers. Enantiomers may be distinguished from one another by their ability to rotate plane-polarised light – light is rotated in opposite directions by each enantiomer. A racemic mixture therefore shows a net rotation of zero. A compound composed of only one enantiomer is optically pure.

Enantiomers are classified as *R* or *S* according to the Cahn, Ingold and Prelog (CIP) system (1966). Using this system, groups around the chiral centre of a molecule are numbered in order of priority, as determined by the atomic number of the immediate substituent atoms followed by the adjacent atoms, e.g. H < C < N < O and CH_3 < C_2H_5 < CH_3O. The lowest priority group is then put to the back, and a curve drawn through

the groups from the highest downwards. If the curve goes in a clockwise direction, the enantiomer is designated *R*, after the Latin *rectus*, meaning right. If the curve goes to the left, the enantiomer is designated *S*, after the Latin *sinister*, meaning left (see Figure 2.7.1).

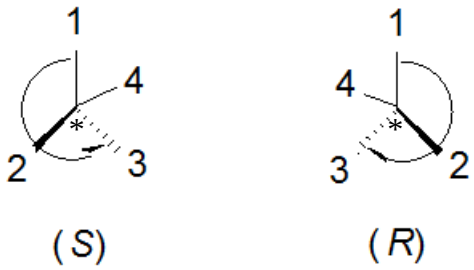

Figure 2.7.1: Classification of chiral molecules by assigning priority to groups around the chiral centre (chiral centre identified by *).

Enantiomerically pure compounds are of importance in the pharmaceutical industry when only one enantiomer is biologically active. The other enantiomer may be either inactive, or may have adverse side-effects. If an enantiomerically pure compound is obtained, the dosage may be halved which would decrease costs and the risk of adverse reactions. Chiral pharmaceuticals manufactured using enantioselective enzymes include anti-anxiety drugs, antiviral and antiretroviral agents, anti-hypertensive drugs, cholesterol-lowering drugs, anti-cancer agents, anti-Alzheimer's drugs, and drugs for the treatment of diabetes (Patel, 2001; 2006; 2008). The anti-Alzheimer's drug rivastigmine is more active in its (*S*) form, intermediates for which can be manufactured by lipase-catalysed reactions (Mangas-Sanchez *et al.*, 2009). The anti-hypertensive drug Omapatrilat has four chiral centres, and can be manufactured using multi-enzyme systems that include enzymes for both chiral resolution and co-factor recycling (Panke & Wubbolts, 2005).

The first methods to be developed for the resolution of racemates were capable of effectively separating the enantiomers, but if only one enantiomer is required the productivity is low as the maximum yield is 50% (Faber, 2001). The goal therefore is the production of an optically pure compound via a method which uses all of the starting material, giving a theoretical yield of 100%.

2.7.1.1 Stereoselective synthesis

Traditionally known as asymmetric synthesis, this describes any process in which an element of chirality is introduced to a molecule, and the two enantiomers are generated in unequal amounts. Kinetic resolution and dynamic kinetic resolution are both examples of stereoselective processes.

2.7.1.2 Kinetic resolution

Kinetic resolution describes a process in which one enantiomer in a racemic mixture has a higher reaction rate than that of the other with a particular enzyme (Figure 2.7.2). This produces an excess of one enantiomer which reaches a maximum, then decreases until the reaction reaches completion. The maximum yield from kinetic resolution techniques is 50%.

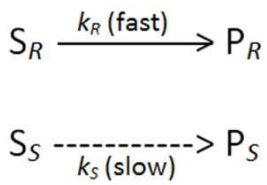

Figure 2.7.2: Kinetic resolution of a racemate. S_R and S_S: substrate enantiomers; P_R and P_S: product enantiomers; k_R and k_S: rate constants.

2.7.1.3 Dynamic kinetic resolution

The problem of the maximum yield of 50% with kinetic resolution is solved by using dynamic kinetic resolution (DKR). In addition to a kinetic resolution step, the enantiomers are equilibrated simultaneously via a racemisation step, as shown in Figure 2.7.3.

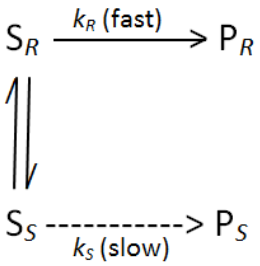

Figure 2.7.3: Dynamic kinetic resolution of a racemate. S_R and S_S: substrate enantiomers; P_R and P_S: product enantiomers; k_R and k_S: rate constants.

In order for DKR to be successful, a number of criteria should be fulfilled. The resolution step should be irreversible, and product should not be involved in the racemisation step. The selectivity of the resolution step should be high, and the rate constant for the racemisation step should be higher than that of the resolution step (Pellissier, 2011). DKR techniques that have been particularly successful have combined a chemocatalytic racemisation step with a biocatalytic enantioselective transformation (Faber, 2001; Pàmies & Bäckvall, 2003). Kim et al (2004a) have developed techniques using a pair of complimentary enzyme-metal combinations for the DKR of racemic secondary alcohols. (*R*)-selective DKR is performed using a lipase-Ru complex combination, and (*S*)-selective DKR is performed using a subtilisin-Ru combination.

2.7.1.4 Enantioconvergent reactions

During enantioconvergent reactions, both enantiomers of a racemate are converted via kinetic resolution to a single enantiomer of product (Figure 2.7.4). The two pathways taken by each enantiomer are completely independent, and show opposing enantiopreference, with both pathways proceeding via separate enantioselective steps. The k_{SR} pathway must also proceed with a stereoinversion step.

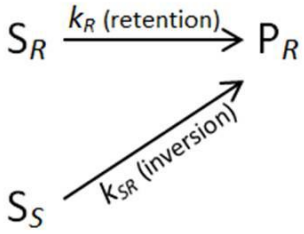

Figure 2.7.4: Enantioconvergent deracemisation. S_R and S_S: substrate enantiomers; P_R: product; k_R and k_{SR}: rate constants.

In practice, enantioconvergent deracemisations are difficult to achieve (Faber, 2001), although a process has been described for the successful resolution of racemic *sec*-alkyl sulfate esters using an alkylsulfatase from *Rhodococcus ruber* (Pogorevc *et al.*, 2002).

2.7.1.5 Cyclic deracemisation

Deracemisation is the interconversion of enantiomers via a stereoinversion process, for example cyclic oxidation and reduction reactions (Turner, 2003). In cyclic deracemisation, an initial enantioselective oxidation step converts one enantiomer to an achiral intermediate, followed by a non-selective reduction step which regenerates both enantiomers of the substrate (see Figure 2.7.5).

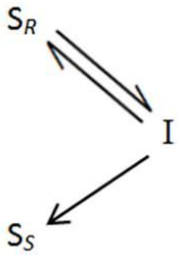

Figure 2.7.5: Cyclic deracemisation of a racemate. An enantioselective oxidation step is followed by a non-selective reduction step. S_R and S_S: substrate enantiomers; I: achiral intermediate.

Oikawa *et al* (2001) successfully used cyclic deracemisation for the generation of pure D-lactate, using an L-selective lactate oxidase from *Aerococcus viridans*, and sodium

borohydride for the non-selective reduction step (see Figure 2.7.6). Shortly afterwards, cyclic deracemisation of the primary amine α-methylbenzylamine was performed using an (*S*)-selective monoamine oxidase from *Aspergillus niger*, and ammonia-borane as the non-selective reductant (Alexeeva *et al.*, 2002).

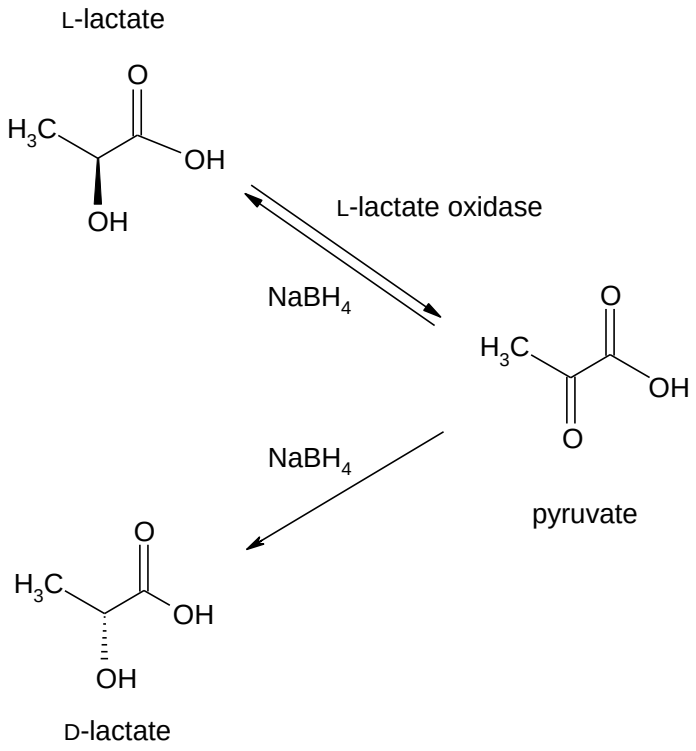

Figure 2.7.6: Cyclic deracemisation of a DL-lactate. An L-selective oxidation step is followed by a non-selective reduction step.

2.8 Amines

Amines are an important class of molecules, and are widely used in their enantiomerically pure forms in pharmaceutical preparations. Amines are derivatives of ammonia, NH_3, and are further classified according to the number of hydrogens that have been replaced by alkyl or aryl groups. Primary amines have one hydrogen replaced, secondary amines have two hydrogens replaced, and tertiary amines have all three hydrogens replaced.

Some examples of amines are shown in Figure 2.8.1.

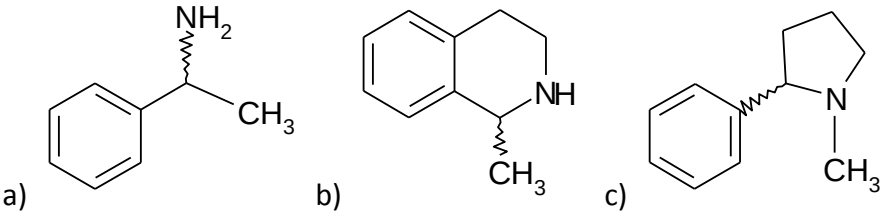

Figure 2.8.1: a) α-methylbenzylamine, a primary amine; b) (*S*)-1-methyltetrahydro-isoquinoline, a secondary amine; c) (*S*)-*N*-methyl-2-phenylpyrrolidine, a tertiary amine.

2.8.1 Enzymes used in the generation of optically pure amines

2.8.1.1 Transaminases

Transaminases, also known as aminotransferases, catalyse the biotransformation of amines by transferring an amino group from a donor molecule to a ketone, and have attracted attention as biocatalysts for either direct asymmetric synthesis from prochiral ketones or by kinetic resolution of racemic amines. The α-transaminases usually transfer amino groups from biologically-produced α-amino acids to α-keto acids, whereas ω-transaminases are usually unable to aminate α-keto acids, but are able to aminate aldehydes or ketones. Hailes *et al* (2010) investigated a ω-transaminase from *Chromobacterium violaceum* which is able to convert a range of aldehydes and ketones, and successfully used it in the conversion of ketodiols to 2-amino-1,3-diols (Hailes *et al.*, 2010; Kaulmann *et al.*, 2007; Smith *et al.*, 2010; Smithies *et al.*, 2009). The enzyme was also found to be particularly useful in that it could accept either the (*R*)- or (*S*)-1,3-dihydroxy ketone, but generated the (2*S*)-amine product in >99% *ee* (Smithies *et al.*, 2009).

Koszelewski *et al.* (2008) tested various commercially available ω-transaminases with ketones as the starting materials for the generation of enantiomerically pure amines. Alanine was used as the amino donor, which was converted to pyruvate, and presented the problem that the equilibrium lay on the side of the starting material. Lactate dehydrogenase was used to reduce pyruvate to lactate, shifting the equilibrium to the product. The group was successful in creating both amine enantiomers in pure form, depending on which ω-transaminase was used. The same

enzymes were later used with a variety of racemic amines as the starting material, in a two-step reaction. Firstly, one ω-transaminase was used in the kinetic resolution of one enantiomer to a ketone; and secondly, a ω-transaminase with the opposite stereopreference was used to convert the ketone to the remaining amine enantiomer (Koszelewski *et al.*, 2009). The enantiomer produced depended on the order in which the two ω-transaminases were used. Recombinant transaminases from the soil bacterium *Bacillus megaterium* have also been used for the deracemisation of amines (Hanson *et al.*, 2008; Koszelewski *et al.*, 2010).

2.8.1.2 Lipases

The most commonly used enzyme in DKR processes for the generation of chiral amines is *C. antarctica* lipase B immobilised in an acrylic resin (Parvulescu *et al.*, 2010), usually with a metal racemisation catalyst, such as ruthenium, iridium, or palladium (Thalén *et al.*, 2009). Selective acylation in a BASF patented process produces an (*S*)-enantiomer and an (*R*)-amide, which can be separated by distillation. The (*R*)-enantiomer is then released through basic hydrolysis of the amide (Breuer *et al.*, 2004). A DKR technique using an (*R*)-selective lipase and palladium nanoparticles for the resolution of primary amines is shown in Figure 2.8.2, which improved on the reaction time and yield of earlier techniques (Kim *et al.*, 2007; 2011).

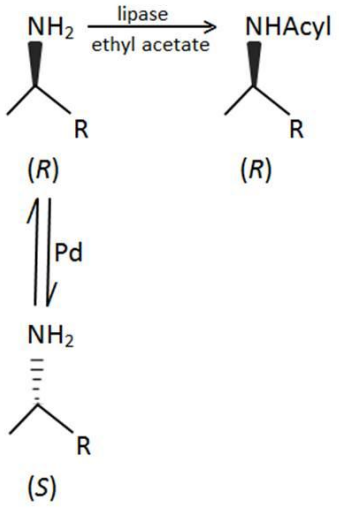

Figure 2.8.2: Dynamic kinetic resolution of primary amines, using an (*R*)-selective lipase and palladium nanoparticles (Kim *et al.*, 2007).

2.8.1.3 Lyases

Phenylalanine ammonia lyase is synthesised by plants to catalyse the reversible conversion of L-phenylalanine to *trans*-cinnamic acid, a precursor of lignin, flavonoids and coumarins (Ward & Wohlgemuth, 2010). Phenylalanine ammonia lyase can also be used in the synthesis of L-phenylalanine derivatives, by supplying high concentrations of ammonia in order that the reverse reaction is catalysed (Gloge *et al.*, 2000).

2.9 Amine oxidases

2.9.1 Classification of amine oxidases

Amine oxidases are oxidoreductases, enzyme class EC 1, which catalyse reactions via the transfer of electrons. Most amine oxidases are in the subclass EC 1.4.3.X, which is comprised of enzymes that act on the CH-NH_2 group of donors (EC 1.4), and use oxygen as the electron acceptor (EC 1.4.3). Some others are in the subclass EC 1.5.3.X, which act on the CH-NH group of donors (EC 1.5), and also use oxygen as the electron acceptor (EC 1.5.3). As oxygen is reduced, the process of oxidative deamination also produces hydrogen peroxide (see Figure 2.9.1). There are four main types of amine oxidase:

1. monoamine oxidases (MAO), EC 1.4.3.4. MAO oxidise primary amines, and also some secondary and tertiary amines. These enzymes are flavoproteins.
2. polyamine oxidases (PAO), EC 1.5.3.13-17. PAO oxidise secondary and tertiary amines, and are also flavoproteins.
3. primary amine oxidases (PrAO), EC 1.4.3.21. PrAO oxidise primary amines only, and contain copper.
4. diamine oxidases, EC 1.4.3.22. These enzymes oxidise diamines, such as histamine, as well as some primary amines. They contain copper, and along with PrAO were previously known as semicarbazide-sensitive oxidases (EC 1.4.3.6, now deleted).

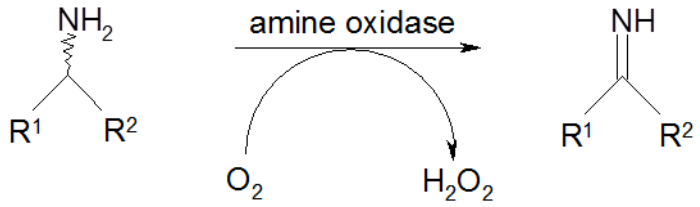

Figure 2.9.1: Oxidative deamination catalysed by amine oxidase. The amine is converted to an imine with the reduction of oxygen, and hydrogen peroxide is produced.

The copper-containing amine oxidases catalyse the deamination of biogenic amines, and have diverse biological roles. They are responsible for nutrient metabolism in prokaryotes, and cell signalling and adhesion in eukaryotes (Kurtis *et al.*, 2011). Polyamines are important in the metabolism of prokaryotes and plants; and monoamine oxidases enable the assimilation of nitrogen as ammonia in fungi (Schilling & Lerch, 1995a), and the regulation of neurotransmitters and deamination of dietary amines in higher eukaryotes (Edmondson *et al.*, 2004).

2.9.2 Monoamine oxidases

The monoamine oxidases of mammals exist in two isoforms, MAO-A and MAO-B, with different but overlapping functions. The two forms are distinguished by differences in substrate specificity, sensitivity to inhibitors, and hormone regulation (Shih *et al.*, 2011; Tipton *et al.*, 2004). The proteins share 70% sequence identity and are encoded by two distinct genes, although identical intron/exons structures indicate a probable origin for both of ancestral gene duplication (Shih *et al.*, 2011). Both isoforms of the enzyme are located in the outer mitochondrial membrane, and contain a covalently-bound flavin adenine dinucleotide (FAD) molecule. FAD is a redox cofactor, which accepts two electrons to become reduced to $FADH_2$. The cofactor consists of riboflavin (vitamin B2) linked to adenosine diphosphate, and is itself linked by the riboflavin moiety to a cysteine residue in the active site of the enzyme (Schilling & Lerch, 1995a).

MAO-B was the first of the two isoenzymes to have its 3-dimensional structure studied, using *Pichia pastoris* as the expression system (Edmondson *et al.*, 2004). The

enzyme is a heterodimer, and each subunit has a molecular mass of 58.8 kDa (Schilling & Lerch, 1995a) and is 520 amino acids long. The subunits each consist of three domains – the membrane-binding domain, the flavin-binding domain, and the substrate-binding domain. The membrane-binding domain is an α-helix made up of 27 residues at the carboxyl terminus of the protein, with an apolar surface to aid membrane insertion. The substrate-binding domain consists of two cavities, an entrance cavity and the active site, entry to which is controlled by a flexible protein loop at the membrane surface. The two cavities connect the opening to the flavin, and may be separate or fused, depending on the conformation of the residue Ile99 which connects the two (Edmondson *et al.*, 2004).

MAO-A was studied the following year and found to be a monomer (De Colibus *et al.*, 2005), with a molecular mass of 59.7 kDa (Schilling & Lerch, 1995a). The enzyme has only one cavity for the active site.

Pathologies linked to MAO in humans include neurological and psychological illnesses, such as anxiety disorders and depression (Riederer *et al.*, 2004). In Alzheimer's disease, levels of prefrontal cortex MAO-B increase by 16%, and prefrontal cortex MAO-A decreases by 17%. These changes occur early in the disease onset, and persist at similar levels throughout its course (Kennedy *et al.*, 2003). A connection has also been made with Parkinson's disease (Youdim & Bakhle, 2006), as MAO inhibitors for the treatment of depressive illness have been found to alleviate the symptoms.

2.9.3 MAO-N

MAO-N is a soluble, tetrameric flavoprotein, each subunit of which has a molecular mass of 55 kDa. FAD is non-covalently bound, and the enzyme itself is not membrane-bound, but located in peroxisomes. Prior to the discovery of the expression of MAO-N by *A. niger* in 1995, the only amine oxidases found in non-vertebrates had been diamine oxidases and polyamine oxidases (Schilling & Lerch, 1995a).

MAO-N is active towards substrates of both MAO-A and MAO-B, and is sensitive to the same inhibitory compounds. It is likely therefore that there are structural similarities

between the proteins. Differences include the FAD cofactor attachment, which is covalently bound in MAO-A and MAO-B, and the location within the cell. However, it is probable that MAO-N is an evolutionary precursor of MAO-A and MAO-B, due to the similarities in sequence and subunit size, which is 59.7 kDa and 58.8 kDa in MAO-A and MAO-B respectively (Schilling & Lerch, 1995a; 1995b).

2.10 The laboratory evolution of enzymes

As biocatalysis has proved useful in many fields, new enzymes are continually being sought that can replace traditional methods of synthesis. New enzymes are initially identified due to some activity towards the substrate of interest, and can be either constructed or homologous genes might be found (Turner, 2009). However, it is likely that there will be a need to enhance one or more of the properties of the enzyme, such as the catalytic activity, substrate specificity, stability (tolerances to organic solvents, temperature, and pH), or selectivity (e.g. enantioselectivity for the synthesis of chiral molecules). Methods used to improve the properties of enzymes are described below, and can be generally assigned to one of the two broad categories of directed evolution and rational design.

2.10.1 Directed evolution

Directed evolution is the process by which an enzyme undergoes repeated cycles of mutagenesis, forming potentially vast libraries from which variants displaying enhanced properties are selected for further work. The advantage of directed evolution as a method for improving enzymes for specific applications is that no prior knowledge of enzyme structure is required, as selection is purely on the basis of enhanced properties. Directed evolution can be applied to a wide range of enzymes, usually with a high success rate.

The first step in directed evolution is to create a library of genetic variants, for which a number of techniques exist. These methods are based either upon the random mutagenesis of DNA, or the recombination of genes. Of the former, the error-prone polymerase chain reaction (epPCR) is commonly employed due to its ease of use. This

method was first used for the evolution of enzymes in 1997, when Reetz and colleagues used epPCR for the random mutagenesis of *Pseudomonas aeruginosa* PAO1 lipase (Reetz *et al.*, 1997). The wild-type enzyme was only very slightly enantioselective for the (*S*)-enantiomer of product in the hydrolysis of racemic *p*-nitrophenyl 2-methyldecanoate, with an *ee* of 2%. The group altered the conditions of the PCR reaction, for example the Mg^{2+} ion concentration, in order to introduce 1-2 errors per lipase gene. Within only four generations, the enantioselectivity had risen from 2% *ee* to 81% *ee*, using epPCR only. A later group used epPCR to improve the specific activity of an *Arthrobacter citreus* aminotransferase, as well as the thermostability of the enzyme, by introducing 17 alterations in amino acid sequence over five generations (Martin *et al.*, 2007). Mutations may also be introduced using the *E. coli* XL1-Red mutator strain for gene cloning. Three independent DNA repair pathways have been inactivated in this strain by the mutations *mutS*, which causes error-prone mismatch repair (Radman *et al.*, 1980); *mutD*, whereby DNA polymerase III lacks the subunit responsible for 3´-5´ exonuclease activity (Scheuermann *et al.*, 1983); and *mutT*, causing an inability to hydrolyse 8-oxo-dGTP (Cox, 1976). The lack of these three repair pathways gives a spontaneous mutation rate of around 5000-fold greater than the wild-type parent (Greener *et al.*, 1997). Another method to induce mutations has been recently developed, known as phage-assisted continuous evolution (PACE), by which genes inserted into the M13 bacteriophage are mutated when incorporated into the host bacterial cell (Esvelt *et al.*, 2011). Potentially rapid and low cost, this method could be applied to enzymes involved in DNA and RNA binding, protein binding, and bond-forming catalysis.

The two most common gene recombination methods are DNA shuffling (Stemmer, 1994), and the staggered extension process (StEP) (Nair *et al.*, 2010; Zhao *et al.*, 1998). In DNA shuffling, copies of the gene of choice are randomly fragmented and then reassembled using a PCR-like process, leading to the incorporation of point mutations in the recombinant genes. The point mutation rate by DNA shuffling is around 0.7%, similar to epPCR. The technique was first demonstrated for the evolution of enzymes by inducing cefotaxime resistance in *E. coli*, achieved by introducing six mutations over two cycles of recombination (Stemmer, 1994). StEP is a process similar to PCR,

but with a very short annealing/extension step, leading to shortened complementary strand fragments. With each cycle, the fragments anneal to a different template and are further extended. The end result is full-length fragments that consist of sequences from numerous different parent templates. When first developed, StEP was used to generate thermostable subtilisin E variants from heat-labile wild-type enzymes. An initial cycle of epPCR identified five variants with enhanced thermostability, which when recombined using StEP lead to the discovery of three mutants with a half-life at 65°C of 25-50 times that of the wild-type (Zhao *et al.*, 1998). In theory, gene recombination methods should be more successful at selecting for advantageous mutations, as wild-type genes are used as templates and natural selection has already removed any mutations that are deleterious (Tobin *et al.*, 2000).

Following random mutagenesis, semi-rational processes may be employed whereby large numbers of mutations in one area are induced by saturation mutagenesis. Site-directed mutagenesis can then be used to optimise individual amino acid residues, for example in the active site, although this does require some knowledge of the structure of the enzyme. The first coordination sphere of the active site, which is in contact with the substrate, is made up of around 10-15 amino acid residues; the second coordination sphere has around 20-30 residues (Turner, 2009). Focussing on these residues can help to further improve the properties of an enzyme that has already been selected via screening for favourable characteristics (Park *et al.*, 2005). A technique known as iterative CASTing (combinatorial active site saturation testing) can help to minimise screening by selecting 2-3 amino acid residues in the active site, and randomising to form small libraries of mutants (Reetz *et al.*, 2006). However, it is possible that by focussing on the active site instead of using further cycles of random mutagenesis, opportunities may be lost for greatly enhancing the required characteristics. Structurally and functionally important amino acid clusters (mutational 'hot spots') have been identified that exert their influence over a considerable distance, which would be difficult to predict using site-specific techniques (Spiller *et al.*, 1999). Others have found similar effects, although it appears that targeting the active site may often be the most successful strategy (Morley & Kazlauskas, 2005).

Screening methods

On possible disadvantage of directed evolution is the requirement for a high throughput screening process following random mutagenesis in order to identify variants with enhanced properties. As there are potentially a large numbers of variants, a rapid and simple method is preferred, for example the use of a pH indicator as a measure of the extent and rate of reaction (Turner, 2009). Approaches include fluorogenic and chromogenic assays (Wahler & Reymond, 2001), genetic selection methods (Reetz *et al.*, 2008), and agar-based selective methods (Leemhuis *et al.*, 2009).

2.10.2 Rational design

In contrast to the random nature of mutations by directed evolution, rational design is the insertion of specific mutations at designated sites with the intentional of altering function in a predetermined manner. As such, knowledge of the structure and mechanisms of the protein in question is required. If the primary sequence of a protein is not precisely known, homology modelling may be used (Cho *et al.*, 2008), or techniques such as iterative saturation mutagenesis (Reetz & Carballeira, 2007), whereby repeated cycles of random mutagenesis are targeted at a specific area.

Lipases are a common target for rational design, as they are popular enzymes for use in biocatalysis. By comparing *C. antarctica* lipase B with two other hydrolases for catalysing the transacylation of acrylates, Syrén *et al* (2010) were able to engineer a mutant with three times the activity of the wild-type enzyme. In another study, the redesign of the stereoselectivity pocket of *C. antarctica* lipase B created a general esterification catalyst, which had previously been hampered by the slow conversion of the (*S*)-enantiomer of the secondary alcohol substrate (Liu *et al.*, 2010).

Rational design of enzymes is commonly used in conjunction with computational design, whereby mutations are modelled *in silico* before being confirmed experimentally. Röthlisberger *et al* (2008) created eight novel kemp elimination catalysts using computer modelling, using random mutagenesis to increase catalytic

efficiency 200-fold. Later improvements to correct features missing from these enzymes increased catalytic efficiency 400-fold (Khersonsky *et al.*, 2011).

The most common reasons for using directed evolution and rational design are to increase the promiscuity of the biocatalyst, to improve enantioselectivity, or to increase its specificity towards minor substrates. A biocatalyst may acquire the ability to catalyse alternative reactions by neutral drift, whilst maintaining its original function. Combined rational design and directed evolution approaches have been employed to first redesign sections of a protein scaffold, then activity is fine-tuned using random mutagenesis and screening. Such approaches have generated enzymes that have switched catalytic function from glyoxalase II to β-lactamase activity (Park *et al.*, 2006), and from esterase to epoxide hydrolase activity (Jochens *et al.*, 2009).

Increased enantioselectivity is a valuable property in a biocatalyst, particularly if the reaction cannot be catalysed in any other way. The rational design of phenylacetone monooxygenase led to the discovery of mutants which showed unusually high activity and enantioselectivity in the oxidative kinetic resolution of a variety of substrates which are not accepted by the wild-type enzyme. The group used bioinformatics data and a knowledge of the enzyme structure to identify sites suitable for mutagenesis (Reetz & Wu, 2009). The same group has also completely reversed the enantioselectivity of *P. aeruginosa* lipase, by using high error rate epPCR and DNA shuffling (Zha *et al.*, 2001).

Increasing the specificity of a biocatalyst can enable the enzyme to accept alternative substrates whilst maintaining its original function, although this may be at the expense of the activity towards the original substrate. One such example is the directed evolution of the phenylalanine dehydrogenase of *B. sphaericus*, an enzyme which normally catalyses the oxidative deamination of phenylalanine to the corresponding keto acid. The switching of specificity to the non-natural amino acid propargylglycine led to a modest activity for the new substrate, and a reduction for the original (Chen & Engel, 2009). Cho *et al* (2008) however were able to rationally

redesign an ω-aminotransferase obtained from *Vibrio fluvialis*, increasing the specificity of two mutants which showed catalytic activity towards a broad range of aliphatic amines without losing the original enantioselectivity and activities toward aromatic amines.

2.11 Directed evolution of MAO-N for the deracemisation of amines

In 2002, the Turner group at the University of Edinburgh reported a conceptually novel method for the preparation of enantiomerically pure chiral amines (Alexeeva *et al.*, 2002). Using the monoamine oxidase of *A. niger*, MAO-N (Schilling & Lerch, 1995a), the group used directed evolution to create a biocatalyst capable of catalysing the enantioselective oxidation of amines to the corresponding imine, which is then non-selectively reduced back to the amine using a chemocatalyst. With further cycles, complete deracemisation is achieved (Figure 2.11.1).

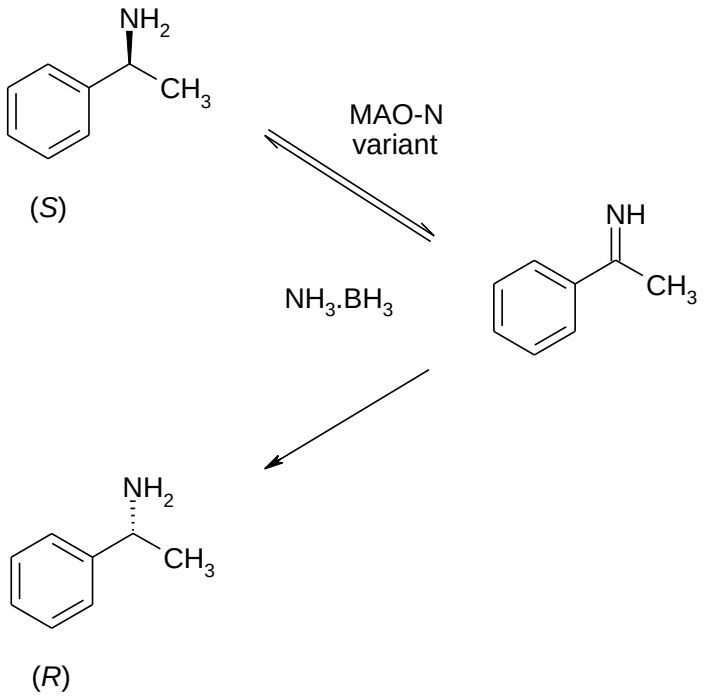

Figure 2.11.1: The cyclic deracemisation of the primary amine α-methylbenzylamine, using the (*S*)-selective biocatalyst MAO-N variant and the non-selective chemocatalyst ammonia borane.

MAO-N first attracted interest due to reports of its high catalytic activity towards simple aliphatic amines, such as benzylamine (k_{cat} ~500 min^{-1}) (Sablin *et al.*, 1998). In order to engineer a biocatalyst with high activity towards primary amines, α-methylbenzylamine was chosen as a model substrate for screening. As the activity of the enzyme was higher towards the (*S*)-enantiomer, it was decided to engineer a biocatalyst with both improved activity and enantioselectivity. The *mao-N* gene was first ligated into the pET16-b plasmid, and the *E. coli* XL1-Red mutator strain used to create a library of variants. Three independent DNA repair pathways have been inactivated in this strain of *E. coli*, giving a spontaneous mutation rate of around 5000-fold greater than the wild-type parent (Greener *et al.*, 1997). Screening of the library was initially by the development of a colorimetric assay applied directly to the colonies. The colonies were transferred to a nitrocellulose filter, and treated with either the (*S*)- or (*R*)-enantiomer and 3,3'-diaminobenzidine (DAB). After incubation at 37°C, any MAO-N activity showed up as pink colonies.

After several rounds of random mutagenesis, a clone was selected for its superior activity (47-fold higher than WT) and enantioselectivity (~6-fold higher than WT). Sequencing showed one mutation, Asn336Ser. The later introduction of a second mutation, Met348Lys, produced higher activity and expression levels, with some activity towards the secondary amine 1-methyltetrahydroisoquinoline (MTQ) (Carr *et al.*, 2003). An additional two mutations, Arg259Lys and Arg260Lys, further improved expression levels, and the fifth mutation Ile246Met improved the k_{cat} towards (*S*)-MTQ 5.5-fold (Carr *et al.*, 2005). A later variant known as MAO-N-D5 which also had five mutations (Ile246Met/Asn336Ser/Met348Lys/Thr384Asn/ Asp385Ser) was examined towards tertiary amines, and out of 10 different substrates good activity towards four was found, with excellent activity towards *N*-methyl-2-phenylpyrrolidine (Dunsmore *et al.*, 2006).

The random mutagenesis of MAO-N had been carried out without prior knowledge of the structure of the protein. However, in order to determine why the random mutations had had the observed effects and to identify possible future improvements, it was necessary to solve the 3-dimensional structure of MAO-N-D5. X-ray

crystallography indicated that the MAO-N-D5 enzyme crystallises as a dimer (Atkin *et al.*, 2008b), and the 3-dimensional structure showed the presence of two channels from the surface of the protein which intersected at the active site. These channels, part of the second coordination sphere of the active site, proved to be the location of four of the mutations (Atkin *et al.*, 2008a). It is thought that these mutations have some effect on the access of the substrate, or the release of the product.
The results of this final study demonstrate the ability of directed evolution to generate superior biocatalysts, without prior knowledge of enzyme structure. Using rational design, it is unlikely that the same residues would have been chosen, as their success in improving activity and enantioselectivity could not be predicted (Turner, 2009).

2.12 Immobilisation of biocatalysts

Biocatalysts are immobilised in order to confine the enzymes or cells to one or more defined zones, whilst maintaining prolonged catalytic activity and if appropriate the viability of the cell. When used in this way, biocatalysts can be more easily removed from the reaction vessel, and may be reused or used in a continuous flow reactor. The biocatalyst is concentrated in one area which may help to improve activity, and as the cells are usually not growing there are fewer secondary reactions which might otherwise cause interference.

The different methodologies used for cell immobilisation include adsorption or bonding to a solid surface, entrapment in a matrix, or physical separation by means of a permeable membrane. A common method is matrix entrapment due to its ease of use, although there may however be problems with mass transfer of the substrate and product. The different types of matrix available include hydrogels, such as calcium alginate and chitosan; thermogels, such as agar or agarose; and synthetic polymers, such as polyacrylamide and sol-gel.

2.12.1 Alginate

Alginate is a biopolymer, produced by many algal species, and is made up of varying proportions of β-D-mannuronic and α-L-guluronic acids. Its popularity as an

immobilisation matrix stems from its ease of use, mild conditions, and general applicability. Cells are mixed with a sodium alginate solution, which is then added drop-wise to a solution of polyvalent cations, usually Ca^{2+}. Ionic crosslinks form between carboxylic acid moieties and the divalent cations, and the droplets immediately solidify, entrapping the cells in a gel lattice. The high porosity of the beads reduces the problems of mass transfer limitations, although it does make the method unsuitable for purified enzymes (Smidsrod & Skjak-Braek, 1990).

Due to its structure of ionic crosslinking, alginate is susceptible to destabilisation by cation scavengers, such as phosphate, sodium citrate, and EDTA (Smeds & Grinstaff, 2001; Smidsrod & Skjak-Braek, 1990), although stability is improved with higher levels of guluronate (Smidsrod & Skjak-Braek, 1990). One advantage of its ease of dissolution is the release of entrapped cells if required.

In a recent study, it was demonstrated that cells encapsulated in alginate could be stored at 4°C for three months without a decrease in enzyme activity (Dey & Roy, 2011). The entrapped cells also showed a higher tolerance to temperature and pH than the free cells.

2.12.2 Chitosan

Chitosan is a nontoxic natural polymer, obtained by extensive deacetylation of chitin, which is found in the shells of crustaceans, molluscs, the cell walls of fungi, and the cuticle of insects (Peniche *et al.*, 2003). It is a weak cationic polysaccharide composed of glucosamine and *N*-acetylglucosamine units, and is a suitable entrapment matrix if alginate cannot be used, for example if a phosphate buffer is to be used during biocatalysis. The method for producing chitosan beads is similar to that used for alginate, whereby a solution of chitosan adjusted to pH 5.5 with acetic acid is mixed with cells and dropped into a crosslinking solution of polyvalent ions. Ionic crosslinking occurs if the chitosan-acetate solution is dropped into a solution of pH <6, as the majority of the NH_2 groups of chitosan are protonated. If dropped into a solution of pH 7.5, crosslinking still takes place but the chitosan is mainly precipitated. The latter

method is suitable if the beads are to be used in reactions taking place at pH >7.5, but these beads will be unstable at lower pH (Vorlop & Klein, 1981).

In a study comparing alginate and chitosan as immobilisation matrices for *Pseudomonas* spp., the latter had greater mechanical stability. With both matrices the enzyme activity was reduced due to mass transfer limitations, but this was compensated for by the long-term viability of the cells (Stocklein *et al.*, 1983).

2.12.3 Polyacrylamide

Polyacrylamide gels attract interest as immobilisation matrices due to their improved mechanical properties, although the neurotoxicity of the acrylamide monomer precursor should be taken into consideration. The acrylamide monomer is cross-linked using bis-acrylamide, at a ratio of 29:1, a reaction which is initiated using ammonium persulfate. Once the gel has set, it can be cut shredded or cut into cubes before use. Studies have demonstrated the ability of polyacrylamide-immobilised bacterial cells to remove toxic metals from waste water (Macaskie, 1990; Tucker *et al.*, 1998).

2.12.4 Sol-gel

Silica sol-gels are created by the polymerisation of two silica sources, one of which is a colloidal silica (sol), triggered by adjusting the pH to form a gel. Following drying, an inert ceramic matrix is formed which is mechanically very strong and protects cells from external stresses. However, a high osmotic pressure due to sodium ions and drying effects during sol-gel formation can be detrimental to cell viability, although the addition of glycerol or gelatin can protect against these effects (Nassif *et al.*, 2002; 2003). The use of aqueous instead of alkoxide precursors is also preferable for the encapsulation of bacteria, as this route does not release alcohol. The leakage of the cytoplasmic enzyme β-galactosidase when alkoxides are used indicates membrane damage, probably from dissolution of the membrane phospholipids (Coiffier *et al.*, 2001; Nassif *et al.*, 2003). Bacteria can be encapsulated in a combination of sol-gel and alginate, combining the advantages of alginate (ease of use and mild conditions) with the mechanical strength of silica (Livage & Coradin, 2006).

Chapter 3: Materials and Methods

Methods

3.1 Bioreduction of palladium

3.1.1 Bioreduction of Pd(II) by *E. coli* K12

The bioreduction of Pd(II) by *E. coli* was first performed using the standard laboratory strain K12, which is a useful model organism since it is facultatively anaerobic and has well-defined molecular tools to elucidate reaction mechanisms under aerobic and anaerobic conditions. The following method used to generate the palladium bionanoparticles ('palladisation') was adapted from that used by Lloyd & Macaskie (1998a).

Starter cultures: Bacterial stocks maintained at -80°C were plated onto LB (Luria-Bertani) agar and incubated at 37°C overnight. 50 ml LB broth in a 500 ml Erlenmeyer flask was inoculated with a single isolated colony of *E. coli* K12 and incubated for 18 hours at 37°C, shaking at 180 rpm.

Aerobic cultures: An 11 ml starter culture was added to 99 ml LB broth in a 1 L Erlenmeyer flask. Flasks were incubated for 24 hours at 37°C, shaking at 180 rpm. The oxygen saturation of a 5 ml aliquot of the broth culture was measured after 24 hours of incubation using an Oakton D06 Acorn Series dissolved oxygen meter.

Anaerobic cultures: An 11 ml starter culture was added to 97.9 ml LB broth containing 20 mM sodium fumarate and supplemented with 1.1 ml 50% vol/vol glycerol in a 120 ml bottle, sealed with a butyl rubber stopper. Bottles were incubated for 24 hours at 37°C, shaking at 180 rpm. The oxygen saturation of a 5 ml aliquot of the broth culture after 24 hours of incubation was measured under anaerobic conditions using an Oakton D06 Acorn Series dissolved oxygen meter.

Although a popular method for the aerobic cultivation of bacteria, flask cultures can become oxygen limiting within a few hours, and the generation of acidic by-products as a result of overflow metabolism can reduce the pH to below optimum growth

conditions. The dissolved oxygen content also decreases rapidly once shaking is stopped, which can reduce the stability of plasmids. However, after 9 hours of incubation the oxygen level rises again and remains high, possibly due to decreased respiration as a result of cell death (Vasala *et al.*, 2006). The flask-grown shaking culture had a dissolved oxygen content of 76% (based on two identical readings on two separate occasions), indicating that the culture was growing aerobically. The pH of the aerobic cultures had increased from 7.2 (uninoculated broth) to 7.7-7.9 at 24 hours of incubation. The anaerobic culture had a dissolved oxygen content of only 2.8%, which is below the level required for anaerobic growth conditions (Vasala *et al.*, 2006). However, the aerobic culture did undergo a period of anaerobiosis, based on dissolved oxygen content readings of 2.5% at two hours incubation, and 2.4% at three hours incubation.

The optical density of cultures were measured using a biochrom WPA Spectrowave S1200 Diode Array Spectrophotometer. Aerobically-grown starter cultures reached an OD_{600} of around 5 after 18 hours of shaking incubation at 37°C. Aerobic broth cultures typically reached an OD_{600} of 5-6 at 24 hours of shaking (180 rpm) incubation at 37°C, yielding a biomass of around 0.7 g ml^{-1} (mass of the wet pellet) from 100 ml liquid culture. This corresponded to a dry weight of 0.12 g. Anaerobic cultures reached an OD_{600} of ~2 following 24 hours of static incubation at 37°C, with a biomass yield of ~0.25 g ml^{-1}.

Palladisation using hydrogen as the electron donor: Each broth culture was divided between two 50 ml Falcon tubes and washed three times in 20 ml MOPS-NaOH (morpholinepropanesulfonic acid) buffer, 20 mM at pH7.6 after centrifugation for 20 minutes at 2500 *g* in a Boeco C-28 A centrifuge. Cell pellets were adjusted to a mass of 250 mg, based on the wet cell pellet, and resuspended MOPS-NaOH to a volume of 1 ml. Each cell pellet was resuspended in 25 ml buffer with 1 mM sodium tetrachloropalladate in 30 ml bottles sealed with butyl rubber stoppers. Bottles were incubated at 30°C for 1 hour for the Pd(II) to biosorb to the cells (Baxter-Plant *et al.*, 2003), then purged with H_2 for 5 minutes, with H_2 allowed to fill the headspace.

Palladisation using formate as the electron donor: The broth cultures were prepared in the same way, and each cell pellet was resuspended in 22.5 ml MOPS-NaOH buffer with 1 mM sodium tetrachloropalladate. Following incubation at 30°C for 1 hour, 2.5 ml 10 mM sodium formate was then added to the bottle to initiate bioreduction of the Pd(II). Bottles were incubated at 30°C until Pd(II) reduction occurred.

3.1.2 X-ray diffraction (XRD) analysis

The cells were coated in a black precipitate forming bioPd within a few minutes in bottles purged with H_2, and in less than 30 minutes in bottles containing formate. The palladised cells settled out leaving a clear colorless supernatant. In order to confirm the presence of palladium in the black precipitate, XRD analysis was performed. The black precipitate was washed once in acetone and air-dried before investigation. The measurements were performed on a Bruker D8 Advance diffractometer, using Cu K alpha1 radiation. The samples were scanned from 5-70 degrees 2theta in steps of 0.2 degrees, with a count time of 2 seconds per step.

3.1.3 Characterisation of palladium nanoparticles by extended X-ray absorption fine structure (EXAFS)

The palladium nanoparticles were analysed using extended X-ray absorption fine structure (EXAFS). Cell/Pd/formate suspensions were prepared as above using *E. coli* BL21(DE3), as this was the strain of choice for later transformation with the *mao-N-D5* gene. Aliquots of the cell/Pd/formate suspension were taken at times 0 and 30 minutes, and 1, 3 and 4 hours from the addition of formate, and frozen immediately in liquid nitrogen. The reduction of Pd(II) to Pd(0) was demonstrated using EXAFS, performed at the European Synchrotron Radiation Facility (ESRF), in Grenoble, France. The samples were transported to the synchrotron at ESRF on dry ice, where they were thawed and injected immediately into sample holders, before freezing once more in liquid nitrogen and placing into the beam. X-ray absorption data were collected on beamline BM29 at the Pd K–edge in the energy range 24,200 – 24,900 eV. Data were recorded at low temperature (77 K) and under vacuum to reduce the thermal Debye-Waller factor and prevent oxidation. A Si(111) double crystal monochromator was used, calibrated with a Pd foil, and the spectra were collected in fluorescence mode

using a 13-element solid-state detector. A reference spectrum of a palladium foil was recorded in transmission mode on station 9.3 at the SRS Daresbury. The data were background subtracted and the EXAFS spectra fitted in DL_Excurv (http://www.cse.scitech.ac.uk/cmg/EXCURV/) using full curved wave theory (Gurman *et al.*, 1984).

3.1.4 Use of transmission electron microscopy (TEM) with energy dispersive X-ray spectroscopy (EDX) to determine location of palladium nanoparticles

TEM was performed on *E. coli* BL21(DE3) cells which had been palladised using both hydrogen and formate, in order to determine the location of the nanoparticles. It was hoped that the location of the nanoparticles would give some indication as to the enzymes involved in their bioreduction, as following the bioreduction of Pd(II) by *D. fructosovorans*, nanoparticles were seen in the periplasm of the cell wall. This is the location of membrane-bound hydrogenases in *D. fructosovorans*, which were later demonstrated to be involved in bioreduction by the use of hydrogenase-negative mutants (Mikheenko *et al.*, 2008). As Pd(II) was reduced by aerobically-grown cultures of *E. coli*, it was expected that the nanoparticles would be deposited in the periplasm, which is the location of the aerobic formate dehydrogenase, FDH-O. However, the reduced palladium was precipitated predominantly in the extracellular matrix of the cultures, which gave no clues as to the biological involvement of the cell in Pd(II) bioreduction.

Preparation of the cell pellets for TEM was performed at the University of Birmingham, School of Biosciences. Following metal challenge, cell pellets were rinsed twice with deionised water, fixed in 2.5% (wt/vol) glutaraldehyde, centrifuged for 5 minutes at 15,996 *g*, resuspended in 1.5 ml of 0.1 M cacodylate buffer (pH 7) and stained in 1% osmium tetroxide in 0.1 M phosphate buffer, pH 7 (60 min). Cells were dehydrated using an ethanol series (70, 90, 100, 100, 100% dried ethanol, 15 min each) and washed twice in propylene oxide (15 min, 9500 g). Cells were embedded in epoxy resin and the mixture was left to polymerise (24 h; 60°C). Sections (100-150 nm thick) were cut from the resin block, placed onto a copper grid and viewed with a JEOL 1200CX2 TEM, accelerating voltage 80 keV. Energy dispersive X-ray spectroscopy (EDX)

was performed on electron-dark areas, to confirm the presence of palladium. The EDX trace and the peaks seen are shown in Figure 3.1.

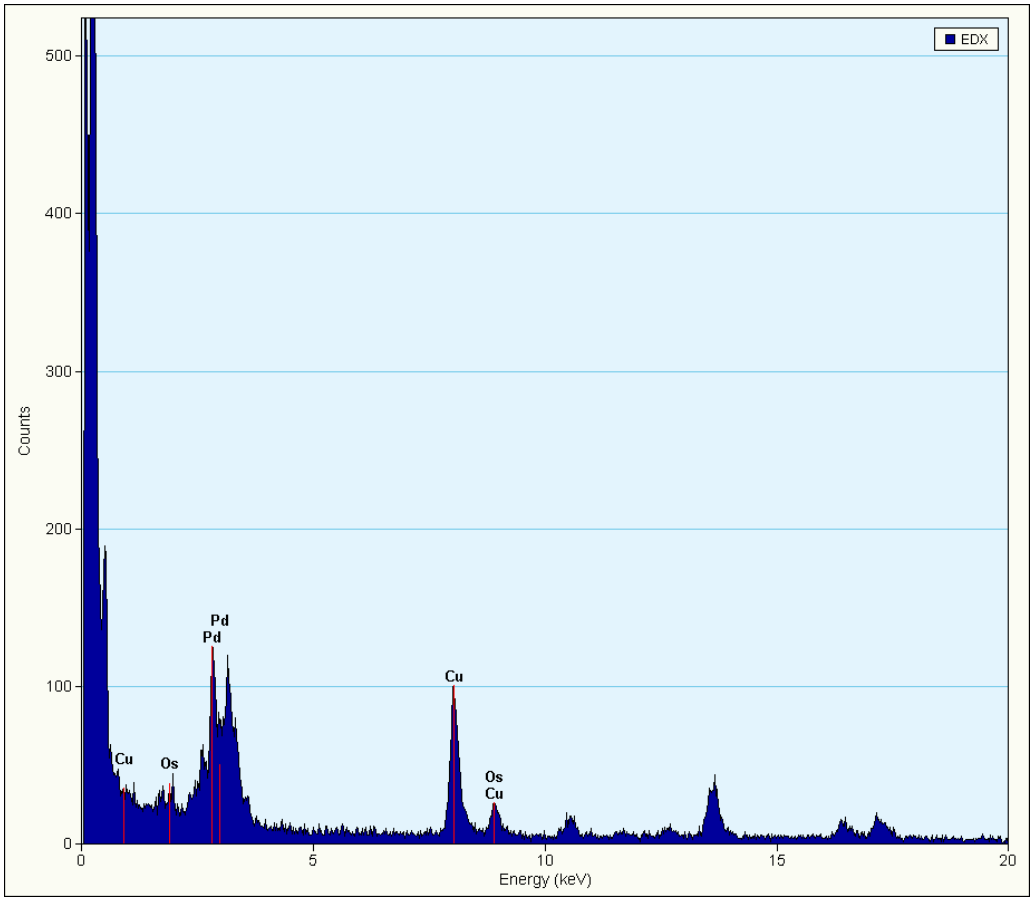

Figure 3.1: EDX trace showing the presence of palladium in the electron-dense precipitates seen by TEM. Peaks are also seen for carbon (far left of trace, >500 counts), copper (composition of the grids used), and osmium (osmium tetroxide was used to stain the sections). The unlabelled peak at around 14 keV does not correspond to any elements and is not recognised by the detector. It is therefore most likely a false peak, and may represent a sum peak (where two X-rays have reached the detector at the same time), or an escape peak (where an X-ray has knocked an electron out of the detector material).

3.1.5 Formate-dependent bioreduction of Pd(II) by different strains of *E. coli*

The bioreduction of Pd(II) by aerobically-grown cultures of *E. coli* indicates the possible involvement of the aerobic formate dehydrogenase, FDH-O. In order to

investigate the possible role of FDH-O and other hydrogenase and formate dehydrogenase enzymes, the rates of reduction by six additional different *E. coli* strains (Table 3.2, page 79) and a series of controls – killed (autoclaved) cells (MC4100), cell-free suspension, and live cells (MC4100) unsupplemented with formate – were compared. The strains were 'palladised' as above using aerobically-grown cultures, using 50 μg ml^{-1} kanamycin as the selective agent for JW2682 and JW3865, and 50 μg ml^{-1} apramycin as the selective agent for MC4100 Δ*moaA*. Aliquots were taken at timed intervals, and centrifuged for 5 minutes at 15,996 *g* to clarify the supernatant. 100 μl supernatant was added to 100 μl 70% nitric acid, and 3.1 ml deionised water was added to give a final concentration of ~2% nitric acid. The samples were filtered and the Pd(II) remaining in solution was measured using inductively coupled plasma mass spectrometry (ICP-MS) with the Agilent 7500cx.

All strains except BL21(DE3) were from the culture collection of Professor Frank Sargent at the College of Life Sciences, University of Dundee. Strain BL21(DE3) was obtained from Invitrogen, Paisley, UK. Strain FTD128 has an in-frame deletion of the *fdhE* gene, which expresses an accessory protein required to locate the FDH-O and FDH-N enzymes to the cytoplasmic membrane. Strains JW2682 and JW3865 were created as part of the Keio collection (Baba *et al.*, 2006) by the in-frame deletion of the *hypF* and *fdoG* genes respectively. The *hypF* gene encodes a hydrogenase maturation protein and the *fdoG* gene encodes α-subunit of FDH-O. Strain MC4100 Δ*moaA* was created by disruption of the *moaA* gene which encodes the molybdenum cofactor biosynthesis protein A, using the method of Datsenko and Wanner (2000) whereby PCR products are used to disrupt the gene of choice by recombination using the plasmid-borne phage λ Red recombinase.

As ICP-MS can be used to measure palladium removal from solution, but not Pd(II) reduction to Pd(0), the precipitation of Pd(II) in the control without formate gave a false-positive result. Also, in two of the experiments the nanoparticles formed were so small as to be impossible to remove from the supernatant by centrifugation or filtration. As a result, the ICP-MS analysis was unable to distinguish between Pd(II) in solution and Pd(0), wrongly giving the impression that bioreduction had not taken

place. A more accurate method of determining Pd(II) reduction would be to use synchrotron radiation, but this method is not practical due to the time taken to secure a beamline allocation.

3.1.6 Investigation of palladium reduction using QEXAFS

In order to determine whether Pd(II) was reduced directly to Pd(0) or if intermediate species were formed, the reduction of Pd(II) to Pd(0) was analyzed by quick-scanning extended X-ray absorption fine structure (QEXAFS) in an *in situ* reduction experiment on beamline BL21 at the Swiss Light Source (SLS) synchrotron facility. *E. coli* strains BL21(DE3), MC4100, and FTD128 were grown aerobically as described previously, frozen and transported to the SLS on dry ice. After thawing, the cells were resuspended in 25 ml 20mM MOPS-NaOH buffer (pH 7.6) and challenged with 1 mM Pd(II), in a 5 cm tube placed longitudinally in the beam (see Figure 3.2). The tube was purged with hydrogen for 30 seconds at 10 minute intervals, until the sample had turned completely black. The reduction of the Pd(II) was slower than under normal laboratory conditions, as hydrogen could not be continuously supplied due to the necessity of vacating the experimental area during use of synchrotron radiation on the beamline. Hydrogen was therefore supplied for only 30 seconds between measurements. The experiment could not be repeated using formate as there was no possibility of incubating the samples whilst in the beam.

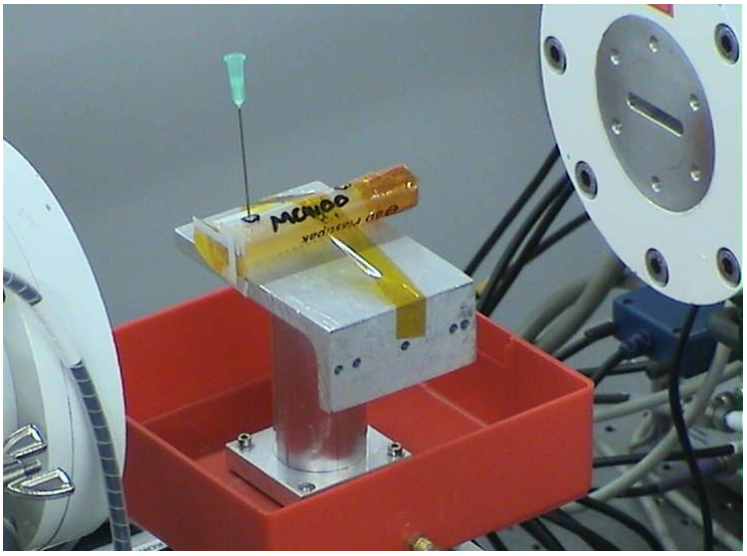

Figure 3.2: Cells challenged with palladium on beamline BL21, Swiss Light Source.

Scans were performed at a rate of 4 scans per minute, for 10 minutes at a time. X-ray absorption data were collected in the energy range 23,970 – 25,727 eV. Data were recorded in transmission, in fast-scanning mode, each run accumulating 118 spectra over 10 minutes. The spectra were isolated, the data range cut to 22,210 – 24,900 eV, and the number of points in each spectrum reduced (and signal-to-noise improved) by averaging adjacent groups of points to a grid finely spaced over the Pd K-edge and after the edge evenly spaced in k-space. The individual spectra were summed into ten groups of ten and one group of eight for each run. This was repeated until all spectra had been processed.

The summed data were background subtracted in the Daresbury program EXBACK. The X-ray absorption near-edge spectroscopy (XANES) spectra were generated by adding back in the E0 defined in the subtraction routine.

3.1.7 Transmission electron microscopy (TEM) of mutant *E. coli* strains

TEM of the different strains of *E. coli* was performed to determine whether the missing enzymes had any influence on the site of Pd(0) nanoparticle deposition. Sections of the metal-loaded cells of strains MC4100 and FTD128 (formate-dependent Pd(II) bioreduction) were provided by EM facility in the Faculty of Life Sciences, University of Manchester. The bacteria were fixed in primary fixative (2.5% glutaraldehyde and 4% formaldehyde in 0.1M sodium cacodylate buffer at pH7.4) and secondary fixative (1% osmium tetroxide and 1.5% potassium ferrocyanide in 0.1M sodium cacodylate buffer at pH7.4) and dehydrated in a graded acetone series (30 minutes each in 50%, 70%, 90% and three changes at 100%) before embedding in TAAB LV medium epoxy resin. Sections were imaged using a FEI Tecnai12 Twin transmission electron microscope. Other bacterial strains were prepared and imaged by the University of Birmingham, as described previously.

3.2 Engineering a whole cell biometallic catalyst

3.2.1 Transformation of *E. coli* BL21(DE3) with pET-16b plasmid containing *mao-N-D5* insert

Strains and plasmid: *E. coli* BL21(DE3) and *E. coli* TOP10/P3 cells were obtained from Invitrogen. The pET16-b plasmid containing the *mao-N-D5* insert and an ampicillin resistance gene was obtained from Dr Andrew Ellis at the Manchester Interdisciplinary Biocentre. Bacterial isolates were stored at -80°C, and the plasmid was stored at -20°C.

Transformation: *E. coli* BL21(DE3) chemically competent cells were transformed according to the supplier's instructions, using approximately 100 ng (2 µl) of plasmid. Transformed BL21(DE3) cells were subcultured onto LB-ampicillin agar, and incubated overnight at 37°C before storage at 4°C for a maximum of 1 week.

3.2.2 Preparation of biocatalyst

Starter culture: 50 ml LB-ampicillin broth in a 500 ml Erlenmeyer flask was inoculated with a single isolated colony of transformed *E. coli* BL21(DE3) and incubated for 18 hours at 37°C, shaking at 180 rpm.

Aerobic cultures: An 11 ml starter culture was added to 99 ml LB-ampicillin broth in a 1 L Erlenmeyer flask. Flasks were incubated for 24 hours at 37°C, shaking at 180 rpm. Each broth culture was then divided between two 50 ml Falcon tubes and washed three times in 20 ml MOPS-NaOH buffer, 20 mM at pH7.6 after centrifugation for 20 minutes at 2500 *g*. Cell pellets were adjusted to a mass of 250 mg based on the wet cell pellet, and resuspended in MOPS-NaOH to a volume of 1 ml. Aliquots were stored at -20°C.

3.2.3 Catalytic activity of biocatalyst

Frozen transformed cells were thawed and added to 8 ml 12.5 mM racemic MTQ, from a stock solution made up in 0.1 M potassium phosphate buffer at pH 7.6. Additional potassium phosphate buffer (1 ml) was added to bring the volume of the reaction mixture to 10 ml. The vessel used was a 120 ml gas bottle sealed with a butyl rubber stopper, and the reaction was allowed to proceed in air at 37°C, with shaking

at 225 rpm. Samples were taken as required, by removing 550 µl in triplicate, centrifuging for 20 minutes at 2500 *g* and storing 500 µl of the supernatant at -20°C in a 2 ml centrifuge tube before extraction with methyl-tert-butyl ether (MTBE).

Solvent extraction: The pH of the samples was first increased to >12 by the addition of 20 µl 10N sodium hydroxide, in order to make the substrate and product more soluble in MTBE. 1 ml MTBE was then added, and the samples vortexed for 30 seconds before centrifuging for 5 minutes at 15,996 *g* to ensure complete separation of the phases, with the MTBE layer on the top. This layer was removed using a glass pipette, and transferred to an eppendorf tube containing ~50 mg anhydrous sodium sulfate, to ensure complete removal of water from the sample. The samples were centrifuged for a few seconds, and the supernatant transferred to an HPLC vial and the MTBE allowed to evaporate under a flow of nitrogen, leaving behind a clear colourless oil.

HPLC analysis: The samples were resuspended in 200 µl isohexane prior to testing by normal phase chiral HPLC on an Agilent 1200 chromatograph, using a Daicel Chiralpak AD-H 4.6 mm x 250 mm column, at a flow rate of 1 ml min^{-1} for 20 minutes at 40°C with a mobile phase of 88% isohexane, 2% ethanol, and 10% isohexane containing 0.5% diethylamine. The analytes were detected by UV-Vis spectroscopy, at wavelengths of 220 nm (MTQ), and 254 nm (MDQ).

Relative standard deviation: The relative standard deviation (RSD) of the data was 2.8%, calculated from three separate measurements using the following equation:

$$\%\text{RSD} = \frac{standard\ deviation\ of\ array}{average\ of\ array} \text{x } 100$$

(Equation 3.1)

3.2.4 Catalytic activity of Pd(0) nanoparticles

Pd-loaded untransformed *E. coli* BL21(DE3) cells were prepared as previously (section 3.1.1), using hydrogen as the electron donor. Cells were washed once in MOPS-NaOH buffer and cell pellets were adjusted to a mass of 250 mg based on the wet cell pellet before resuspending in MOPS-NaOH buffer to a volume of 1 ml. Aliquots were stored at -20°C.

Reduction of MDQ using formate as the electron donor: Frozen transformed cells were thawed and added to 8 ml 12.5 mM MDQ, from a stock solution made up in 0.1 M potassium phosphate buffer at pH 7.6, and 1 ml 70 mM sodium formate in buffer. The vessel used was a 120 ml gas bottle sealed with a butyl rubber stopper, and the reaction was allowed to proceed in air at 37°C, with shaking at 225 rpm. Samples were taken as required, by removing 550 µl in triplicate, centrifuging for 20 minutes at 2500 *g* and storing 500 µl of the supernatant at -20°C before extraction with MTBE and analysis by HPLC. Reduction of MDQ was complete within one hour.

Reduction of MDQ using hydrogen gas as the electron donor: Frozen transformed cells were thawed and added to 8 ml 12.5 mM MDQ, from a stock solution made up in 0.1 M potassium phosphate buffer at pH 7.6, in a 120 ml gas bottle. Additional potassium phosphate buffer (1 ml) was added to bring the volume of the reaction mixture to 10 ml, and the bottle was sealed with a butyl rubber stopper. The bottle was sparged with H_2 for 90 seconds, before incubation at 37°C with shaking at 225 rpm. Samples were taken as required, by removing 550 µl in triplicate, centrifuging for 20 minutes at 2500 *g* and storing 500 µl of the supernatant at -20°C before extraction with MTBE and analysis by HPLC. Reduction of MDQ was complete within 30-40 minutes.

3.2.5 Integration of processes for deracemisation

Deracemisation with sodium formate as the electron donor: The two reactions were combined by using palladised transformed cells in the reaction mixture, and with the addition of 70 mM sodium formate (final concentration). The bottles were incubated as above.

Despite the rapid conversion of the starting materials in both the oxidation and reduction experiments, when initially combined into one system and incubated for 24 hours, deracemisation did not proceed beyond the initial oxidation step. This was due to the unexpected formation of another product from MDQ by further chemical oxidation (Figure 3.3). This molecule was identified as 1-methylisoquinoline (MIQ)

using reverse-phase LC-MS. The sample was dissolved in 200 µl acetonitrile and water in a 1:1 ratio, and run on an Agilent 1100 LC / MSD SC using a Phenomenex Luna C18 (2) 150 x 4.60 mm 3 µm column, at a flow rate of 1 ml min^{-1} with a mobile phase of 2% acetonitrile and 98% water, ramping to 98% acetonitrile over 30 minutes.

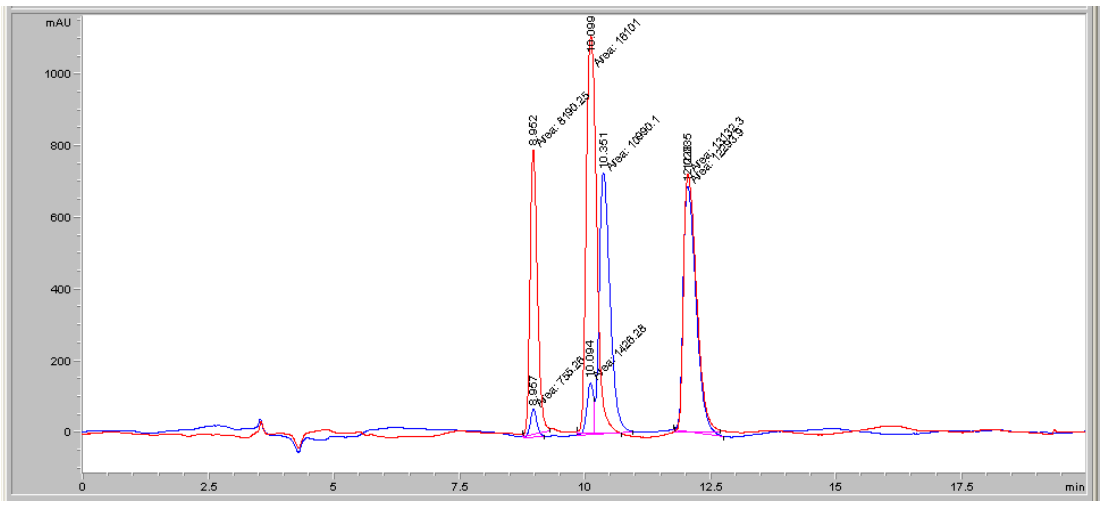

Figure 3.3: HPLC traces, showing trace soon after start of oxidation (blue trace) with large peaks for (*S*)-MTQ (retention time 10.35 minutes) and (*R*)-MTQ (12.03 minutes) and small peaks for MDQ (8.95 minutes) and MIQ (10.1 minutes); and after 3 hours of incubation at 37°C (red trace), showing large peaks for MDQ and MIQ, no peak for (*S*)-MTQ, and no change to the peak for (*R*)-MTQ.

Deracemisation with hydrogen as the electron donor: The two reactions were combined by using palladised transformed cells in the reaction mixture. Oxidation and reduction steps were performed as separate cycles, by flushing the vessel alternately with air or hydrogen. The reaction vessel was a 120 ml gas bottle with a 10 ml reaction volume, providing a 110 ml headspace. The vessel was first flushed with nitrogen to avoid the mixing of air and hydrogen. Based on the initial separate oxidation and reduction experiments, each oxidation step was two hours long, and each reduction step was 45 minutes. Samples were taken at the end of each reduction step, for 4 cycles. The pH of the reaction supernatant following the biotransformation was 7.5, indicating that it was still in the range of activity for the MAO-N-D5 enzyme which has an optimum activity at pH 7.5-8.1 (Reiss, 2008), and not detrimental to the viability of the biocatalyst. Production of MIQ was not observed when hydrogen gas was used

instead of formate as the electron donor for the reduction step, possibly as hydrogen drives the reduction of MDQ at a faster rate than formate (see section 3.2.4).

3.2.6 Re-use of cells

Palladised transformed cells were used in a 5-cycle biotransformation as described in section 3.2.5, using hydrogen as the electron donor. The used cells were then recovered by centrifuging for 20 minutes at 2500 *g*, and resuspended to 1 ml in 20 mM potassium phosphate buffer, pH 7.6. The cells were frozen in liquid nitrogen and stored at -20°C until used in an oxidation experiment, as described in section 3.2.3.

3.2.7 Comparison with commercially available palladium on a carbon support (Pd/C).

The activity of the biometallic catalyst was compared with non-palladised cells and 0.0221 g commercially available 10% palladium on carbon (Pd/C). The biotransformation was carried out over 5 cycles of alternating air and hydrogen.

Measuring loss of palladium into the reaction supernatant: In order to determine whether palladium was leached into the reaction supernatant, contaminating the products, the supernatant was obtained by centrifugation of 1 ml at 15,996 *g* for 5 minutes, before digestion with an equal volume of 70% nitric acid for 24 hours. Samples were then diluted to 2% nitric acid, and filtered before analysis for the presence of palladium using ICP-MS.

3.2.8 Immobilisation of biocatalyst in alginate

The method used for the immobilisation of palladised transformed cells in alginate beads was adapted from that of Hartmeier (1988). 1.2 g sodium alginate was dissolved in 42 ml deionised water, and 6 ml of palladised transformed *E. coli* cells (250 mg ml^{-1} in 20 mM MOPS-NaOH buffer at pH 7.6) were added to 350 ml dissolved alginate solution. The alginate-cell suspension was then dropped into 200 ml of a 2% w/v calcium chloride solution using a plastic Pasteur pipette, whilst gently stirring to prevent bead aggregation. Alginate beads were left stirring for 1 hour to harden, after which time the $CaCl_2$ solution was diluted to 0.5% w/v with the addition of a further 600 ml deionised water. Beads were stored in the 0.5% w/v $CaCl_2$ solution at 10°C

until use. The beads were approximately 3-4 mm in diameter (Figure 3.4), and each 250 mg aliquot of biocatalyst produced around 110 beads.

Figure 3.4: Alginate beads containing immobilised palladised *E. coli*.

Before use in oxidation, reduction, or deracemisation experiments, the beads were rinsed in MOPS-NaOH buffer at pH 7.6. All experiments were carried out using reagents made up in MOPS-NaOH buffer rather than potassium phosphate buffer, as phosphate would destabilise the beads and release the biocatalyst (Smidsrod & Skjak-Braek, 1990). Otherwise, the experiments were carried out as for planktonic cells, in 120 ml gas bottles (see Figure 3.5). Culture of the reaction supernatant following biotransformation revealed no viable cells had been released from the beads.

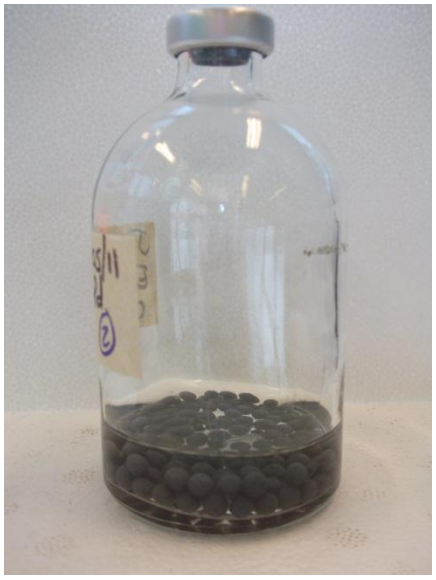

Figure 3.5: Alginate beads in reaction vessel, showing 10 ml substrate and 110 ml headspace.

3.2.9 Environmental scanning electron microscopy (ESEM)

Biocatalyst-containing beads were examined using a Philips XL30 ESEM-FEG using ionised water vapour to disperse the charge from the sample surface, thus avoiding the need to carbon coat. The beads were imaged both before and after use in a deracemisation reaction, in order to determine any possible effects on the integrity of the beads.

3.2.10 Use of freeze-dried beads in oxidation and reduction reactions

To assess the suitability of freeze-drying for the long-term storage of the biocatalyst, beads were frozen in liquid nitrogen and dried for 24 hours. The beads were stored at 10°C under vacuum until use, and were used in oxidation experiments on day one, after two weeks, and after six weeks.

3.3 Materials

Most of the culture media, buffers, enzymes and chemicals used in this study were obtained from Fisher Scientific or Sigma Aldrich. Any materials not obtained from these sources are listed in Table 3.1.

Table 3.1: Materials used in this study.

Material	**Source**
Culture media:	
SOC medium	In 200 ml deionised water: Tryptone 4 g Yeast extract 1 g NaCl 0.1 g
Buffers:	
MOPS buffer	Acros Organics
Chemicals:	

Material	Source
Acrylamide:bis-acrylamide (29:1)	BioRad
Diethylamine	Fluka
Hydrogen gas	BOC Gases
Isohexane	Romil
MDQ	Acros Organics
MTQ	GSK
Nitrogen gas	BOC Gases
Oxygen gas	BOC Gases
Pyrogallol red dye	Acros Organics
Sodium sulfate	BDH
Sodium tetrachloropalladate	Alfa Aesar
HPLC columns:	
Daicel Chiralpak AD-H 4.6 mm x 250 mm column	Chiral Technologies Europe
Phenomenex Luna C18 (2) 150 x 4.60 mm 3 µm column	Phenomenex

3.3.1 Bacterial strains and plasmid

The bacterial strains and plasmid used in this study are listed in Table 3.2, which includes the genotypes and source of the strains.

Table 3.2: *E. coli* strains and plasmid used in this study.

Strain	Genotype	Phenotype	Reference	Source
K12 JM109	F´ *tra*D36 *pro*A^{+}B^{+} *lacI*^{q} Δ*(lacZ)*M15/ Δ*(lac-pro*AB*) gln*V44 *e14*$^{-}$ *gyr*A96 *rec*A1 *rel*A1 *end*A1 *thi hsd*R17	Strain commonly used for recombinant protein expression.	(Yanisch-Perron *et al.*, 1985)	New England BioLabs
TOP10/P3	F^{-} *mcr*A Δ(*mrr-hsd*RMS-*mcr*BC) ϕ80*lac*ZΔM15 Δ*lac*X74 *rec*A1 *ara*Δ139	Strain commonly used for plasmid amplification.	Invitrogen	Invitrogen

	Δ(*ara-leu*)7697 *gal*U *gal*K *rps*L (Str^R) *end*A1 *nup*G.			
BL21(DE3)	*F2 ompT gal dcm lon* $hsdS_B(r_B^- m_B^-)$ λ(DE3 [*lacI lacUV5-T7 gene 1 ind1 sam7 nin5*])	Strain commonly used for recombinant protein expression.	(Studier & Moffatt, 1986)	Invitrogen
MC4100	*F-* Δ*lacU169 araD139 rpsL150 relA1 ptsF rbs flbB5301*	Parental strain for FTD128 and MC4100 Δ*moaA*.	(Casadaban & Cohen, 1979)	From the collection of Professor F. Sargent, University of Dundee.
BW25113	$lacI^q$ $rrbB_{T14}$ Δ$lacZ_{WJ16}$ *hsd*R514 Δ$araBAD_{AH33}$ Δ$rhaBAD_{LD78}$	Parental strain for JW2682 and JW3865.	(Datsenko & Wanner, 2000)	As above
FTD128	As MC4100, with in-frame deletion in the *fdhE* gene.	FDH-O & FDH-N negative.	(Luke *et al.*, 2008)	As above
JW2682	As BW25113, with in-frame deletion of the *hypF* gene.	Deficient in all hydrogenases.	(Baba *et al.*, 2006)	As above
JW3865	As BW25113, with in-frame deletion of the *fdoG* gene.	FDH-O negative.	(Baba *et al.*, 2006)	As above
MC4100 Δ*moaA*	As MC4100, disruption of the *moaA* gene.	Deficient in all molybdoenzymes.	This study.	As above
pET 16-b plasmid	T7 promoter, T7 transcription start, His•Tag sequence, MCS (*Nde* I -*Bam*H I), T7 terminator, *lacI* coding sequence, pBR322 *ori*, *bla* coding sequence.	High-level expression plasmid.	Novagen	Novagen

Chapter 4: Engineering a biometallic whole cell catalyst for enantioselective deracemization reactions

Engineering a biometallic whole cell catalyst for enantioselective deracemization reactions

Joanne M. Foulkes[†], Kirk J. Malone[‡], Victoria S. Coker[†], Nicholas J. Turner[‡], Jonathan R. Lloyd[†]*

[†]*Williamson Research Centre for Molecular Environmental Science and School of Earth, Atmospheric and Environmental Sciences, University of Manchester, Oxford Road, Manchester M13 9PL, UK*

[‡]*School of Chemistry, University of Manchester, Manchester Interdisciplinary Biocentre, 131 Princess Street, Manchester M1 7DN, UK*

**Corresponding author;*

Tel: +44 (0)161 275 7155

Fax: +44 (0)161 306 3961

e-mail: jon.lloyd@manchester.ac.uk

ABSTRACT The ability of microbial cells to synthesize highly reactive nano-scale functional materials provides the basis for a novel synthetic biology tool for developing the next generation of multifunctional industrial biocatalysts. Here we demonstrate that aerobic cultures of *Escherichia coli*, genetically engineered to overproduce a recombinant monoamine oxidase (MAO-N) possessing high enantioselectivity against chiral amines, can be augmented with nano-scale Pd(0) precipitated *via* bioreduction

reactions. The result is a novel biometallic catalyst for the deracemization of racemic amines. This deracemization process is normally achieved by discrete sequential oxidation/reduction steps using a separate enantiomer-specific biocatalyst and metal catalyst respectively. Here, use of *E. coli* cultures carrying the cloned monoamine oxidase gene and nano-scale bioreduced Pd(0) particles was used successfully for the conversion of racemic 1-methyltetrahydroisoquinoline (MTQ) to (*R*)-MTQ, *via* the intermediate 1-methyl-3,4-dihydroisoquinoline (MDQ), with an enantiomeric excess of up to 96%. There was no loss of catalyst activity following the five rounds of oxidation and reduction, and importantly there was minimal loss of palladium into the reaction supernatant. This first demonstration of a whole cell biometallic catalyst mixture for "single-pot", multi-step reactions opens up the way for a wide range of integrated processes, offering a scalable and highly flexible platform technology.

Keywords: palladium catalyst, *Escherichia coli*, biocatalysis, biotransformation, deracemization.

The fabrication of functional biominerals by microbial cells offers the potential to revolutionize the synthesis of nanomaterials. These biosynthetic routes are potentially highly scalable, work at ambient pressures and temperatures in the absence of toxic compounds such as capping agents, and their properties can be fine-tuned using genetic or physiological manipulations.[1] In several examples, waste materials can be used as the feedstock for biomineral synthesis, offering a green chemistry solution to nanomaterial synthesis.[2] Functional biominerals produced recently by microbial routes include precious metal catalysts,[2, 3] nanomagnets for hyperthermic cancer treatment,[4] quantum dots,[5] bioremediation agents,[6] silver-based antimicrobials,[7] and SERS probes.[8] The model organisms used for these processes are all amenable to manipulations using the rapidly advancing tools of synthetic biology. Thus, they have the potential to form the basis of complex multifunctional systems, when integrated with the microbial host's cellular physiology.

A particularly promising area for this type of approach is the development of multifunctional biocatalysts. The application of recombinant whole cell biocatalysts is an established technology for a broad range of industrial conversions including notable examples such as the reduction of ketones to alcohols using ketoreductases[9] and also the asymmetric synthesis of chiral amines using transaminases.[10]

The requirement for enantiomerically pure chiral amines in the pharmaceutical and agrochemicals industries has led to the development of asymmetric transformations, dynamic kinetic resolutions (DKR) and deracemization reactions using biocatalysts that can efficiently generate products in up to 100% yield and 100% e.e.[11] Previous work has reported the use of lipases with a carbon-supported palladium catalyst for the DKR of racemic amines.[12] However, this method takes up to five days at 60°C to give

moderate yields, and generates unwanted by-products. Lipases are suitable for use with primary amines and some secondary amines, but cannot be applied to tertiary amines.[13] By contrast, monoamine oxidase-N (MAO-N), has attracted attention as a result of its enantioselectivity towards the (*S*)-form of the primary amine α-methyl-benzylamine.[14] MAO-N is a tetrameric flavoprotein that catalyzes the oxidative deamination of terminal amine groups.[15] The use of this enzyme for the deracemization of racemic chiral amines is based on the creation of imine intermediates by oxidation of the (*S*)-enantiomer. The addition of a chemical reductant, such as ammonia-borane or palladium-formate/hydrogen, results in the non-selective conversion of the imine back to the racemic amine. After several oxidation/reduction cycles, a very high enantiomeric excess and yield of the (*R*)-enantiomer is achieved.

The directed evolution of *mao-N* from *Aspergillus niger* has led to the generation of enzymes with enhanced activity and specificity towards primary,[11] secondary[16] and tertiary amines.[13] The advantage of directed evolution as a method for improving enzymes for specific applications is that no prior knowledge of enzyme structure is required, as screening is carried out purely on the basis of the desired functional properties.[17] After several cycles of mutagenesis and screening, a variant enzyme was identified with activity towards the secondary amine 1-methyltetrahydroisoquinoline (MTQ)[16] and the tertiary amine *N*-methyl-2-phenylpyrrolidine.[13] The latter variant has five point mutations in the gene, giving rise to the alterations Ile246Met/Asn336Ser/Met348Lys/Thr384Asn/Asp385Ser in the product. This enzyme is designated MAO-N-D5.[13, 18]

It has been known for more than a century that a range of specialist prokaryotes can reduce metals by using them as the terminal electron acceptor during anaerobic

respiration.[19] These microbial activities can be used in the bioremediation of land contaminated with toxic metals and also in the reclamation of potentially valuable precious metals.[1] For example, the obligately anaerobic sulfate-reducing bacterium *Desulfovibrio desulfuricans* has been shown to reduce soluble Pd(II) to insoluble Pd(0), which is precipitated in the periplasm as nanoparticles.[20] This property has allowed the use of the palladized organism (known as Bio-Pd) directly in a broad range of reactions, showing good activity compared with a commercially available carbon-supported palladium catalyst for the dehalogenation of chlorophenol, polychlorinated biphenyls, and polybrominated diphenyl ethers. [21, 22] Here we outline how Bio-Pd can be produced without the use of strict anaerobic culture, or complicated washing steps to remove sulfide formed by the sulfate-reducing bacterium (which can poison palladium catalysts) by using the facultative anaerobe *Escherichia coli* grown under aerobic conditions. *E. coli* is also easily transformed with plasmid DNA, and hence can be used to express foreign genes, making this organism ideal for use as a biocatalyst in a one-pot reaction utilizing recombinant enzymes such as MAO-N-D5 in combination with Bio-Pd . The aim of this study was to demonstrate for the first time the coupled activity of a functional biomineral catalyst and enzyme in a novel engineered catalyst, in this case for the deracemization of racemic amines, providing a prototype for multi-step transformations and other hybrid biometallic systems (Figure 1).

Figure 1: The cyclic deracemization of 1-methyltetrahydroisoquinoline (MTQ) via the imine 1-methyl-3,4-dihydroisoquinoline (MDQ) using palladized biocatalyst with the *mao-N-D5* insert.

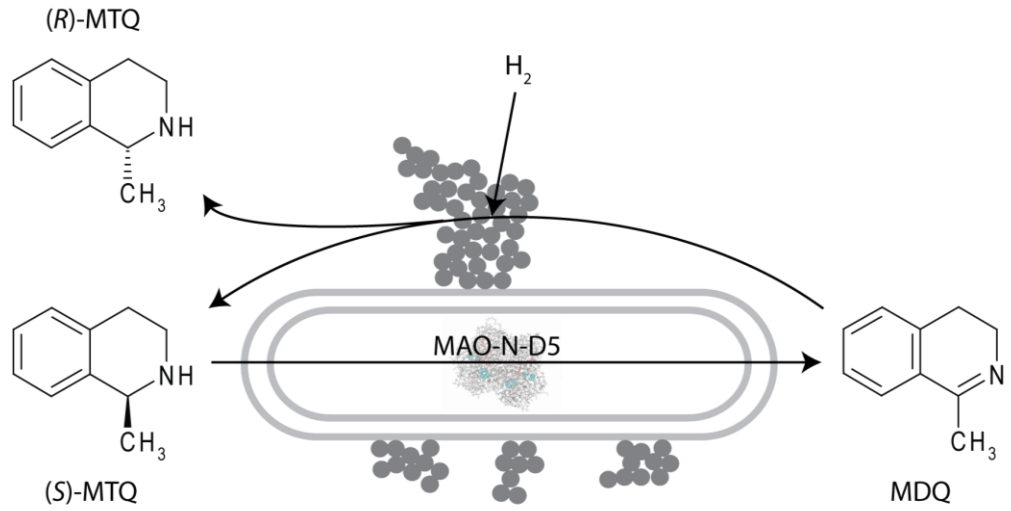

RESULTS AND DISCUSSION

PALLADIZATION OF *E. COLI* BL21

In order to develop a multifunctional biometallic whole-cell catalyst for deracemization reactions, washed aerobically-grown *E. coli* BL21 cells containing the cloned gene expressing the enzyme MAO-N-D5 were palladized by challenging with 1 mM Pd(II) and hydrogen gas as an electron donor. The cells were coated in a black precipitate within a few minutes (Figure 2a), indicating the reduction of Pd(II) to insoluble particles of Pd(0).[20] Pd(II) did not reduce to Pd(0) in bottles that were not purged with H_2. The black precipitate was analyzed by X-ray diffraction to confirm the presence of elemental palladium (Figure 2b), although the signal was weak due the nanoparticulate nature of the sample. The size of the particles was calculated to be approximately 1 nm in diameter, as measured using the Scherrer equation.

Figure 2: a) Biomass with palladium (II) (left), and reduced palladium (right); b) XRD showing presence of palladium on in the microbial cultures supplied with Pd(II) and hydrogen as the electron donor; c) TEM of thin sections of aerobically grown cells

showing extracellular palladium (scale bar = 1 µm); d) TEM of a cell showing intracellular nanoparticles associated with the inner surface of the plasma membrane (scale bar = 50 nm).

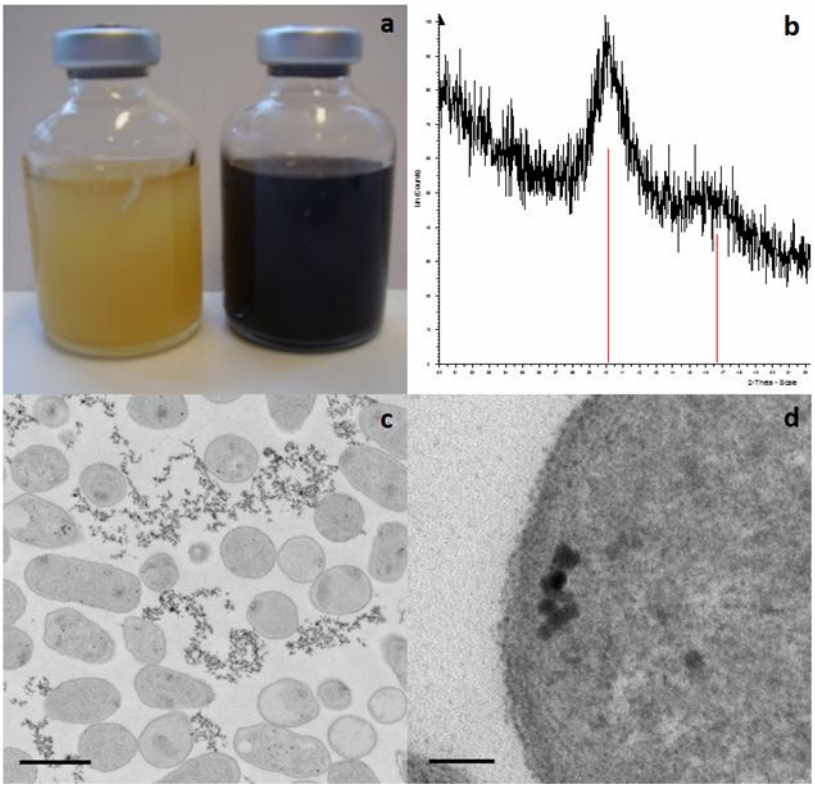

TEM images of thin sections of cells showed that the reduced palladium was precipitated predominantly in the extracellular matrix of the cultures (Figure 2c). Occasionally, larger nanoparticles (~10 nm) were seen inside the cell, possibly located on the inner surface of the plasma membrane (Figure 2d). Energy dispersive X-ray spectroscopy (EDS) confirmed the presence of palladium in these electron dense nano-scale precipitates.

QEXAFS analysis at the Swiss Light Source showed that the Pd(II) is reduced to Pd(0) with no evidence of intermediate species (Figure 3). However, the reduction of the Pd(II) was slower than under normal laboratory conditions, as hydrogen could not be continuously supplied due to the necessity of vacating the experimental area during use

of synchrotron radiation on the beamline. Hydrogen was therefore supplied for only 30 seconds between measurements.

Figure 3: EXAFS spectra showing reduction of Pd(II) to Pd(0) within 1 hour (in situ experiment). Times shown are in minutes.

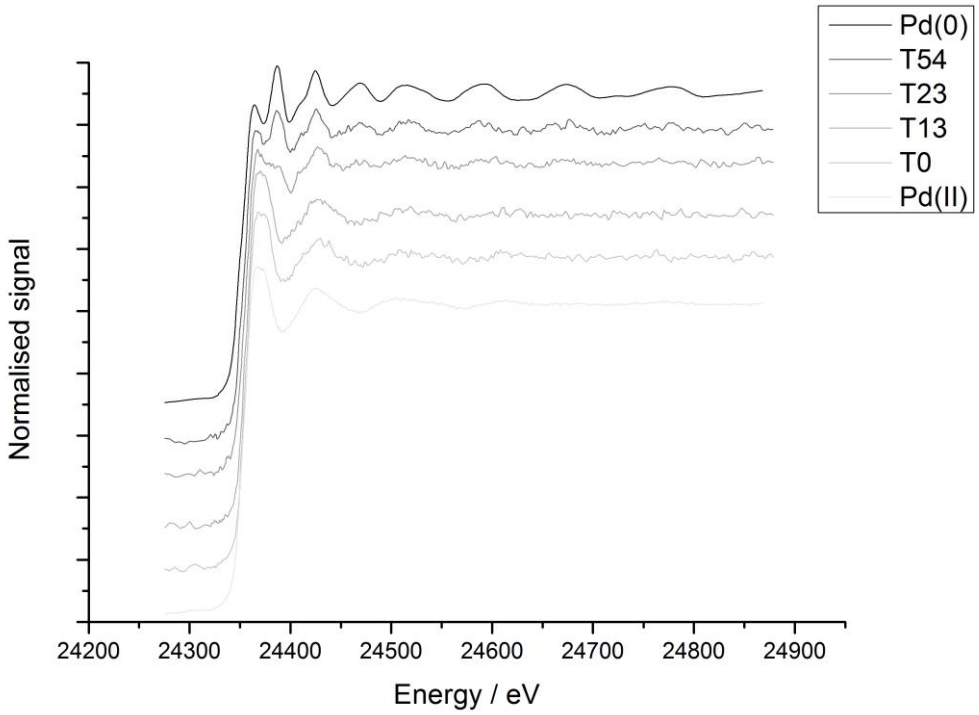

SUBSTRATE OXIDATION AND REDUCTION

When *E. coli* transformed with the *mao-N-D5* gene insert was added to 10 mM racemic MTQ and incubated at 37°C, all of the (*S*)-enantiomer of the MTQ was oxidized to MDQ within two hours (Figure 4).

Figure 4: The oxidation of (*S*)-MTQ to MDQ within 2 hours at 37°C, by *E. coli* transformed with the *mao-N-D5* gene insert.

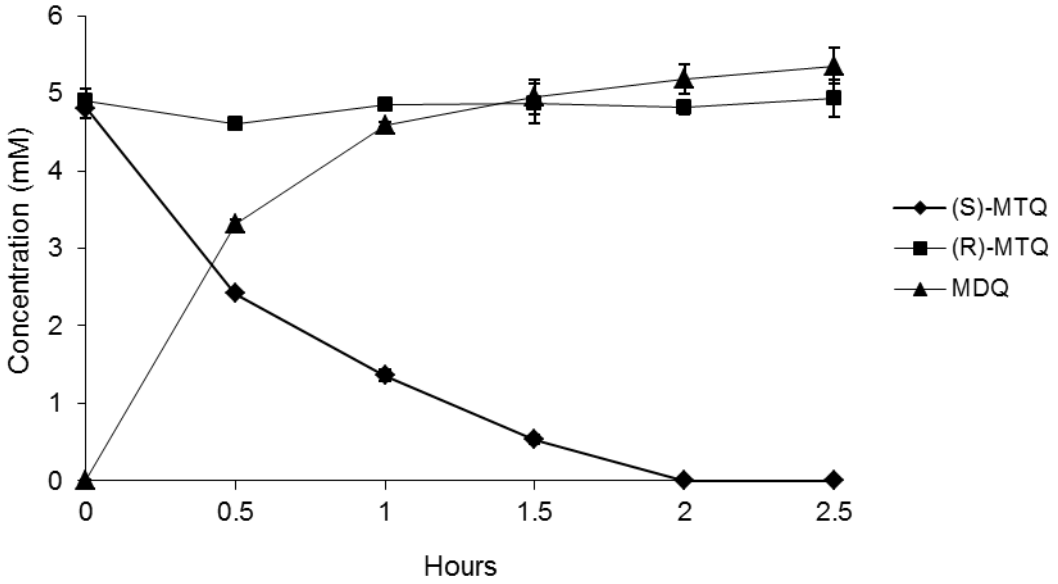

When palladized untransformed *E. coli* was added to 10 mM MDQ and 70 mM sodium formate and incubated at 37°C, all of the MDQ was reduced to racemic MTQ within 1 hour. Subsequent experiments using hydrogen gas showed complete reduction of MDQ within 30 minutes (Figure 5). Thus both the oxidative and reductive steps required for the deracemization of chiral amines such as MTQ were active in the same culture of recombinant, palladized *E. coli* developed in this study.

Figure 5: The reduction of MDQ to racemic MTQ within 30 minutes at 37°C, by palladized *E. coli* using hydrogen gas as the electron donor.

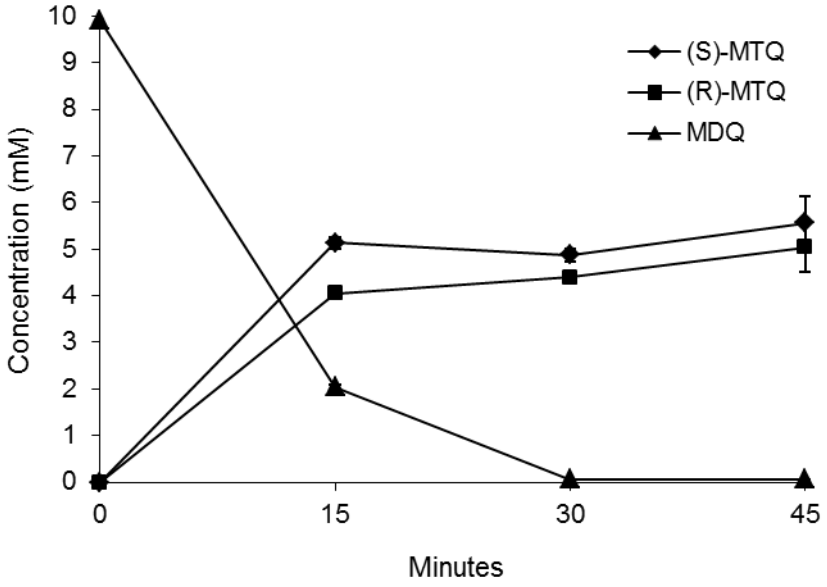

INTEGRATION OF PROCESSES FOR DERACEMIZATION

Despite the rapid conversion of the starting materials in both the oxidation and reduction experiments, when initially combined into one system and incubated for 24 hours, deracemization did not proceed beyond the initial oxidation step. This was due to the unexpected formation of 1-methylisoquinoline (MIQ) from MDQ by further chemical oxidation. However, production of MIQ was not observed when hydrogen gas was used instead of formate as the electron donor for the reduction step, possibly indicating that hydrogen drives the bioreduction of MDQ at a faster rate than formate. To avoid the potentially hazardous mixing of air and hydrogen in the reaction vessel, oxidation and reduction steps were performed as separate cycles. Based on the results from the separate oxidation and reduction reactions, each oxidation step was maintained for two hours, and each reduction step was 45 minutes, to allow each reaction to proceed to completion. After four cycles of oxidation and reduction, the (*R*)-enantiomer was present in an enantiomeric excess (*e.e.*) of 89%. The hypothetical value at this stage after 4 cycles of oxidation and reduction is a 96.875% e.e. Increasing the

experiment from 4 cycles to 5 cycles increased the e.e. to 96% (Figure 6), which would be the standard required for commercial application.

Figure 6: The deracemization of MTQ, giving an e.e. of 96% (*R*)-MTQ (5 cycles of air alternated with 5 cycles of hydrogen).

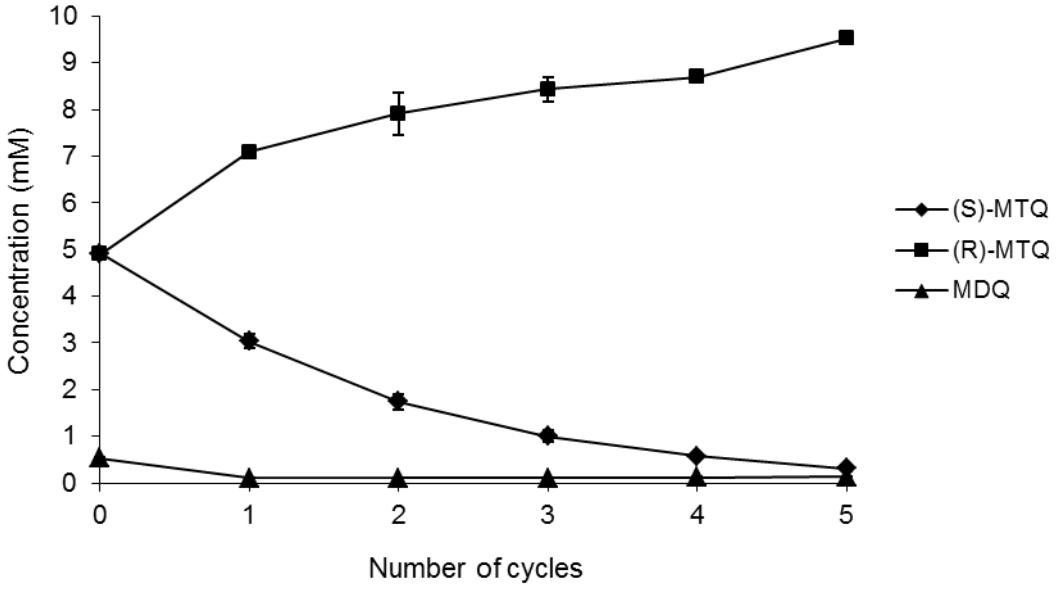

When cells used in a 5-cycle biotransformation were collected by centrifugation and washed with potassium phosphate buffer and used in further oxidation-only and reduction-only experiments, it was found that the activity of both the MAO-N-D5 enzyme and the palladium was the same as that prior to the biotransformation. Thus both the recombinant enzyme and Bio-Pd were stable for multiple rounds of biotransformation.

COMPARISON OF ACTIVITY WITH COMMERCIALLY AVAILABLE PALLADIUM.

When the performance of the palladized cells was compared to that of recombinant non-palladized cells with an equivalent amount of conventional-Pd (carbon with 10% palladium) in a biotransformation of 5 cycles of oxidation and reduction, there was a

97% conversion to (*R*)-MTQ by both the Bio-Pd and the conventional-Pd. However, the total mass of the final product (*R*)-MTQ was low at 85% of the expected total produced for the Bio-Pd and 75% for the conventional-Pd. Washing the cell pellets three times with methyl-tert-butyl ether recovered the (*R*)-MTQ from the Bio-Pd cell pellet, however 10% of the missing (*R*)-MTQ was still not recoverable at this stage from the conventional-Pd cell pellet. The third wash for the conventional-Pd samples continued to yield (*R*)-MTQ, indicating retention of the amine through adsorption onto the carbon support, which was difficult to recover through washing. The recovery of product from the Bio-Pd was 100%, with no further (*R*)-MTQ recovered after the second wash. With the additional material taken into account from the washing of the cell pellets, both the Bio-Pd and the conventional-Pd showed a 92% conversion to (*R*)-MTQ. However, the yield was 10% lower than expected for the conventional-Pd. In this respect, Bio-Pd is superior to conventional-Pd for use in deracemization reactions due to the comparative ease of product recovery.

MEASURING LOSS OF PALLADIUM INTO THE REACTION SUPERNATANT

Although centrifugation was sufficient to remove all Bio-Pd nanoparticles from the reaction supernatant, visible particles of conventional-Pd remained in the supernatant after centrifugation and required filtering to remove. The ICP-MS results also showed that more palladium was lost to the supernatant when using conventional-Pd than with Bio-Pd. The Bio-Pd reaction supernatant contained 0.17 mg l^{-1} palladium, whereas the conventional-Pd reaction supernatant contained 0.24 mg l^{-1}.

CONCLUSIONS

Recent advances in the field of synthetic biology allow us to anticipate the possibility of creating a “designer” biometallic catalyst, engineered precisely to the requirements

of the desired chemical transformation. This study has shown that it is already possible to engineer a biometallic catalyst mixture capable of one-pot deracemization reactions.

Although previous studies investigating the bioreduction of palladium have used anaerobic cultures, this study has demonstrated that palladium reduction is possible with aerobic cultures of *E. coli*, using hydrogen as the electron donor. Although Pd(II) is reduced by hydrogen without the presence of bacteria, there is likely to be a biological mechanism for Pd(II) reduction in this cultures, due to the significantly increased time taken for reduction to complete in cell-free controls and killed (autoclaved) cell controls (based on visual interpretation), as also seen by others.[23] The aerobic expression of hydrogenases known to mediate Pd(II) reduction in anaerobic cultures,[24] is one possibility that is being investigated in our laboratory, or the expression of another macromolecular system with the capability to catalyze hydrogen oxidation and Pd(II) reduction. The use of aerobic cultures for the production of biometallic catalysts is preferable, due to increased cell yield, higher yields of recombinant proteins[25] and in the case of SRB no production of H_2S which can poison metallic catalysts.[26] TEM images show the presence of elemental palladium as extracellular nanoparticles, associated with the cell surface and possibly with exopolysaccharides. It may be this association which prevents the removal of the palladium nanoparticles during washing of the biocatalyst. Occasionally nanoparticles were seen inside the cell, possibly located on the inner surface of the plasma membrane. QEXAFS data confirms the reduction of Pd(II) directly to Pd(0), without the production of intermediate species.

Palladized *E. coli* transformed with the *mao-N-D5* plasmid is capable of performing both oxidation and reduction reactions required for the deracemization reactions

studied here. However, it was not possible to perform both reactions simultaneously, with aerobic cells supplied with formate as an electron donor for the Pd-catalyzed reaction, due to the formation of the unwanted product MIQ under these conditions. However, this product was not seen when hydrogen was used instead of formate as the electron donor in the reduction reaction. The use of hydrogen required the two reactions to be performed separately but in the same reaction vessel, in a cyclical manner. This simple approach should be amenable for use in a broad range of reactor configurations, including those using high densities of cells immobilized on a suitable support for easy re-use. As the two reactions are not run simultaneously, each discrete reaction step can be optimized fully, with prolonged activity for the catalyst demonstrated in this study.

When the performance of enzymatically produced Bio-Pd was compared to that of commercially available "conventional-Pd" in a biotransformation of 5 cycles of oxidation and reduction, both were found to adsorb the reactants and products of the biotransformation. However, the conventional-Pd adsorbed around 10% more than the Bio-Pd (1 mM of the potential 10 mM final product in our study), indicating that the amine could not be desorbed from the catalyst even with multiple washing steps. It was also found that the conventional-Pd was present in the reaction supernatant at higher levels than the Bio-Pd, and had to be removed by an additional filtration step complicating downstream processing. The ease of removal of Bio-Pd from the reaction mixture indicates both reduced contamination of the products with palladium, and improved recyclability of the catalyst. The re-use of Bio-Pd cells following a 5-cycle biotransformation confirmed that the activity of these cells was the same as in previous experiments.

In conclusion, we have demonstrated that it is possible to create a biometallic catalyst that expresses MAO-N as a model oxidase enzyme in palladized cells, and can perform both oxidation and reduction reactions leading to a 96% deracemization of a secondary amine, without the addition of a separate chemical reductant and with limited contamination or adsorption of the reaction products by the catalyst. This method has a broad potential for simplifying or improving other enzyme/inorganic catalyst combinations, not being specific to either *E. coli* or palladium, and could be potentially useful for a range of industrial and biotechnological applications. This study, therefore, illustrates the exciting potential of applying the rapidly evolving synthetic biology toolkit available to biotechnologists to engineer biocatalysts and novel nano-scale biomineral precipitates in a single organism for multi-step catalysis.

EXPERIMENTAL SECTION

TRANSFORMATION OF *E. COLI* BL21 WITH PET-16B PLASMID CONTAINING THE *MAO-N-D5* INSERT

Strains and plasmid: *E. coli* BL21 cells were obtained from Invitrogen. The pET16-b plasmid containing the *mao-N-D5* insert and an ampicillin resistance gene was obtained from Dr Andrew Ellis at the Manchester Interdisciplinary Biocentre. Bacterial isolates were stored at -80°C, and the plasmid was stored at -20°C.

Transformation: Cells were transformed according to the supplier's instructions, using approximately 100 ng of plasmid. Transformed BL21 cells were subcultured onto LB agar plates containing 100 μg ml^{-1} ampicillin, and incubated overnight at 37°C before storage at 4°C for a maximum of 1 week.

PALLADIZATION OF *E. COLI* BL21

The method used was adapted from that used by Lloyd & Macaskie.[20]

Starter cultures: 50 ml LB broth in a 500 ml Erlenmeyer flask was inoculated with a single isolated colony of the transformed *E. coli* and incubated overnight at 37°C, shaking at 180 rpm.

Aerobic cultures: An 11 ml starter culture was added to 99 ml LB broth containing 100 μg ml^{-1} ampicillin, in a 1 L Erlenmeyer flask. Flasks were incubated for 24 hours at 37°C, shaking at 180 rpm. An oxygen saturation of 72% was measured using an Oakton D06 Acorn Series dissolved oxygen meter.

Palladization: Each culture was divided between two 50 ml Falcon tubes (supplied by Fisher) and washed three times in 20 ml MOPS-NaOH (morpholinepropanesulfonic acid) buffer, 20 mM at pH7.6 after centrifugation for 20 minutes at 2500 *g*. Cell pellets were adjusted to a mass of 250 mg, based on the wet cell pellet, and resuspended MOPS-NaOH to a volume of 1 ml. Two tubes of each culture were resuspended in 25 ml buffer with 1 mM sodium tetrachloropalladate (supplied by Alfa Aesar) in 30 ml bottles sealed with butyl rubber stoppers (two bottles per culture). Bottles were incubated in the dark at 30°C for 1 hour for the Pd(II) to biosorb to the cells.[21] One of each of the two different cultures was then purged with H_2 for 5 minutes, with H_2 allowed to fill the headspace to promote the enzymatic reduction of the Pd(II). The final loading of bioreduced, elemental Pd(0) in the biomass was approximately 1% by mass. The remaining two bottles were H_2-negative controls.

X-RAY DIFFRACTION (XRD) ANALYSIS

The cells were coated in a black precipitate within a few minutes in bottles containing cells as Pd(II) purged with H_2. The palladized cells settled out leaving a clear colorless supernatant. The black precipitate was washed once in acetone and air-dried, before investigation by XRD. The measurements were performed on a Bruker D8 Advance

diffractometer, using Cu Kalpha1 radiation. The samples were scanned from 5-70 degrees 2theta in steps of 0.2 degrees, with a count time of 2 seconds per step.

TRANSMISSION ELECTRON MICROSCOPY (TEM) AND ENERGY DISPERSIVE X-RAY SPECTROSCOPY (EDS)

Sections of the palladized cells were provided by EM facility in the Faculty of Life Sciences, University of Manchester. The bacteria were fixed in primary fixative (2.5% glutaraldehyde and 4% formaldehyde in 0.1M sodium cacodylate buffer at pH7.4) and secondary fixative (1% osmium tetroxide and 1.5% potassium ferrocyanide in 0.1M sodium cacodylate buffer at pH7.4) and dehydrated in a graded acetone series (30 minutes each in 50%, 70%, 90% and three changes at 100%) before embedding in TAAB LV medium epoxy resin. EDS was performed on electron-dark areas, to confirm the presence of palladium.

QUICK-SCANNING EXTENDED X-RAY ABSORPTION FINE STRUCTURE (QEXAFS)

The reduction of Pd(II) to Pd(0) was analyzed by QEXAFS in an *in situ* reduction experiment on beamline BL21 at the Swiss Light Source (SLS) synchrotron facility. Cells were grown aerobically as described previously, frozen and transported to the SLS on dry ice. After thawing, the cells were resuspended in 25 ml 20mM MOPS-NaOH buffer (pH 7.6) and challenged with 1 mM Pd(II), in a 5 cm tube placed longitudinally in the beam. The tube was purged with hydrogen for 30 seconds at 10 minute intervals, until the sample had turned completely black. Scans were performed at a rate of 4 scans per minute, for 10 minutes at a time. X-ray absorption data were collected in the energy range 23,970 – 25,727 eV. Data were recorded in transmission, in fast-scanning mode, each run accumulating 118 spectra over 10 minutes. The spectra were isolated, the data range cut to 22,210 – 24,900 eV, and the number of points in

each spectrum reduced (and signal-to-noise improved) by averaging adjacent groups of points to a grid finely spaced over the Pd K-edge and after the edge evenly spaced in k-space. The individual spectra were summed into ten groups of ten and one group of eight for each run. This was repeated until all spectra had been processed.

The summed data were background subtracted in the Daresbury program EXBACK.

SUBSTRATE OXIDATION AND REDUCTION

Oxidation: Frozen transformed cells (250 mg ml^{-1} in 20 mM MOPS-NaOH buffer at pH 7.6) were thawed and added to 8 ml 12.5 mM racemic MTQ, from a stock solution made up in 0.1 M potassium phosphate buffer at pH 7.6. Potassium phosphate buffer (1 ml) was added to bring the volume of the reaction mixture to 10 ml. The vessel used was a 120 ml gas bottle sealed with a butyl rubber stopper, and the reaction was allowed to proceed in air at 37°C, with shaking at 225 rpm. Samples were taken as required, by removing 550 μl in triplicate, centrifuging for 20 minutes at 2500 *g* and storing 500 μl of the supernatant at 20°C before extraction with methyl-tert-butyl ether (MTBE).

Reduction with sodium formate as the electron donor: Frozen palladized untransformed cells (250 mg ml^{-1} in 20 mM MOPS-NaOH buffer at pH 7.6, with 1% Pd loading by mass) were thawed and added to 8 ml 12.5 mM MDQ (1-methyl-3,4-dihydroisoquinoline, supplied by Acros Organics), from a stock solution made up in 0.1 M potassium phosphate buffer at pH 7.6. Sodium formate (1 ml) was added to a final concentration of 70 mM, giving a total reaction volume of 10 ml. The conditions of incubation and MTBE extraction were the same as for the oxidation step.

Reduction with hydrogen as the electron donor: The procedure was carried out as above, with 1 ml 0.1 M potassium phosphate buffer replacing the sodium formate in the

reaction mixture. The reaction volume was 10 ml, in a 120 ml gas bottle, providing a 110 ml headspace. The bottle was sparged with hydrogen for 2 minutes before incubating and extracting as previously.

HPLC analysis: The samples were resuspended in 200 μl isohexane prior to testing by normal phase chiral HPLC on an Agilent 1200 chromatograph, using a Daicel Chiralpak AD-H 4.6 mm x 250 mm column, at a flow rate of 1 ml min^{-1} for 20 minutes at 40°C with a mobile phase of 88% isohexane, 2% ethanol, and 10% isohexane containing 0.5% diethylamine. The analytes were detected by UV-Vis spectroscopy, at wavelengths of 220 nm (MTQ), and 254 nm (MDQ) (see Supplementary Fig. 1 online). The error (RSD) was 2.8%.

INTEGRATION OF PROCESSES FOR DERACEMIZATION

Deracemization with sodium formate as the electron donor: The two reactions were combined by using palladized transformed cells in the reaction mixture, and with the addition of 70 mM sodium formate (final concentration). The bottles were incubated as above.

Deracemization with hydrogen as the electron donor: The two reactions were combined by using palladized transformed cells in the reaction mixture. Oxidation and reduction steps were performed as separate cycles, by flushing the vessel alternately with air or hydrogen. The reaction vessel was a 120 ml gas bottle with a 10 ml reaction volume, providing a 110 ml headspace. The vessel was first flushed with nitrogen to avoid the mixing of air and hydrogen. Each oxidation step was two hours long, and each reduction step was 45 minutes. Samples were taken at the end of each reduction step, for 4 cycles. The deracemisation took a total of 11 hours, with intervention for the flushing of gases at the end of each oxidation and each reduction step (8 interventions in total). Increasing the deracemisation step from 4 cycles to 5 cycles required an

additional 2 interventions for the flushing of gases, over a total of 13 hours and 45 minutes.

COMPARISON OF ACTIVITY WITH COMMERCIALLY AVAILABLE PALLADIUM

The activity of the biometallic catalyst was compared with non-palladized cells and commercially available 10% palladium on carbon (conventional-Pd), supplied by Sigma Aldrich. The biotransformation was carried out over 5 cycles of air and hydrogen.

MEASURING LOSS OF PALLADIUM INTO THE REACTION SUPERNATANT

In order to determine whether palladium was leached into the reaction supernatant, contaminating the products, the supernatant was obtained by centrifugation of 1 ml at 15,682 *g* for 5 minutes, before digestion with an equal volume of 70% nitric acid for 24 hours. Samples were then diluted to 2% nitric acid, and filtered before analysis for the presence of palladium using the ICP-MS Agilent 7500cx.

ACKNOWLEDGEMENTS

The authors thank the staff in the EM facility in the Faculty of Life Sciences, The University of Manchester for their assistance, and the Wellcome Trust for equipment grant support to the EM facility. We also thank Dr John Charnock of the University of Manchester for analysis of QEXAFS data, and Dr Valentin Koehler of the University of Basel for assistance with HPLC analysis.

Supporting Information Available: Additional data, including details of HPLC analysis, controls for palladium reduction with hydrogen, re-use of the biocatalyst, and a

comparison of Bio-Pd with conventional-Pd. This material is available free of charge via the Internet at http://pubs.acs.org.

REFERENCES

1. Lloyd, J. R.; Pearce, C. I.; Coker, V. S.; Pattrick, R. A. D.; Van Der Laan, G.; Cutting, R.; Vaughan, D. J.; Paterson-Beedle, M.; Mikheenko, I. P.; Yong, P.; Macaskie, L. E., Biomineralization: linking the fossil record to the production of high value functional materials. *Geobiology* **2008,** 6, (3), 285-297.

2. Macaskie, L. E.; Mikheenko, I. P.; Yong, P.; Deplanche, K.; Murray, A. J.; Paterson-Beedle, M.; Coker, V. S.; Pearce, C. I.; Cutting, R.; Pattrick, R. A. D.; Vaughan, D.; van der Laan, G.; Lloyd, J. R., Today's wastes, tomorrow's materials for environmental protection. *Hydrometallurgy* **2010,** 104, (3-4), 483-487.

3. Coker, V. S.; Bennett, J. A.; Telling, N. D.; Henkel, T.; Charnock, J. M.; van der Laan, G.; Pattrick, R. A. D.; Pearce, C. I.; Cutting, R. S.; Shannon, I. J.; Wood, J.; Arenholz, E.; Lyon, I. C.; Lloyd, J. R., Microbial engineering of nanoheterostructures: biological synthesis of a magnetically recoverable palladium nanocatalyst. *ACS Nano* **2010,** 4, (5), 2577-2584.

4. Coker, V. S.; Telling, N. D.; van der Laan, G.; Pattrick, R. A. D.; Pearce, C. I.; Arenholz, E.; Tuna, F.; Winpenny, R. E. P.; Lloyd, J. R., Harnessing the extracellular bacterial production of nanoscale cobalt ferrite with exploitable magnetic properties. *ACS Nano* **2009,** 3, (7), 1922-1928.

5. Pearce, C. I.; Coker, V. S.; Charnock, J. M.; Pattrick, R. A. D.; Mosselmans, J. F. W.; Law, N.; Beveridge, T. J.; Lloyd, J. R., Microbial manufacture of chalcogenide-based nanoparticles via the reduction of selenite using *Veillonella atypica*: an in situ EXAFS study. *Nanotechnology* **2008,** 19, (15), -.

6. Cutting, R. S.; Coker, V. S.; Fellowes, J. W.; Lloyd, J. R.; Vaughan, D. J., Mineralogical and morphological constraints on the reduction of Fe(III) minerals by *Geobacter sulfurreducens*. *Geochimica Et Cosmochimica Acta* **2009,** 73, (14), 4004-4022.

7. Suresh, A. K.; Pelletier, D. A.; Wang, W.; Moon, J. W.; Gu, B. H.; Mortensen, N. P.; Allison, D. P.; Joy, D. C.; Phelps, T. J.; Doktycz, M. J., Silver nanocrystallites: biofabrication using *Shewanella oneidensis*, and an evaluation of their comparative toxicity on Gram-negative and Gram-positive bacteria. *Environmental Science & Technology* **2010,** 44, (13), 5210-5215.

8. Jarvis, R. M.; Law, N.; Shadi, L. T.; O'Brien, P.; Lloyd, J. R.; Goodacre, R., Surface-enhanced Raman scattering from intracellular and extracellular bacterial locations. *Analytical Chemistry* **2008,** 80, (17), 6741-6746.

9. Moore, J. C.; Pollard, D. J.; Kosjek, B.; Devine, P. N., Advances in the enzymatic reduction of ketones. *Acc Chem Res* **2007,** 40, (12), 1412-9.

10. Savile, C. K.; Janey, J. M.; Mundorff, E. C.; Moore, J. C.; Tam, S.; Jarvis, W. R.; Colbeck, J. C.; Krebber, A.; Fleitz, F. J.; Brands, J.; Devine, P. N.; Huisman, G. W.; Hughes, G. J., Biocatalytic asymmetric synthesis of chiral amines from ketones applied to sitagliptin manufacture. *Science* **2010,** 329, (5989), 305-9.

11. Alexeeva, M.; Enright, A.; Dawson, M. J.; Mahmoudian, M.; Turner, N. J., Deracemization of alpha-methylbenzylamine using an enzyme obtained by in vitro evolution. *Angewandte Chemie-International Edition* **2002,** 41, (17), 3177-3180.

12. Choi, Y. K.; Kim, M. J.; Ahn, Y.; Kim, M. J., Lipase/palladium-catalyzed asymmetric transformations of ketoximes to optically active amines. *Organic Letters* **2001,** 3, (25), 4099-4101.

13. Dunsmore, C. J.; Carr, R.; Fleming, T.; Turner, N. J., A chemo-enzymatic route to enantiomerically pure cyclic tertiary amines. *Journal of the American Chemical Society* **2006,** 128, (7), 2224-2225.

14. Alexeeva, M.; Enright, A.; Dawson, M. J.; Mahmoudian, M.; Turner, N. J., Deracemization of α-methylbenzylamine using an enzyme obtained by in vitro evolution. *Angewandte Chemie-International Edition* **2002,** 41, (17), 3177-3180.

15. Schilling, B.; Lerch, K., Amine oxidases from *Aspergillus niger* - identification of a novel flavin-dependent enzyme. *Biochimica Et Biophysica Acta-General Subjects* **1995,** 1243, (3), 529-537.

16. Carr, R.; Alexeeva, M.; Dawson, M. J.; Gotor-Fernandez, V.; Humphrey, C. E.; Turner, N. J., Directed evolution of an amine oxidase for the preparative deracemisation of cyclic secondary amines. *Chembiochem* **2005,** 6, (4), 637-639.

17. Alexeeva, M., Carr, R., Turner, N. J., Directed evolution of enzymes: new biocatalysts for asymmetric synthesis. *Organic and Biomolecular Chemistry* **2003,** 1, 4133-4137.

18. Atkin, K. E.; Reiss, R.; Turner, N. J.; Brzozowski, A. M.; Grogan, G., Cloning, expression, purification, crystallization and preliminary X-ray diffraction analysis of variants of monoamine oxidase from *Aspergillus niger*. *Acta Crystallographica Section F-Structural Biology and Crystallization Communications* **2008,** 64, 182-185.

19. Lloyd, J. R., Microbial reduction of metals and radionuclides. *FEMS Microbiology Reviews* **2003,** 27, (2-3), 411-425.

20. Lloyd, J. R.; Yong, P.; Macaskie, L. E., Enzymatic recovery of elemental palladium by using sulfate-reducing bacteria. *Applied and Environmental Microbiology* **1998,** 64, (11), 4607-4609.

21. Baxter-Plant, V.; Mikheenko, I. P.; Macaskie, L. E., Sulphate-reducing bacteria, palladium and the reductive dehalogenation of chlorinated aromatic compounds. *Biodegradation* **2003,** 14, (2), 83-90.

22. De Windt, W.; Aelterman, P.; Verstraete, W., Bioreductive deposition of palladium (0) nanoparticles on *Shewanella oneidensis* with catalytic activity towards reductive dechlorination of polychlorinated biphenyls. *Environmental Microbiology* **2005,** 7, (3), 314-325.

23. Yong, P.; Rowson, N. A.; Farr, J. P. G.; Harris, I. R.; Macaskie, L. E., Bioreduction and biocrystallization of palladium by *Desulfovibrio desulfuricans* NCIMB 8307. *Biotechnology and Bioengineering* **2002,** 80, (4), 369-379.

24. Deplanche, K.; Caldelari, I.; Mikheenko, I. P.; Sargent, F.; Macaskie, L. E., Involvement of hydrogenases in the formation of highly catalytic Pd(0) nanoparticles by bioreduction of Pd(II) using *Escherichia coli* mutant strains. *Microbiology-SGM* **2010,** 156, 2630-2640.

25. Krause, M.; Ukkonen, K.; Haataja, T.; Ruottinen, M.; Glumoff, T.; Neubauer, A.; Neubauer, P.; Vasala, A., A novel fed-batch based cultivation method provides high cell-density and improves yield of soluble recombinant proteins in shaken cultures. *Microbial Cell Factories* **2010,** 9, 11.

26. Redwood, M. D.; Deplanche, K.; Baxter-Plant, V. S.; Macaskie, L. E., Biomass-supported palladium catalysts on *Desulfovibrio desulfuricans* and *Rhodobacter sphaeroides*. *Biotechnology and Bioengineering* **2008,** 99, (5), 1045-1054.

For Table of Contents Use Only. Engineering a biometallic whole cell catalyst for enantioselective deracemization reactions. Joanne M. Foulkes, Kirk J. Malone, Victoria S. Coker, Nicholas J. Turner, Jonathan R. Lloyd.

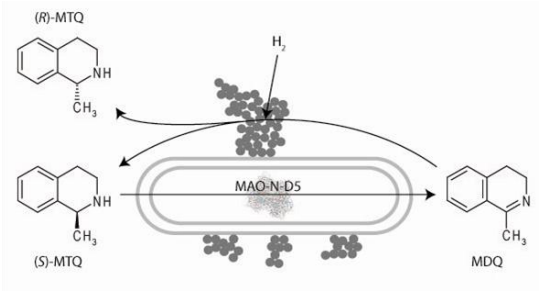

SUPPORTING INFORMATION

FOR

ENGINEERING A BIOMETALLIC WHOLE CELL CATALYST FOR ENANTIOSELECTIVE DERACEMIZATION REACTIONS

Joanne M. Foulkes, Kirk J. Malone, Victoria S. Coker, Nicholas J. Turner, Jonathan R. Lloyd*

**Corresponding author;*

Tel: +44 (0)161 275 7155

Fax: +44 (0)161 306 3961

e-mail: jon.lloyd@manchester.ac.uk

HPLC analysis

Supplementary Figure 1: HPLC traces, showing trace soon after start of oxidation (blue trace) with large peaks for (*S*)-MTQ (retention time 10.35 minutes) and (*R*)-MTQ (12.03 minutes) and small peaks for MDQ (8.95 minutes) and MIQ (10.1 minutes), and after 3 hours of incubation at 37°C (red trace), showing large peaks for MDQ and MIQ, no peak for (*S*)-MTQ, and no change to the peak for (*R*)-MTQ.

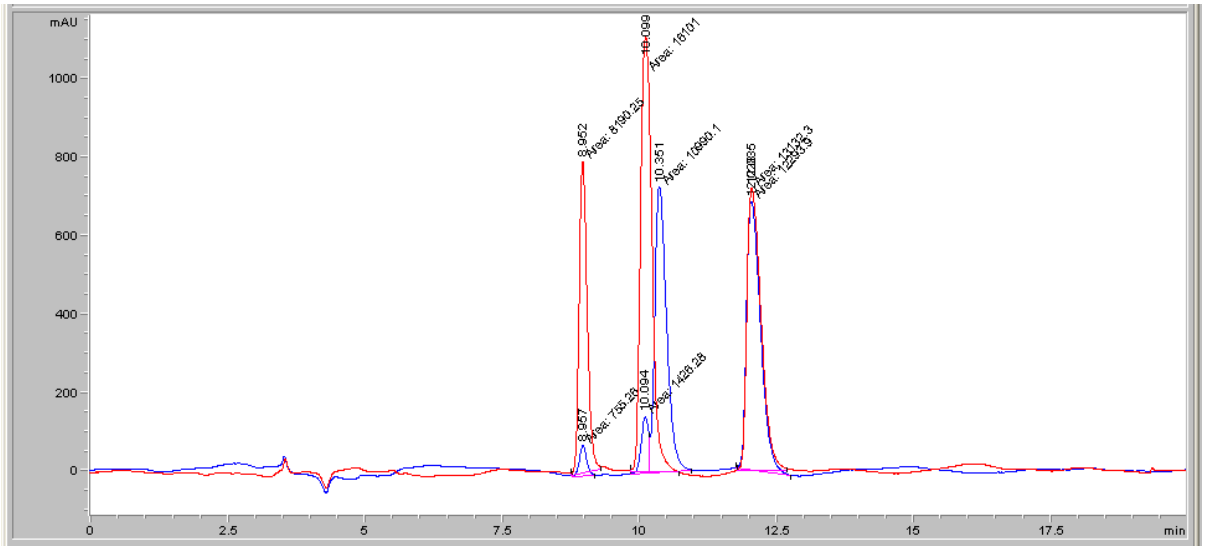

Enantiomeric excess (*e.e.*) of (*R*)-MTQ

Supplementary Table 1: Expected and actual percentages of (*S*)-MTQ and (*R*)-MTQ after repeated cycles of oxidation and reduction.

	Percentage after					
	0 cycles	1 cycle	2 cycles	3 cycles	4 cycles	5 cycles
(*S*)-MTQ (expected)	50	25	12.5	6.25	3.125	1.563
(*R*)-MTQ (expected)	50	75	87.5	93.75	96.875	98.438
(*S*)-MTQ (actual)	49	29	16	9	6	2
(*R*)-MTQ (actual)	51	71	84	91	94	98

Pd(II) reduction rates using hydrogen

Supplementary Figure 2: Removal of soluble Pd(II) from solution during reduction by *E. coli* MC4100, with hydrogen as the electron donor. Palladium in the supernatant was measured using the Perkin-Elmer Optima 5300 dual view ICP-AES.

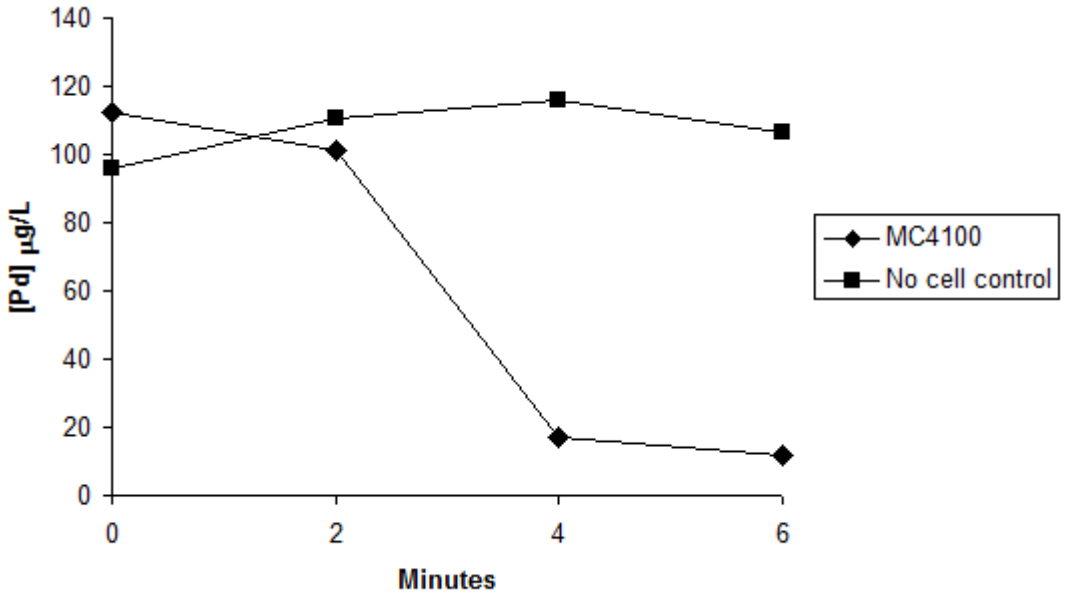

Oxidation and reduction experiments using cells previously used in a 5 cycle biotransformation

Supplementary Figure 3: cells used in a 5-cycle biotransformation were collected by centrifugation and washed with potassium phosphate buffer and used in further oxidation-only experiments. The activity of the MAO-N-D5 enzyme in the whole cells after the 5-cycle biotransformation remained the same as that prior to the biotransformation steps. All data points represent mean values from triplicate measurements, with standard error bars.

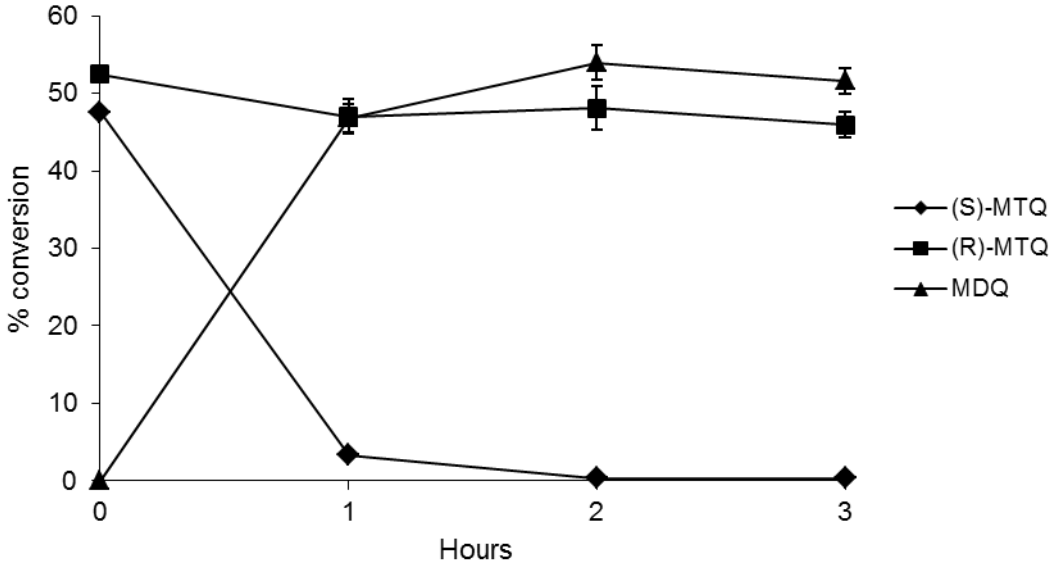

Supplementary Figure 4: cells used in a 5-cycle biotransformation were collected by centrifugation and washed with potassium phosphate buffer and used in further reduction-only experiments. The activity of the palladium after the 5-cycle biotransformation remained the same as that prior to the biotransformation steps. All data points represent mean values from triplicate measurements, with standard error bars.

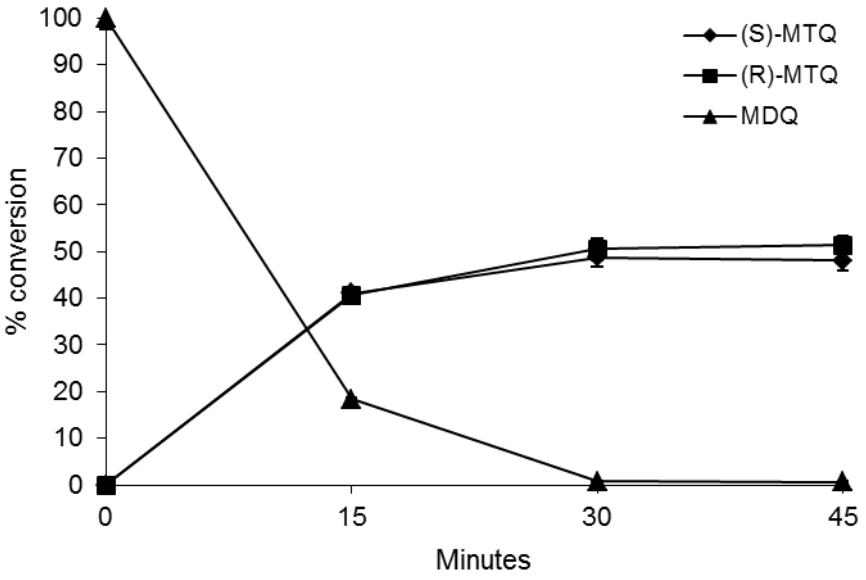

Comparison of activity with commercially available palladium

Supplementary Figure 5: A comparison of loss of palladium into the reaction supernatant from Bio-Pd and commercial Pd. After standing overnight, the Bio-Pd nanoparticles settled to the bottom of the experimental vessel (left), whereas the commercial Pd (right) could not be fully removed from the supernatant without filtering.

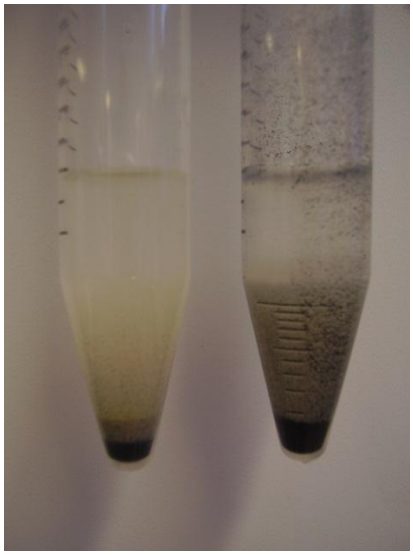

Chapter 5: A novel aerobic mechanism for palladium bioreduction and recovery by *Escherichia coli*

A novel aerobic mechanism for palladium bioreduction and recovery by *Escherichia coli*

Running title: Aerobic Pd(II) reduction

Contents category: Physiology and biochemistry

Joanne M. Foulkes[a], Kevin Deplanche[b], Frank Sargent[c], Lynne E. Macaskie[b], Jonathan R. Lloyd[a]*

a. Williamson Research Centre for Molecular Environmental Science and School of Earth, Atmospheric and Environmental Sciences, University of Manchester, Oxford Road, Manchester M13 9PL, UK

b. Unit of Functional Bionanomaterials, School of Biosciences, University of Birmingham, Edgbaston, Birmingham B15 2TT, UK

c. Division of Molecular Microbiology, College of Life Sciences, University of Dundee, Dundee DD1 5EH, UK

*Corresponding author, email jon.lloyd@manchester.ac.uk

Tel: +44 (0)161 275 7155

Fax: +44 (0)161 306 3961

Escherichia coli is a Gram-negative bacterium with a flexible respiratory metabolism. *E. coli* grows optimally aerobically while utilising molecular oxygen (O_2) as terminal electron acceptor. In the absence of O_2, *E. coli* continues to survive by switching to either a fermentative growth or by utilising alternative compounds, e.g. nitrate, as

terminal electron acceptors. The respiratory activity of *E. coli* can also be harnessed to drive biotechnologically-important activities, for example on in the bio-reduction of precious metal ions to recover the metal. In this work, aerobically-grown whole cells of *E. coli* were shown to reduce Pd(II) and precipitate Pd(0) nanoparticles via a novel mechanism using formate as the electron donor. The reductive transformation of palladium was monitored in real-time using extended X-ray absorption fine structure (EXAFS), and subsequent TEM analysis showed that the Pd(0) nanoparticles, confirmed by XRD, were precipitated outside the cells. The rate of reduction of Pd(II) was measured using *E. coli* mutants deficient in a range of oxidoreductases, including the [NiFe] hydrogenases and the molybdenum-dependent formate dehydrogenases. Results from these aerobic experiments suggested a novel, molybdoprotein-mediated mechanism is at play, which is completely distinct from the hydrogenase-mediated Pd(II) reduction previously described for anaerobically-grown *E. coli* cultures. The potential implications for Pd(II) recovery and bioPd catalyst fabrication are discussed.

INTRODUCTION

The microbial reduction of metals and radionuclides has attracted much recent interest, as it can be potentially harnessed for bioremediation, metal recovery, the fabrication of novel nanobiominerals and even energy generation in biobatteries (Lloyd, 2003; Lloyd *et al.*, 2008; Lovley, 2006). For example, the sulfate-reducing bacterium (SRB) *Desulfovibrio desulfuricans* has been shown to use a periplasmic hydrogenase supplied with hydrogen to reduce soluble Pd(II), resulting in the precipitation of Pd(0) nanoparticles in the periplasm of the cell, however SRB produce H_2S, a potent catalyst poison that must be removed before making the bioPd. Other organisms capable of this metal bioreduction include the Gram-negative bacteria *Shewanella oneidensis* (De Windt *et al.*, 2005), *Escherichia coli* (Mabbett *et al.*, 2006), *Pseudomonas putida*,

Cupriavidus necator (Sobjerg *et al.*, 2009), *C. metallidurans* (Gauthier *et al.*, 2010), *Paracoccus denitrificans* (Bunge *et al.*, 2010), *Rhodobacter sphaeroides* (Redwood *et al.*, 2008) and *R. capsulatus* (Wood *et al.*, 2010), and the Gram-positive bacteria *Bacillus sphaericus* (Creamer *et al.*, 2007a; Creamer *et al.*, 2007b), *Arthrobacter oxidans* (Wood *et al.*, 2010), *Staphylococcus sciuri* (Sobjerg *et al.*, 2009) and *Clostridium pasteurianum* (Chidambaram *et al.*, 2010; Deplanche *et al.*, 2011). This property has allowed the use of the palladised whole cell or processed biomineral ("bioPd") directly in industrially important reactions, often showing superior activity compared with a commercially available carbon-supported palladium catalyst. A number of studies have investigated the catalytic activity of bioPd, demonstrating its use in the evolution of H_2 from sodium hypophosphite (Yong *et al.*, 2002), the reduction of Cr(VI) to Cr(III) (Mabbett *et al.*, 2002; Mabbett *et al.*, 2004), the dehalogenation of chlorophenol, polychlorinated biphenyls, polybrominated diphenyl ethers (Baxter-Plant *et al.*, 2003; De Windt *et al.*, 2005; Harrad *et al.*, 2007), trichloroethylene (Hennebel *et al.*, 2009a; Hennebel *et al.*, 2009b), and the pesticide γ-hexachlorocyclohexane (Mertens *et al.*, 2007), the hydrogenation of itaconic acid (Creamer *et al.*, 2007a; Creamer *et al.*, 2007b) and 2-pentyne (Bennett *et al.*, 2010), and the application of bioPd as a fuel cell electrocatalyst to produce electricity from hydrogen (Yong *et al.*, 2007). In each case where the bioPd was compared with an abiotically-produced palladium catalyst (finely-divided or supported on a carbon matrix), the bioPd was more active or at least as active as the commercially available alternative.

Of the organisms shown to produce bioPd to date, *E. coli* provides a very useful model organism since it is facultatively anaerobic and has well-defined molecular tools to elucidate reaction mechanisms under aerobic and anaerobic conditions. The enzymes

thought to be involved in the bioreduction of palladium by *E. coli* under the latter conditions are the nickel-dependent hydrogenase enzymes Hyd-1, Hyd-2, and Hyd-3, and the formate dehydrogenase molybdoenzymes FDH-N, and FDH-H. Another molybdoenzyme, FDH-O, is expressed under both aerobic and anaerobic conditions. A possible role for FDH-O is to allow bacteria to adapt rapidly to a sudden shift from aerobic respiration to anaerobiosis, before FDH-N has been produced in sufficient amounts to continue formate metabolism (Abaibou *et al.*, 1995). Hyd-1, Hyd-2, FDH-O, and FDH-N are membrane-bound and periplasmically oriented, whereas Hyd-3 and FDH-H are subunits of the formate hydrogenlyase (FHL) complex, an intracellular enzyme complex that is also membrane-bound but which faces into the cytoplasm. The mechanisms responsible for the formate-dependent bioreduction by anaerobically-grown cultures of *E. coli* have been studied, and it has been shown that the hydrogenase enzymes Hyd-1 and Hyd-2 are mainly responsible for Pd(II) bioreduction (Deplanche *et al.*, 2010). In a study of formate-dependent Pd(II) bioreduction by *D. fructosovorans*, the deletion of the periplasmic hydrogenases caused the Pd(0) nanoparticles to be relocated to the cytoplasmic membrane site of the remaining hydrogenases, indicating that the periplasmic hydrogenases are at least partially involved (Mikheenko *et al.*, 2008).

The growth yield of anaerobic cultures is also lower than that of aerobic cultures, and for economic production at scale a method of growth of high biomass density is required. When using anaerobic cultures there is also the cost of supplementing with sodium fumarate and glycerol. For production of hydrogen by *E. coli* aerobic pre-growth to high cell density followed by anaerobiosis yielded cells capable of making bioPd catalytically active in the hydrogenation of soybean oil (Zhu *et al.*, 2011). However the catalytic activity of bioPd made by cells which were used for hydrogen

fermentation and then transferred into anaerobic conditions to 'prime' the hydrogenases was lower than for cells grown anaerobically throughout (Zhu *et al.*, 2011). Since the catalytic activity of bioPd relates to the specific enzyme responsible for its manufacture (Deplanche *et al.*, 2010; Rousset *et al.*, 2006) and it is not known to what extent 'aerobic' enzymes cease to be active under anaerobic conditions, the purpose of this study was to investigate the role of enzymes in aerobically-grown cells in the reduction of Pd(II). It is possible that such enzymes may 'dilute out' anaerobic enzymes responsible for the manufacture of the highest quality bioPd and such a nuisance effect may need to be removed for industrial bionanocatalyst production.

The dual aims of this study are to establish whether *E. coli* cells grown aerobically are capable of manufacturing bioPd and to identify the enzyme(s) responsible for such metal reduction. A move away from the need for anaerobic growth would simplify the preparation of catalyst at industrial scale.

METHODS

Bacterial growth

Starter cultures: 50 ml LB broth in a 500 ml Erlenmeyer flask was inoculated with a single isolated colony of the *E. coli* strain under investigation and incubated aerobically (37°C, shaking at 180 rpm for 18 hours).

Aerobic cultures: An 11 ml starter culture was added to 99 ml LB broth in a 1 L Erlenmeyer flask. Flasks were incubated for 24 hours (37°C, 180 rpm) to produce stationary phase "resting" cells. The pH of the cells after 24 hours incubation was measured to determine that organic acids had not been produced that would lower the pH considerably (Vasala *et al.*, 2006). Oxygen saturation of a 5 ml aliquot of the broth

culture was measured immediately after 24 hours of incubation using an Oakton D06 Acorn Series dissolved oxygen meter.

Reduction of Pd(II) to produce bioPd on bacteria

The aerobically grown liquid culture was divided between two 50 ml Falcon tubes and washed three times in 20 ml MOPS-NaOH (morpholinepropanesulfonic acid) buffer, 20 mM at pH7.6 after centrifugation for 20 minutes at 2500 *g*. Cell pellets were adjusted to a mass of 250 mg wet pellet weight, and resuspended in the MOPS-NaOH buffer to a volume of 1 ml. One tube of 250 mg wet weight cells was resuspended in 22.5 ml MOPS-NaOH buffer with 1 mM sodium tetrachloropalladate in a 30 ml bottle sealed with a butyl rubber stopper. The bottle was incubated in the dark at 30°C for 1 hour for the Pd(II) to biosorb to the cells (Baxter-Plant *et al.*, 2003). 2.5 ml 10 mM sodium formate was then added to the bottle to initiate bioreduction of the Pd(II).

Extended X-ray absorption fine structure (EXAFS)

Aliquots of the cell/Pd/formate suspension were taken at times 0 and 30 minutes, and 1, 3 and 4 hours from the addition of formate, and frozen immediately in liquid nitrogen. The direct reduction of Pd(II) to Pd(0) was demonstrated using EXAFS, performed at the European Synchrotron Radiation Facility (ESRF), in Grenoble, France. The samples were transported to the synchrotron at ESRF on dry ice, where they were thawed and injected immediately into sample holders, before freezing once more in liquid nitrogen and placing into the beam. X-ray absorption data were collected on beamline BM29 at the Pd K–edge in the energy range 24,200 – 24,900 eV. Data were recorded at low temperature (77 K) and under vacuum to reduce the thermal Debye-Waller factor and prevent oxidation. A Si(111) double crystal monochromator was used, calibrated with a Pd foil, and the spectra were collected in fluorescence mode using a

13-element solid-state detector. A reference spectrum of a palladium foil was recorded in transmission mode on station 9.3 at the SRS Daresbury. The data were background subtracted and the EXAFS spectra fitted in DL_Excurv (http://www.cse.scitech.ac.uk/cmg/EXCURV/) using full curved wave theory (Gurman *et al.*, 1984).

Use of mutants to determine electron transfer pathway to Pd(II)

In order to investigate the possible role of the aerobic formate dehydrogenase (FDH-O) and other hydrogenase/formate dehydrogenase enzymes in the reduction of Pd(II) by aerobically-grown cells of *E. coli*, the rates of reduction by six additional different strains (Table 1) were compared by measuring the Pd(II) remaining in solution by ICP-MS. The strains were 'palladised' as above, and rates of reduction/removal compared to that in a series of controls – killed cells (MC4100), cell-free suspension, and live cells (MC4100) unsupplemented with formate.

All strains except BL21(DE3) were from the culture collection of Professor Frank Sargent at the College of Life Sciences, University of Dundee. Strain BL21(DE3) was obtained from Invitrogen, Paisley, UK. Strain MC4100 Δ*moaA* was created by disruption of the *moaA* gene which encodes the molybdenum cofactor biosynthesis protein A, using the method of Datsenko and Wanner (2000) whereby PCR products are used to disrupt the gene of choice by recombination using the plasmid-borne phage λ Red recombinase.

Table 1: *E. coli* strains used to determine biological involvement in the reduction of palladium (II) using formate as the electron donor.

Strain	**Genotype**	**Phenotype**	**Reference**
BL21(DE3)	*F2 ompT gal dcm lon* $hsdS_B(r_B^- m_B^-)$ λ(DE3 [*lacI lacUV5-T7 gene 1 ind1 sam7 nin5*])	Wild type strain commonly used for recombinant protein expression.	(Studier & Moffatt, 1986)
MC4100	*F-* Δ*lacU169 araD139 rpsL150 relA1 ptsF rbs flbB5301*	Parental strain for FTD128 and Δ*moaA*.	(Casadaban & Cohen, 1979)
BW25113	$lacI^q$ $rrbB_{T14}$ Δ$lacZ_{WJ16}$ *hsd*R514 Δ$araBAD_{AH33}$ Δ$rhaBAD_{LD78}$	Parental strain for JW2682 and JW3865.	(Datsenko & Wanner, 2000)
FTD128	As MC4100, with in-frame deletion in the *fdhE* gene.	FDH-O & FDH-N negative.	(Luke *et al.*, 2008)
JW2682	As BW25113, with in-frame deletion of the *hypF* gene.	Deficient in all hydrogenases.	(Baba *et al.*, 2006)
JW3865	As BW25113, with in-frame deletion of the *fdoG* gene.	FDH-O negative.	(Baba *et al.*, 2006)
MC4100 Δ*moaA*	As MC4100, disruption of the *moaA* gene.	Deficient in all molybdoenzymes	This study.

X-ray diffraction (XRD) analysis

The black precipitates were washed once in acetone and air dried, before analysis by X-ray diffraction (XRD). The measurements were performed on a Bruker D8 Advance diffractometer, using Cu K alpha1 radiation. The samples were scanned from 5-70 degrees 2theta in steps of 0.2 degrees, with a count time of 2 seconds per step.

Transmission electron microscopy (TEM) and energy dispersive X-ray spectroscopy (EDS)

Following Pd(II) reduction, cells were stored at 10°C. After 24 hours, the cell pellets were rinsed twice with deionised water, fixed in 2.5% (wt/vol) glutaraldehyde, centrifuged for 5 minutes at 15,996 *g*, resuspended in 1.5 ml of 0.1 M cacodylate buffer (pH 7) and stained in 1% osmium tetroxide in 0.1 M phosphate buffer, pH 7 (60 min). Cells were dehydrated using an ethanol series (70, 90, 100, 100, 100% dried ethanol, 15 min each) and washed twice in propylene oxide (15 min, 9500 g). Cells were embedded in epoxy resin and the mixture was left to polymerise (24 h; 60°C). Sections (100-150 nm thick) were cut from the resin block, placed onto a copper grid and viewed with a JEOL 1200CX2 TEM, accelerating voltage 80 keV. EDS was performed on electron-dark areas, to confirm the presence of palladium.

RESULTS

Palladisation of *E. coli* BL21(DE3)

The pH of the aerobically-grown liquid culture was between 7.7-7.9, indicating that there was no considerable production of organic acids due to overflow metabolism. Oxygen saturation measurements showed that the liquid culture was 72% saturated following 24 hours of incubation, indicating that it was not oxygen-limited. The palladium was seen to be completely removed from solution within 45 minutes (Fig. 1a) as confirmed by ICP-MS, and the presence of crystalline Pd(0) was confirmed using XRD.

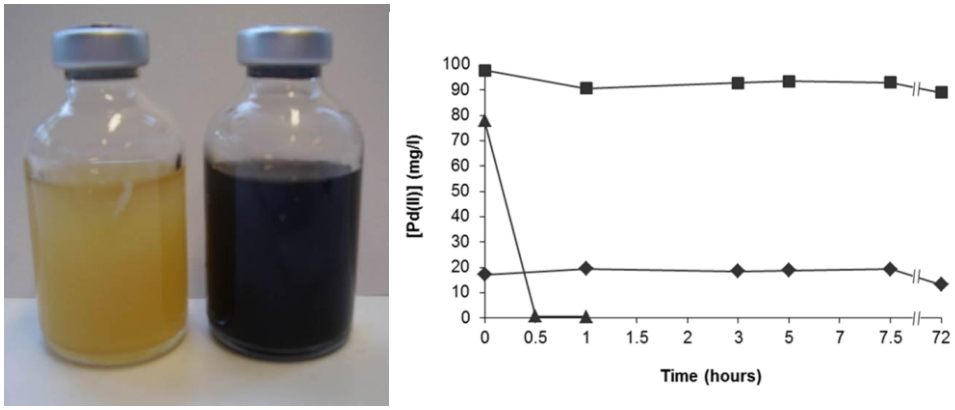

Figure 1: a) complete reduction of Pd(II) to Pd(0) by an aerobically-grown culture of *E. coli*. Both bottles contain cells resuspended in 20 mM MOPS buffer at pH7.6, and 1 mM sodium tetrachloropalladate (total volume 25 ml). This image was taken 45 minutes after the addition of formate to the bottle on the right. b) controls showing no abiotic reduction of Pd(II). Time is in hours from the addition of formate. Controls used were killed (autoclaved) cells, cell-free suspension, and a positive control containing MC4100. Soluble Pd(II) in the supernatant was measured using ICP-MS. ▲= MC4100; ■ = no cells; ♦ = killed cells.

Extended X-ray absorption fine structure (EXAFS)

The features in EXAFS are due to the wave-like nature of the photoelectron, which is released from the atom with increasing energy and scattered from surrounding atoms with new waves being emitted. With increasing photon energy, the interference between the waves alternates between constructive and destructive, which leads to oscillations in the spectrum. Examining these oscillations gives information on the number, species and distance of the surrounding atoms. As seen in Figure 4.3, the samples taken at times 0 and 30 minutes, which contain Pd(II), have identical EXAFS spectra. The samples taken at 60 minutes onwards are identical to the Pd(0) foil control, which indicates that only Pd(0) was present. Reduction of the Pd(II) to Pd(0) was

therefore complete in less than 30 minutes, which was later confirmed by ICP-MS analysis.

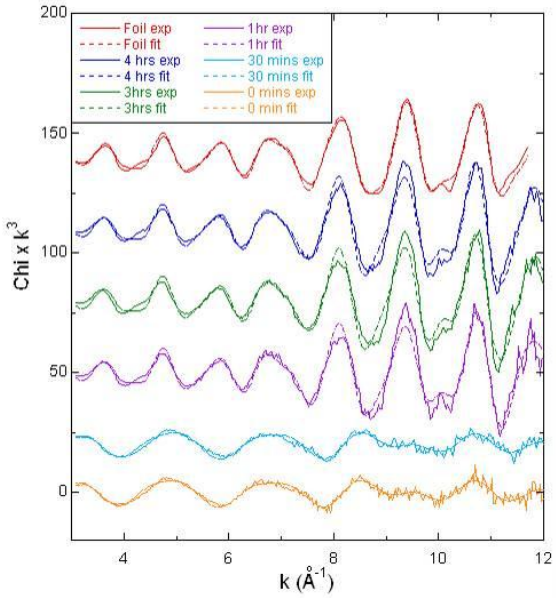

Figure 2: EXAFS data showing the presence of Pd(II) at 0 and 30 minutes (bottom two traces), and Pd(0) at 1, 3 and 4 hours. The top trace is palladium foil.

Use of mutants to determine electron transfer pathway to Pd(II)

Controls: The controls showed no abiotic reduction of Pd(II) using formate (Fig. 1b), although a brown precipitate was seen in the no-formate control. The X-ray diffraction pattern did not show the presence of any peaks characteristic of Pd(0) in this precipitate, indicating that it was probably amorphous and non-crystalline. Time 0 on Fig. 3 is the point at which formate was added, following one hour of incubation to allow biosorption of the Pd(II) to the cells. As the killed cell control has less than 20% of the original Pd(II) remaining, this indicates that an increased amount of sorption has taken place, possibly due to the increased surface area of the biomass.

Mutants: The parental strains MC4100 and BW25113 and the strain which lacked all hydrogenases (JW2682) removed Pd(II) identically with no residual Pd(II) detected after 30 minutes (Fig. 3). Removal of the hydrogenase enzymes had no effect of the

rate of palladium removal from solution, indicating that hydrogenases have no role in the aerobic reduction of Pd(II). The FDH-O-negative strain JW3865 reduced Pd(II) within 1 hour, and the FDH-O/FDH-N-negative strain FTD128 within 2 hours. Strain MC4100 Δ*moaA*, lacking all molybdoenzymes, reduced the palladium within 7 hours. These results indicate the likely involvement of the FDH-O enzyme in the reduction of Pd(II) by aerobically-grown *E. coli* using formate, although other Mo-containing enzymes must also be involved given the impaired metal reduction noted with the Δ*moa* mutant.

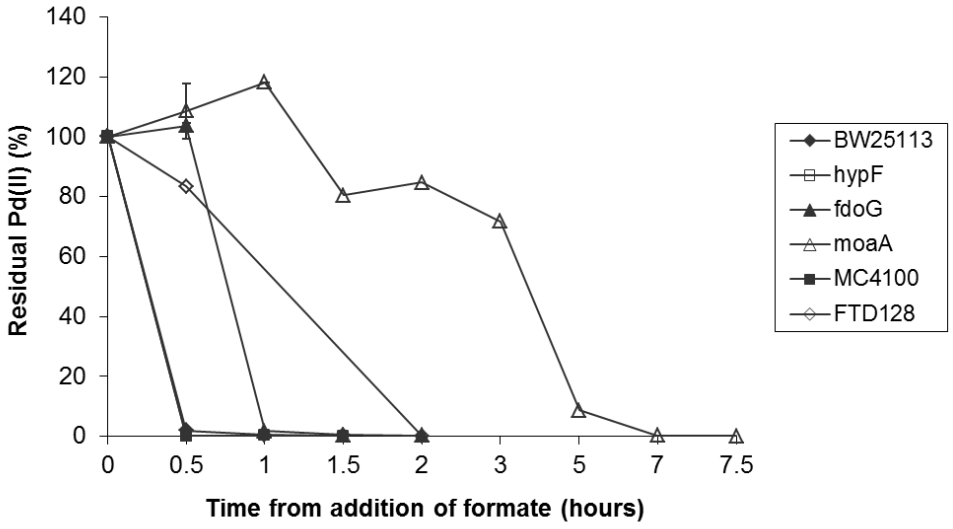

Figure 3: Pd(II) reduction by six different strains of *E. coli*, using formate as the electron donor. Soluble Pd(II) in the supernatant was measured using ICP-MS. ♦ = BW25113; □ = JW2682; ▲= JW3865; Δ = MC4100 Δ*moaA*; ■ = MC4100; ◊ = FTD128. Data points for BW25113, JW2682 and JW3865 are mean values of triplicate readings, with standard error shown.

Transmission electron microscopy (TEM)

TEM images of thin sections of cells showed that with all strains the reduced palladium was precipitated predominantly in the extracellular matrix of the cultures (Fig. 4),

although it appears that the nanoparticles may be associated with the outer membrane of the cells. Energy dispersive X-ray spectroscopy (EDS) confirmed the presence of palladium in these precipitates.

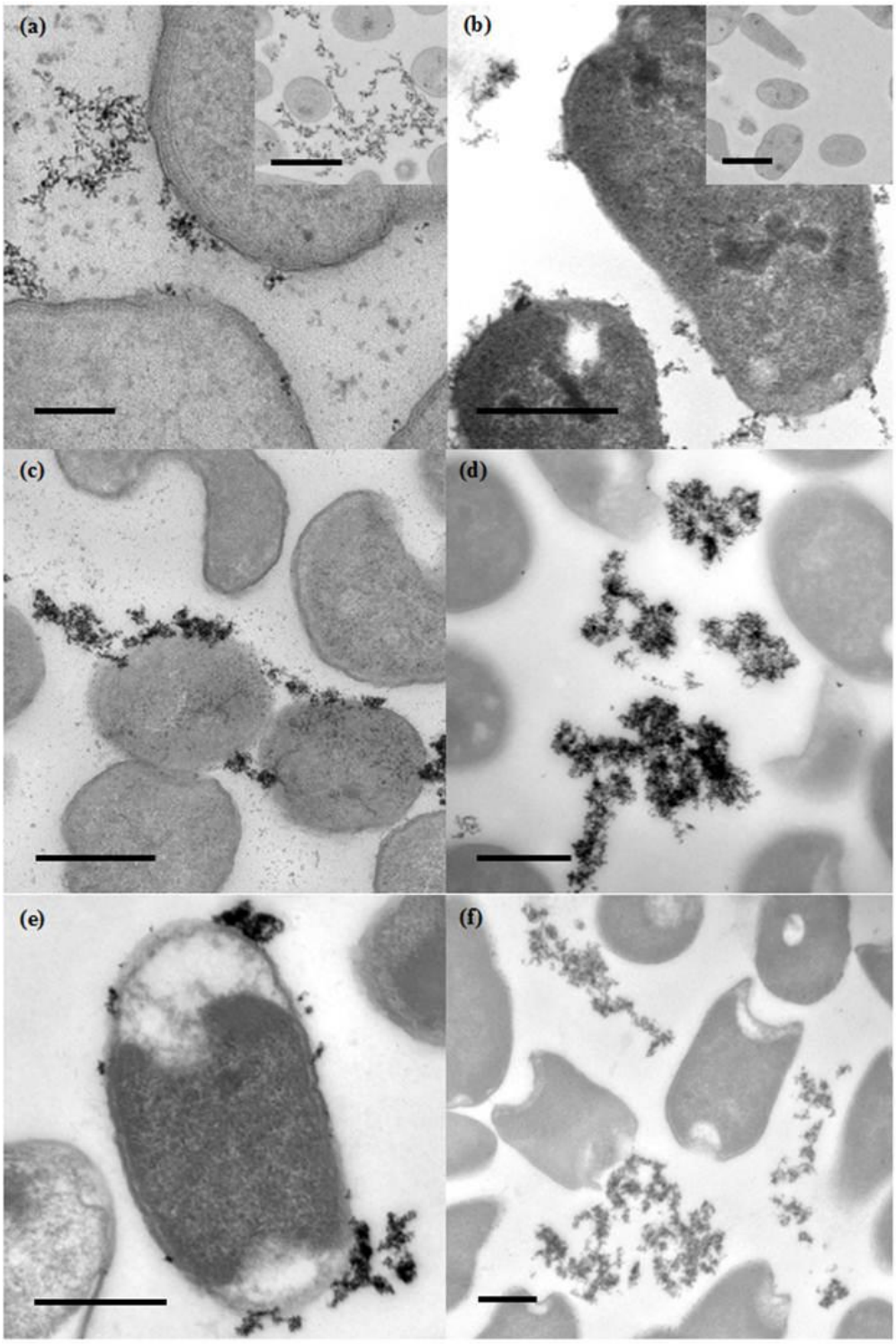

Figure 4: TEM of thin sections of aerobically grown cells showing extracellular palladium; a) MC4100, inset BL21(DE3); b) BW25113, inset BL21(DE3) (no Pd); c) FTD128; d) JW2682; e) MC4100 Δ*moaA*; f) JW3865. Scale bar a) = 100 nm; b)-f) = 500 nm; insets = 1μm.

DISCUSSION

The results above demonstrate that it is possible for aerobically-grown cultures of *E. coli* to enzymatically reduce Pd(II), with no need to de-aerate the experimental system during the bioreduction step. The only known aerobically-expressed molybdoenzyme (FDH-O) is involved, but it is not the only enzyme implicated. Autoclaved control experiments indicate that Pd(II) bioreduction in these cultures is enzymatic, with reduction of palladium not occurring in the absence of viable cells irrespective of the length of incubation. The major enzymes shown to be involved include the formate dehydrogenases FDH-O and FDH-N, although bioreduction still occurs in strains without these enzymes albeit at a much lower rate. Other molybdoenzymes must therefore be involved. The strain that lacked all molybdoenzymes however did still reduce the palladium, although this took 7 hours, compared with less than 30 minutes by the wild-type strains. Hydrogenases, implicated as the dominant Pd(II) reductases in other experimental systems (Deplanche *et al.*, 2010; Mikheenko *et al.*, 2008) are not expressed in aerobically grown cultures, and their lack of involvement was evident as the strain lacking any hydrogenase enzymes reduced palladium at the same rate as the wild-type strains.

Furthermore, whichever biological system is responsible for the aerobic bioreduction system, there seems to be little impact on the site of Pd(0) deposition. The location of the bioreduced Pd(0) in our experiments is almost always extracellular, although often

associated with the outer membrane of the cells. This is particularly the case with the MC4100 Δ*moaA* strain (which lacks all molybdoenzymes), in which the majority of the Pd(0) nanoparticles are closely associated with the outer membrane (Figure 4e). One conclusion that may be drawn from this is that whilst cells that lack the formate dehydrogenases are still capable of reducing Pd(II), when all of these enzymes are missing a cellular component associated with the outer membrane may be responsible. Furthermore, this formate oxidation activity is much weaker than that seen with the strains containing formate dehydrogenases, where Pd(II) reduction is more rapid. It is possible however that following the initial enzymatic reduction of a small percentage of the Pd(II), the Pd(0) nanoparticles formed may themselves be responsible for catalysing the reduction of the remainder of the Pd(II) (Yong *et al.*, 2002), which would mean that only a minor, initial biological input is required.

Although the formate dehydrogenase enzyme systems implicated in Pd(II) bioreduction by *E. coli* are periplasmic, the majority of the reduced Pd(0) precipitates outside the cell. It is possible that an electron shuttle system exists similar to that found in *Geobacter sulfurreducens* and *Shewanella oneidensis* (Lloyd *et al.*, 2003) that is as yet undiscovered in *E. coli*. It is also possible that the first Pd(0) nanoparticles to form breach the outer membrane, and themselves form an electron conduit for further Pd(II) reduction outside the cell. The pH of these experiments is also higher than others where Pd(0) nanoparticles accumulated in the periplasm (Redwood *et al.*, 2008), which could indicate the higher biosorption of cationic metals to the outer membrane and extracellular polymeric substances, which are then not able to enter the periplasm. The influence of a higher pH in the location of the Pd(0) may be confirmed by the observation that Pd(0) nanoparticles were located on the cell surface of *D. desulfuricans* when the bioreduction was performed at pH 7 (Yong *et al.*, 2002).

One limitation of using ICP-MS for the measurement of Pd(II) in solution is that palladium removal is measured rather than palladium reduction. This meant that the formation of a brown precipitate in the cell control lacking formate, and from 3-7 hours following formate addition in the MC4100 Δ*moaA* strain, implied Pd(II) reduction to Pd(0) where none had occurred. This precipitate may be formed due to increased biosorption of the Pd(II) to viable cells over time. There is also removal of soluble Pd(II) when using autoclaved cells, possibly indicating that the increased surface area of the lysed cells leads to increased sorption of the Pd(II) to the biomass. In some cases, such as with the strains MC4100 and FTD128, the reduced palladium particles were so small that they could not be removed from the reaction supernatant, and gave a false impression of the amount of Pd(II) remaining in solution. Synchrotron radiation techniques such as X-ray absorption would be better to measure bioreduction, as it provides the oxidation state of the palladium. However, the time constraints involved in securing beam time made this approach unfeasible.

This study has demonstrated the presence of a novel biological mechanism responsible for the bioreduction of Pd(II) in aerobically-grown cultures of *E. coli*, catalysed mainly by molybdenum-containing enzyme systems. Subsequent studies will investigate the catalytic activity of the Pd(0) nanoparticles produced under aerobic conditions in a range of industrially important reactions. If active, this new form of bioPd has the advantage over that produced by anaerobic culture as it is easier to produce and perform and provides increased biomass. There is also no requirement for additional processing steps to remove H_2S (produced by SRB systems), and the use of formate instead of hydrogen gas means that the procedure is less hazardous and more controllable.

Acknowledgements The authors would like to thank Dr John Charnock of the University of Manchester for analysis of EXAFS data.

REFERENCES

Abaibou, H., Pommier, J., Benoit, S., Giordano, G. & Mandrandberthelot, M. A. (1995). Expression and characterization of the *Escherichia coli fdo* Locus and a possible physiological role for aerobic formate dehydrogenase. *Journal of Bacteriology* **177**, 7141-7149.

Baba, T., Ara, T., Hasegawa, M. & other authors (2006). Construction of *Escherichia coli* K-12 in-frame, single-gene knockout mutants: the Keio collection. *Molecular Systems Biology* **2**, Article no. 2006.0008.

Baxter-Plant, V., Mikheenko, I. P. & Macaskie, L. E. (2003). Sulphate-reducing bacteria, palladium and the reductive dehalogenation of chlorinated aromatic compounds. *Biodegradation* **14**, 83-90.

Bennett, J. A., Creamer, N. J., Deplanche, K., Macaskie, L. E., Shannon, I. J. & Wood, J. (2010). Palladium supported on bacterial biomass as a novel heterogeneous catalyst: A comparison of Pd/Al_2O_3 and bio-Pd in the hydrogenation of 2-pentyne. *Chemical Engineering Science* **65**, 282-290.

Bunge, M., Sobjerg, L. S., Rotaru, A. E. & other authors (2010). Formation of palladium(0) nanoparticles at microbial surfaces. *Biotechnology and Bioengineering* **107**, 206-215.

Casadaban, M. J. (1976). Transposition and fusion of the *lac* genes to selected promoters in *Escherichia coli* using bacteriophage lambda and mu. *Journal of Molecular Biology* **104**, 541-555.

Chidambaram, D., Hennebel, T., Taghavi, S., Mast, J., Boon, N., Verstraete, W., van der Lelie, D. & Fitts, J. P. (2010). Concomitant microbial generation of palladium nanoparticles and hydrogen to immobilize chromate. *Environmental Science & Technology* **44**, 7635-7640.

Creamer, N. J., Mikheenko, I. P., Deplanche, K., Yong, P., Wood, J., Pollmann, K., Selenska-Pobell, S. & Macaskie, L. E. (2007a). A novel hydrogenation and hydrogenolysis catalyst using palladized biomass of Gram-negative and Gram-positive bacteria. *Advanced Materials Research* **20-21**, 603-606.

Creamer, N. J., Mikheenko, I. P., Yong, P. & other authors (2007b). Novel supported Pd hydrogenation bionanocatalyst for hybrid homogeneous/heterogeneous catalysis. *Catalysis Today* **128**, 80-87.

Datsenko, K. A. & Wanner, B. L. (2000). One-step inactivation of chromosomal genes in *Escherichia coli* K-12 using PCR products. *Proceedings of the National Academy of Sciences of the United States of America* **97**, 6640-6645.

De Windt, W., Aelterman, P. & Verstraete, W. (2005). Bioreductive deposition of palladium (0) nanoparticles on *Shewanella oneidensis* with catalytic activity towards

reductive dechlorination of polychlorinated biphenyls. *Environmental Microbiology* **7**, 314-325.

Deplanche, K., Caldelari, I., Mikheenko, I. P., Sargent, F. & Macaskie, L. E. (2010). Involvement of hydrogenases in the formation of highly catalytic Pd(0) nanoparticles by bioreduction of Pd(II) using *Escherichia coli* mutant strains. *Microbiology* **156**, 2630-2640.

Deplanche, K., Murray, A. J., Mennan, C., Taylor, S. & Macaskie, L. E. (2011). Biorecycling of precious metals and rare earth elements. In *Nanomaterials*: InTech Publishing, in submission.

Gauthier, D., Sobjerg, L. S., Jensen, K. M., Lindhardt, A. T., Bunge, M., Finster, K., Skrydstrup, T. & Meyer, R. L. (2010). Environmentally benign recovery and reactivation of palladium from industrial waste by using Gram-negative bacteria. *Chemsuschem* **3**, 1036-1039.

Gurman, S. J., Binsted, N. & Ross, I. (1984). A Rapid, Exact Curved-Wave Theory for EXAFS Calculations. *Journal of Physics C-Solid State Physics* **17**, 143-151.

Harrad, S., Robson, M., Hazrati, S., Baxter-Plant, V. S., Deplanche, K., Redwood, M. D. & Macaskie, L. E. (2007). Dehalogenation of polychlorinated biphenyls and polybrominated diphenyl ethers using a hybrid bioinorganic catalyst. *Journal of Environmental Monitoring* **9**, 314-318.

Hennebel, T., Verhagen, P., Simoen, H., De Gusseme, B., Vlaeminck, S. E., Boon, N. & Verstraete, W. (2009a). Remediation of trichloroethylene by bio-precipitated and encapsulated palladium nanoparticles in a fixed bed reactor. *Chemosphere* **76**, 1221-1225.

Hennebel, T., Simoen, H., De Windt, W., Verloo, M., Boon, N. & Verstraete, W. (2009b). Biocatalytic dechlorination of trichloroethylene with bio-palladium in a pilot-scale membrane reactor. *Biotechnology and Bioengineering* **102**, 995-1002.

Lloyd, J. R. (2003). Microbial reduction of metals and radionuclides. *FEMS Microbiology Reviews* **27**, 411-425.

Lloyd, J. R., Lovley, D. R. & Macaskie, L. E. (2003). Biotechnological application of metal-reducing microorganisms. *Advances in Applied Microbiology* **53**, 85-128.

Lloyd, J. R., Pearce, C. I., Coker, V. S. & other authors (2008). Biomineralization: linking the fossil record to the production of high value functional materials. *Geobiology* **6**, 285-297.

Lovley, D. R. (2006). Microbial fuel cells: novel microbial physiologies and engineering approaches. *Current Opinion in Biotechnology* **17**, 327-332.

Luke, I., Butland, G., Moore, K. & other authors (2008). Biosynthesis of the respiratory formate dehydrogenases from *Escherichia coli*: characterization of the FdhE protein. *Archives of Microbiology* **190**, 685-696.

Mabbett, A. N., Lloyd, J. R. & Macaskie, L. E. (2002). Effect of complexing agents on reduction of Cr(VI) by *Desulfovibrio vulgaris* ATCC 29579. *Biotechnology and Bioengineering* **79**, 389-397.

Mabbett, A. N., Yong, P., Farr, J. P. G. & Macaskie, L. E. (2004). Reduction of Cr(VI) by "palladized" biomass of *Desulfovibrio desulfuricans* ATCC 29577. *Biotechnology and Bioengineering* **87**, 104-109.

Mabbett, A. N., Sanyahumbi, D., Yong, P. & Macaskie, L. E. (2006). Biorecovered precious metals from industrial wastes: Single-step conversion of a mixed metal liquid waste to a bioinorganic catalyst with environmental application. *Environmental Science & Technology* **40**, 1015-1021.

Mertens, B., Blothe, C., Windey, K., De Windt, W. & Verstraete, W. (2007). Biocatalytic dechlorination of lindane by nano-scale particles of Pd(0) deposited on *Shewanella oneidensis*. *Chemosphere* **66**, 99-105.

Mikheenko, I. P., Rousset, M., Dementin, S. & Macaskie, L. E. (2008). Bioaccumulation of palladium by *Desulfovibrio fructosivorans* wild-type and hydrogenase-deficient strains. *Applied and Environmental Microbiology* **74**, 6144-6146.

Redwood, M. D., Deplanche, K., Baxter-Plant, V. S. & Macaskie, L. E. (2008). Biomass-supported palladium catalysts on *Desulfovibrio desulfuricans* and *Rhodobacter sphaeroides*. *Biotechnology and Bioengineering* **99**, 1045-1054.

Rousset, M., Casalot, L., de Philip, P., Bélaich, A., Mikheenko, I. P. & Macaskie, L. E. (2006). Use of bacterium strains for the preparation of metallic biocatalysts, in particular for the preparation of palladium biocatalysts. European Patent Application Number: WO/2006/087334. International Application No. PCT/EP2006/05094.

Sobjerg, L. S., Gauthier, D., Lindhardt, A. T., Bunge, M., Finster, K., Skrydstrup, T. & Meyer, R. L. (2009). Bio-supported palladium nanoparticles as a catalyst for Suzuki-Miyaura and Mizoroki-Heck reactions. *Green Chemistry* **11**, 2041-2046.

Studier, F. W. & Moffatt, B. A. (1986). Use of bacteriophage T7 RNA polymerase to direct selective high level expression of cloned genes. *Journal of Molecular Biology* **189**, 113-130.

Vasala, A., Panula, J., Bollok, M., Illmann, L., Halsig, C. & Neubauer, P. (2006). A new wireless system for decentralised measurement of physiological parameters from shake flasks. *Microbial Cell Factories* **5**.

Wood, J., Bodenes, L., Bennett, J., Deplanche, K. & Macaskie, L. E. (2010). Hydrogenation of 2-butyne-1,4-diol using novel bio-palladium catalysts. *Industrial & Engineering Chemistry Research* **49**, 980-988.

Yong, P., Rowson, N. A., Farr, J. P. G., Harris, I. R. & Macaskie, L. E. (2002). Bioreduction and biocrystallization of palladium by *Desulfovibrio desulfuricans* NCIMB 8307. *Biotechnology and Bioengineering* **80**, 369-379.

Yong, P., Paterson-Beedle, M., Mikheenko, I. P. & Macaskie, L. E. (2007). From bio-mineralisation to fuel cells: biomanufacture of Pt and Pd nanocrystals for fuel cell electrode catalyst. *Biotechnology Letters* **29**, 539-544.

Zhu, J., Mikheenko, I. P., Deplanche, K., Bennett, S. J., Redwood, M. D., Orozco, R. L., Wood, J. & Macaskie, L. E. (2011). Hydrogenation of soybean oil using Bio-Pd catalyst. In *Second Int Conf on Multifunctional Hybrid Nanomaterials*. Strasbourg, France, 6-10 March, 2011: Proceedings,Hybrid Materials 2011.

Chapter 6: The immobilisation of a biometallic whole cell catalyst for multi-step transformations

The immobilisation of a biometallic whole cell catalyst for multi-step transformations

Joanne M Foulkes[a], Kirk J Malone[b], Nicholas J Turner[b], Jonathan R Lloyd[a]*

a. Williamson Research Centre for Molecular Environmental Science and School of Earth, Atmospheric and Environmental Sciences, University of Manchester, Oxford Road, Manchester M13 9PL, UK

b. School of Chemistry, University of Manchester, Manchester Interdisciplinary Biocentre, 131 Princess Street, Manchester M1 7DN, UK

**Corresponding author;*

Tel: +44 (0)161 275 7155

Fax: +44 (0)161 306 3961

e-mail: jon.lloyd@manchester.ac.uk

ABSTRACT

We have previously developed a biometallic catalyst for the cyclic deracemisation of amines, using *Escherichia coli* transformed with a variant monoamine oxidase gene (*mao-N-D5*), and loaded with bioreduced Pd(0) nanoparticles. Here, this new biocatalyst is immobilised in alginate beads, to facilitate re-use, and through freeze-drying to increase its stability during storage. Encapsulation had no effect on the activity of either the enzyme or the biogenic Pd(0) catalyst, as the amine substrate was deracemised to give the (*R*)-enantiomer in up to 91% enantiomeric excess following

five cycles of oxidation and reduction reactions using either immobilised or planktonic cells. Loss of palladium from the immobilised biometallic catalyst was minimised, with ICP-MS data showing that only 9.8 μg l^{-1} palladium was lost into the reaction supernatant following deracemisation using the immobilised biocatalyst, compared with 63.4 μg l^{-1} without immobilisation in alginate. The storage time of the beads was successfully increased to up to six weeks (the time limit of this experiment) by freeze-drying the beads and storing under vacuum.

Keywords: palladium catalyst, *Escherichia coli*, biocatalysis, biotransformation, deracemisation, immobilisation, alginate.

INTRODUCTION

The production of functional biominerals by microbial routes presents a green technology capable of leading to a permanent shift towards the biosynthesis of nanomaterials. Recent developments in the production of biominerals include precious metal catalysts (Coker *et al.*, 2010; Macaskie *et al.*, 2010), nanomagnets for hyperthermic cancer treatment (Coker *et al.*, 2009), quantum dots (Pearce *et al.*, 2008), bioremediation agents (Cutting *et al.*, 2009), silver-based antimicrobials (Suresh *et al.*, 2010), and SERS probes (Jarvis *et al.*, 2008). We have previously also engineered a recombinant whole cell biocatalyst, exploiting the ease with which *Escherichia coli* can be genetically manipulated, as well as its ability to reduce soluble palladium (II) to nanoparticulate Pd(0) suitable for use in reduction reactions (Foulkes *et al.*, 2011).

The bioreduction of soluble Pd(II) to insoluble Pd(0) was first reported in anaerobic cultures of the sulphate-reducing bacterium (SRB) *Desulfovibrio desulfuricans* (Lloyd *et al.*, 1998), with the aim of recovering of palladium from industrial wastewaters. *D.*

desulfuricans was chosen for its high metal reductase activity and broad specificity. Using pyruvate, formate, and hydrogen as electron donors, the bacteria catalysed the reduction of Pd(II) to form nano-scale clusters of Pd(0) in the periplasm (detected by electron microscopy), via a process referred to as palladisation. A number of studies have investigated the catalytic activity of this material ("Bio-Pd"), demonstrating its use in processes including the evolution of H_2 from sodium hypophosphite (Yong *et al.*, 2002), the dehalogenation of chlorophenol, polychlorinated biphenyls, polybrominated diphenyl ethers (Baxter-Plant *et al.*, 2003; De Windt *et al.*, 2005; Harrad *et al.*, 2007), trichloroethylene (Hennebel *et al.*, 2009a; Hennebel *et al.*, 2009b), and the pesticide γ-hexachlorocyclohexane (Mertens *et al.*, 2007), the hydrogenation of itaconic acid (Creamer *et al.*, 2007a; Creamer *et al.*, 2007b), and the reduction of Cr(VI) to Cr(III) (Mabbett *et al.*, 2002; Mabbett *et al.*, 2004). In each case where the Bio-Pd was compared with an abiotically-produced palladium catalyst (finely-divided or supported on a carbon matrix), the Bio-Pd was more active or at least as active as the commercially available alternative. The mechanisms responsible for the formate-dependent bioreduction of Pd(II) by anaerobic cultures of *E. coli* have been studied, and have implicated the involvement of the hydrogenase enzymes Hyd-1 and Hyd-2 (Deplanche *et al.*, 2010).

The requirement for enantiomerically pure chiral amines in the pharmaceutical and agrochemicals industries has led to the requirement for biocatalysts that can generate up to 100% yield of products, with up to 100% *e.e.* (enantiomeric excess) (Alexeeva *et al.*, 2002). Previously published work has investigated the use of lipases and transaminases, using lipases for hydrolysis reactions and transaminases for the conversion of ketones to chiral amines. Lipases are also suitable for use with primary amines and some secondary amines only, with no activity towards tertiary amines

(Dunsmore *et al.*, 2006). Using a conceptually different approach, we have used the monoamine oxidase enzyme MAO-N-D5, a variant of the MAO-N enzyme of *Aspergillus niger* produced by directed evolution of the *mao-N* gene as an alternative enzyme in deracemisation reactions (Atkin *et al.*, 2008; Dunsmore *et al.*, 2006). *E. coli* cells transformed with the *mao-N-D5* gene can then be palladised to produce a multifunctional biocatalyst which generates imine intermediates by oxidation of the (*S*)-enantiomer of the amine, which are then non-selectively reduced back to the racemic amine by the Pd(0) catalyst (Figure 1). After several cycles of oxidation and reduction, a high yield and e.e. of the (*R*)-enantiomer is achieved (Foulkes *et al.*, 2011).

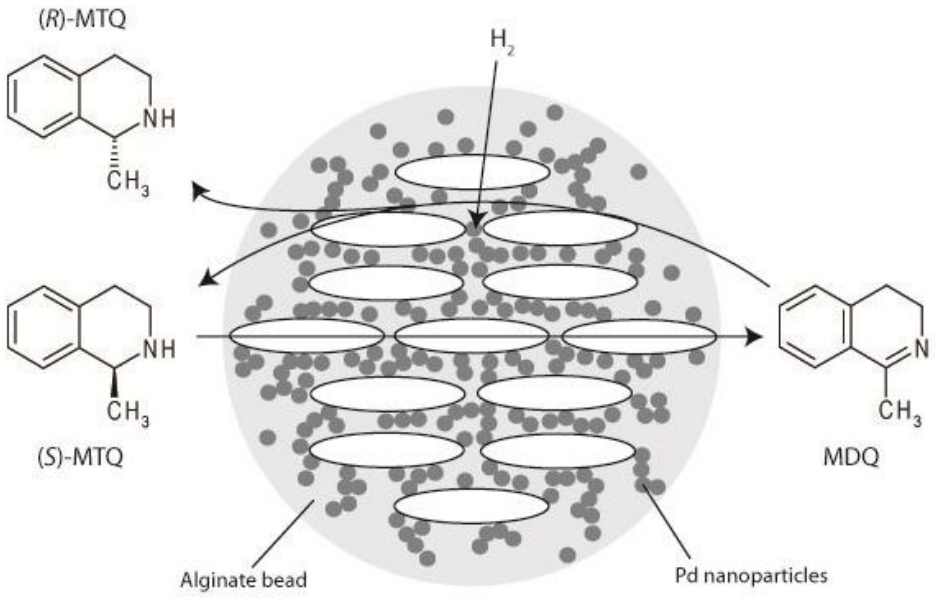

Figure 1: The cyclic deracemisation of 1-methyltetrahydroisoquinoline (MTQ) via the imine 1-methyl-3,4-dihydroisoquinoline (MDQ) using palladised *E. coli* cells with the *mao-N-D5* gene expressed, immobilised in an alginate bead.

Immobilisation matrices for biocatalysts are being used increasingly as they extend the viability of the cells, increase recyclability of the biocatalyst, and facilitate the separation of the biocatalyst from their products. Matrices used for the entrapment of

whole cells include hydrogels, such as calcium alginate and chitosan; thermogels, such as agar or agarose; and synthetic polymers, such as polyacrylamide and sol-gel.

The aim of this study was to demonstrate that palladised transformed *E. coli* cells that can be used for the deracemisation of amines can be immobilised successfully in a suitable polymeric matrix, in this case alginate, providing a superior biometallic catalyst for industrial use. The advantage of immobilisation is that the cells are kept separate from the substrate facilitating removal when the reaction is complete. Alginate was used in this study as it is non-toxic, and the method used for cell immobilisation avoids the use of toxic reagents or harsh processing steps (Hartmeier, 1988).

METHODS

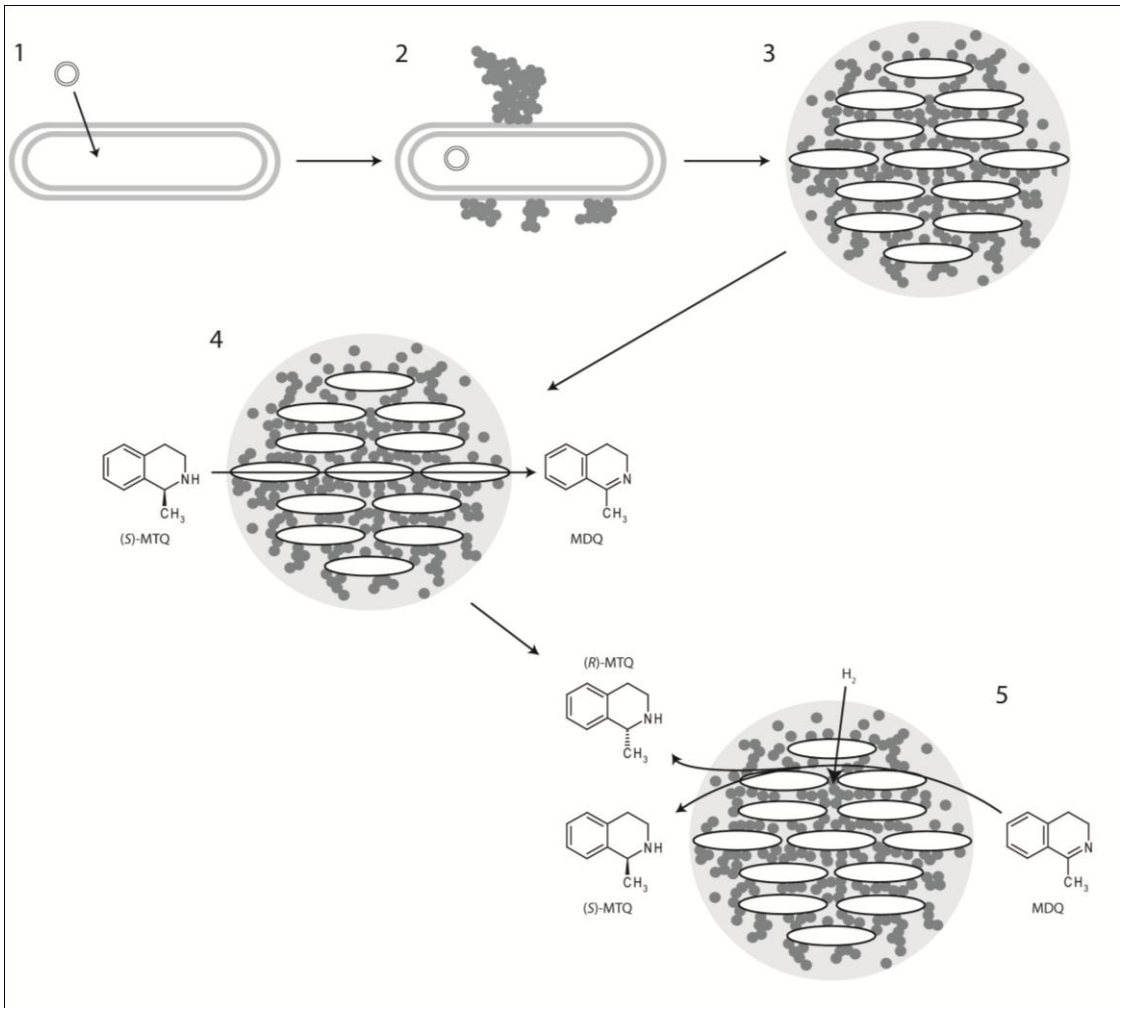

Figure 2: Schematic of methods. 1) transformation of *E. coli* with pET-16b plasmid containing *mao-N-D5* gene insert; 2) palladisation of transformed *E. coli*; 3) immobilisation of palladised cells in alginate beads; 4) oxidation of (*S*)-MTQ via expressed MAO-N-D5 enzyme; 5) reduction of MDQ via Pd(0) nanoparticles and hydrogen.

TRANSFORMATION OF *E. COLI* BL21 WITH PET-16B PLASMID CONTAINING THE *MAO-N-D5* INSERT

Strains and plasmid: *E. coli* BL21 cells were obtained from Invitrogen. The pET16-b plasmid containing the *mao-N-D5* insert and an ampicillin resistance gene was obtained from Dr Andrew Ellis at the Manchester Interdisciplinary Biocentre. Bacterial isolates were stored at -80°C, and the plasmid was stored at -20°C.

Transformation: Cells were transformed according to the supplier's instructions, using approximately 100 ng of plasmid. Transformed BL21 cells were subcultured onto LB agar plates containing 100 μg ml^{-1} ampicillin, and incubated overnight at 37°C before storage at 4°C for a maximum of 1 week.

PALLADISATION OF *E. COLI* BL21

The method used was that used previously, as adapted from that used by Lloyd and Macaskie (1998), as follows.

Starter cultures: 50 ml LB broth in a 500 ml Erlenmeyer flask was inoculated with a single isolated colony of the transformed *E. coli* and incubated overnight at 37°C, shaking at 180 rpm.

Flask cultures: An 11 ml starter culture was added to 99 ml LB broth containing 100 μg ml^{-1} ampicillin, in a 1 L Erlenmeyer flask. Flasks were incubated for 24 hours at 37°C, shaking at 180 rpm.

Palladisation: Each culture was divided between two 50 ml Falcon tubes (supplied by Fisher) and washed three times in 20 ml MOPS-NaOH (morpholinepropanesulfonic acid) buffer, 20 mM at pH7.6 after centrifugation for 20 minutes at 2500 *g*. Cell pellets were adjusted to a mass of 250 mg, based on the wet cell pellet, and resuspended MOPS-NaOH to a volume of 1 ml. Two tubes of each culture were resuspended in 25 ml buffer with 1 mM sodium tetrachloropalladate (supplied by Alfa Aesar) in 30 ml bottles sealed with butyl rubber stoppers (two bottles per culture). Bottles were incubated in the dark at 30°C for 1 hour for the Pd(II) to biosorb to the cells (Humphries *et al.*, 2006). One of each of the two different cultures was then purged with H_2 for 5 minutes, with H_2 allowed to fill the headspace. The remaining two bottles were H_2-negative controls.

X-RAY DIFFRACTION (XRD) ANALYSIS

The cells were coated in a black precipitate within a few minutes in bottles containing cells as Pd(II) purged with H_2. The palladised cells settled out leaving a clear colourless supernatant. The black precipitate was washed once in acetone and air-dried, before investigation by XRD. The measurements were performed on a Bruker D8 Advance diffractometer, using Cu Kalpha1 radiation. The samples were scanned from 5-70 degrees 2theta in steps of 0.2 degrees, with a count time of 2 seconds per step.

TRANSMISSION ELECTRON MICROSCOPY (TEM) AND ENERGY DISPERSIVE X-RAY SPECTROSCOPY (EDX)

Sections of the palladised cells were provided by EM facility in the Faculty of Life Sciences, University of Manchester. The bacteria were fixed in primary fixative (2.5% glutaraldehyde and 4% formaldehyde in 0.1M sodium cacodylate buffer at pH7.4) and secondary fixative (1% osmium tetroxide and 1.5% potassium ferrocyanide in 0.1M sodium cacodylate buffer at pH7.4) and dehydrated in a graded acetone series (30 minutes each in 50%, 70%, 90% and three changes at 100%) before embedding in TAAB LV medium epoxy resin. EDX was performed on electron-dark areas, to confirm the presence of palladium.

IMMOBILISATION OF PALLADISED TRANSFORMED CELLS IN ALGINATE

The method used for the immobilisation of palladised transformed cells in alginate beads was adapted from that of Hartmeier (1988). 1.2 g sodium alginate was dissolved in 42 ml distilled water, and 6 ml of palladised transformed *E. coli* cells (250 mg ml^{-1} in 20 mM MOPS-NaOH buffer at pH 7.6) were added to 350 ml dissolved alginate solution. The alginate-cell suspension was then dropped into 200 ml of a 2% w/v $CaCl_2$ solution using a plastic Pasteur pipette, whilst gently stirring to prevent bead aggregation. Alginate beads were left stirring for 1 hour to harden, after which time the $CaCl_2$ solution was diluted to 0.5% w/v with the addition of a further 600 ml distilled water. Beads were stored in the 0.5% w/v $CaCl_2$ solution and refrigerated until use (Figure 3c).

KINETICS OF SUBSTRATE OXIDATION AND REDUCTION

Oxidation: 5.35 g beads (equivalent to 250 mg ml^{-1} cells in 20 mM MOPS-NaOH buffer at pH 7.6) were rinsed in 0.1 M MOPS, and added to 10 ml 10 mM racemic

MTQ (obtained from GSK), made up in 0.1 M MOPS buffer at pH 7.6. The vessel used was a 120 ml gas bottle sealed with a butyl rubber stopper, providing a 110 ml headspace (Figure 3d). The reaction was allowed to proceed in air at 37°C, with shaking at 225 rpm. Samples were taken as required, by removing 500 µl supernatant in triplicate, and storing at -20°C before extraction with methyl-tert-butyl ether (MTBE). Beads were tested on day one, after one week, and after two weeks, in order to determine the loss of activity following storage at 10°C.

Reduction of MDQ with hydrogen as the electron donor: 5.35 g beads (equivalent to 250 mg ml^{-1} cells in 20 mM MOPS-NaOH buffer at pH 7.6) were rinsed in 0.1 M MOPS, and added to 10 ml 10 mM MDQ (1-methyl-3,4-dihydroisoquinoline, supplied by Acros Organics), made up in 0.1 M MOPS buffer at pH 7.6. The reaction volume was 10 ml, in a 120 ml gas bottle, providing a 110 ml headspace. The bottle was sparged with hydrogen for 90 seconds before incubating and extracting as previously. Beads were tested on day one, after one week, and after two weeks, in order to determine the loss of activity following storage.

HPLC analysis: The MTBE phase of the sample extract was dried with Na_2SO_4 and concentrated *in vacuo* to yield the MTQ as a colourless oil. The samples were resuspended in 200 µl isohexane prior to testing by normal phase chiral HPLC on an Agilent 1200 chromatograph, using a Daicel Chiralpak AD-H 4.6 mm x 250 mm column, at a flow rate of 1 ml min^{-1} for 20 minutes at 40°C with a mobile phase of 88% isohexane, 2% ethanol, and 10% isohexane containing 0.5% diethylamine. The analytes were detected by UV-Vis spectroscopy, at wavelengths of 220 nm (MTQ), and 254 nm (MDQ). The error (RSD) was 2.8%.

Integration of Processes for Deracemisation

Oxidation and reduction steps were performed as separate cycles, by flushing the vessel alternately with air or hydrogen. The reaction vessel was a 120 ml gas bottle with a 10 ml reaction volume, providing a 110 ml headspace. The vessel was first flushed with nitrogen to avoid the mixing of air and hydrogen. Each oxidation step was two hours long, and each reduction step was 45 minutes. Samples were taken at the end of each reduction step, for 5 cycles. The same beads were used in three consecutive deracemisation reactions over three days, with storage in the reaction mixture at 10°C overnight between reactions. Beads were rinsed briefly with 0.1 M MOPS buffer before addition to the substrate.

Measuring the loss of palladium into the reaction supernatant

Aliquots of reaction supernatant were analysed following a biotransformation, in order to measure the amount of palladium lost from the biocatalyst. The supernatant was digested with an equal volume of 70% nitric acid for 24 hours, diluted to 2% nitric acid, and filtered before analysis for the presence of palladium using an Agilent 7500cx ICP-MS.

Environmental Scanning Electron Microscopy (ESEM)

Biocatalyst-containing beads were examined using a Philips XL30 ESEM-FEG using ionised water vapour to disperse the charge from the sample surface, thus avoiding the need to carbon coat. The beads were imaged both before and after use in a deracemisation reaction, in order to determine any possible effects on the integrity of the beads.

USE OF FREEZE-DRIED BEADS IN OXIDATION AND REDUCTION REACTIONS

To assess the suitability of freeze-drying for the long-term storage of the biocatalyst, beads were frozen in liquid nitrogen and dried for 24 hours. The beads were stored at 10°C under vacuum until use.

RESULTS

PALLADISATION OF *E. COLI* BL21

Washed aerobically-grown *E. coli* BL21 cells containing the cloned gene expressing the enzyme MAO-N-D5 were palladised by challenging with 1 mM Pd(II) and hydrogen gas as an electron donor. The cells were coated in a black precipitate within a few minutes, indicating the reduction of Pd(II) to insoluble particles of Pd(0) (Lloyd *et al.*, 1998). Pd(II) did not reduce to Pd(0) in bottles that were not purged with H_2, or in the absence of cells. The black precipitate was analysed by X-ray diffraction to confirm the presence of elemental palladium (Figure 3a), although the signal was weak due the nanoparticulate nature of the sample. The size of the particles was calculated to be approximately 1 nm in diameter using the Scherrer equation.

TEM images of thin sections of cells showed that the reduced palladium was precipitated predominantly in the extracellular matrix of the cultures (Figure 3b). Energy dispersive X-ray spectroscopy (EDX) confirmed the presence of palladium in these electron dense nano-scale precipitates.

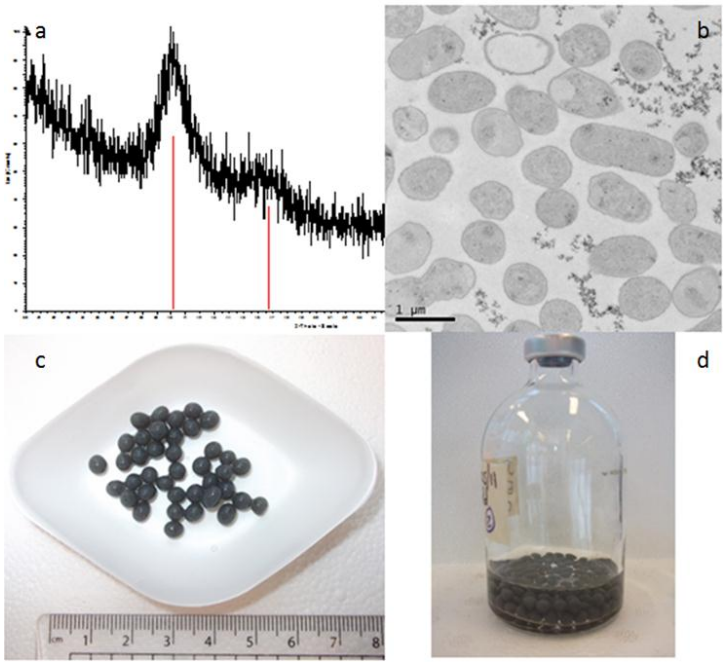

Figure 3: a) XRD showing presence of palladium on in the microbial cultures supplied with Pd(II) and hydrogen as the electron donor; b) TEM of thin sections of aerobically grown cells showing extracellular palladium; c) Alginate beads containing immobilised palladised *E. coli*; d) Alginate beads in reaction vessel, showing 10 ml substrate and 110 ml headspace.

KINETICS OF SUBSTRATE OXIDATION AND REDUCTION

When palladised transformed cells of *E. coli* immobilised in alginate beads were added to 10 mM racemic MTQ and incubated at 37°C, less than 7% (*S*)-enantiomer (0.7 mM) of the MTQ remained after two and a half hours (Figure 4a). The remainder was oxidised to MDQ, which made up 48% of the total product (4.8 mM). On consecutive oxidation reactions however, there was a loss of activity. By the third oxidation, 18% (*S*)-enantiomer (1.8 mM) still remained after 2.5 hours.

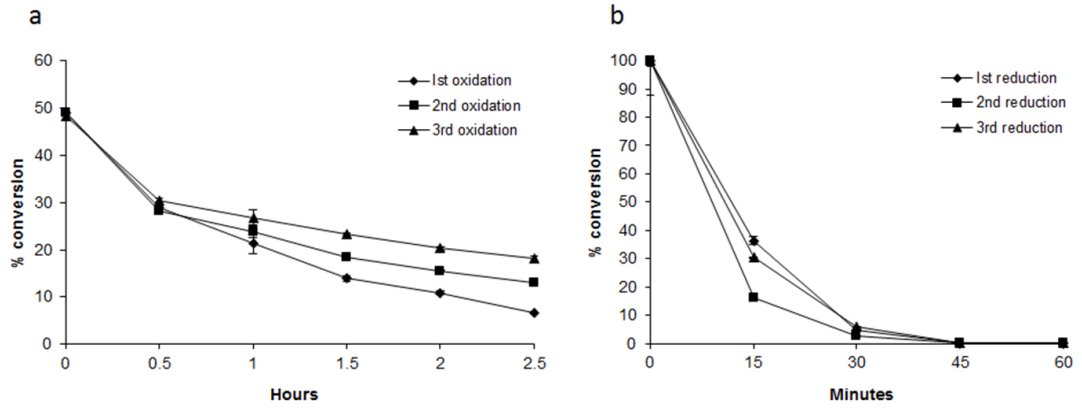

Figure 4: a) Three consecutive oxidations of (*S*)-MTQ to MDQ at 37°C, by cells of *E. coli* transformed with the *mao-N-D5* gene insert and immobilised in alginate beads; b) Three consecutive reductions of MDQ to racemic MTQ at 37°C, by palladised *E. coli* immobilised in alginate beads, using hydrogen gas as the electron donor. Triplicates of each time point were tested, and the error bars show the standard error.

When the immobilised cells were added to 10 mM MDQ, sparged with hydrogen gas for 90 seconds and incubated at 37°C, all of the MDQ was reduced to racemic MTQ within 45 minutes (Figure 4b). Re-use of the biocatalyst (three consecutive oxidation reactions followed by three consecutive reduction reactions) had no effect on the activity of the Pd(0) nanoparticles.

INTEGRATION OF PROCESSES FOR DERACEMISATION

To avoid the potentially hazardous mixing of air and hydrogen in the reaction vessel, oxidation and reduction steps for deracemisation were performed as separate cycles. Based on the results from the separate oxidation and reduction reactions using planktonic cells (Foulkes *et al.*, 2011), each oxidation step was maintained for two hours, and each reduction step was 45 minutes, to allow each reaction to proceed to completion. After five cycles of oxidation and reduction, the (*R*)-enantiomer was

present in an enantiomeric excess (*e.e.*) of 85% (Figure 5). The hypothetical value at this stage after 5 cycles of oxidation and reduction is a 96.876% e.e.

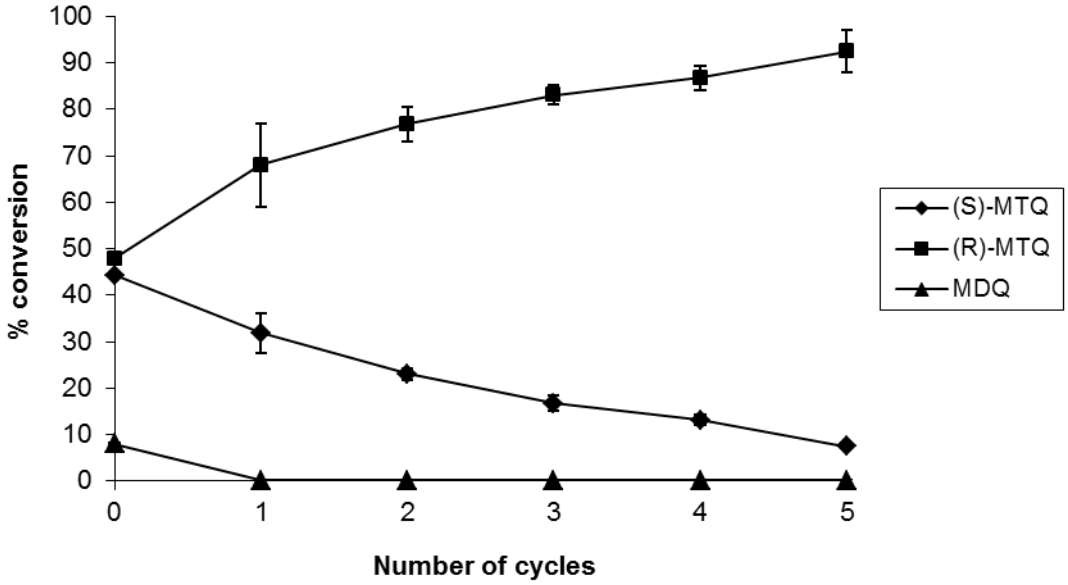

Figure 5: The deracemisation of MTQ by palladised *E. coli* transformed with the *mao-N-D5* gene insert and immobilised in alginate beads, giving an *e.e.* of 85% (*R*)-MTQ (5 cycles of air alternated with 5 cycles of hydrogen). Triplicates of each time point were tested, and the error bars show the standard error.

When beads used in a 5-cycle biotransformation that generated an enantiomeric excess of 91% were collected and washed with MOPS buffer and used in further biotransformation experiments, it was found that the enantiomeric excess of (*R*)-MTQ was 88% in the second biotransformation and 78% in the third biotransformation (Table 1). Thus both the activity of either the recombinant enzyme or the Bio-Pd was slightly reduced in multiple rounds of biotransformation.

In order to determine the impact of storage on the performance of the biocatalyst, beads that had been stored for 2 weeks were used in oxidation-only experiments. The results

showed the production of 24% MDQ in 2.5 hours, with 34% (*S*)-MTQ remaining. The same beads were subsequently used in a reduction-only experiment, in which all MDQ was reduced to racemic MTQ within 45 minutes, showing no loss in activity of the Bio-Pd.

Table 1: Enantiomeric excess following a biotransformation of five cycles of oxidation and reduction.

Biocatalyst	**% (*S*)-MTQ**	**% (*R*)-MTQ**	**% e.e.**
Planktonic cells	3	95	90
Immobilised cells (first biotransformation)	4	95	91
Immobilised cells (second biotransformation)	6	94	88
Immobilised cells (third biotransformation)	11	89	78

MEASURING THE LOSS OF PALLADIUM INTO THE REACTION SUPERNATANT

Palladium in the reaction supernatant was measured in triplicate by ICP-MS, in order to determine the extent of Pd leaching by the immobilised biocatalyst compared with planktonic cells. The ICP-MS results showed that 9.8 ±0.2 μg l^{-1} palladium was lost into the reaction supernatant following deracemisation of MTQ using immobilised biocatalyst. When using planktonic cells, the level of palladium in the supernatant was 63.4 ±0.3 μg l^{-1}, demonstrating the improved stability of the palladium nanoparticles when immobilised in alginate.

ENVIRONMENTAL SCANNING ELECTRON MICROSCOPY (ESEM)

ESEM was used to examine the structural integrity of the beads following their use in a biotransformation experiment. Little difference was seen in the surface integrity of the

beads following their use in a 5-cycle deracemisation reaction (Figure 6), although some pitting of the surface appears.

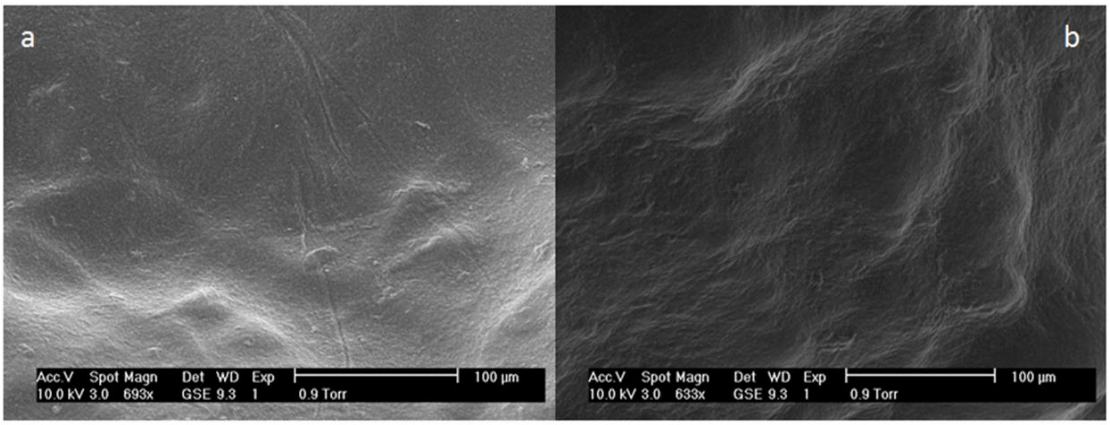

Figure 6: a) ESEM image of the surface of an alginate bead with immobilised palladised *E. coli*, before use in a 5-cycle deracemisation reaction; b) ESEM image of a bead after use in a deracemisation reaction.

USE OF FREEZE-DRIED BEADS IN OXIDATION AND REDUCTION REACTIONS

In order to discover whether the life of the biocatalyst could be extended, beads were freeze-dried and stored for up to six weeks under vacuum at 10°C. When freeze-dried beads were used immediately in oxidation-only experiments, results showed the production of 34% MDQ in 2.5 hours, with 20% (*S*)-MTQ remaining (Figure 7a). The same beads were subsequently used in a reduction experiment, in which all MDQ was reduced to racemic MTQ within 45 minutes, showing no loss in activity of the Bio-Pd. Freeze-dried beads that had been stored at 10°C for 2 weeks when used in an oxidation-only experiment showed the production of 34% MDQ in 2.5 hours, with 20% (*S*)-MTQ remaining. Freeze-dried beads that had been stored at 10°C for 6 weeks when used in an oxidation-only experiment showed the production of 38% MDQ in 2.5 hours, with 14% (*S*)-MTQ remaining. Despite the loss in activity due to freeze-drying therefore, the activity remained constant following storage, unlike the fresh beads which showed a considerable drop in activity after only 2 weeks. In the reduction-only experiment, all

MDQ was reduced to racemic MTQ within 45 minutes (Figure 7b), showing no loss in activity of the Bio-Pd despite freeze-drying and storage.

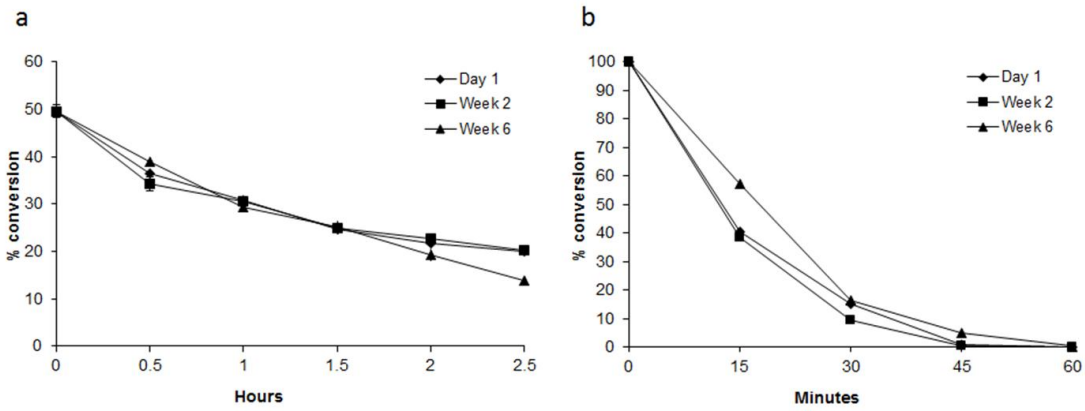

Figure 7: a) The oxidation of (*S*)-MTQ to MDQ at 37°C, by E. coli transformed with the *mao-N-D5* gene insert and immobilised in alginate beads before freeze-drying and testing immediately, after storage at 10°C for 2 weeks, and after storage at 10°C for 6 weeks; b) The reduction of MDQ to *rac*-MTQ at 37°C, by palladised *E. coli* cells immobilised in alginate beads before freeze-drying and testing immediately using hydrogen gas as the electron donor, after storage at 10°C for 2 weeks, and after storage at 10°C for 6 weeks. Triplicates of each time point were tested, and the error bars show the standard error.

DISCUSSION

Having demonstrated that it is possible to engineer a biometallic catalyst capable of one-pot deracemization reactions, we have now shown that this biocatalyst can be successfully immobilised in an alginate matrix to improve its performance. These biocatalyst-containing beads facilitate the use of the biocatalyst and increase its stability based on the leaching of palladium into the reaction supernatant, and freeze-drying prolongs the activity of the enzyme.

This study used aerobic cultures of *E. coli* for the hydrogen-dependent reduction of Pd(II), a procedure previously only performed using anaerobically grown cells. In addition to being easier to manipulate, aerobic cultures give higher cell yields, higher expression of recombinant proteins (Krause *et al.*, 2010), and do not require additional processing steps for the removal of H_2S which would otherwise poison the metal catalyst (Redwood *et al.*, 2008). The reduction of Pd(II) using hydrogen as the electron donor is likely to involve biological mechanisms, as the time taken for complete reduction is significantly increased in cell-free controls and killed (autoclaved) controls (Yong *et al.*, 2002). Pd(0) nanoparticles approximately 1 nm in diameter are located extracellularly, as shown in the transmission electron micrograph of the palladised cells (Figure 3c), although the nanoparticles appear to be associated with the outer membrane of the cells.

Palladised *E. coli* transformed with the *mao-N-D5* plasmid is capable of performing both oxidation and reduction reactions required for the deracemisation of amines, as shown here and previously (Foulkes *et al.*, 2011). The immobilisation of the biocatalyst in alginate was performed in order to facilitate its re-use, and extend its storage life. The activity of the immobilised biocatalyst was at first as high as that of the planktonic cells, and the product yield after three consecutive biotransformations was still high at 89%. The capacity of the Pd(0) catalyst to reduce MDQ to MTQ was not affected by the re-use or storage of the beads, but the activity of the MAO-N-D5 enzyme was reduced over time. However, freeze-drying the beads prevented loss of activity of the enzyme, which was unaffected by six weeks of storage of the beads (the time limit of this particular experiment). The activity of the Pd(0) was also unaffected by freeze-drying, making this a useful method for prolonging the life of this immobilised biocatalyst.

In conclusion, we have developed an immobilised biometallic catalyst, suitable for use in the two-step one pot deracemisation of 1-methyltetrahydroisoquinoline with high yield and *e.e.*, and suitable for long-term storage without loss of activity. This method should also be applicable to the deracemisation of a range of other amine substrates, as demonstrated previously (Carr *et al.*, 2005; Dunsmore *et al.*, 2006), and using other enzyme/metal combinations, could be potentially useful for a range of industrial and biotechnological applications.

ACKNOWLEDGEMENTS

The authors thank the staff in the EM facility in the Faculty of Life Sciences, The University of Manchester for their assistance, and the Wellcome Trust for equipment grant support to the EM facility. We would also like to thank the BBSRC for providing funding for this study.

REFERENCES

Alexeeva, M., Enright, A., Dawson, M. J., Mahmoudian, M. & Turner, N. J. (2002). Deracemization of alpha-methylbenzylamine using an enzyme obtained by in vitro evolution. *Angewandte Chemie-International Edition* **41**, 3177-3180.

Atkin, K. E., Reiss, R., Turner, N. J., Brzozowski, A. M. & Grogan, G. (2008). Cloning, expression, purification, crystallization and preliminary X-ray diffraction analysis of variants of monoamine oxidase from *Aspergillus niger*. *Acta Crystallographica Section F-Structural Biology and Crystallization Communications* **64**, 182-185.

Baxter-Plant, V., Mikheenko, I. P. & Macaskie, L. E. (2003). Sulphate-reducing bacteria, palladium and the reductive dehalogenation of chlorinated aromatic compounds. *Biodegradation* **14**, 83-90.

Carr, R., Alexeeva, M., Dawson, M. J., Gotor-Fernandez, V., Humphrey, C. E. & Turner, N. J. (2005). Directed evolution of an amine oxidase for the preparative deracemisation of cyclic secondary amines. *Chembiochem* **6**, 637-639.

Coker, V. S., Telling, N. D., van der Laan, G., Pattrick, R. A. D., Pearce, C. I., Arenholz, E., Tuna, F., Winpenny, R. E. P. & Lloyd, J. R. (2009). Harnessing the Extracellular Bacterial Production of Nanoscale Cobalt Ferrite with Exploitable Magnetic Properties. *ACS Nano* **3**, 1922-1928.

Coker, V. S., Bennett, J. A., Telling, N. D. & other authors (2010). Microbial Engineering of Nanoheterostructures: Biological Synthesis of a Magnetically Recoverable Palladium Nanocatalyst. *ACS Nano* **4**, 2577-2584.

Creamer, N. J., Mikheenko, I. P., Deplanche, K., Yong, P., Wood, J., Pollmann, K., Selenska-Pobell, S. & Macaskie, L. E. (2007a). A novel hydrogenation and hydrogenolysis catalyst using palladized biomass of Gram-negative and Gram-positive bacteria. *Advanced Materials Research* **20-21**, 603-606.

Creamer, N. J., Mikheenko, I. P., Yong, P. & other authors (2007b). Novel supported Pd hydrogenation bionanocatalyst for hybrid homogeneous/heterogeneous catalysis. *Catalysis Today* **128**, 80-87.

Cutting, R. S., Coker, V. S., Fellowes, J. W., Lloyd, J. R. & Vaughan, D. J. (2009). Mineralogical and morphological constraints on the reduction of Fe(III) minerals by Geobacter sulfurreducens. *Geochimica Et Cosmochimica Acta* **73**, 4004-4022.

De Windt, W., Aelterman, P. & Verstraete, W. (2005). Bioreductive deposition of palladium (0) nanoparticles on *Shewanella oneidensis* with catalytic activity towards reductive dechlorination of polychlorinated biphenyls. *Environmental Microbiology* **7**, 314-325.

Deplanche, K., Caldelari, I., Mikheenko, I. P., Sargent, F. & Macaskie, L. E. (2010). Involvement of hydrogenases in the formation of highly catalytic Pd(0) nanoparticles by bioreduction of Pd(II) using *Escherichia coli* mutant strains. *Microbiology* **156**, 2630-2640.

Dunsmore, C. J., Carr, R., Fleming, T. & Turner, N. J. (2006). A chemo-enzymatic route to enantiomerically pure cyclic tertiary amines. *Journal of the American Chemical Society* **128**, 2224-2225.

Foulkes, J. M., Malone, K. J., Coker, V. S., Turner, N. J. & Lloyd, J. R. (2011). Engineering a biometallic whole cell catalyst for enantioselective deracemization reactions. *In revision*.

Harrad, S., Robson, M., Hazrati, S., Baxter-Plant, V. S., Deplanche, K., Redwood, M. D. & Macaskie, L. E. (2007). Dehalogenation of polychlorinated biphenyls and polybrominated diphenyl ethers using a hybrid bioinorganic catalyst. *Journal of Environmental Monitoring* **9**, 314-318.

Hartmeier, W. (1988). *Immobilized Biocatalysts*: Springer Verlag, Berlin.

Hennebel, T., Verhagen, P., Simoen, H., De Gusseme, B., Vlaeminck, S. E., Boon, N. & Verstraete, W. (2009a). Remediation of trichloroethylene by bio-precipitated and encapsulated palladium nanoparticles in a fixed bed reactor. *Chemosphere* **76**, 1221-1225.

Hennebel, T., Simoen, H., De Windt, W., Verloo, M., Boon, N. & Verstraete, W. (2009b). Biocatalytic dechlorination of trichloroethylene with bio-palladium in a pilot-scale membrane reactor. *Biotechnology and Bioengineering* **102**, 995-1002.

Humphries, A. C., Mikheenko, I. P. & Macaskie, L. E. (2006). Chromate reduction by immobilized palladized sulfate-reducing bacteria. *Biotechnology and Bioengineering* **94**, 81-90.

Jarvis, R. M., Law, N., Shadi, L. T., O'Brien, P., Lloyd, J. R. & Goodacre, R. (2008). Surface-enhanced Raman scattering from intracellular and extracellular bacterial locations. *Analytical Chemistry* **80**, 6741-6746.

Krause, M., Ukkonen, K., Haataja, T., Ruottinen, M., Glumoff, T., Neubauer, A., Neubauer, P. & Vasala, A. (2010). A novel fed-batch based cultivation method provides high cell-density and improves yield of soluble recombinant proteins in shaken cultures. *Microbial Cell Factories* **9**, 11.

Lloyd, J. R., Yong, P. & Macaskie, L. E. (1998). Enzymatic recovery of elemental palladium by using sulfate-reducing bacteria. *Applied and Environmental Microbiology* **64**, 4607-4609.

Mabbett, A. N., Lloyd, J. R. & Macaskie, L. E. (2002). Effect of complexing agents on reduction of Cr(VI) by *Desulfovibrio vulgaris* ATCC 29579. *Biotechnology and Bioengineering* **79**, 389-397.

Mabbett, A. N., Yong, P., Farr, J. P. G. & Macaskie, L. E. (2004). Reduction of Cr(VI) by "palladized" biomass of *Desulfovibrio desulfuricans* ATCC 29577. *Biotechnology and Bioengineering* **87**, 104-109.

Macaskie, L. E., Mikheenko, I. P., Yong, P. & other authors (2010). Today's wastes, tomorrow's materials for environmental protection. *Hydrometallurgy* **104**, 483-487.

Mertens, B., Blothe, C., Windey, K., De Windt, W. & Verstraete, W. (2007). Biocatalytic dechlorination of lindane by nano-scale particles of Pd(0) deposited on *Shewanella oneidensis*. *Chemosphere* **66**, 99-105.

Pearce, C. I., Coker, V. S., Charnock, J. M., Pattrick, R. A. D., Mosselmans, J. F. W., Law, N., Beveridge, T. J. & Lloyd, J. R. (2008). Microbial manufacture of chalcogenide-based nanoparticles via the reduction of selenite using *Veillonella atypica*: an in situ EXAFS study. *Nanotechnology* **19**, -.

Redwood, M. D., Deplanche, K., Baxter-Plant, V. S. & Macaskie, L. E. (2008). Biomass-supported palladium catalysts on *Desulfovibrio desulfuricans* and *Rhodobacter sphaeroides*. *Biotechnology and Bioengineering* **99**, 1045-1054.

Suresh, A. K., Pelletier, D. A., Wang, W. & other authors (2010). Silver Nanocrystallites: Biofabrication using Shewanella oneidensis, and an Evaluation of Their Comparative Toxicity on Gram-negative and Gram-positive Bacteria. *Environmental Science & Technology* **44**, 5210-5215.

Yong, P., Rowson, N. A., Farr, J. P. G., Harris, I. R. & Macaskie, L. E. (2002). Bioreduction and biocrystallization of palladium by *Desulfovibrio desulfuricans* NCIMB 8307. *Biotechnology and Bioengineering* **80**, 369-379.

Chapter 7: The use of monoamine oxidase and biogenic palladium in the deracemization of the secondary amine 1-methyltetrahydroisoquinoline

1. The use of monoamine oxidase and biogenic palladium in the deracemization of the secondary amine 1-methyltetrahydroisoquinoline

Joanne M. Foulkes, Kirk J. Malone, Nicholas J. Turner, Jonathan R. Lloyd

A method was reported previously for a two-step, one pot deracemization of primary,[1] secondary,[2] and tertiary[3] amines. This method employs the enantioselective monoamine oxidase MAO-N-D5,[4, 5] and a non-selective reducing agent. We have developed this method further by employing genetically transformed *Escherichia coli* cells expressing the monoamine oxidase, and biogenic nanoparticulate palladium produced extracellularly by the bacterium as the reducing agent (Figure 1).

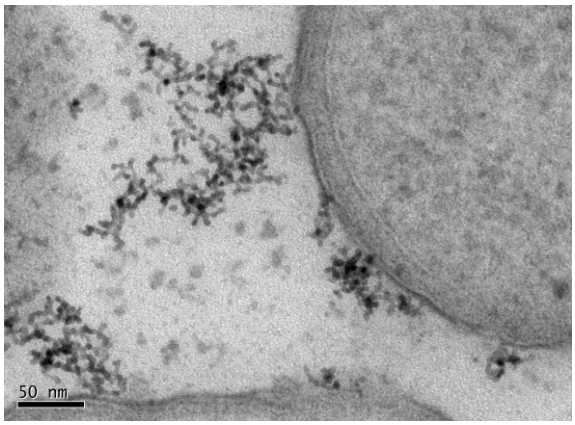

Figure 1 *Transmission electron micrograph of thin sections of cells of* E. coli *with extracellular biogenic palladium associated with the outer membrane.*

This biometallic catalyst was used successfully for the conversion of racemic 1-methyltetrahydroisoquinoline (MTQ) to (*R*)-MTQ, *via* the intermediate 1-methyldihydroisoquinoline (MDQ), with an enantiomeric excess of 93% (Figure 2).

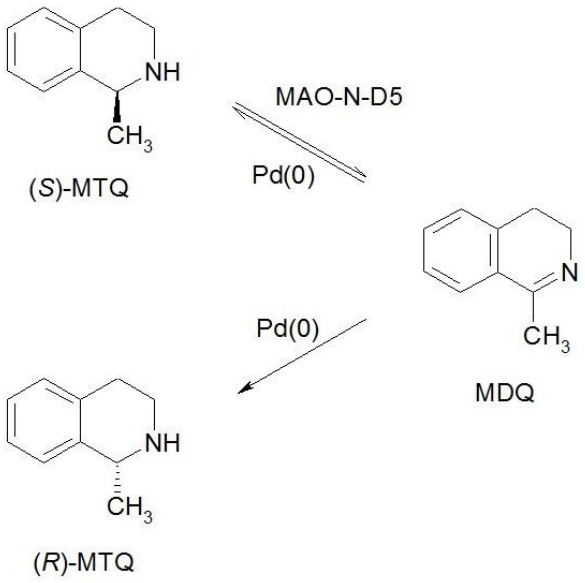

Figure 2 *The cyclic deracemisation of 1-methyltetrahydroisoquinoline (MTQ) via the imine 1-methyldihydroisoquinoline (MDQ) using palladised bacterial cells with the* mao-N-D5 *gene expressed.*

1.1 Procedure 1: Transformation and palladisation of *Escherichia coli*

1.1.1 Materials and Equipment

- *E. coli* BL21 competent cells (50 μL – Invitrogen)
- plasmid pET16b (Novagen) containing the variant mao-N-D5 gene (2 μL)
- SOC broth
- Luria-Bertani (LB) agar in Petri dishes containing 100 μg mL^{-1} ampicillin
- ice bath
- water bath at 42°C
- static incubator
- Erlenmeyer flasks (500 mL and 1 L) with foam bungs
- LB broth containing 100 μg mL^{-1} ampicillin
- shaker/incubator
- centrifuge
- morpholinepropanesulfonic acid (MOPS) buffer (20 mM, pH 7.6)
- gas bottles (25 mL), with butyl rubber stoppers and metal sealable caps
- sodium tetrachloropalladate (7.3553 mg, 0.025 mmol)
- hydrogen gas

1.1.2 Procedure

1. The plasmid was transformed into *E. coli* BL21 competent cells according to the manufacturer's instructions.
2. The transformed cell suspension (30 μL) was spread onto an LB-ampicillin agar plate and incubated at 37°C for 18 h.
3. A single colony was used to inoculate 50 mL LB-ampicillin broth in a 500 mL Erlenmeyer flask (starter culture). This was incubated at 37°C, 180 rpm for 18 h.
4. The cell suspension (11 mL) was used to inoculate 99 mL of fresh LB-ampicillin broth in a 1 L Erlenmeyer flask. This was incubated at 37°C, 180 rpm for 24 h.
5. Cells were harvested by centrifugation at 3000 *g* for 20 minutes.
6. Cells were washed three times in MOPS buffer (12.5 mL), and wet cell pellets were resuspended in MOPS buffer to a cell mass of 250 mg mL^{-1}.
7. Cells (1 mL, 250 mg mL^{-1}) were added to MOPS buffer (21.5 mL) in a 30 mL gas bottle, and sodium tetrachloropalladate solution (10 mM, 2.5 mL) was added.
8. The cell suspension was incubated at 30°C, 180 rpm for 1 h, in order for the Pd(II) to biosorb to the cells.[6]
9. The cell suspension was sparged with hydrogen gas for up to 5 minutes, during which time the soluble Pd(II) (light brown in colour) was reduced to insoluble Pd(0) enzymatically (black precipitate).
10. Palladised cells were harvested by centrifugation at 3000 *g* for 20 minutes.
11. Cells were resuspended in MOPS buffer to a volume of 1 mL, and used directly in Procedure 2 (Section 1.2).

1.2 Procedure 2: Deracemization of *rac*-MTQ

1.2.1 Materials and Equipment

- whole palladised cells expressing the variant MAO-N-D5 enzyme (250 mg mL^{-1})
- potassium phosphate buffer (K_2HPO_4-KH_2PO_4) (9 mL, 0.1 M, pH 7.6)
- racemic MTQ (14.7 mg, 0.1 mmol)
- methyl-tert-butyl ether (MTBE)
- anhydrous Na_2SO_4
- gas bottle (100 mL), with butyl rubber stopper and metal sealable cap
- shaker/incubator
- microcentrifuge
- hydrogen gas
- nitrogen gas

1.2.2 Procedure

1. A 1 mL aliquot of palladised cells expressing the MAO-N-D5 variant enzyme was suspended in potassium phosphate buffer (0.1 M, pH 7.6, 9 mL). Racemic MTQ (14.7 mg, 0.1 mmol) was added. The gas bottle was sealed with a butyl rubber stopper and metal cap, and was incubated at 37°C, 225 rpm for 2 h.
2. The cell/MTQ suspension was flushed with nitrogen gas, then sparged with hydrogen gas for 2 minutes, and was further incubated at 37°C, 225 rpm for 1 h.
3. Five cycles of air/hydrogen incubation were performed with nitrogen flushing between each step, and samples (0.5 mL) were taken for analysis at the end of each reduction step.
4. For high-performance liquid chromatography (HPLC) analysis: the reaction mixture was clarified by centrifugation at 14 000 g for 5 minutes, and the supernatant decanted and extracted with 1 mL MTBE. The MTBE phase was dried with Na_2SO_4 and concentrated *in vacuo* to yield the MTQ as a colourless oil. Samples were resuspended in 200 µL iso-hexane.
5. Enantiomeric excess was determined by HPLC with a Daicel Chiralpak AD-H 4.6 mm x 250 mm column, at a flow rate of 1 ml min^{-1} for 20 minutes at 40°C with a mobile phase of 88% isohexane, 2% ethanol, and 10% isohexane containing 0.5% diethylamine. The analytes were detected by UV-Vis spectroscopy, at wavelengths of 220 nm (MTQ), and 254 nm (MDQ). Major enantiomer R_t = 12.03 min, 93% ee.

1.3 Conclusion

This biometallic whole-cell catalyst provides a reproducible method for the deracemisation of amines that can potentially be applied to a wide range of substrates including primary, secondary, and tertiary amines, as reported previously.[1-3]

References

1. Alexeeva, M., Enright, A., Dawson, M.J., Mahmoudian, M. & Turner, N.J. Deracemization of alpha-methylbenzylamine using an enzyme obtained by in vitro evolution. *Angewandte Chemie-International Edition* **41**, 3177-3180 (2002).
2. Carr, R. et al. Directed evolution of an amine oxidase for the preparative deracemisation of cyclic secondary amines. *Chembiochem* **6**, 637-639 (2005).
3. Dunsmore, C.J., Carr, R., Fleming, T. & Turner, N.J. A chemo-enzymatic route to enantiomerically pure cyclic tertiary amines. *Journal of the American Chemical Society* **128**, 2224-2225 (2006).
4. Alexeeva, M., Carr, R., Turner, N. J. Directed evolution of enzymes: new biocatalysts for asymmetric synthesis. *Organic and Biomolecular Chemistry* **1**, 4133-4137 (2003).
5. Carr, R. et al. Directed evolution of an amine oxidase possessing both broad substrate specificity and high enantioselectivity. *Angewandte Chemie-International Edition* **42**, 4807-4810 (2003).
6. Baxter-Plant, V., Mikheenko, I.P. & Macaskie, L.E. Sulphate-reducing bacteria, palladium and the reductive dehalogenation of chlorinated aromatic compounds. *Biodegradation* **14**, 83-90 (2003).

Chapter 8: Conclusions and future work

Recent advances in the field of synthetic biology allow us to anticipate the possibility of creating “designer” biometallic catalysts, engineered precisely to the requirements of the desired chemical transformation. This study has shown that it is already possible to engineer an aerobically-grown biometallic catalyst capable of one-pot deracemisation reactions, and to extend the life of this biometallic catalyst by freeze-drying whilst immobilised in an alginate matrix.

Using chiral HPLC for the detection of (*S*)-MTQ, (*R*)-MTQ and MDQ, it was found that palladised *E. coli* transformed with the *mao-N-D5* plasmid is capable of performing both oxidation and reduction reactions required for the deracemisation reactions studied here. However, it was not possible to perform both reactions simultaneously, with aerobic cells supplied with formate as an electron donor for the Pd-catalysed reaction, due to the formation of an unwanted product under these conditions, later identified as MIQ using LC-MS. However, this product was not seen when hydrogen was used instead of formate as the electron donor in the reduction reaction possibly as hydrogen drives the reduction of MDQ at a faster rate than formate (see section 3.2.4). The use of hydrogen required the two reactions to be performed separately but in the same reaction vessel, in a cyclical manner. This simple approach should be amenable for use in a broad range of reactor configurations, including those using high densities of cells immobilised on a suitable support for easy re-use. As the two reactions are not run simultaneously, each discrete reaction step can be optimised fully, with prolonged activity for the catalyst demonstrated in this study.

When the performance of enzymatically produced bioPd was compared to that of commercially available “conventional-Pd” in a biotransformation of 5 cycles of oxidation and reduction, both were found to adsorb the reactants and products of the biotransformation. However, the conventional-Pd adsorbed around 10% more than the bioPd (1 mM of the potential 10 mM final product in our study), indicating that the amine could not be desorbed from the catalyst even with multiple washing steps. It was also found that the conventional-Pd was present in the reaction supernatant at

higher levels than the bioPd, and had to be removed by an additional filtration step complicating downstream processing. The ease of removal of bioPd from the reaction mixture indicates both reduced contamination of the products with palladium, and improved recyclability of the catalyst. The re-use of bioPd cells following a 5-cycle biotransformation confirmed that the activity of the metallic biocatalyst was not affected significantly by recycling in this experiment.

The immobilisation of the biocatalyst in a variety of matrices was performed in order to facilitate its re-use, and extend its storage life. Chitosan, sol-gel, and polyacrylamide were found to be unsuitable as immobilisation matrices in this case, primarily due to the instability of the matrix with the addition of Pd-loaded cells or when added to the amine substrate in solution. Alginate was found to be a suitable matrix as it remained stable throughout the deracemisation reaction, maintained the viability of the majority of the biocatalyst, and less than one-sixth the amount of palladium was lost into the reaction supernatant compared with planktonic cells. The activity of the alginate-immobilised biocatalyst was at first as high as that of the planktonic cells, and the product yield after three consecutive biotransformations was still high at 89%. Culture-based analysis of the reaction supernatant following biotransformation indicated that no viable cells were lost from the beads, and ESEM images showed that the integrity of the beads was not affected. The capacity of the Pd(0) catalyst to reduce MDQ to MTQ was not affected by the re-use or storage of the beads, but the activity of the MAO-N-D5 enzyme was reduced over time. However, freeze-drying the beads prevented loss of activity of the enzyme, which was unaffected by six weeks of storage of the beads (the time limit of this particular experiment). The activity of the Pd(0) was also unaffected by freeze-drying, making this a useful method for prolonging the life of this immobilised biocatalyst.

Although previous studies investigating the bioreduction of palladium have used anaerobic cultures, this study has demonstrated that palladium reduction is possible with aerobic cultures of *E. coli*, using either hydrogen or formate as the electron donor. The use of aerobic cultures for the production of biometallic catalysts is preferable, due to increased cell yield, higher yields of recombinant proteins (Krause *et al.*, 2010)

and in the case of SRB no production of H_2S which can poison metallic catalysts (Redwood *et al.*, 2008a). Although Pd(II) is reduced by hydrogen without the presence of bacteria, there is likely to be a biological mechanism for hydrogen-dependent Pd(II) reduction, due to the significantly increased time taken for reduction to complete in cell-free and killed (autoclaved) controls (based on visual interpretation), as also seen by others (Yong *et al.*, 2002b). For formate-dependent bioreduction of Pd(II), using ICP-MS to measure Pd(II) removal from solution indicates that Pd(II) bioreduction in these cultures is enzymatic, with reduction of palladium not occurring in the cell-free and autoclaved cells experiments irrespective of the length of incubation. Further investigation of the enzymatic systems involved using mutant *E. coli* strains with absent or disrupted hydrogenase and formate dehydrogenase enzymes indicated that the major enzymes involved include the formate dehydrogenases FDH-O and FDH-N, although bioreduction still occurs in strains without these enzymes albeit at a much lower rate. Other molybdoenzymes are most likely involved. The strain that lacked all molybdoenzymes however did still reduce the palladium, although this took 7 hours, compared with less than 30 minutes by the wild-type strains. Hydrogenases, implicated as the dominant Pd(II) reductases in other experimental systems (Deplanche *et al.*, 2010; Mikheenko *et al.*, 2008) are not expressed in aerobically grown cultures, and their lack of involvement was evident as the strain lacking any hydrogenase enzymes reduced palladium at the same rate as the wild-type strains.

Although it was hoped that the location of the Pd(0) nanoparticles would implicate the enzymes responsible for their reduction, TEM images show the presence of elemental palladium as extracellular nanoparticles, associated with the cell surface and possibly with exopolysaccharides. EDX was used to confirm the presence of Pd(0) in these precipitates. Occasionally nanoparticles were seen inside the cell, possibly located on the inner surface of the plasma membrane. Furthermore, the extracellular precipitation of Pd(0) occurs with all strains of *E. coli* used in this study, including mutants, indicating that whichever biological system is responsible for the aerobic bioreduction system, there seems to be little impact on the site of Pd(0) deposition. It is possible that an electron transfer system to the surface of the outer membrane exists similar to that found in *Geobacter sulfurreducens* and *Shewanella oneidensis*

(Lloyd *et al.*, 2003) that is as yet undiscovered in *E. coli*. It is also possible, as suggested by the electron tomography images obtained (Figure A2.1), that the first Pd(0) nanoparticles to form breach the outer membrane, and themselves form an electron conduit for further Pd(II) reduction outside the cell. The pH of the experiments in this study is also higher than others where Pd(0) nanoparticles accumulated in the periplasm (Redwood *et al.*, 2008a), which were performed at around pH 2. The higher pH used here could result in the higher biosorption of cationic metals to the outer membrane and extracellular polymeric substances, which are then not able to enter the periplasm. The influence of a higher pH in the location of the Pd(0) may be confirmed by the observation that Pd(0) nanoparticles were located on the cell surface of *D. desulfuricans* when the bioreduction was performed at pH 7 (Yong *et al.*, 2002b).

One further conclusion that may be drawn from the extracellular location of the Pd(0) nanoparticles is that whilst cells that lack the formate dehydrogenases are still capable of reducing Pd(II), when all of these enzymes are missing a cellular component associated with the outer membrane may be responsible. This is implicated by the TEM images of the MC4100 Δ*moaA* strain (which lacks all molybdoenzymes), in which the majority of the Pd(0) nanoparticles are closely associated with the outer membrane (Figure 4e, Chapter 5). Furthermore, this formate oxidation activity is much weaker than that seen with the strains containing formate dehydrogenases, where Pd(II) reduction occurs much earlier. It is possible however that following the initial enzymatic reduction of a small percentage of the Pd(II), the Pd(0) nanoparticles formed may themselves be responsible for catalysing the reduction of the remainder of the Pd(II) (Yong *et al.*, 2002b), which would mean that only a minor, initial biological input is required.

One limitation of using ICP-MS for the measurement of the rate of Pd(II) reduction is that palladium removal is measured rather than a direct measurement of metal reduction. This meant that the formation of a brown precipitate which was not Pd(0) in the cell control lacking formate, and from 3-7 hours following formate addition in the MC4100 Δ*moaA* strain, implied Pd(II) reduction to Pd(0) where none had

occurred. This precipitate may be formed due to increased biosorption of the Pd(II) to viable cells over time. The X-ray diffraction pattern did not show the presence of any peaks characteristic of Pd(0) in this precipitate, indicating that it was probably amorphous and non-crystalline. There is also removal of soluble Pd(II) when using autoclaved cells, possibly indicating that the increased surface area of the lysed cells leads to increased sorption of the Pd(II) to the biomass. In some cases, the reduced palladium particles were so small that they could not be removed from the reaction supernatant, and gave a false impression of the amount of Pd(II) remaining in solution. Synchrotron radiation techniques such as X-ray absorption spectroscopy would be better to measure bioreduction directly, as it supplies information on the oxidation state of the palladium. EXAFS data confirm that the complete reduction of Pd(II) to Pd(0) occurs within minutes, and QEXAFS data confirm the reduction of Pd(II) directly to Pd(0), without the production of intermediate species. However, the time constraints involved in securing beam time meant that this approach was only available for the investigation of some of the bacterial strains used in this study.

In conclusion, we have demonstrated the presence of a novel biological mechanism responsible for the bioreduction of Pd(II) in aerobically-grown cultures of *E. coli*, catalysed mainly by molybdenum-containing enzyme systems. If active in a range of industrially important reactions, this new form of bioPd has the advantage over that produced by anaerobic culture as it is easier to produce and perform and provides increased biomass. There is also no requirement for additional processing steps to remove H_2S (produced by SRB systems), and the use of formate instead of hydrogen gas means that the procedure is less hazardous and more controllable. This study has also demonstrated that it is possible to create an alginate-immobilised biometallic catalyst that expresses MAO-N as a model oxidase enzyme in palladised cells, and can perform both oxidation and reduction reactions leading to a 96% deracemisation of a secondary amine, without the addition of a separate chemical reductant and with limited contamination or adsorption of the reaction products by the catalyst. The biometallic catalyst can also be stored long-term entrapped in freeze-dried alginate beads without loss of activity. This method has a broad potential for simplifying or improving other enzyme/inorganic catalyst combinations, not being specific to either

E. coli or palladium, and could be potentially useful for a range of industrial and biotechnological applications.

8.1 Future work

The development of a biometallic catalyst for use in the deracemisation of MTQ has proved that the concept is possible, and it should be feasible to use the same catalyst for the deracemisation of a range of other primary, secondary and tertiary amine substrates, as previously performed using the MAO-N-D5 enzyme and a separate chemocatalyst (Alexeeva *et al.*, 2002; Carr *et al.*, 2003; Dunsmore *et al.*, 2006). Using other racemic amines as substrates it may also be possible to develop the system using formate as the electron donor in the reduction step, rather than hydrogen gas which requires more complex bioprocess engineering. It may also be possible to develop a range of new metallic biocatalysts by transforming the bacterial host cell with alternative enzymes, for use in two-step biotransformations where metal catalysts are used, or in multi-step biotransformations where more than one enzyme is used. The bacterial host cell could also be loaded with other metals as required, such as platinum or gold nanoparticles, or a combination of metals. Biogenic gold nanoparticles have previously been used as the catalyst in oxidation reactions such as the oxidation of glycerol (Deplanche *et al.*, 2007), and in combination with palladium for the oxidation of alcohols (Deplanche, 2010). Biogenic platinum has been used as the catalyst in fuel cells (Yong *et al.*, 2007), and for the reduction of Cr(VI) to Cr(III) (Murray *et al.*, 2007). Subsequent studies will investigate the catalytic activity of the Pd(0) nanoparticles produced during this current work in a range of industrially important reactions.

Future work with the mutant strains of *E. coli* for the investigation of the processes of formate-dependent Pd(II) bioreduction should include a repeat of the data obtained using ICP-MS by synchrotron radiation techniques, such as EXAFS. This would show conclusively the rate of reduction of Pd(II) by strains where ICP-MS data is ambiguous, such as with the strain MC4100 Δ*moaA*. ICP-MS however is useful for comparing rates of reduction between different strains. In order to determine exactly the mechanisms responsible for Pd(II) bioreduction in strain MC4100 Δ*moaA*, more genes could be

knocked out, although this might prove to be detrimental to viability. It would be interesting to discover how the lack of hydrogenase and molybdoenzymes affects the cell metabolism, as the cell may be using alternative systems for the same functions which could include Pd(II) reduction.

Further work could be performed with the alginate-immobilised biocatalyst, to investigate the viability of cells in freeze-dried beads, and also to determine the precise lifespan of the biocatalyst, which in the limited time available to this study was found to be at least six weeks with no loss of activity compared with day 1. The immobilised biocatalyst could also be used in a flow-through bioreactor, for the continuous production of the optically pure amine. Other immobilisation methods could also be used in which the cells are maintained in as natural a state as possible, such as membranes (Hartmeier, 1988) or biofilms (Cheng *et al.*, 2010; Rosche *et al.*, 2009). Recently, a biofilm of *E. coli* transformed with the tryptophan synthase gene of *Salmonella enterica* was used to convert haloindoles and serine to L-halotryptophans, with improved activity over both planktonic cells and the immobilised enzyme itself. No loss of activity was reported with repeated re-use of the biofilm (Tsoligkas *et al.*, 2011). It is possible that this system could also be used to immobilise palladised biocatalyst for biotransformations.

Appendices

Appendix 1: Analytical Techniques

In this section, techniques that have been employed in this project are described.

A1.1 High performance liquid chromatography (HPLC)

Chromatography is used for the separation of substances, based on the way they distribute between two immiscible phases. This is known as the distribution or partition coefficient (K_d), derived by dividing the concentration in phase A by that in phase B, and is constant at a given temperature. The two phases are known as the stationary phase, which is immobilised onto a particulate matrix; and the mobile phase, or eluent, a liquid or a gas that is passed through the stationary phase after the addition of the analyte mixture. In high-pressure liquid chromatography, the matrix is packed into a stainless steel column and the samples are added to the top via an injector system. Separated analytes leave the column at different times based on their distribution coefficients; and a detector, such as a spectrophotometer or mass spectrometer, analyses the eluate as it leaves the column (see Figure A1.1). The back-pressure generated within the HPLC column is more than 50 bar. This provides improved resolution of analytes, and so the technique is also known as high performance liquid chromatography. The system may be either normal-phase, where the stationary phase is polar and the mobile phase is non-polar; or reverse-phased, where the opposite situation is in effect. In reverse-phased LC, the most commonly used stationary phases are hydrocarbons chemically attached to silica, such as butyl (C_4), octyl (C_8), and octadecyl (C_{18}) (Wilson, 2005). Analytes are drawn into the stationary phase by hydrophobic interactions with these molecules. The mobile phase may be constant, such as an aqueous buffer, methanol, or acetonitrile, or a pre-mixed solution of more than one of these (isocratic elution); or the composition may change gradually during column development (gradient elution), to improve separation of analytes.

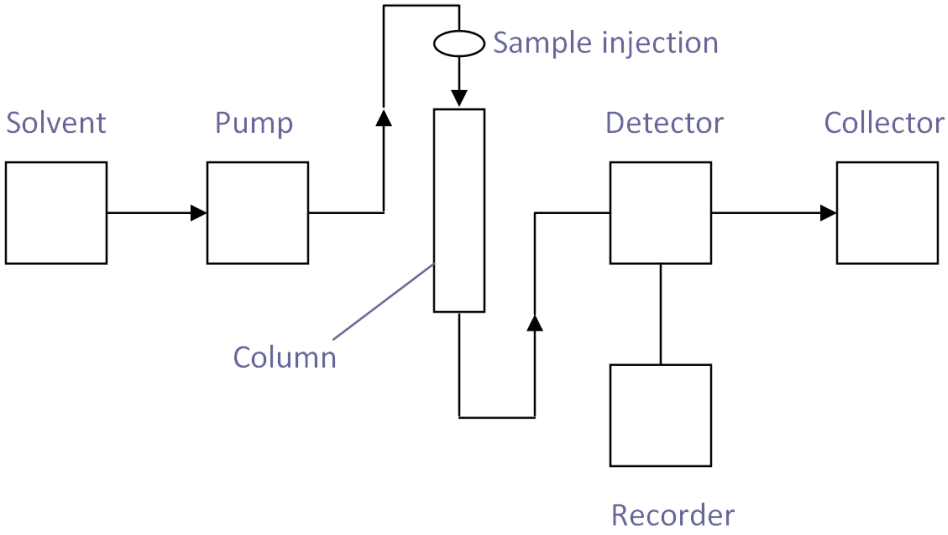

Figure A1.1: Schematic representation of an HPLC system (adapted from Wilson, 2005).

The data provided by the detector system is in the form of a chart known as a chromatogram, or chromatograph (see Figure A1.2). The presence of an analyte is demonstrated by peaks, with the position of each peak corresponding to the retention time of that particular analyte. If the analytes have been successfully separated, the peaks are said to be resolved. The use of mass spectrometry as a detection system however allows the identification of overlapping peaks, as detection is based on the molecular mass of the analyte. The area inside the peak on a chromatogram corresponds to analyte concentration, giving a quantitative result when compared to a calibration curve produced from a series of known standards.

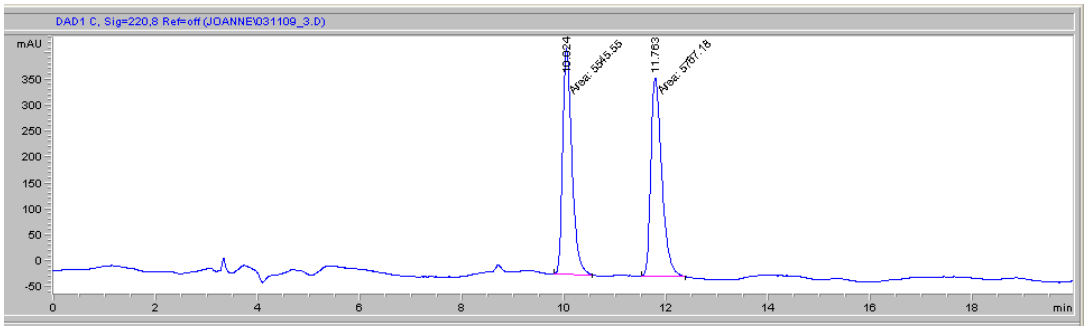

Figure A1.2: Chromatogram – each peak represents a different analyte; (*S*)-MTQ at 10.024 minutes, and (*R*)-MTQ at 11.763 minutes.

A1.2 Mass spectrometry

Mass spectrometry is a technique whereby molecules are detected on the basis of their mass-to-charge ratio (*m*/*z*) following conversion to gaseous ions. The abundance of ions at each *m*/*z* ratio provides the mass spectrum. The technique is useful for separating molecules that are very similar, and it also provides an accurate relative molecular mass (M_r). Molecules can be ionised by bombardment with electrons, photons, ions, or molecules (Skoog *et al.*, 1998b). One new method for the ionisation of molecules is electrospray (ES), whereby molecules are sprayed into an electrical field. The ions are then accelerated to a specific velocity, and separated in a mass analyser according to their *m*/*z* ratio (Aitken, 2005).

A1.3 Chiral chromatography

Chiral compounds are those in which two forms of the molecule exist, often as mirror images. The two molecules, known as enantiomers, differ in the way they interact with plane-polarised light. A commonly used naming convention is the Cahn-Ingold-Prelog system, whereby enantiomers are classified as *R* (Latin, *rectus*) and *S* (*sinister*) (Wilson, 2005), according to a set of rules regarding the atoms attached to carbon within the molecule. Although the functional groups on the two enantiomers are identical, their physical properties are different and thus they can be separated by chiral chromatography. The stationary phase may be Pirkle phases (amino acid derivatives), triacetylcellulose or cyclodextrins, bonded to silica. Separation may be due to hydrophobic interactions and van der waals forces (Pirkle phases), or the creation of a molecular cage in which the enantiomer is housed (cyclodextrins) (Wilson, 2005).

A1.4 UV and visible light spectroscopy

This technique measures the extent of absorption of light by a coloured sample (or chromophore) in solution, by determining the ratio of transmitted to incident radiation (transmittance) which when considered with the pathlength of the sample gives the absorbance (*A*). When the measurement is based on the scattering of light

rather than absorption (for example when estimating bacterial cell numbers), the term attenuation (D; previously known as optical density) is used instead of absorbance. The Beer-Lambert law (Equation A1 below) states that absorbance is proportional to both the concentration of a substance and its pathlength,

$$A = \in_{\lambda} cl$$

(Equation A1.1: The Beer-Lambert law)

where ε is the molar extinction coefficient at a particular wavelength of light (λ), *c* is the concentration of the solution, and *l* is the pathlength. The sample is compared to a solvent blank in order to minimise the effect of absorption by the solvent, and so the area illuminated by incident light is the same for both reference and sample and can be ignored. In order to determine the concentration of a compound, a calibration curve based on the absorbance versus concentration of a set of standards is produced, from which concentration of an unknown may be interpolated. The linearity of the curve is not indefinite, a phenomenon known as the Job effect, and results therefore should not be extrapolated from beyond the curve as to do so would introduce errors (Gordon, 2005).

In a simple single beam spectrophotometer (see Figure A1.3), visible light is produced by a tungsten filament lamp, and UV light by a hydrogen or deuterium lamp, in order to produce a continuous spectrum. The light passes through a monochromator (either a prism or diffraction grating) to produce the required wavelength, which then passes through the sample contained in a low-absorbance plastic cuvette. Two photosensitive detectors (usually photocells, which produce a current proportionate to the intensity of light) are used, one for incident light and one for transmitted light.

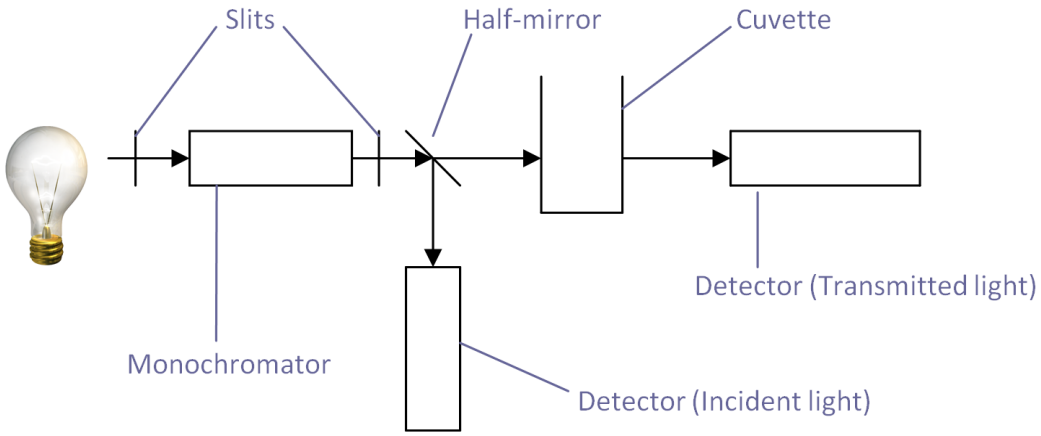

Figure A1.3: The optical arrangements in a single-beam spectrophotometer (adapted from Gordon, 2005).

In double-beam spectrophotometers, the light is split into two beams, one of which passes through the sample, and one through the reference. This prevents errors being introduced, for example from variations in beam intensity (Miller, 1993).

As spectrophotometers can scan over the whole range from UV to visible light, an absorption spectrum for a particular molecule can be produced, by plotting absorbance against wavelength (Figure A1.4). Such spectra show at which wavelengths a chromophore absorbs light most strongly, for use in further spectrophotometric experiments.

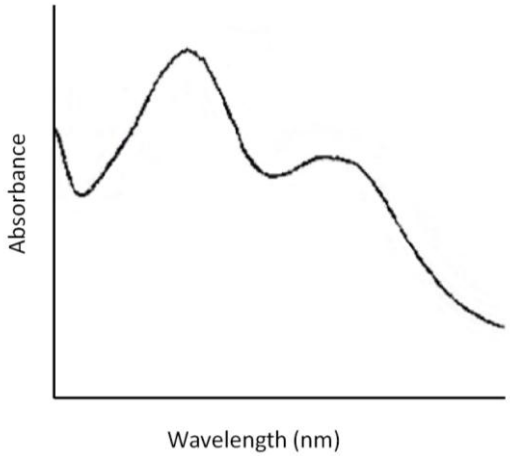

Figure A1.4: UV absorption spectrum of a Palladium (II) complex showing strong absorption at 350 nm (adapted from Park et al., 2008).

A1.5 Inductively coupled plasma - mass spectrometry (ICP-MS)

Inductively coupled plasma - mass spectrometry (ICP-MS) is a technique for the characterisation of the elemental composition of samples, with a limit of detection potentially as low as 0.01 ppb. Inductively coupled plasma is formed by igniting a very high temperature inert gas with a high voltage discharge, and maintaining a radiofrequency (RF) current. The gas is ionised, making it electrically conductive, and reaches temperatures of up to 10 000 K. Liquid samples are aerosolised and introduced to the plasma via an argon gas stream. The plasma decomposes the sample contents to individual atoms, before stripping them of electrons to form ions. The ions are separated within the mass spectrometer, the commonest type of which is the quadropole mass filter. This is an arrangement of four rods, with alternating AC and DC voltages applied to opposite pairs of rods. Rapid switching of the voltages and an RF field allow the passage of ions of only a single mass-to-charge ratio at a time, making multi-element analysis of a sample possible (Abou-Shakra, 2004; Taylor, 2001).

A1.6 X-ray diffraction (XRD)

When an X-ray beam at angle θ strikes a crystal, some of the beam is scattered by the surface atoms and some of the beam passes through. This beam reaches the second layer of atoms, where the same events occur, and so on. The scattering of X-rays takes place only when striking the crystal faces at certain angles, and is also dependent on both the distance between the planes of atoms and the wavelength of the radiation. The pattern of diffraction of X-rays is therefore specific to a crystal, and depends on satisfying Bragg's law:

$$n\lambda = 2d \sin \theta$$

(Equation A1.2: Bragg Equation)

where n is an integer and *d* is the interplanar space (Skoog *et al.*, 1998a). Thus, the atoms that make up a crystal can be identified using this technique.

A1.7 X-ray absorption spectroscopy (XAS)

X-ray absorption spectroscopy (XAS) provides information on the species and local arrangement of atoms in a sample by measuring the absorption of photons as a function of their energy. The energy of the X-ray beam is set below the binding energy of the core electrons (K-level) of the element studied, at which point there is no excitation of the electrons. With an increase in photon energy, a point is reached at which the core level electrons are excited (the K-edge), and begin to populate the empty states. This is known as the near edge region (see Figure A1.5), with XAS at this point specifically known as X-ray absorption near-edge spectroscopy (XANES). As the photon energy increases further, the photoelectron leaves the atom. This region is known as extended X-ray absorption fine structure (EXAFS), and extends for up to around 1000 eV. For isolated atoms, both XANES and EXAFS are featureless, but where atoms are surrounded by other atoms their local arrangement causes oscillations in the EXAFS region. The features in EXAFS are due to the wave-like nature of the photoelectron, which is scattered from surrounding atoms with new waves being emitted. With increasing photon energy, the interference between the waves alternates between constructive and destructive, which leads to oscillations in the spectrum. Examining these oscillations gives information on the number, species and distance of the surrounding atoms. A Fourier transform of the EXAFS region allows the contributions of different atoms to be detected. For heavier elements, it may not be possible to supply X-rays of sufficient energy, and so L3-edge EXAFS may be used instead of K-edge (University of Slovenia Group for Experimental Atomic Physics website).

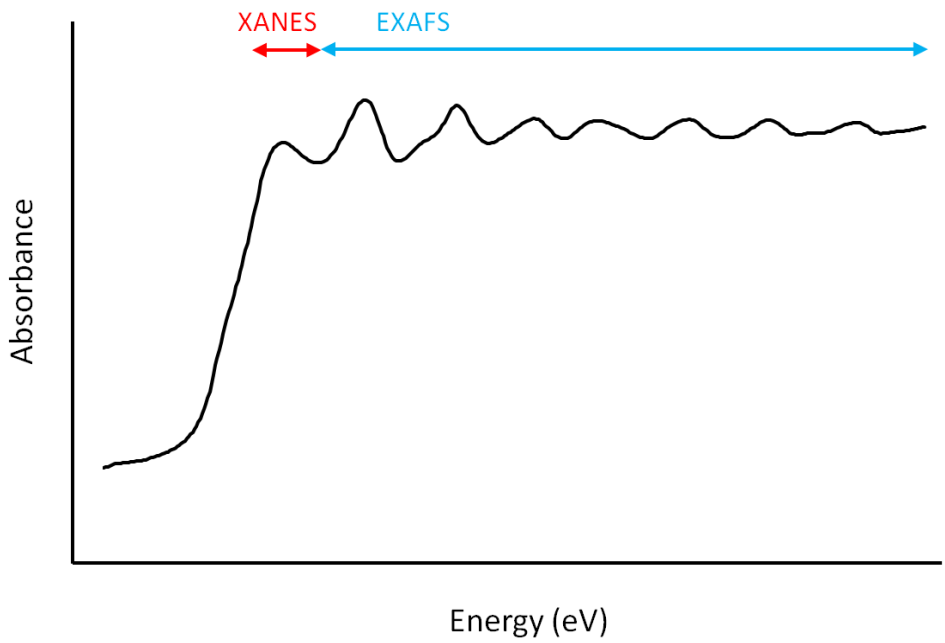

Figure A1.5: XAS spectrum, showing near-edge and fine structure regions.

Historically XAS spectra are recorded by comparing the intensity of the incident X-ray beam (I_0) with the transmitted beam (I_t). If greater sensitivity is required, for example in very dilute specimens, fluorescence or total electron emission can be measured instead (Charnock, 1995; Sebilleau, 2006).

The advantage of XAS over other X-ray spectroscopy techniques is that the technique can be used with solids, liquids or gases, without the need for long-range order of atoms within the sample (University of Slovenia Group for Experimental Atomic Physics website).

A1.7.1 Synchrotron radiation for XAS

The X-ray source for XAS is provided by synchrotron radiation. Figure A1.6 below shows a schematic representation of a synchrotron. To begin with, electrons are fired into the linac and boosted to almost the speed of light before entering the storage ring, which is actually a series of straight sections with electromagnets to direct the electrons between them. The RF system boosts the electrons with each circuit of the storage ring. Whilst in the storage ring, the constant acceleration experienced by the electrons causes them to lose energy in the form of X-rays, which are directed down

beamlines when the electrons pass through the bending magnets. Very high energy experiments use the more intense light produced when the electrons pass through insertion devices, arrays of magnets arranged as “wigglers” or “undulators”.

After the X-rays are directed into a beamline, the beam is passed through a monochromator to generate photons of a single wavelength. The beam is then passed through a detector to measure the intensity of the beam, before passing through the sample and a further detector for measuring the intensity of the transmitted beam (see Figure A1.7).

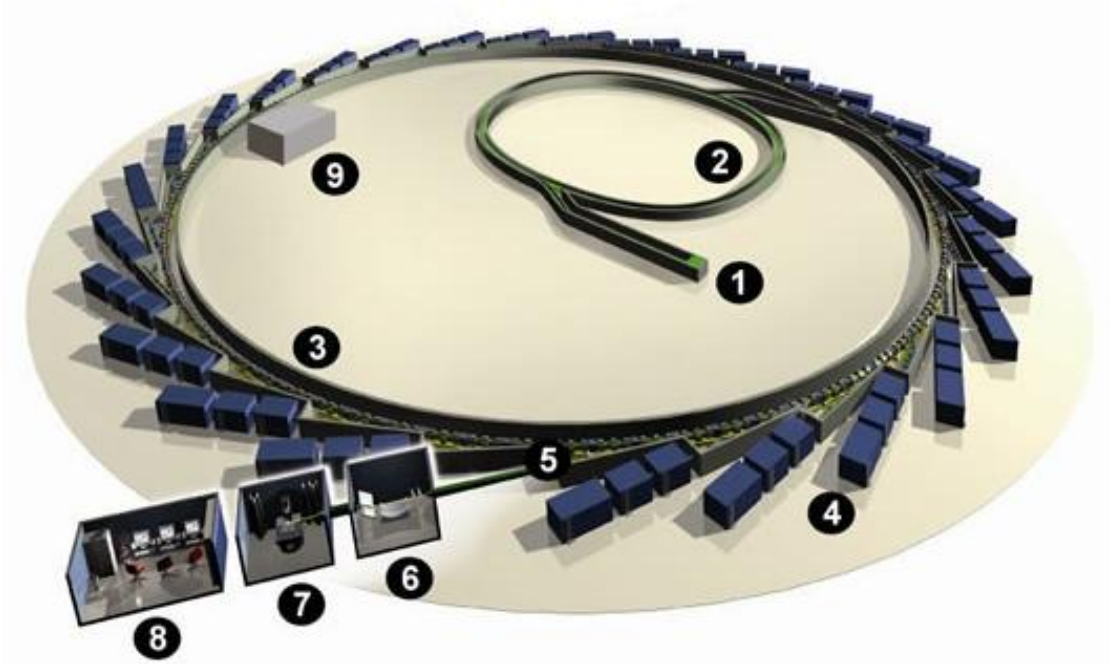

Figure A1.6: Schematic representation of a synchrotron. 1) linear accelerator (Linac), 2) booster ring, 3) storage ring and experimental hall, 4) insertion devices, 5) front end, 6) optics hutch, 7) experimental hutch, 8) user cabin, 9) radiofrequency (RF) system. Image courtesy of Diamond Light Source Ltd.

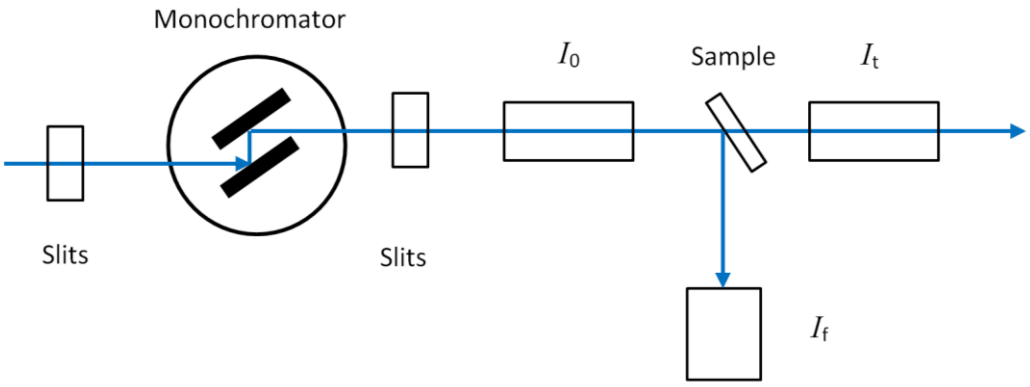

Figure A1.7: Experimental setup for EXAFS (adapted from Charnock, 1995). The arrow shows the path of the X-rays as they leave the synchrotron and enter the beamline. I_0 and I_t are the ion chambers for detection of incident and transmitted light, I_f is the fluorescence detector.

EXAFS data for this study was collected from the XAS beamline (BM29) at the European Synchrotron Research Facility (ESRF), Grenoble, France, and the Super-XAS beamline at the Swiss Light Source (SLS), Paul Scherrer Institut, Villigen, Switzerland.

A1.8 Transmission electron microscopy (TEM)

The limit of resolution using light microscopy is based on the wavelength of the light used. In order to resolve images smaller than around 200 nm, electrons are used instead of light, which improves resolution by three orders of magnitude. The image formation in transmission electron microscopy (TEM) comes from the combination of both elastic scattering (where electrons are deflected by nuclei within a sample without loss of energy) and inelastic scattering (where interaction leads to energy loss) (Ellisman, 2006). Sectioning work for TEM studies in this thesis was performed at the School of Biological Sciences, University of Birmingham, and the EM facility in the Faculty of Life Sciences, University of Manchester.

A1.9 Electron tomography

Electron tomography is a process using transmission electron microscopy by which tilt/rotate cartridges are used that allow a TEM sample grid to be tilted to 70° and rotated to 90°. By scanning through the thick section as it is being tilted, a series of images are produced at different angles which can then be recompiled in a stack to generate a 3-dimensional image, providing information for example about a bacterial cell surface and any structures associated with it. Precision is essential when moving the sample within the beam, as any errors in stage movement will interfere with the imaging process. The cartridge-based system increases stability and reduces such errors.

Appendix 2: Unpublished work

A2.1 Pd(II) biosorption by *E. coli* BL21(DE3) cells

Method

To determine the amount of Pd(II) lost from solution by biosorption to the bacterial cells, rather than by bioreduction to Pd(0), cell suspensions were challenged with 1 mM sodium tetrachloropalladate as previously (section 3.1.1) and incubated at 30°C for 1 hour. Aliquots were taken prior to and following incubation and centrifuged for 5 minutes at 15,996 *g* in a Boeco M-24 microcentrifuge. The supernatant was added to an equal volume of 70% nitric acid and diluted to a final concentration of 2% nitric acid, and filtered using a syringe-driven 0.22 µm Millipore filter before analysis for the presence of palladium using ICP-MS.

Results

When cells were challenged with Pd(II) and incubated for one hour at 30°C, the level of Pd(II) found in the supernatant was reduced from 90 µg ml^{-1} to 87 µg ml^{-1}. However, using killed (autoclaved) cells the level found in the supernatant following incubation was 18 µg ml^{-1}. Live cells therefore take up very little Pd(II) by biosorption, but killed cells remove most of the Pd(II) from the supernatant, possibly due to the increased surface area of the biomass (due to cell lysis).

In a 1 mM solution of sodium tetrachloropalladate, the amount of Pd(II) should be 106.42 mg l^{-1}, but the ICP-MS results consistently show less than this. The Pd(II) control (no cells) is measured at 97-99 mg l^{-1}. This can be partially explained by the reported % of palladium in the Na_2PdCl_4, which is 35.4% (rather than 36.2%). This would return a result of 104 mg l^{-1}. Of the remainder, it is possible that some Pd(II) sorbs to the cells immediately, reducing the Pd(II) in solution to a level between ~98 mg l^{-1} and 90 mg l^{-1}.

In a previous study of Pd(II) biosorption to D desulfuricans, Yong *et al*. (2002c) determined that biosorption of palladium in $PdCl_4^{2+}$ complexes was pH-dependent, with up to 70% removal of Pd(II) from solution at pH 4. At pH 7, the removal due to biosorption was <20%. They concluded that the high concentration of Cl^- ions may

cause complexes with Pd(II) to form and reduce its affinity for cationic-specific biosorption sites. When a different Pd(II) complex, $Pd(NH_3)_4^{2+}$ was used, less than 30% biosorption was observed irrespective of pH (Yong *et al.*, 2002c). As this current study uses pH 7.6 for bioreduction experiments in order to maintain the viability of the bacterial cells, this could explain the lower levels of biosorption seen in strains of *E. coli*.

A2.2 Viability of cells

Method

Viability of palladised cells: Viability of palladised cells was determined using the Miles and Misra colony counting technique (Miles & Misra, 1938), whereby 20 µl of serial dilutions of the cell suspension were plated onto LB agar in triplicate. The dilution showing the closest to ~20 colonies is counted, and the number of colony forming units (cfu) in the original suspension calculated as follows:

$$cfu\ ml^{-1} = average\ number\ of\ colonies\ in\ dilution \times 50 \times dilution\ factor$$

(Equation A2.1)

Viability of cells following deracemisation: The viability of biocatalyst used in a deracemisation reaction over 5 cycles of air and hydrogen was determined using the Miles and Misra colony counting technique.

Viability of cells in alginate beads: The viability of the cells encapsulated in alginate was determined by first destabilising the ionic cross-linking of the alginate using potassium phosphate buffer (Smidsrod & Skjak-Braek, 1990), before plating out using the Miles and Misra colony counting technique. Cells were counted on day 1, immediately following encapsulation, and after 1 week of storage in 0.5% w/v $CaCl_2$ solution at 10°C.

Results

Viability of palladised cells: Palladisation of the cells reduced the viability of the cells from 10^8 cfu ml^{-1} (thawed biocatalyst, 250 mg ml^{-1}) to 10^6-10^7 cfu ml^{-1}. This reduction in viability was most likely due to the disruption in the outer cell membrane seen in transmission electron micrographs (see section 4.1.9 and Figure 4.9).

Viability of cells following deracemisation: The viability of the biocatalyst as determined using the Miles and Misra colony counting technique was calculated to be 8×10^7 cfu ml^{-1} prior to the biotransformation, and 2×10^5 cfu ml^{-1} following the biotransformation, a reduction of two orders of magnitude. The fragility of the cells following palladisation was probably a factor, but the cells would also have been starved of nutrients at this point.

Viability of cells in alginate beads: Immediately following encapsulation in alginate, the viable count for the biocatalyst was 4.5×10^5 cfu ml^{-1}, a reduction in two orders of magnitude from 10^7 cfu ml^{-1}. The alginate is non-toxic and the encapsulation conditions are very mild, which suggests that the increased fragility of the palladised cells is responsible. After one week of storage in 0.5% w/v $CaCl_2$ at 10°C, the viable count was further reduced to 6×10^3 cfu ml^{-1}. However, the cells had been starved of nutrients for all this period, and it is possible that a nutrient supply would extend the viability of the biocatalyst.

A2.3 Electron tomography

Method

3-dimensional images of the palladised bacterial strains *E. coli* BL21(DE3), MC4100 and FTD128 were prepared using the FEI Polara 300kV FEG transmission electron microscope in the University of Manchester EM facility. These images were taken in order to provide clearer information as to the nature of the association of the Pd(0) nanoparticles with the cell surface. The sections were prepared in the same way as those used for TEM (section 3.1.8).

Results

The 3-dimensional images of palladised cells obtained using the FEI Polara 300kV FEG transmission electron microscope in the University of Manchester EM facility showed the association of the Pd(0) nanoparticles with the outer membrane of the cells, and indicated that the clusters of nanoparticles might possibly cross the membrane into the periplasm (Figure A2.1). Similar results were obtained from cells with formate-dependent bioreduced Pd(0) (MC4100 and FTD128) and hydrogen-dependent bioreduced Pd(0) (BL21(DE3)). However, the limitation of this technique is that the data must be viewed using animation software, otherwise the image is two-dimensional only.

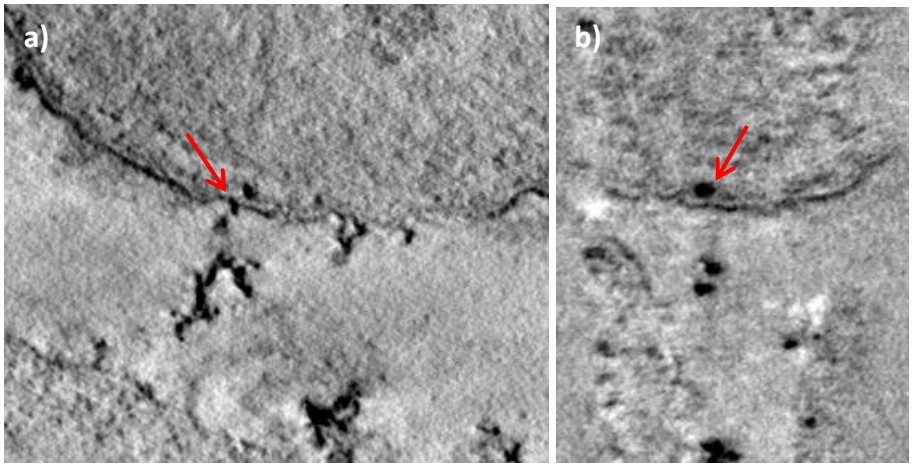

Figure A2.1: Polara transmission electron micrographs of *E. coli* MC4100, showing palladium nanoparticles breaching the outer membrane (a) and located within the periplasm (b) (red arrows). Scales bars are not available, as these images were taken as screenshots from an animated sequence.

A2.4 Amplification and purification of plasmid

Method

E. coli TOP10/P3 chemically competent cells were thawed on ice before adding 1 µl plasmid and incubating on ice for 30 minutes. The cells were heat shocked at 42°C for 30 seconds and transferred back to the ice for 2-3 minutes. 250 µl SOC medium (super optimal broth with catabolite repression) was added to the cells, which were then incubated at 37°C for one hour. Transformed cells were subcultured onto LB agar

plates containing 100 µg ml^{-1} ampicillin (LB-ampicillin agar), and incubated overnight at 37°C. Three isolated colonies were used to inoculate three 5 ml aliquots of LB-broth with 100 µg ml^{-1} ampicillin (LB-ampicillin broth), which were then incubated at 37°C, shaking at 180 rpm for 18 hours. After centrifuging and removing all broth supernatant, the plasmid was purified using the QIAprep Spin Miniprep Kit from QIAGEN.

Quantification of plasmid: Using a crystal microcuvette, the amount of plasmid obtained through amplification and purification was measured using a Camspec M501 Single Beam Scanning UV/Visible spectrophotometer.

Results

Quantification of plasmid: DNA can be quantified using spectrophotometry, by measuring the absorbance of a sample at 260 nm. At this wavelength, an absorbance measurement of 1 is equal to 50 ng μl^{-1}. As protein absorbs light at a wavelength of 280 nm, the $A_{260/280}$ ratio is used to detect protein contamination, with a ratio of 1.8-1.9 for pure DNA.

The amount of DNA obtained was calculated to be 56.31 ng μl^{-1}, requiring 2 µl (~100 ng) to be used in the transformation of *E. coli* BL21(DE3) cells. The $A_{260/280}$ ratio was 2.1, indicating that there was no protein contamination detected (although there may have been some RNA present).

A2.5 Colorimetric assay

The principle of the colorimetric assay is based on the reduction of molecular oxygen that accompanies the oxidation of MTQ, forming hydrogen peroxide. Horseradish peroxidase (HRP) catalyses the oxidation of the dye pyrogallol red, with the associated reduction of hydrogen peroxide. This leads to a colour change in the dye from deep red to straw-coloured, which can be measured by spectrophotometry.

Method

Reagents were prepared by diluting in 100 mM potassium phosphate buffer at pH 7.6, to produce 1 mg ml^{-1} HRP, 0.6 mg ml^{-1} pyrogallol red dye, and 12.5 mM MTQ. Aerobic cells were used diluted 1:10, anaerobic cells were used neat. Twelve wells of a 96-well plate were used for the assay with samples and controls wells tested in triplicate, with each well containing a final volume of 100 µl as shown in Table A2.

Table A2: Experimental set-up in a 96-well plate for the oxidation of pyrogallol red dye.

1	2	3	4	5	6	7	8	9	10	11	12
5 µl HRP 5 µl cells 10 µl dye 80 µl MTQ			5 µl HRP 5 µl cells 10 µl dye 80 µl KPO_4			5 µl HRP 5 µl KPO_4 10 µl dye 80 µl MTQ			5 µl KPO_4 5 µl cells 10 µl dye 80 µl MTQ		

The plate was placed immediately into the Bio-Tek Elx800 plate reader, and the absorbance read at 550 nm every 30 seconds for 45 minutes.

Results

The colorimetric assay produced a colour change in wells 1-3, which contained biocatalyst, horseradish peroxidase (HRP), pyrogallol red dye, and the MTQ substrate (see Figure A2.2). A slower change in colour was seen in wells 4-6, which were missing the substrate, and wells 7-9, which were missing the biocatalyst. No colour change was seen in wells 10-12, which were missing the HRP enzyme.

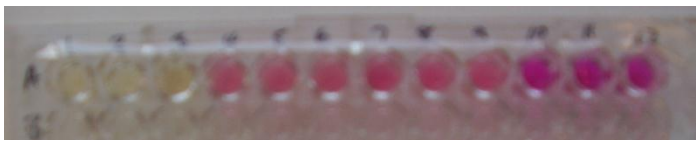

Figure A2.2: Colorimetric plate assay, demonstrating the complete reduction of the pyrogallol red dye by horseradish peroxidase (wells 1-3), with partial reduction in wells 4-6 (no MTQ substrate) and wells 7-9 (no biocatalyst), and no reduction in wells 10-12 (no HRP).

The rate of pyrogallol reduction by HRP (wells 1-3 only) can be seen in Figure A2.3, which compares three separate batches of biocatalyst. The rate of reduction is similar in all three batches.

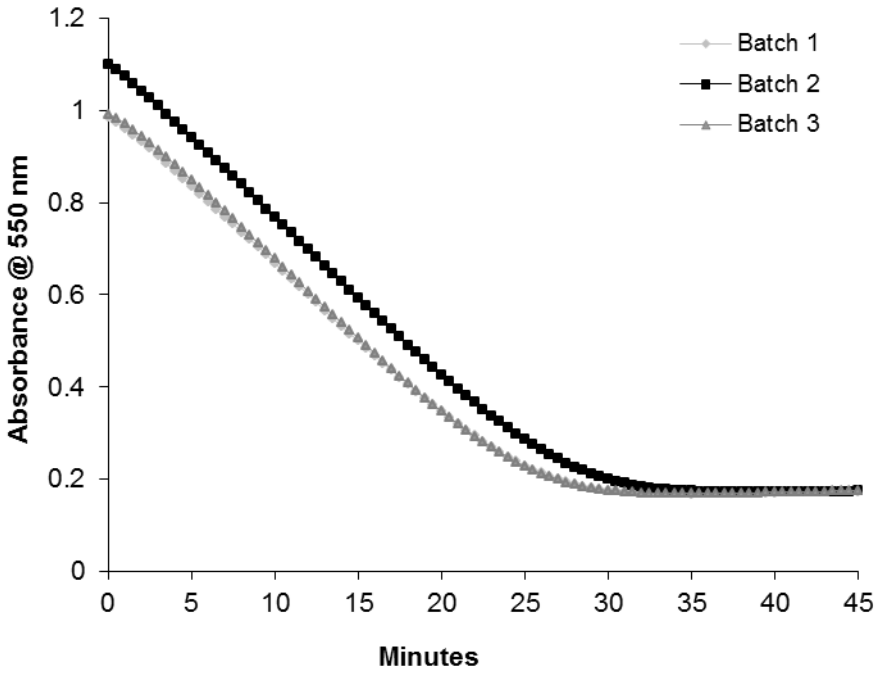

Figure A2.3: Rate of reduction of pyrogallol red by HRP for the comparison of batches of biocatalyst, as measured by UV/visible spectrophotometry. Each point is based on a single measurement.

The colorimetric assay demonstrates the expression of MAO-N-D5 enzyme, but measures the activity of the HRP enzyme and so is useful only for comparing the activity of different batches of biocatalyst, for example as a screening assay for variants produced by directed evolution. A further assay using HPLC analysis was therefore designed in order to measure the activity of the MAO-N-D5 directly, based on the oxidation of (*S*)-MTQ to MDQ.

A2.6 Optimisation of oxidation step 1 – different biomasses of biocatalyst

Methods

The biocatalyst was prepared as in section 3.2.2. Cell pellets were adjusted to a mass of either 125 mg, 250 mg, or 500 mg based on the wet cell pellet, and resuspended in MOPS-NaOH to a volume of 1 ml. Aliquots were stored at -20°C.

Results

In a comparison of three different biomasses of biocatalyst, the 250 mg ml^{-1} biocatalyst performed the best (Figure A2.4). The oxidation of (*S*)-MTQ with this biomass was complete within 2 hours, whereas the rate of oxidation with the 500 mg ml^{-1} biocatalyst was faster at the beginning, but slower when the substrate concentration was <0.5 mM remaining and did not reach completion. With the 125 mg ml^{-1} biocatalyst, >1 mM substrate still remained at 2.5 hours.

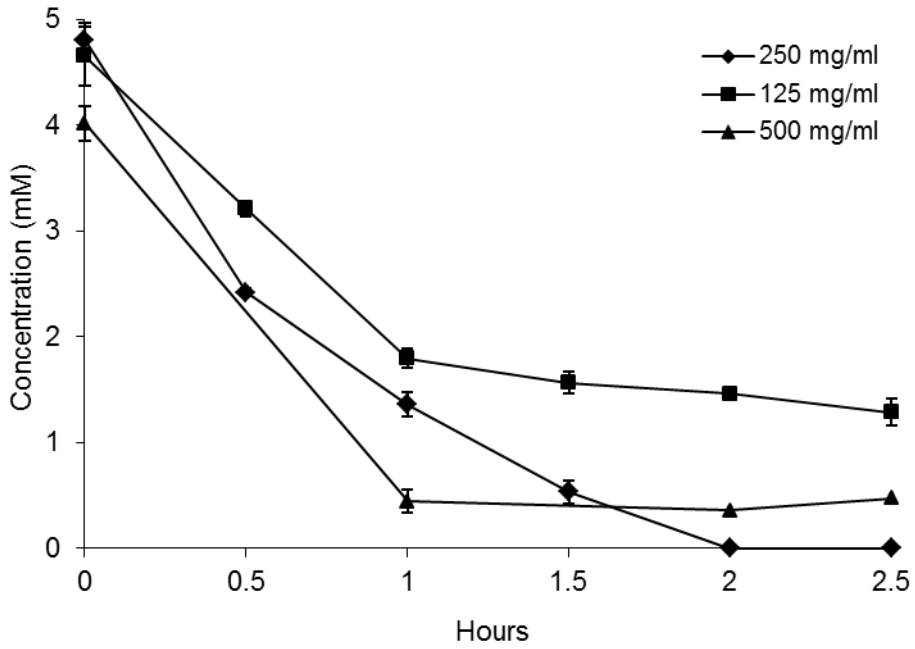

Figure A2.4: Comparison of three different biomasses of biocatalyst in the oxidation of (*S*)-MTQ to MDQ. For clarity, (*S*)-MTQ only is shown. All data points represent mean values from triplicate measurements, with standard error bars.

A2.7 Optimisation of oxidation step 2 – different shaking speeds during incubation

Methods

Two different shaking speeds were compared with static incubation to determine the optimum conditions for deracemisation. The deracemisation experiment was prepared as in section 3.2.5. Samples were mixed on a 1 ml scale in a thermomixer at 900 rpm, in a shaking incubator at 225 rpm, and in a static incubator. The incubation temperature was 37°C in all three experiments. Samples for extraction in MTBE (see section 3.2.3) were taken at 0 and 3 hours.

Results

Very little MDQ was produced in the samples shaking at 900 rpm (Figure A2.5), indicating that the speed was too fast for efficient reaction kinetics to take place, or that the enzyme was denatured. Slightly more MDQ was produced in the static samples, where the reaction kinetics were hindered by the lack of mixing of the substrate with the enzyme. Mixing at 225 rpm allowed the oxidation reaction to complete within 3 hours, and thus was the speed chosen for further experiments.

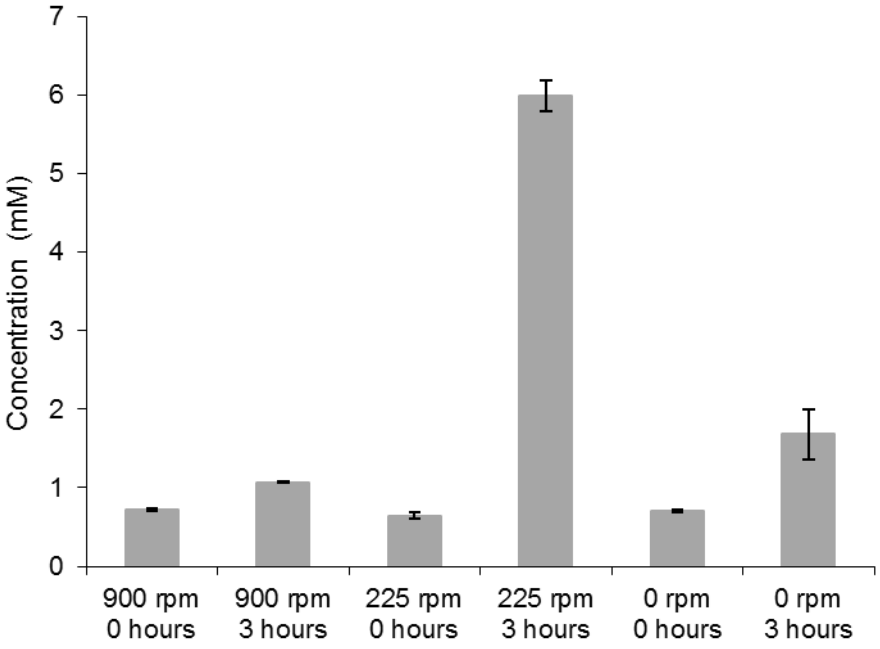

Figure A2.5: MDQ generated from the oxidation of (*S*)-MTQ over three hours at 37°C, using three different speeds of shaking – 900 rpm, 225 rpm, and static incubation.

A2.8 Optimisation of reduction step 1 – reduction of MDQ with formate only

This experiment was to demonstrate that reduction of MDQ to racemic MTQ does not take place with formate only, and that a palladium is necessary to catalyse the reaction.

Methods

Biocatalyst without palladium loading was prepared as previously (see section 3.2.2), and a reduction step was performed using formate (see section 3.2.4 for method).

Results

Over a 24 hour period, no MTQ was formed (see Figure A2.6), indicating that formate alone is insufficient for the reduction of MDQ to racemic MTQ to take place, and that a palladium catalyst is necessary.

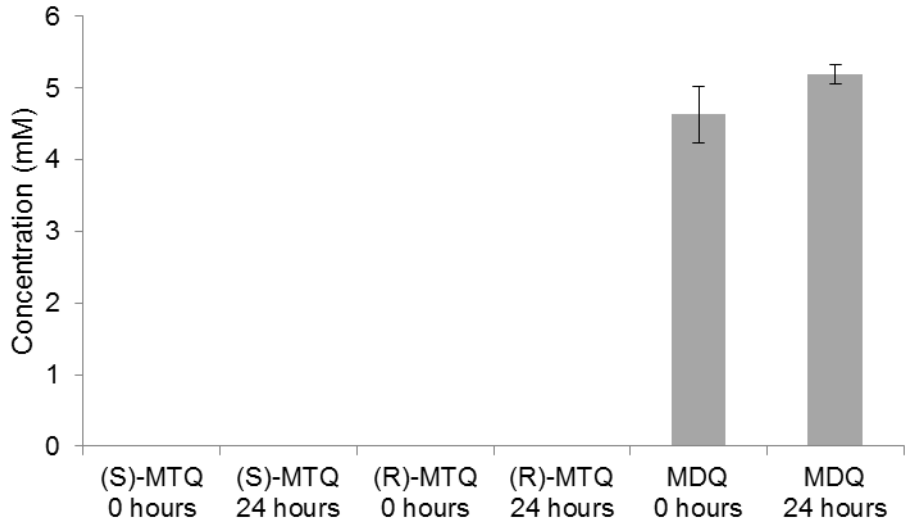

Figure A2.6: Incubation of substrate with cells and formate, no palladium. No reduction of MDQ takes place over a 24 hour period.

A2.9 Optimisation of reduction step 2 – loading of biomass with different concentrations of Pd(0)

Method

Pd-loaded untransformed *E. coli* BL21(DE3) cells were prepared as previously (section 3.1.1), using hydrogen as the electron donor, with concentrations of either 0.5 mM or 1 mM Pd(II). The Pd-loaded cells were then used to catalyse the reduction of MDQ to racemic MTQ, using hydrogen gas as the electron donor (see section 3.2.4 for method).

Results

When two different concentrations of palladium were used in the palladisation of the biocatalyst and compared in the reduction of MDQ, the higher concentration (1 mM palladium) performed better. The reduction of MDQ using the lower concentration of palladium (0.5 mM) was slower from the start, and had not reached completion by 45 minutes, with almost 1 mM MDQ remaining (Figure A2.7).

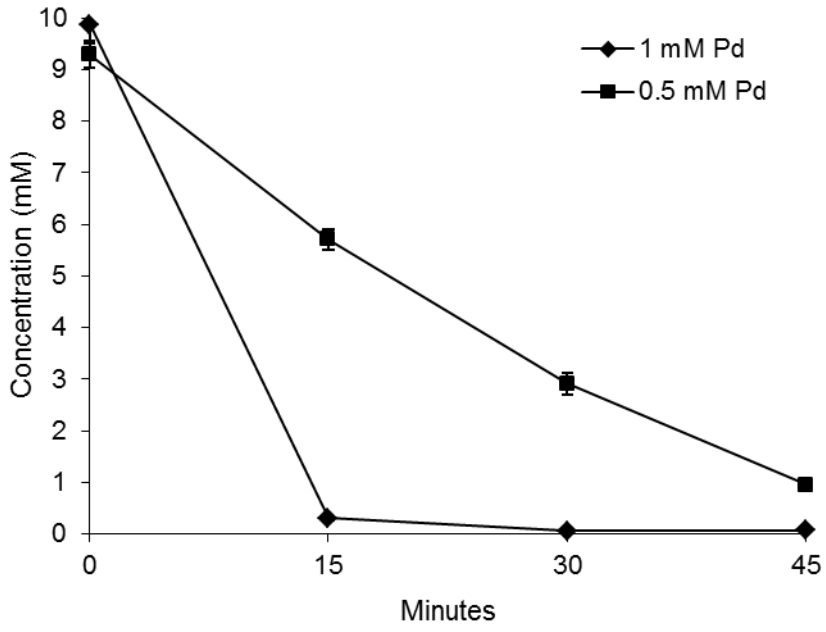

Figure A2.7: Comparison of two different concentrations of palladium in the generation of palladised cells, for the reduction of MDQ to racemic MTQ. For clarity, MDQ only is shown. All data points represent mean values from triplicate measurements, with standard error bars.

A2.10 Improving enantiomeric excess

Methods

In order to improve the enantiomeric excess of product obtained from a 4-cycle biotransformation using hydrogen as the electron donor, deracemisation was performed using various additional strategies as follows:

1. The biotransformation was carried out at 40°C, instead of 37°C.
2. The oxidation step was performed under pure oxygen, rather than air.
3. The inducer isopropyl β-D-1-thiogalactopyranoside (IPTG) was used to upregulate expression of the MAO-N-D5 enzyme. IPTG (1 ml, 1 mM) was added to the 100 ml LB broth flask culture after 6.5 hours of incubation, during the mid-exponential growth phase.
4. Catalase (0.1 mg ml^{-1}) was added to the biotransformation, to ensure the removal of hydrogen peroxide from the reaction.
5. 5 cycles of alternating oxidation and reduction were performed, rather than 4.

Results

Of the various strategies used, increasing the temperature to 40°C, using oxygen for the oxidation step, inducing expression of the enzyme, and the addition of catalase to the biotransformation had no effect on improving the e.e. Increasing the experiment from 4 cycles to 5 cycles increased the e.e. to 93% (Figure A2.8).

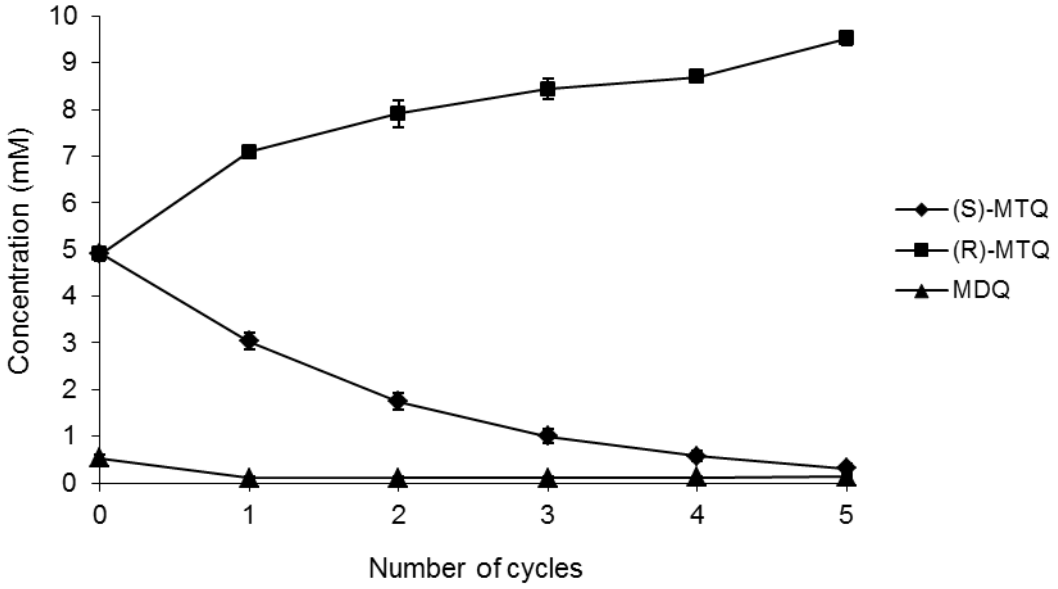

Figure A2.8: The deracemisation of MTQ, giving an e.e. of 93% (*R*)-MTQ (5 cycles of air alternated with 5 cycles of hydrogen). All data points represent mean values from triplicate measurements, with standard error bars.

A2.11 Immobilisation of cells in chitosan

Method

Cells were immobilised in chitosan beads by adapting the method of Vorlop and Klein (1981). 72 µl acetic acid was added to 7.1 ml deionised water, into which 0.16 g chitosan was then dissolved.

0.16 g chitosan was dissolved in 42 ml deionised water with 72 µl acetic acid, and 1 ml of palladised transformed *E. coli* cells (250 mg ml^{-1} in 20 mM MOPS-NaOH buffer at pH 7.6) were added. The chitosan-cell suspension was then dropped into 50 ml of a 1.5% w/v sodium pyrophosphate solution at pH 9 using a plastic Pasteur pipette, whilst gently stirring to prevent bead aggregation. Chitosan beads were left stirring for 1 hour to harden, after which time the beads were rinsed in 0.1 M potassium phosphate buffer at pH 7.6. Beads were stored potassium phosphate buffer at 10°C until use.

Results

After storage overnight in 0.1 M potassium phosphate buffer, the cells had begun to drop out of the chitosan beads, as determined by the turbidity of the buffer. As the solution into which the beads were dropped was pH 9, the chitosan would have been precipitated rather than cross-linked (pH <6). The higher pH was chosen for its milder conditions, in producing beads of neutral pH, but was possibly the reason for the instability of the beads. The chitosan beads were therefore discarded without use in a deracemisation reaction.

A2.12 Immobilisation of cells in sol-gel

Method

The method used for sol-gel encapsulation of biocatalyst was adapted from those of Nguyen-Ngoc and Tran-Minh (2007), and Nassif *et al* (2002). The sol-gel was prepared by mixing 2 ml 0.4 M sodium silicate with 6 ml 8.5 M LUDOX HS-40, and adjusting to pH 7 with 4 M hydrochloric acid. 1 ml of palladised transformed *E. coli* cells (250 mg ml^{-1} in 10% v/v glycerol) were added, and the mixture transferred to a 96-well plate where the sol-gel was left to harden overnight into pellets.

Results

Cells that had not been loaded with palladium were encapsulated into hardened sol-gel pellets. Pd-loaded cells however were not, as the palladium appeared to have interfered with the cross-linking of the sol-gel in some way. The sol-gel pellets were therefore discarded without use in a deracemisation reaction.

A2.13 Immobilisation of cells in polyacrylamide

Method

The polyacrylamide gel was prepared by mixing 15 ml acrylamide:bis-acrylamide (29:1) with 150 µl ammonium persulfate, and adding 1 ml of palladised transformed *E. coli* cells (250 mg ml^{-1} in 20 mM MOPS-NaOH buffer at pH 7.6). The gel was allowed to set

for one hour, before cutting into small cubes and storing in 0.1 M potassium phosphate buffer at pH 7.6 at 10°C until use.

Results

When the polyacrylamide gel cubes were added to the MTQ substrate, it immediately began to depolymerise and release the biocatalyst. The polyacrylamide gel was therefore discarded without use in a deracemisation reaction.

A2.14 Activity of alginate-immobilised biocatalyst following storage

Methods

In order to determine the activity of the biocatalyst following storage at 10°C, the activity of beads used on day 1 in oxidation-only experiments was compared with that used after 1 week and 2 weeks of storage (see section 3.2.8 for method). The same beads were used immediately afterwards in reduction-only experiments.

Results

As can be seen from Figure A2.9, the activity of the MAO-N-D5 in alginate-immobilised biocatalyst is considerably reduced with time. On day 1, the (*S*)-MTQ is oxidised from 50% to 7% within 2.5 hours, but after one week of storage, the amount of (*S*)-MTQ remaining is 26%. After a further week of storage, the amount of (*S*)-MTQ remaining is 34%. With the reduction-only experiments however, it can be seen from Figure A2.10 that there is no loss of activity of the Pd(0) nanoparticles.

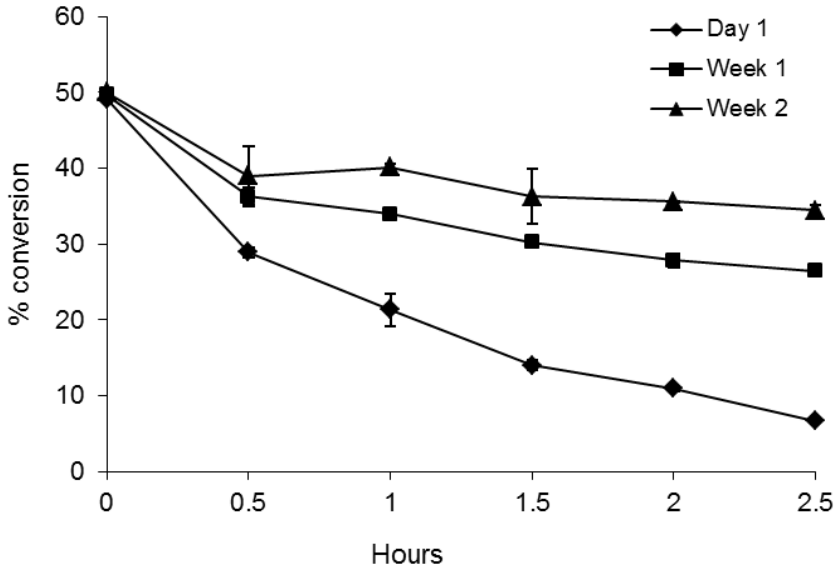

Figure A2.9: The oxidation of (*S*)-MTQ to MDQ at 37°C, by *E. coli* transformed with the *mao-N-D5* gene insert and immobilised in alginate beads before testing immediately, after storage at 10°C for 1 week, and after storage at 10°C for 2 weeks. Only (*S*)-MTQ is shown for clarity. All data points represent mean values from triplicate measurements, with standard error bars.

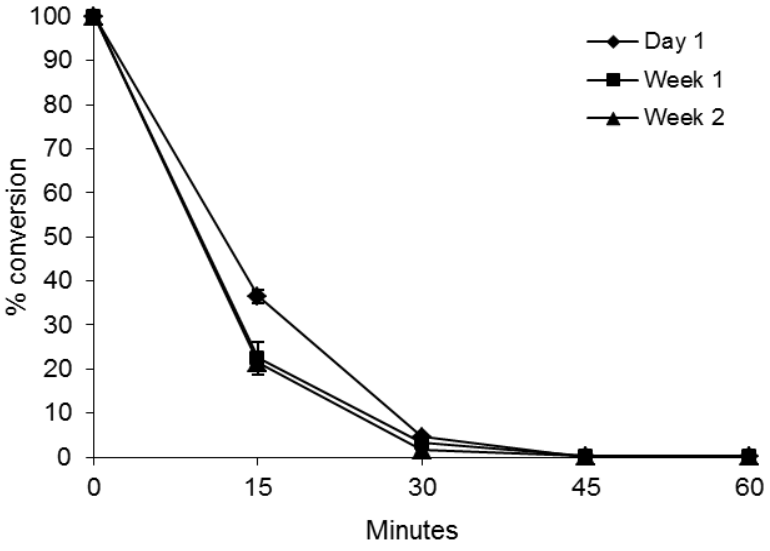

Figure A2.10: The reduction of MDQ to *rac*-MTQ at 37°C, by palladised *E. coli* cells immobilised in alginate beads before testing immediately using hydrogen gas as the electron donor, after storage at 10°C for 1 week, and after storage at 10°C for 2 weeks. Only MDQ is shown for clarity. All data points represent mean values from triplicate measurements, with standard error bars.

Appendix 3: Conferences Attended

10th-13th December 2010; Biocatalysis 2010, Cancun Mexico. Presentation entitled "Engineering microbial cells for bio-metallic catalysis".

6th-9th September 2010; Society for General Microbiology Autumn Meeting 2010, University of Nottingham.

21st April 2009; RSC Biotechnology Group and the RSC Chemistry Biology Interface Forum meeting Advances in Biocatalysis, University College London.

15th July 2008; 5th NW Microbiology Group Meeting. Ness Gardens, Liverpool.

References

Abaibou, H., Pommier, J., Benoit, S., Giordano, G. & Mandrandberthelot, M. A. (1995). Expression and characterization of the *Escherichia coli fdo* Locus and a possible physiological role for aerobic formate dehydrogenase. *Journal of Bacteriology* **177**, 7141-7149.

Abou-Shakra, F. R. (2004). Biomedical applications of inductively coupled plasma mass spectrometry (ICP-MS) as an element specific detector for chromatographic separations. In *Bioanalytical Separations*, pp. 351-371. Edited by I. D. Wilson: Elsevier Science.

Aitken, A. (2005). Chapter 9 Mass spectrometric techniques. In *Principles and techniques of biochemistry and molecular biology*. Edited by K. Wilson & J. M. Walker. New York: Cambridge University Press.

Alexeeva, M., Enright, A., Dawson, M. J., Mahmoudian, M. & Turner, N. J. (2002). Deracemization of α-methylbenzylamine using an enzyme obtained by in vitro evolution. *Angewandte Chemie-International Edition* **41**, 3177-3180.

Anderson, R. T., Rooney-Varga, J. N., Gaw, C. V. & Lovley, D. R. (1998). Anaerobic benzene oxidation in the Fe(III) reduction zone of petroleum-contaminated aquifers. *Environmental Science & Technology* **32**, 1222-1229.

Andrews, S. C., Berks, B. C., McClay, J., Ambler, A., Quail, M. A., Golby, P. & Guest, J. R. (1997). A 12-cistron *Escherichia coli* operon (*hyf*) encoding a putative proton-translocating formate hydrogenlyase system. *Microbiology* **143**, 3633-3647.

Anraku, Y. & Gennis, R. B. (1987). The aerobic respiratory chain of *Escherichia coli*. *Trends in Biochemical Sciences* **12**, 262-266.

Atkin, K. E., Reiss, R., Koehler, V., Bailey, K. R., Hart, S., Turkenburg, J. P., Turner, N. J., Brzozowski, A. M. & Grogan, G. (2008a). The structure of monoamine oxidase from *Aspergillus niger* provides a molecular context for improvements in activity obtained by directed evolution. *Journal of Molecular Biology* **384**, 1218-1231.

Atkin, K. E., Reiss, R., Turner, N. J., Brzozowski, A. M. & Grogan, G. (2008b). Cloning, expression, purification, crystallization and preliminary X-ray diffraction analysis of variants of monoamine oxidase from *Aspergillus niger*. *Acta Crystallographica Section F-Structural Biology and Crystallization Communications* **64**, 182-185.

Baba, T., Ara, T., Hasegawa, M. & other authors (2006). Construction of *Escherichia coli* K-12 in-frame, single-gene knockout mutants: the Keio collection. *Molecular Systems Biology* **2**, Article no. 2006.0008.

Baxter-Plant, V., Mikheenko, I. P. & Macaskie, L. E. (2003). Sulphate-reducing bacteria, palladium and the reductive dehalogenation of chlorinated aromatic compounds. *Biodegradation* **14**, 83-90.

Baxter-Plant, V. S., Mikheenko, I. P., Robson, M., Harrad, S. J. & Macaskie, L. E. (2004). Dehalogenation of chlorinated aromatic compounds using a hybrid bioinorganic catalyst on cells of *Desulfiovibrio desulfuricans*. *Biotechnology Letters* **26**, 1885-1890.

Beauregard, D. A., Yong, P., Macaskie, L. E. & Johns, M. L. (2010). Using non-invasive magnetic resonance imaging (MRI) to assess the reduction of Cr(VI) using a biofilm-palladium catalyst. *Biotechnology and Bioengineering* **107**, 11-20.

Bennett, J. A., Creamer, N. J., Deplanche, K., Macaskie, L. E., Shannon, I. J. & Wood, J. (2010). Palladium supported on bacterial biomass as a novel heterogeneous catalyst: A comparison of Pd/Al_2O_3 and bio-Pd in the hydrogenation of 2-pentyne. *Chemical Engineering Science* **65**, 282-290.

Berg, B. L., Li, J., Heider, J. & Stewart, V. (1991). Nitrate-inducible formate dehydrogenase in *Escherichia coli* K-12 .1. Nucleotide sequence of the *fdnGHI* operon and evidence that opal (UGA) encodes selenocysteine. *Journal of Biological Chemistry* **266**, 22380-22385.

Berks, B. C., Ferguson, S. J., Moir, J. W. B. & Richardson, D. J. (1995). Enzymes and associated electron transport systems that catalyse the respiratory reduction of nitrogen oxides and oxyanions. *Biochimica Et Biophysica Acta-Bioenergetics* **1232**, 97-173.

Bohm, R., Sauter, M. & Bock, A. (1990). Nucleotide sequence and expression of an operon in *Escherichia coli* coding for formate hydrogenlyase components. *Molecular Microbiology* **4**, 231-243.

Breuer, M., Ditrich, K., Habicher, T., Hauer, B., Kesseler, M., Sturmer, R. & Zelinski, T. (2004). Industrial methods for the production of optically active intermediates. *Angewandte Chemie-International Edition* **43**, 788-824.

Bunge, M., Sobjerg, L. S., Rotaru, A. E. & other authors (2010). Formation of palladium(0) nanoparticles at microbial surfaces. *Biotechnology and Bioengineering* **107**, 206-215.

Burton, P. D., Boyle, T. J. & Datye, A. K. (2011). Facile, surfactant-free synthesis of Pd nanoparticles for heterogeneous catalysts. *Journal of Catalysis* **280**, 145-149.

Cahn, R. S., Ingold, C. & Prelog, V. (1966). Specification of molecular chirality. *Angewandte Chemie-International Edition* **5**, 385-415.

Carr, R., Alexeeva, M., Enright, A., Eve, T. S. C., Dawson, M. J. & Turner, N. J. (2003). Directed evolution of an amine oxidase possessing both broad substrate specificity and high enantioselectivity. *Angewandte Chemie-International Edition* **42**, 4807-4810.

Carr, R., Alexeeva, M., Dawson, M. J., Gotor-Fernandez, V., Humphrey, C. E. & Turner, N. J. (2005). Directed evolution of an amine oxidase for the preparative deracemisation of cyclic secondary amines. *Chembiochem* **6**, 637-639.

Casadaban, M. J. & Cohen, S. N. (1979). Lactose genes fused to exogenous promoters in one-step using a Mu-*lac* Bacteriophage - *In vivo* probe for transcriptional control sequences. *Proceedings of the National Academy of Sciences of the United States of America* **76**, 4530-4533.

Charnock, J. M. (1995). Biological applications of EXAFS spectroscopy. *Radiation Physics and Chemistry* **45**, 385-391.

Chen, S. H. & Engel, P. C. (2009). Efficient screening for new amino acid dehydrogenase activity: Directed evolution of *Bacillus sphaericus* phenylalanine dehydrogenase towards activity with an unsaturated non-natural amino acid. *Journal of Biotechnology* **142**, 127-134.

Cheng, K. C., Demirci, A. & Catchmark, J. M. (2010). Advances in biofilm reactors for production of value-added products. *Applied Microbiology and Biotechnology* **87**, 445-456.

Chidambaram, D., Hennebel, T., Taghavi, S., Mast, J., Boon, N., Verstraete, W., van der Lelie, D. & Fitts, J. P. (2010). Concomitant microbial generation of palladium nanoparticles and hydrogen to immobilize chromate. *Environmental Science & Technology* **44**, 7635-7640.

Cho, B. K., Park, H. Y., Seo, J. H., Kim, J. H., Kang, T. J., Lee, B. S. & Kim, B. G. (2008). Redesigning the substrate specificity of ω-aminotransferase for the kinetic resolution of aliphatic chiral amines. *Biotechnology and Bioengineering* **99**, 275-284.

Coates, J. D., Phillips, E. J. P., Lonergan, D. J., Jenter, H. & Lovley, D. R. (1996). Isolation of *Geobacter* species from diverse sedimentary environments. *Applied and Environmental Microbiology* **62**, 1531-1536.

Coiffier, A., Coradin, T., Roux, C., Bouvet, O. M. M. & Livage, J. (2001). Sol-gel encapsulation of bacteria: a comparison between alkoxide and aqueous routes. *Journal of Materials Chemistry* **11**, 2039-2044.

Cox, E. C. (1976). Bacterial mutator genes and control of spontaneous mutation. *Annual Review of Genetics* **10**, 135-156.

Creamer, N. J., Baxter-Plant, V. S., Henderson, J., Potter, M. & Macaskie, L. E. (2006). Palladium and gold removal and recovery from precious metal solutions and electronic scrap leachates by *Desulfovibrio desulfuricans*. *Biotechnology Letters* **28**, 1475-1484.

Creamer, N. J., Mikheenko, I. P., Deplanche, K., Yong, P., Wood, J., Pollmann, K., Selenska-Pobell, S. & Macaskie, L. E. (2007a). A novel hydrogenation and hydrogenolysis catalyst using palladized biomass of Gram-negative and Gram-positive bacteria. *Advanced Materials Research* **20-21**, 603-606.

Creamer, N. J., Mikheenko, I. P., Yong, P. & other authors (2007b). Novel supported Pd hydrogenation bionanocatalyst for hybrid homogeneous/heterogeneous catalysis. *Catalysis Today* **128**, 80-87.

Creamer, N. J., Deplanche, K., Snape, T. J. & other authors (2008). A biogenic catalyst for hydrogenation, reduction and selective dehalogenation in non-aqueous solvents. *Hydrometallurgy* **94**, 138-143.

Datsenko, K. A. & Wanner, B. L. (2000). One-step inactivation of chromosomal genes in *Escherichia coli* K-12 using PCR products. *Proceedings of the National Academy of Sciences of the United States of America* **97**, 6640-6645.

De Colibus, L., Li, M., Binda, C., Lustig, A., Edmondson, D. E. & Mattevi, A. (2005). Three-dimensional structure of human monoamine oxidase A (MAO A): Relation to the structures of rat MAO A and human MAO B. *Proceedings of the National Academy of Sciences of the United States of America* **102**, 12684-12689.

de Vargas, I., Macaskie, L. E. & Guibal, E. (2004). Biosorption of palladium and platinum by sulfate-reducing bacteria. *Journal of Chemical Technology and Biotechnology* **79**, 49-56.

De Windt, W., Aelterman, P. & Verstraete, W. (2005). Bioreductive deposition of palladium (0) nanoparticles on *Shewanella oneidensis* with catalytic activity towards reductive dechlorination of polychlorinated biphenyls. *Environmental Microbiology* **7**, 314-325.

De Windt, W., Boon, N., Van den Bulcke, J., Rubberecht, L., Prata, F., Mast, J., Hennebel, T. & Verstraete, W. (2006). Biological control of the size and reactivity of catalytic Pd(0) produced by *Shewanella oneidensis*. *Antonie Van Leeuwenhoek International Journal of General and Molecular Microbiology* **90**, 377-389.

Demain, A. L. & Adrio, J. L. (2008). Contributions of microorganisms to industrial biology. *Molecular Biotechnology* **38**, 41-55.

Deplanche, K., Attard, G. A. & Macaskie, L. E. (2007). Biorecovery of gold from jewellery wastes by *Escherichia coli* and biomanufacture of active Au-nanomaterial. *Advanced Materials Research* **20-21**, 647-650.

Deplanche, K., Snape, T. J., Hazrati, S., Harrad, S. & Macaskie, L. E. (2009). Versatility of a new bioinorganic catalyst: Palladized cells of *Desulfovibrio desulfuricans* and application to dehalogenation of flame retardant materials. *Environmental Technology* **30**, 681-692.

Deplanche, K. (2010). Novel gold/palladium bioinorganic catalysts for selective oxidation of alcohols. *Journal of Biotechnology* **150**, S198-S198.

Deplanche, K., Caldelari, I., Mikheenko, I. P., Sargent, F. & Macaskie, L. E. (2010). Involvement of hydrogenases in the formation of highly catalytic Pd(0) nanoparticles by bioreduction of Pd(II) using *Escherichia coli* mutant strains. *Microbiology* **156**, 2630-2640.

Deplanche, K., Murray, A. J., Mennan, C., Taylor, S. & Macaskie, L. E. (2011). Biorecycling of precious metals and rare earth elements. In *Nanomaterials*: InTech Publishing, in submission.

Dey, K. & Roy, P. (2011). Degradation of chloroform by immobilized cells of *Bacillus* sp. in calcium alginate beads. *Biotechnology Letters* **33**, 1101-1105.

Dunsmore, C. J., Carr, R., Fleming, T. & Turner, N. J. (2006). A chemo-enzymatic route to enantiomerically pure cyclic tertiary amines. *Journal of the American Chemical Society* **128**, 2224-2225.

Eberhardt, W. (2002). Clusters as new materials. *Surface Science* **500**, 242-270.

Edmondson, D. E., Mattevi, A., Binda, C., Li, M. & Hubalek, F. (2004). Structure and mechanism of monoamine oxidase. *Current Medicinal Chemistry* **11**, 1983-1993.

Ellisman, M. H. (2006). Chapter 19 Image Production Using Transmission Electron Microscopy. In *Basic Methods in Microscopy*. Edited by D. L. Spector & R. D. Goldman. New York: Cold Spring Press.

Esvelt, K. M., Carlson, J. C. & Liu, D. R. (2011). A system for the continuous directed evolution of biomolecules. *Nature* **472**, 499-U550.

Faber, K. (2001). Non-sequential processes for the transformation of a racemate into a single stereoisomeric product: Proposal for stereochemical classification. *Chemistry-a European Journal* **7**, 5004-5010.

Forzi, L. & Sawers, R. G. (2007). Maturation of [NiFe]-hydrogenases in *Escherichia coli*. *Biometals* **20**, 565-578.

Fotheringham, I. (2000). Engineering biosynthetic pathways: new routes to chiral amino acids. *Current Opinion in Chemical Biology* **4**, 120-124.

Gauthier, D., Sobjerg, L. S., Jensen, K. M., Lindhardt, A. T., Bunge, M., Finster, K., Skrydstrup, T. & Meyer, R. L. (2010). Environmentally benign recovery and reactivation of palladium from industrial waste by using Gram-negative bacteria. *Chemsuschem* **3**, 1036-1039.

Gloge, A., Zon, J., Kovari, A., Poppe, L. & Retey, J. (2000). Phenylalanine ammonia-lyase: The use of its broad substrate specificity for mechanistic investigations and biocatalysis - Synthesis of L-arylalanines. *Chemistry-a European Journal* **6**, 3386-3390.

Gordon, D. B. (2005). Chapter 12 Spectroscopic Techniques: Atomic and Molecular Electronic Spectroscopy. In *Principles and techniques of biochemistry and molecular biology*. Edited by K. Wilson & J. M. Walker. New York: Cambridge University Press.

Greener, A., Callahan, M. & Jerpseth, B. (1997). An efficient random mutagenesis technique using an *E. coli* mutator strain. *Molecular Biotechnology* **7**, 189-195.

Grogan, G. (2009). *Practical Biotransformations*. Chichester: John Wiley & Sons Ltd.

Grunwaldt, J. D., van Vegten, N. & Baiker, A. (2007). Insight into the structure of supported palladium catalysts during the total oxidation of methane. *Chemical Communications*, 4635-4637.

Gurman, S. J., Binsted, N. & Ross, I. (1984). A Rapid, Exact Curved-Wave Theory for EXAFS Calculations. *Journal of Physics C-Solid State Physics* **17**, 143-151.

Hailes, H. C., Dalby, P. A., Lye, G. J., Baganz, F., Micheletti, M., Szita, N. & Ward, J. M. (2010). α,α'-dihydroxy ketones and 2-amino-1,3-diols: synthetic and process strategies using biocatalysts. *Current Organic Chemistry* **14**, 1883-1893.

Hamilton, W. A. (1998). Bioenergetics of sulphate-reducing bacteria in relation to their environmental impact. *Biodegradation* **9**, 201-212.

Hanson, R. L., Davis, B. L., Chen, Y. J., Goldberg, S. L., Parker, W. L., Tully, T. P., Montana, M. A. & Patel, R. N. (2008). Preparation of (*R*)-amines from racemic amines with an (*S*)-amine transaminase from *Bacillus megaterium*. *Advanced Synthesis & Catalysis* **350**, 1367-1375.

Harrad, S., Robson, M., Hazrati, S., Baxter-Plant, V. S., Deplanche, K., Redwood, M. D. & Macaskie, L. E. (2007). Dehalogenation of polychlorinated biphenyls and polybrominated diphenyl ethers using a hybrid bioinorganic catalyst. *Journal of Environmental Monitoring* **9**, 314-318.

Hartmeier, W. (1988). *Immobilized Biocatalysts*: Springer Verlag, Berlin.

Hennebel, T., Van Nevel, S., Verschuere, S. & other authors (2011). Palladium nanoparticles produced by fermentatively cultivated bacteria as catalyst for diatrizoate removal with biogenic hydrogen. *Applied Microbiology and Biotechnology* **91**, 1435-1445.

Humphries, A. C., Mikheenko, I. P. & Macaskie, L. E. (2006). Chromate reduction by immobilized palladized sulfate-reducing bacteria. *Biotechnology and Bioengineering* **94**, 81-90.

Ishige, T., Honda, K. & Shimizu, S. (2005). Whole organism biocatalysis. *Current Opinion in Chemical Biology* **9**, 174-180.

Jia, L. S., Zhang, Q., Li, Q. B. & Song, H. (2009). The biosynthesis of palladium nanoparticles by antioxidants in *Gardenia jasminoides Ellis*: long lifetime nanocatalysts for *p*-nitrotoluene hydrogenation. *Nanotechnology* **20**.

Jochens, H., Stiba, K., Savile, C., Fujii, R., Yu, J. G., Gerassenkov, T., Bornscheuer, U. T. & Kazlauskas, R. J. (2009). Converting an esterase into an epoxide hydrolase. *Angewandte Chemie-International Edition* **48**, 3532-3535.

Jollie, D. (2008).PLATINUM 2008. United Kingdom: Johnson Matthey.

Kashefi, K., Tor, J. M., Nevin, K. P. & Lovley, D. R. (2001). Reductive precipitation of gold by dissimilatory Fe(III)-reducing bacteria and Archaea. *Applied and Environmental Microbiology* **67**, 3275-3279.

Kaulmann, U., Smithies, K., Smith, M. E. B., HaileS, H. C. & Ward, J. M. (2007). Substrate spectrum of ω-transaminase from *Chromobacterium violaceum* DSM30191 and its potential for biocatalysis. *Enzyme and Microbial Technology* **41**, 628-637.

Kennedy, B. P., Ziegler, M. G., Alford, M., Hansen, L. A., Thal, L. J. & Masliah, E. (2003). Early and persistent alterations in prefrontal cortex MAO A and B in Alzheimer's disease. *Journal of Neural Transmission* **110**, 789-801.

Khersonsky, O., Röthlisberger, D., Wollacott, A. M. & other authors (2011). Optimization of the *in-silico*-designed Kemp eliminase KE70 by computational design and directed evolution. *Journal of Molecular Biology* **407**, 391-412.

Kim, M. J., Kim, H. M., Kim, D., Ahn, Y. & Park, J. (2004a). Dynamic kinetic resolution of secondary alcohols by enzyme-metal combinations in ionic liquid. *Green Chemistry* **6**, 471-474.

Kim, M. J., Kim, W. H., Han, K., Choi, Y. K. & Park, J. (2007). Dynamic kinetic resolution of primary amines with a recyclable Pd nanocatalyst for racemization. *Organic Letters* **9**, 1157-1159.

Kim, Y., Park, J. & Kim, M. J. (2011). Dynamic kinetic resolution of amines and amino acids by enzyme-metal cocatalysis. *ChemCatChem* **3**, 271-277.

Kim, Y. H., Shin, W. S. & Ko, S. O. (2004b). Reductive dechlorination of chlorinated biphenyls by palladized zero-valent metals. *Journal of Environmental Science and Health Part a-Toxic/Hazardous Substances & Environmental Engineering* **39**, 1177-1188.

Kirk, O., Borchert, T. V. & Fuglsang, C. C. (2002). Industrial enzyme applications. *Current Opinion in Biotechnology* **13**, 345-351.

Koszelewski, D., Lavandera, I., Clay, D., Rozzell, D. & Kroutil, W. (2008). Asymmetric synthesis of optically pure pharmacologically relevant amines employing ω-transaminases. *Advanced Synthesis & Catalysis* **350**, 2761-2766.

Koszelewski, D., Clay, D., Rozzell, D. & Kroutil, W. (2009). Deracemisation of α-chiral primary amines by a one-pot, two-step cascade reaction catalysed by ω-transaminases. *European Journal of Organic Chemistry*, 2289-2292.

Koszelewski, D., Goritzer, M., Clay, D., Seisser, B. & Kroutil, W. (2010). Synthesis of optically active amines employing recombinant ω-transaminases in *E. coli* cells. *ChemCatChem* **2**, 73-77.

Krause, M., Ukkonen, K., Haataja, T., Ruottinen, M., Glumoff, T., Neubauer, A., Neubauer, P. & Vasala, A. (2010). A novel fed-batch based cultivation method provides high cell-density and improves yield of soluble recombinant proteins in shaken cultures. *Microbial Cell Factories* **9**, 11.

Kurtis, C. R. P., Knowles, P. F., Parsons, M. R., Gaule, T. G., Phillips, S. E. V. & McPherson, M. J. (2011). Tyrosine 381 in *E. coli* copper amine oxidase influences substrate specificity. *Journal of Neural Transmission* **118**, 1043-1053.

Leemhuis, H., Kelly, R. M. & Dijkhuizen, L. (2009). Directed evolution of enzymes: Library screening strategies. *IUBMB Life* **61**, 222-228.

Lengke, M. F., Fleet, M. E. & Southam, G. (2007). Synthesis of palladium nanoparticles by reaction of filamentous cyanobacterial biomass with a palladium(II) chloride complex. *Langmuir* **23**, 8982-8987.

Liu, D. N., Trodler, P., Eiben, S. & other authors (2010). Rational design of *Pseudozyma antarctica* lipase B yielding a general esterification catalyst. *Chembiochem* **11**, 789-795.

Liu, J. C., He, F., Gunn, T. M., Zhao, D. Y. & Roberts, C. B. (2009). Precise seed-mediated growth and size-controlled synthesis of palladium nanoparticles using a green chemistry approach. *Langmuir* **25**, 7116-7128.

Livage, J. & Coradin, T. (2006). Living cells in oxide glasses. *Medical Mineraology and Geochemistry* **64**, 315-332.

Lloyd, J. R. & Macaskie, L. E. (1996). A novel PhosphorImager-based technique for monitoring the microbial reduction of technetium. *Applied and Environmental Microbiology* **62**, 578-582.

Lloyd, J. R., Harding, C. L. & Macaskie, L. E. (1997). Tc(VII) reduction and accumulation by immobilized cells of *Escherichia coli*. *Biotechnology and Bioengineering* **55**, 505-510.

Lloyd, J. R., Yong, P. & Macaskie, L. E. (1998a). Enzymatic recovery of elemental palladium by using sulfate-reducing bacteria. *Applied and Environmental Microbiology* **64**, 4607-4609.

Lloyd, J. R., Nolting, H. F., Sole, V. A. & Bosecker, K. (1998b). Technetium reduction and precipitation by sulfate-reducing bacteria. *Geomicrobiology Journal* **15**, 45-58.

Lloyd, J. R., Sole, V. A., Van Praagh, C. V. G. & Lovley, D. R. (2000). Direct and Fe(II)-mediated reduction of technetium by Fe(III)-reducing bacteria. *Applied and Environmental Microbiology* **66**, 3743-3749.

Lloyd, J. R., Mabbett, A. N., Williams, D. R. & Macaskie, L. E. (2001). Metal reduction by sulphate-reducing bacteria: physiological diversity and metal specificity. *Hydrometallurgy* **59**, 327-337.

Lloyd, J. R. (2003). Microbial reduction of metals and radionuclides. *Fems Microbiology Reviews* **27**, 411-425.

Lloyd, J. R., Lovley, D. R. & Macaskie, L. E. (2003). Biotechnological application of metal-reducing microorganisms. *Advances in Applied Microbiology* **53**, 85-128.

Lloyd, J. R. & Renshaw, J. C. (2005). Bioremediation of radioactive waste: radionuclide-microbe interactions in laboratory and field-scale studies. *Current Opinion in Biotechnology* **16**, 254-260.

Lovley, D. R. (1991). Dissimilatory Fe(III) and Mn(IV) reduction. *Microbiological Reviews* **55**, 259-287.

Lovley, D. R., Phillips, E. J. P., Gorby, Y. A. & Landa, E. R. (1991). Microbial reduction of uranium. *Nature* **350**, 413-416.

Lovley, D. R. & Phillips, E. J. P. (1992). Reduction of uranium by *Desulfovibrio desulfuricans*. *Applied and Environmental Microbiology* **58**, 850-856.

Lovley, D. R., Giovannoni, S. J., White, D. C., Champine, J. E., Phillips, E. J. P., Gorby, Y. A. & Goodwin, S. (1993). *Geobacter metallireducens* gen. nov. sp. nov., a microorganism capable of coupling the complete oxidation of organic compounds to the reduction of iron and other metals. *Archives of Microbiology* **159**, 336-344.

Lovley, D. R., Woodward, J. C. & Chapelle, F. H. (1994). Stimulated anoxic biodegradation of aromatic hydrocarbons using Fe(III) ligands. *Nature* **370**, 128-131.

Lovley, D. R. (1995). Bioremediation of organic and metal contaminants with dissimilatory metal reduction. *Journal of Industrial Microbiology* **14**, 85-93.

Lovley, D. R., Coates, J. D., BluntHarris, E. L., Phillips, E. J. P. & Woodward, J. C. (1996a). Humic substances as electron acceptors for microbial respiration. *Nature* **382**, 445-448.

Lovley, D. R., Woodward, J. C. & Chapelle, F. H. (1996b). Rapid anaerobic benzene oxidation with a variety of chelated Fe(III) forms. *Applied and Environmental Microbiology* **62**, 288-291.

Lovley, D. R. (2000). *Environmental Microbe-Metal Interactions*. Washington: ASM Press.

Lovley, D. R. & Anderson, R. T. (2000). Influence of dissimilatory metal reduction on fate of organic and metal contaminants in the subsurface. *Hydrogeology Journal* **8**, 77-88.

Lovley, D. R., Holmes, D. E. & Nevin, K. P. (2004). Dissimilatory Fe(III) and Mn(IV) reduction. *Advances in Microbial Physiology, Vol 49* **49**, 219-286.

Luke, I., Butland, G., Moore, K. & other authors (2008). Biosynthesis of the respiratory formate dehydrogenases from *Escherichia coli*: characterization of the FdhE protein. *Archives of Microbiology* **190**, 685-696.

Ma, J., Ji, Y., Sun, H., Chen, Y., Tang, Y., Lu, T. & Zheng, W. (2011). Synthesis of carbon supported palladium nanoparticles catalyst using a facile homogeneous precipitation-reduction reaction method for formic acid electrooxidation. *Applied Surface Science*, in press.

Mabbett, A. N., Lloyd, J. R. & Macaskie, L. E. (2002). Effect of complexing agents on reduction of Cr(VI) by *Desulfovibrio vulgaris* ATCC 29579. *Biotechnology and Bioengineering* **79**, 389-397.

Mabbett, A. N., Yong, P., Farr, J. P. G. & Macaskie, L. E. (2004). Reduction of Cr(VI) by "palladized" biomass of *Desulfovibrio desulfuricans* ATCC 29577. *Biotechnology and Bioengineering* **87**, 104-109.

Mabbett, A. N., Sanyahumbi, D., Yong, P. & Macaskie, L. E. (2006). Biorecovered precious metals from industrial wastes: Single-step conversion of a mixed metal liquid waste to a bioinorganic catalyst with environmental application. *Environmental Science & Technology* **40**, 1015-1021.

Macaskie, L. E. (1990). An immobilized cell bioprocess for the removal of heavy metals from aqueous flows. *Journal of Chemical Technology and Biotechnology* **49**, 357-379.

Macaskie, L. E., Baxter-Plant, V. S., Creamer, N. J., Humphries, A. C., Mikheenko, I. P., Mikheenko, P. M., Penfold, D. W. & Yong, P. (2005). Applications of bacterial hydrogenases in waste decontamination, manufacture of novel bionanocatalysts and in sustainable energy. *Biochemical Society Transactions* **33**, 76-79.

Macy, J. M., Michel, T. A. & Kirsch, D. G. (1989). Selenate reduction by a *Pseudomonas* species - a new mode of anaerobic respiration. *FEMS Microbiology Letters* **61**, 195-198.

Macy, J. M., Nunan, K., Hagen, K. D., Dixon, D. R., Harbour, P. J., Cahill, M. & Sly, L. I. (1996). *Chrysiogenes arsenatis* gen. nov., sp. nov.; a new arsenate-respiring bacterium isolated from gold mine wastewater. *International Journal of Systematic Bacteriology* **46**, 1153-1157.

Madler, L., Stark, W. J. & Pratsinis, S. E. (2003). Simultaneous deposition of Au nanoparticles during flame synthesis of TiO_2 and SiO_2. *Journal of Materials Research* **18**, 115-120.

Maeda, T., Sanchez-Torres, V. & Wood, T. K. (2007). *Escherichia coli* hydrogenase 3 is a reversible enzyme possessing hydrogen uptake and synthesis activities. *Applied Microbiology and Biotechnology* **76**, 1035-1042.

Mangas-Sanchez, J., Rodriguez-Mata, M., Busto, E., Gotor, V. & Gotor-Fernandez, V. (2009). Chemoenzymatic synthesis of rivastigmine based on lipase-catalyzed processes. *Journal of Organic Chemistry* **74**, 5304-5310.

Martin, A. R., DiSanto, R., Plotnikov, I., Kamat, S., Shonnard, D. & Pannuri, S. (2007). Improved activity and thermostability of (*S*)-aminotransferase by error-prone polymerase chain reaction for the production of a chiral amine. *Biochemical Engineering Journal* **37**, 246-255.

Megonigal, J. P., Hines, M. E. & Visscher, P. T. (2003). *Anaerobic Metabolism: Linkages to Trace Gases and Aerobic Processes*. Pergamon: Elsevier.

Mekasuwandumrong, O., Phothakwanpracha, S., Jongsomjit, B., Shotipruk, A. & Panpranot, J. (2011). Influence of flame conditions on the dispersion of Pd on the flame spray-derived Pd/TiO_2 nanoparticles. *Powder Technology* **210**, 328-331.

Menon, N. K., Robbins, J., Peck, H. D., Chatelus, C. Y., Choi, E. S. & Przybyla, A. E. (1990). Cloning and sequencing of a putative *Escherichia coli* [Nife] hydrogenase-1 operon containing 6 open reading frames. *Journal of Bacteriology* **172**, 1969-1977.

Menon, N. K., Chatelus, C. Y., Dervartanian, M., Wendt, J. C., Shanmugam, K. T., Peck, H. D. & Przybyla, A. E. (1994). Cloning, sequencing, and mutational analysis of the *hyb* operon encoding *Escherichia coli* hydrogenase-2. *Journal of Bacteriology* **176**, 4416-4423.

Mertens, B., Blothe, C., Windey, K., De Windt, W. & Verstraete, W. (2007). Biocatalytic dechlorination of lindane by nano-scale particles of Pd(0) deposited on *Shewanella oneidensis*. *Chemosphere* **66**, 99-105.

Mikheenko, I. P., Rousset, M., Dementin, S. & Macaskie, L. E. (2008). Bioaccumulation of palladium by *Desulfovibrio fructosivorans* wild-type and hydrogenase-deficient strains. *Applied and Environmental Microbiology* **74**, 6144-6146.

Miles, A. A. & Misra, S. S. (1938). The estimation of the bactericidal power of the blood. *The Journal of Hygiene* **38**, 732-749.

Miller, J. N. (1993). Chapter 2 Instrumentation for UV-visible and fluorescence spectroscopy. In *UV spectroscopy: techniques, instrumentation, data handling*. Edited by B. J. Clark, T. Frost & M. A. Russell. London: Chapman & Hall.

Mnatsakanyan, N., Vassilian, A., Navasardyan, L., Bagramyan, K. & Trchounian, A. (2002). Regulation of *Escherichia coli* formate hydrogenlyase activity by formate at alkaline pH. *Current Microbiology* **45**, 281-286.

Morley, K. L. & Kazlauskas, R. J. (2005). Improving enzyme properties: when are closer mutations better? *Trends in Biotechnology* **23**, 231-237.

Murray, A. J., Mikheenko, I. P., Goralska, E., Rowson, N. A. & Macaskie, L. E. (2007). Biorecovery of platinum group metals from secondary sources. *Advanced Materials Research* **20-21**, 651-654.

Mutti, F. G., Sattler, J., Tauber, K. & Kroutil, W. (2011). Creating a biocatalyst for the production of an optically pure sterically hindered amine. *ChemCatChem* **3**, 109-111.

Nair, N. U., Denard, C. A. & Zhao, H. M. (2010). Engineering of enzymes for selective catalysis. *Current Organic Chemistry* **14**, 1870-1882.

Nassif, N., Bouvet, O., Rager, M. N., Roux, C., Coradin, T. & Livage, J. (2002). Living bacteria in silica gels. *Nature Materials* **1**, 42-44.

Nassif, N., Coiffier, A., Coradin, T., Roux, C., Livage, J. & Bouvet, O. (2003). Viability of bacteria in hybrid aqueous silica gels. *Journal of Sol-Gel Science and Technology* **26**, 1141-1144.

Nguyen-Ngoc, H. & Tran-Minh, C. (2007). Sol-gel process for vegetal cell encapsulation. *Materials Science & Engineering C-Biomimetic and Supramolecular Systems* **27**, 607-611.

Ogawa, J., Shimizu, S. & Yamada, H. (1994). Enzymatic asymmetric synthesis of α-methyl arylalkylamines and α-methyl arylalkylalcohols by arylalkyl acylamidases. *Bioorganic & Medicinal Chemistry* **2**, 429-432.

Ogi, T., Honda, R., Tamaoki, K., Saitoh, N. & Konishi, Y. (2011). Direct room-temperature synthesis of a highly dispersed Pd nanoparticle catalyst and its electrical properties in a fuel cell. *Powder Technology* **205**, 143-148.

Oikawa, T., Mukoyama, S. & Soda, K. (2001). Chemo-enzymatic D-enantiomerization of DL-lactate. *Biotechnology and Bioengineering* **73**, 80-82.

Orozco, R. L., Redwood, M. D., Yong, P., Caldelari, I., Sargent, F. & Macaskie, L. E. (2010). Towards an integrated system for bio-energy: hydrogen production by *Escherichia coli* and use of palladium-coated waste cells for electricity generation in a fuel cell. *Biotechnology Letters* **32**, 1837-1845.

Pàmies, O. & Bäckvall, J. E. (2003). Combined metal catalysis and biocatalysis for an efficient deracemization process. *Current Opinion in Biotechnology* **14**, 407-413.

Panke, S., Held, M. & Wubbolts, M. (2004). Trends and innovations in industrial biocatalysis for the production of fine chemicals. *Current Opinion in Biotechnology* **15**, 272-279.

Panke, S. & Wubbolts, M. (2005). Advances in biocatalytic synthesis of pharmaceutical intermediates. *Current Opinion in Chemical Biology* **9**, 188-194.

Park, H. S., Nam, S. H., Lee, J. K., Yoon, C. N., Mannervik, B., Benkovic, S. J. & Kim, H. S. (2006). Design and evolution of new catalytic activity with an existing protein scaffold. *Science* **311**, 535-538.

Park, S., Morley, K. L., Horsman, G. P., Holmquist, M., Hult, K. & Kazlauskas, R. J. (2005). Focusing mutations into the *P. fluorescens* esterase binding site increases enantioselectivity more effectively than distant mutations. *Chemistry & Biology* **12**, 45-54.

Park, S., Kadkin, O. N., Tae, J. G. & Choi, M. G. (2008). Photoresponsive palladium(II) complexes with azobenzene incorporated into benzyl aryl ether dendrimers. *Inorganica Chimica Acta* **361**, 3063-3068.

Parvulescu, A., Janssens, J., Vanderleyden, J. & De Vos, D. (2010). Heterogeneous catalysts for racemization and dynamic kinetic resolution of amines and secondary alcohols. *Topics in Catalysis* **53**, 931-941.

Patel, R. N. (2001). Biocatalytic synthesis of intermediates for the synthesis of chiral drug substances. *Current Opinion in Biotechnology* **12**, 587-604.

Patel, R. N. (2006). Biocatalysis: Synthesis of chiral intermediates for pharmaceuticals. *Current Organic Chemistry* **10**, 1289-1321.

Patel, R. N. (2008). Synthesis of chiral pharmaceutical intermediates by biocatalysis. *Coordination Chemistry Reviews* **252**, 659-701.

Pellissier, H. (2011). Recent developments in dynamic kinetic resolution. *Tetrahedron* **67**, 3769-3802.

Peniche, C., Arguelles-Monal, W., Peniche, H. & Acosta, N. (2003). Chitosan: An attractive biocompatible polymer for microencapsulation. *Macromolecular Bioscience* **3**, 511-520.

Plunkett, G., Burland, V., Daniels, D. L. & Blattner, F. R. (1993). Analysis of the *Escherichia coli* genome .3. DNA sequence of the region from 87.2 to 89.2 minutes. *Nucleic Acids Research* **21**, 3391-3398.

Pogorevc, M., Kroutil, W., Wallner, S. R. & Faber, K. (2002). Enantioselective stereoinversion in the kinetic resolution of *rac-sec*-alkyl sulfate esters by hydrolysis with an alkylsulfatase from *Rhodococcus ruber* DSM 44541 furnishes homochiral products. *Angewandte Chemie-International Edition* **41**, 4052-4054.

Poole, R. K. (1983). Bacterial cytochrome oxidases - a structurally and functionally diverse group of electron-transfer proteins. *Biochimica Et Biophysica Acta* **726**, 205-243.

Radman, M., Wagner, R. E., Glickman, B. W. & Meselson, M. (1980). *DNA methylation, mismatch correction, and genetic stability*: In *Progress in Environmental Mutagenesis* (Alevic, M., ed.). Elsevier, Amsterdam, pp. 121-130.

Redwood, M. D., Deplanche, K., Baxter-Plant, V. S. & Macaskie, L. E. (2008a). Biomass-supported palladium catalysts on *Desulfovibrio desulfuricans* and *Rhodobacter sphaeroides*. *Biotechnology and Bioengineering* **99**, 1045-1054.

Redwood, M. D., Mikheenko, I. P., Sargent, F. & Macaskie, L. E. (2008b). Dissecting the roles of *Escherichia coli* hydrogenases in biohydrogen production. *FEMS Microbiology Letters* **278**, 48-55.

Reetz, M. T., Zonta, A., Schimossek, K., Liebeton, K. & Jaeger, K. E. (1997). Creation of enantioselective biocatalysts for organic chemistry by in vitro evolution. *Angewandte Chemie-International Edition* **36**, 2830-2832.

Reetz, M. T., Wang, L. W. & Bocola, M. (2006). Directed evolution of enantioselective enzymes: Iterative cycles of CASTing for probing protein-sequence space. *Angewandte Chemie-International Edition* **45**, 1236-1241.

Reetz, M. T. & Carballeira, J. D. (2007). Iterative saturation mutagenesis (ISM) for rapid directed evolution of functional enzymes. *Nature Protocols* **2**, 891-903.

Reetz, M. T., Hobenreich, H., Soni, P. & Fernandez, L. (2008). A genetic selection system for evolving enantioselectivity of enzymes. *Chemical Communications*, 5502-5504.

Reetz, M. T. & Wu, S. (2009). Laboratory evolution of robust and enantioselective Baeyer-Villiger monooxygenases for asymmetric catalysis. *Journal of the American Chemical Society* **131**, 15424-15432.

Reiss, R. (2008). Engineering monoamine oxidase-N for the deracemisation of racemic amines: PhD Thesis, University of Manchester.

Richardson, D. J. (2000). Bacterial respiration: a flexible process for a changing environment. *Microbiology-SGM* **146**, 551-571.

Riederer, P., Lachenmayer, L. & Laux, G. (2004). Clinical applications of MAO-inhibitors. *Current Medicinal Chemistry* **11**, 2033-2043.

Roberts, S. M., Turner, N. J., Willetts, A. J. & Turner, M. K. (1995). *Introduction to Biocatalysis Using Enzymes and Micro-organisms*. Milton Keynes: Cambridge University Press.

Rosche, B., Li, X. Z., Hauer, B., Schmid, A. & Buehler, K. (2009). Microbial biofilms: a concept for industrial catalysis? *Trends in Biotechnology* **27**, 636-643.

Röthlisberger, D., Khersonsky, O., Wollacott, A. M. & other authors (2008). Kemp elimination catalysts by computational enzyme design. *Nature* **453**, 190-U194.

RSC (2008). Visual Elements website (Accessed 03/10/08). http://www.rsc.org/chemsoc/visualelements/pages/palladium.html Royal Society of Chemistry.

Sablin, S. O., Yankovskaya, V., Bernard, S., Cronin, C. N. & Singer, T. P. (1998). Isolation and characterization of an evolutionary precursor of human monoamine oxidases A and B. *European Journal of Biochemistry* **253**, 270-279.

Savile, C. K., Janey, J. M., Mundorff, E. C. & other authors (2010). Biocatalytic asymmetric synthesis of chiral amines from ketones applied to sitagliptin manufacture. *Science* **329**, 305-309.

Sawers, G., Heider, J., Zehelein, E. & Bock, A. (1991). Expression and operon structure of the *sel* genes of *Escherichia coli* and identification of a 3rd selenium-containing formate dehydrogenase isoenzyme. *Journal of Bacteriology* **173**, 4983-4993.

Sawers, G. (1994). The hydrogenases and formate dehydrogenases of *Escherichia coli*. *Antonie Van Leeuwenhoek International Journal of General and Molecular Microbiology* **66**, 57-88.

Sawers, R. G., Ballantine, S. P. & Boxer, D. H. (1985). Differential expression of hydrogenase isoenzymes in *Escherichia coli* K-12 - evidence for a 3rd isoenzyme. *Journal of Bacteriology* **164**, 1324-1331.

Sawers, R. G. (2005). Formate and its role in hydrogen production in *Escherichia coli*. *Biochemical Society Transactions* **33**, 42-46.

Scheuermann, R., Tam, S., Burgers, P. M. J., Lu, C. & Echols, H. (1983). Identification of the epsilon-subunit of *Escherichia coli* DNA polymerase III holoenzyme as the *dnaQ* gene product - a fidelity subunit for DNA replication. *Proceedings of the National Academy of Sciences of the United States of America-Biological Sciences* **80**, 7085-7089.

Schilling, B. & Lerch, K. (1995a). Amine oxidases from *Aspergillus niger* - Identification of a novel flavin-dependent enzyme. *Biochimica Et Biophysica Acta-General Subjects* **1243**, 529-537.

Schilling, B. & Lerch, K. (1995b). Cloning, sequencing and heterologous expression of the monoamine oxidase gene from *Aspergillus niger*. *Molecular & General Genetics* **247**, 430-438.

Schröfel, A. & Kratošová, G. (2011). Biosynthesis of metallic nanoparticles and their applications. In *Intracellular Delivery: Fundamentals and Applications*, pp. 373-409. Edited by A. Prokop: Springer Science.

Sebilleau, D. (2006). X-ray and electron spectroscopies: An introduction. *Magnetism: A Synchrotron Radiation Approach* **697**, 15-57.

Shih, J. C., Wu, J. B. & Chen, K. (2011). Transcriptional regulation and multiple functions of MAO genes. *Journal of Neural Transmission* **118**, 979-986.

Skoog, D. A., Holler, F. J. & Nieman, T. A. (1998a). Chapter 12 Atomic X-ray Spectroscopy. In *Principles of Instrumental Analysis*. Edited by D. A. Skoog, F. J. Holler & T. A. Nieman. London: Saunders College Publishing.

Skoog, D. A., Holler, F. J. & Nieman, T. A. (1998b). Chapter 11 Atomic Mass Spectrometry. In *Principles of Instrumental Analysis*. Edited by D. A. Skoog, F. J. Holler & T. A. Nieman. London: Saunders College Publishing.

Smeds, K. A. & Grinstaff, M. W. (2001). Photocrosslinkable polysaccharides for *in situ* hydrogel formation. *Journal of Biomedical Materials Research* **54**, 115-121.

Smidsrod, O. & Skjak-Braek, G. (1990). Alginate as immobilization matrix for cells. *Trends in Biotechnology* **8**, 71-78.

Smith, M. E. B., Chen, B. H., Hibbert, E. G. & other authors (2010). A multidisciplinary approach toward the rapid and preparative-scale biocatalytic synthesis of chiral amino alcohols: a concise transketolase-/ω-transaminase-mediated synthesis of (2*S*,3*S*)-2-aminopentane-1,3-diol. *Organic Process Research & Development* **14**, 99-107.

Smithies, K., Smith, M. E. B., Kaulmann, U., Galman, J. L., Ward, J. M. & Hailes, H. C. (2009). Stereoselectivity of an ω-transaminase-mediated amination of 1,3-dihydroxy-1-phenylpropane-2-one. *Tetrahedron-Asymmetry* **20**, 570-574.

Sobjerg, L. S., Gauthier, D., Lindhardt, A. T., Bunge, M., Finster, K., Skrydstrup, T. & Meyer, R. L. (2009). Bio-supported palladium nanoparticles as a catalyst for Suzuki-Miyaura and Mizoroki-Heck reactions. *Green Chemistry* **11**, 2041-2046.

Sobjerg, L. S., Lindhardt, A. T., Finster, K., Meyer, R. L. & Skrydstrup, T. (2011). Size control and catalytic activity of bio-supported palladium nanoparticles. *Colloids and Surfaces B-Biointerfaces* **85**, 373-378.

Spiller, B., Gershenson, A., Arnold, F. H. & Stevens, R. C. (1999). A structural view of evolutionary divergence. *Proceedings of the National Academy of Sciences of the United States of America* **96**, 12305-12310.

Stemmer, W. P. C. (1994). Rapid evolution of a protein *in vitro* by DNA shuffling. *Nature* **370**, 389-391.

Stocklein, W., Eisgruber, A. & Schmidt, H. L. (1983). Conversion of L-phenylalanine to L-tyrosine by immobilized bacteria. *Biotechnology Letters* **5**, 703-708.

Straathof, A. J. J., Panke, S. & Schmid, A. (2002). The production of fine chemicals by biotransformations. *Current Opinion in Biotechnology* **13**, 548-556.

Studier, F. W. & Moffatt, B. A. (1986). Use of bacteriophage T7 RNA polymerase to direct selective high level expression of cloned genes. *Journal of Molecular Biology* **189**, 113-130.

Syrén, P. O., Lindgren, E., Hoeffken, H. W., Branneby, C., Maurer, S., Hauer, B. & Hult, K. (2010). Increased activity of enzymatic transacylation of acrylates through rational design of lipases. *Journal of Molecular Catalysis B-Enzymatic* **65**, 3-10.

Taylor, H. E. (2001). *Inductively Coupled Plasma-Mass Spectrometry. Practices and Techniques*: Academic Press, San Diego.

Thalén, L. K., Zhao, D. B., Sortais, J. B., Paetzold, J., Hoben, C. & Bäckvall, J. E. (2009). A chemoenzymatic approach to enantiomerically pure amines using dynamic kinetic resolution: application to the synthesis of norsertraline. *Chemistry-a European Journal* **15**, 3403-3410.

Tipton, K. F., Boyce, S., O'Sullivan, J., Davey, G. P. & Healy, J. (2004). Monoamine oxidases: Certainties and uncertainties. *Current Medicinal Chemistry* **11**, 1965-1982.

Tobin, M. B., Gustafsson, C. & Huisman, G. W. (2000). Directed evolution: the 'rational' basis for 'irrational' design. *Current Opinion in Structural Biology* **10**, 421-427.

Tsoligkas, A. N., Winn, M., Bowen, J., Overton, T. W., Simmons, M. J. H. & Goss, R. J. M. (2011). Engineering biofilms for biocatalysis. *ChemBioChem* **12**, 1391-1395.

Tucker, M. D., Barton, L. L. & Thomson, B. M. (1998). Reduction of Cr, Mo, Se and U by *Desulfovibrio desulfuricans* immobilized in polyacrylamide gels. *Journal of Industrial Microbiology & Biotechnology* **20**, 13-19.

Turner, N. J. (2003). Controlling chirality. *Current Opinion in Biotechnology* **14**, 401-406.

Turner, N. J. (2009). Directed evolution drives the next generation of biocatalysts. *Nature Chemical Biology* **5**, 568-574.

Unden, G. & Bongaerts, J. (1997). Alternative respiratory pathways of *Escherichia coli*: Energetics and transcriptional regulation in response to electron acceptors. *Biochimica Et Biophysica Acta-Bioenergetics* **1320**, 217-234.

Vasala, A., Panula, J., Bollok, M., Illmann, L., Halsig, C. & Neubauer, P. (2006). A new wireless system for decentralised measurement of physiological parameters from shake flasks. *Microbial Cell Factories* **5**.

Vignais, P. M., Billoud, B. & Meyer, J. (2001). Classification and phylogeny of hydrogenases. *Fems Microbiology Reviews* **25**, 455-501.

Vignais, P. M. & Billoud, B. (2007). Occurrence, classification, and biological function of hydrogenases: An overview. *Chemical Reviews* **107**, 4206-4272.

Vignais, P. M. (2008). Hydrogenases and H^+-reduction in primary energy conservation. *Results and Problems in Cell Differentiation* **45**, 223-252.

Vorlop, K. D. & Klein, J. (1981). Formation of spherical chitosan biocatalysts by ionotropic gelation. *Biotechnology Letters* **3**, 9-14.

Wahler, D. & Reymond, J. L. (2001). High-throughput screening for biocatalysts. *Current Opinion in Biotechnology* **12**, 535-544.

Ward, J. & Wohlgemuth, R. (2010). High-yield biocatalytic amination reactions in organic synthesis. *Current Organic Chemistry* **14**, 1914-1927.

Wilson, K. (2005). Chapter 11 Chromatographic techniques. In *Principles and techniques of biochemistry and molecular biology*. Edited by K. Wilson & J. M. Walker. New York: Cambridge University Press.

Wood, J., Bodenes, L., Bennett, J., Deplanche, K. & Macaskie, L. E. (2010). Hydrogenation of 2-butyne-1,4-diol using novel bio-palladium catalysts. *Industrial & Engineering Chemistry Research* **49**, 980-988.

Yang, X., Li, Q. B., Wang, H. X. & other authors (2010). Green synthesis of palladium nanoparticles using broth of *Cinnamomum camphora* leaf. *Journal of Nanoparticle Research* **12**, 1589-1598.

Yanisch-Perron, C., Vieira, J. & Messing, J. (1985). Improved M13 phage cloning vectors and host strains - nucleotide sequences of the M13mp18 and pUC19 vectors. *Gene* **33**, 103-119.

Yong, P., Farr, J. P. G., Harris, I. R. & Macaskie, L. E. (2002a). Palladium recovery by immobilized cells of *Desulfovibrio desulfuricans* using hydrogen as the electron donor in a novel electrobioreactor. *Biotechnology Letters* **24**, 205-212.

Yong, P., Rowson, N. A., Farr, J. P. G., Harris, I. R. & Macaskie, L. E. (2002b). Bioreduction and biocrystallization of palladium by *Desulfovibrio desulfuricans* NCIMB 8307. *Biotechnology and Bioengineering* **80**, 369-379.

Yong, P., Rowson, N. A., Farr, J. P. G., Harris, I. R. & Macaskie, L. E. (2002c). Bioaccumulation of palladium by *Desulfovibrio desulfuricans*. *Journal of Chemical Technology and Biotechnology* **77**, 593-601.

Yong, P., Rowson, N. A., Farr, J. P. G., Harris, I. R. & Macaskie, L. E. (2003). A novel electrobiotechnology for the recovery of precious metals from spent automotive catalysts. *Environmental Technology* **24**, 289-297.

Yong, P., Paterson-Beedle, M., Mikheenko, I. P. & Macaskie, L. E. (2007). From bio-mineralisation to fuel cells: biomanufacture of Pt and Pd nanocrystals for fuel cell electrode catalyst. *Biotechnology Letters* **29**, 539-544.

Yong, P., Mikheenko, I. P., Deplanche, K., Redwood, M. D. & Macaskie, L. E. (2010). Biorefining of precious metals from wastes: an answer to manufacturing of cheap nanocatalysts for fuel cells and power generation via an integrated biorefinery? *Biotechnology Letters* **32**, 1821-1828.

Youdim, M. B. H. & Bakhle, Y. S. (2006). Monoamine oxidase: isoforms and inhibitors in Parkinson's disease and depressive illness. *British Journal of Pharmacology* **147**, S287-S296.

Zha, D. X., Wilensek, S., Hermes, M., Jaeger, K. E. & Reetz, M. T. (2001). Complete reversal of enantioselectivity of an enzyme-catalyzed reaction by directed evolution. *Chemical Communications*, 2664-2665.

Zhao, H. M., Giver, L., Shao, Z. X., Affholter, J. A. & Arnold, F. H. (1998). Molecular evolution by staggered extension process (StEP) in vitro recombination. *Nature Biotechnology* **16**, 258-261.

Zinoni, F., Birkmann, A., Stadtman, T. C. & Bock, A. (1986). Nucleotide sequence and expression of the selenocysteine-containing polypeptide of formate dehydrogenase (formate hydrogen lyase-linked) from *Escherichia coli*. *Proceedings of the National Academy of Sciences of the United States of America* **83**, 4650-4654.